MUSCLE DISORDER OR METABOLIC DISORDER: GENOMIC, TRANSCRIPTOMIC, AND METABOLOMIC INSIGHTS INTO THE PATHOGENESIS OF WOODEN BREAST AND WHITE STRIPING IN COMMERCIAL BROILER CHICKENS

by

Juniper Ada Lake

A dissertation submitted to the Faculty of the University of Delaware in partial fulfillment of the requirements for the degree of Doctor of Philosophy in Bioinformatics Data Science

Summer 2021

MUSCLE DISORDER OR METABOLIC DISORDER:

GENOMIC, TRANSCRIPTOMIC, AND METABOLOMIC INSIGHTS INTO THE PATHOGENESIS OF WOODEN BREAST AND WHITE STRIPING IN COMMERCIAL BROILER CHICKENS

by

Juniper Ada Lake

Approved: _____

Erin E. Connor, Ph.D.
Chair of the Department of Animal and Food Sciences

Approved: _____

Calvin L. Keeler Jr., Ph.D.
Interim Dean of the College of Agriculture and Natural Resources

Approved: _____

Louis F. Rossi, Ph.D.
Vice Provost for Graduate and Professional Education and
Dean of the Graduate College

I certify that I have read this dissertation and that in my opinion it meets the academic and professional standard required by the University as a dissertation for the degree of Doctor of Philosophy.

Signed: _____

Behnam Abasht, Ph.D.
Professor in charge of dissertation

I certify that I have read this dissertation and that in my opinion it meets the academic and professional standard required by the University as a dissertation for the degree of Doctor of Philosophy.

Signed: _____

Randall J. Wisser, Ph.D.
Member of dissertation committee

I certify that I have read this dissertation and that in my opinion it meets the academic and professional standard required by the University as a dissertation for the degree of Doctor of Philosophy.

Signed: _____

Shawn W. Polson, Ph.D.
Member of dissertation committee

I certify that I have read this dissertation and that in my opinion it meets the academic and professional standard required by the University as a dissertation for the degree of Doctor of Philosophy.

Signed: _____

Jack C.M. Dekkers, Ph.D.
Member of dissertation committee

I certify that I have read this dissertation and that in my opinion it meets the academic and professional standard required by the University as a dissertation for the degree of Doctor of Philosophy.

Signed: _____

Erin Seifert, Ph.D.
Member of dissertation committee

ACKNOWLEDGMENTS

I am sincerely grateful to my research advisor, Dr. Behnam Abasht, who welcomed me into his lab and has treated me with immense kindness, support, and understanding ever since. He has given me the space and provided the knowledge to guide my rabbit-hole research through many missed deadlines, venturing into realms not quite in the scope of my original doctoral plan. Long before he was my advisor, he helped ignite in me an interest in genetics and bioinformatics during a graduate course called Genetics and Breeding that he co-instructed alongside Dr. Randy Wisser. That course was undoubtedly the best learning experience I've ever been exposed to and drastically shaped not only my understanding of genetics, but also my views on pedagogy and teamwork. I can only hope that they still teach with the creativity and enthusiasm that I was so lucky to witness.

Luckily, Dr. Randy Wisser has also continued to play a role in my life as a professor, committee member, and friend. He has seen me cry in a full-blown meltdown and has watched me foment a minor rebellion in a new class that he was trying to develop, but for some reason he continues to stay involved in my education and research.

I would also like to acknowledge Dr. Jack Dekkers, who has taught me many complex ideas in a very casual manner and welcomed me into his lab for a few invaluable weeks at the beginning of my foray into the world of genomics analysis. Maybe someday we'll get to ride bikes together.

The final member of my committee, Dr. Erin Seifert, was a somewhat late addition but has proved immensely helpful in learning and writing about metabolic diseases and human biology. She has contributed her knowledge and time to helping me out of pure generosity and I can't thank her enough.

There are many others who have contributed to this research, including many who I have never met. Over the last year of remote work, I am particularly nostalgic for interactions with lab members and fellow students such as Ziqing, Heidi, Michael, Joe, Zhu, Connor, and Emma among others. I am also grateful for my friends, who all listened to me talk about "chicken diabetes" for years and never once asked me to stop talking.

Finally, I must thank my partner and our three dogs – Barley, Goose, and Orville Redenbarker – who make me question a career at all if the alternative is spending time with them all day.

TABLE OF CONTENTS

LIST OF TABLES

LIST OF FIGURES

ABSTRACT

Commercial broilers represent a remarkable feat in the optimization of meat production, principally due to many generations of intensive artificial selection for economically important production traits such as rapid growth, high breast muscle yield, and low feed utilization. One of the unintended consequences of such selection among modern broiler chickens has been the relatively recent emergence of several muscle disorders mainly affecting the pectoralis major muscle and severely impacting meat quality. Two such myopathies, wooden breast and white striping, are the focus of this dissertation due to their high prevalence and economic importance. Severe wooden breast presents grossly as pale, enlarged, and palpably firm pectoralis major muscle, with visible signs of inflammation such as petechial hemorrhages and tissue edema. White striping, which often co-occurs with wooden breast and is considered by many to be part of the same disease spectrum, presents as fatty white striations running parallel to the muscle fiber.

The overarching objective of this dissertation was to improve our understanding of the pathogenesis of wooden breast and white striping in modern commercial broiler chickens primarily using ‘omics technologies and techniques. However, the first section eschews primary research and instead presents a novel hypothesis on the etiology and pathogenesis of these myopathies founded in existing literature, unpublished data from our lab, and an examination of the intricacies of avian glucose transport and metabolism. It purports that evident dysfunction of glucose and lipid metabolism in wooden breast closely aligns with similar changes

associated with type 2 diabetes and metabolic syndrome in mammals, and that reliance on insulin-independent glucose transport in the skeletal muscle of chickens may produce the wooden breast phenotype in lieu of increased plasma glucose levels. The remaining studies investigated hematologic, metabolomic, transcriptomic, and genomic changes associated with development of the wooden breast phenotype in a crossbred commercial broiler population that was raised to 7 weeks of age and scored for both wooden breast and white striping.

The first study assessed the association of wooden breast with perturbations in various venous blood parameters – blood gases, electrolytes, etc. – acquired through a rapid blood test and also examined changes in body weight distribution and lung morphology. Chickens with wooden breast were found to exhibit blood gas disturbances potentially indicative of insufficient respiratory gas exchange and elevated metabolism, including higher potassium and total carbon dioxide and lower oxygen saturation and pH. A microscopic comparison of lung tissues did not provide any evidence that lung morphology was a contributing factor, but affected broilers possessed a significantly heavier pectoralis major muscle and whole feathered wing compared to unaffected broilers, which could contribute to increased metabolic demand or impaired respiration.

The second study involved untargeted metabolomic profiling of blood plasma in 250 male broilers to find metabolites associated with wooden breast and white striping and to identify plasma biomarkers that could be used as a diagnostic tool for future research. Two statistical approaches were employed to achieve the two distinct goals of this study – mixed linear modeling and stepwise feature selection for a support vector machine. The findings from this study revealed changes in histidine

metabolism, lipid metabolism, and nucleotide metabolism associated with wooden breast and found that metabolites associated with white striping were almost entirely a subset of those associated with wooden breast. The metabolite 3-methylhistidine, which is often used as an index of myofibrillar breakdown in skeletal muscle and is increased in plasma of individuals with uncontrolled diabetes mellitus, was the top metabolite for both wooden breast and white striping in our mixed linear model and was also the metabolite with highest marginal prediction accuracy (82%) for wooden breast in our support vector machine. The final support vector machine achieved a prediction accuracy of 94% using only 6 metabolites, supporting the use of plasma biomarkers as an objective and quantitative measure of wooden breast severity for future research.

The third study looked at early changes in gene expression in the pectoralis major muscle associated with later development of wooden breast at market age. Biopsy samples of the left pectoralis major muscle were collected from birds at 14 days of age, and birds were subsequently raised to 7 weeks of age to allow sample selection based on the wooden breast phenotype at market age. RNA sequencing was performed on 5 unaffected and 8 affected female chicken samples, and differential expression analysis found wooden breast status at market age to be associated mainly with increased lipid metabolism and altered calcium homeostasis at 2 weeks of age. The genes *peroxisome proliferator-activated receptor gamma* (*PPARG*) and *lipoprotein lipase* (*LPL*) were two of many lipid metabolism genes expressed higher in wooden breast affected birds, and encode proteins that function respectively as an important transcription factor for lipid uptake and adipogenesis and as the rate-limiting catalyst for hydrolysis of triglycerides in circulating lipoproteins. A large proportion

of differentially expressed genes were also found to be linked to type 2 diabetes in humans, with *Ras related glycolysis inhibitor and calcium channel regulator* (*RRAD*) perhaps the best example of this. This gene was originally named *Ras-related associated with diabetes* because it was identified via subtraction cloning as the only gene out of 4000 cDNA clones that was overexpressed in skeletal muscle of type 2 diabetic individuals compared to non-diabetic or type 1 diabetic individuals.

The fourth and final study was a genome-wide association study of nearly 1200 broilers to investigate the genetic basis of wooden breast and white striping and identify candidate genes using genomic marker data. Heritability was estimated at 0.5 for both wooden breast and white striping with high genetic correlation between them (0.9). The majority of quantitative trait loci identified for both myopathies were located in a ~8 Mb region of chicken chromosome 5, which has highly conserved synteny with a portion of human chromosome 11 containing a cluster of imprinted genes associated with growth and metabolic disorders such as type 2 diabetes and Beckwith-Wiedemann syndrome. Top candidate genes include *potassium voltage-gated channel subfamily Q member 1* (*KCNQ1*), involved in insulin secretion and cardiac electrical activity, *lymphocyte-specific protein 1* (*LSP1*), involved in inflammation and immune response, and *dynamin 2* (*DNM2*), involved in biphasic insulin secretion and associated with two congenital neuromuscular diseases in humans.

Collectively, this dissertation frames the pathogenesis of wooden breast and white striping as closely related metabolic muscle disorders involving and potentially resulting from extensive dysregulation of glucose and lipid metabolism. Most importantly, this work emphasizes the systemic nature of these breast muscle disorders

and highlights the need for future research on other organs that likely contribute to myopathy development, including the pancreas, liver, and adipose tissue.

Chapter 1

INTRODUCTION

This dissertation comprises a broad, but by no means exhaustive, study of molecular and physiological changes – DNA, RNA, metabolites, and blood gases – associated with two economically important muscle disorders of modern commercial broiler chickens called wooden breast and white striping. The two highlights of this work are undoubtedly (1) the novel hypothesis on the etiology and pathogenesis of wooden breast and white striping described in Chapter 2 and (2) the genome-wide association (GWA) study described in Chapter 6. Because Chapter 2 provides a relatively comprehensive review of the literature surrounding wooden breast and white striping, it would be redundant to provide additional background on these disorders here. Instead, the remainder of this introduction is dedicated to discussing some of the important considerations underlying the GWA study of Chapter 6, including genotyping, association testing, and interpretation of results.

1.1 Genotyping

Technologies for genotyping genetic variants generally fall into one of two categories, genomic sequencing or DNA probe-based microarrays. Several commercial microarrays currently exist for *Gallus gallus*, including the Axiom Genome-Wide Chicken Genotyping 600k array (Kranis et al., 2013) and the 60k Illumina SNP BeadChip (Groenen et al., 2011), which were both designed using individuals from several broiler and layer populations. Due to their low cost and

convenience, genotyping arrays are the most popular genotyping technology in GWA studies although their popularity is starting to wane as the cost of sequencing falls (Tam et al., 2019). Several drawbacks of DNA microarrays make next-generation sequencing (NGS)-based methods of genotyping more attractive for certain types of studies.

One important limitation of microarrays is that they are designed using a specific population and therefore may not be representative of the genomic variation in the research population (Bumgarner, 2013). For example, the major chicken genotyping arrays were designed for use in western commercial broiler and layer populations and do not capture genomic variation in heritage chicken breeds or non-domesticated ancestors of the modern chicken (Liu et al., 2019). This is an even greater challenge for those who study non-model organisms which may require custom arrays, although there is support for cross-species applications such as the use of the Axiom 600k chicken array in several species of grouse (Minias et al. 2019).

Another limitation of microarrays that is more relevant to the study described in Chapter 6 is their bias toward common variants with relatively high minor allele frequencies even though rare variants have been demonstrated to contribute substantial fractions of complex disease heritability (Bomba et al., 2017). This issue is mitigated by the use of newer high-density microarrays, which can be used alongside whole-genome sequencing to impute low-frequency variants (Ros-Freixedes et al., 2020). However, many studies are still under-powered to detect significant effects of low-frequency variants especially if effects sizes are small (Bomba et al., 2017).

The GWA study described in this dissertation utilizes an NGS-based genotyping method called genotyping-by-sequencing (GBS), which involves constructing reduced

representation DNA libraries with restriction enzymes that target specific genomic sequences (Elshire et al., 2011). Compared to microarrays, some of the major advantages of this method are (1) the flexibility to target different areas of the genome depending on which restriction enzymes are used, (2) the ability to genotype without a pre-existing reference genome, and (3) the ability to lower costs by pooling samples and reducing genomic representation.

The low-depth genotyping-by-sequencing (GBS) method described in Chapter 6 (Dodds et al., 2015) has relatively high levels of missing data because it relies on a relatively low amount of sequence data, measured in sequence reads, for each individual. A reduction in the amount of sequence reads for an individual's genome is accomplished by reducing the percentage of a genome that is targeted for sequencing or by reducing the number of reads at each locus (average read depth). A lower read depth reduces our ability to confidently determine the true genotype at a given locus and requires special treatment in genotype calling.

The study described in Chapter 6 doesn't have an exceedingly low average read depth, but the read depth varies considerably from locus to locus. To accommodate this variation, a Bayesian genotype caller such as PolyRad (Clark et al., 2019) can be used to calculate the probability of each possible genotype informed by data other than just sequence reads (e.g. linkage disequilibrium and allele frequency). Genotype probabilities can then be converted to continuous genotype calls, which allow the uncertainty about a genotype to be reflected in the genotype call itself.

1.2 Association Testing

Mixed linear models (MLMs) are a highly popular method of testing for association in GWA studies because of their effectiveness in accounting for

relatedness among individuals (Zhou and Stephens, 2012). The inclusion of a random polygene effect with variance dependent on a kinship matrix reflecting genetic similarity across individuals eliminates the need for pedigree knowledge and mitigates the threat of spurious associations caused by cryptic relatedness and unknown admixture (Kang et al., 2008). A major challenge of MLMs, however, is the computational impracticality of explicitly accounting for pairwise relatedness with large sample sizes. To address this, several approximate methods have been developed to reduce computational time by, for example, using pre-estimated variance components or eigen decompositions of the genomic relatedness matrix (Kang et al., 2010; Zhang et al., 2010; Zhou and Stephens, 2012).

Mixed linear models are generally used to estimate additive genetic variation captured by markers in a dataset, but can also be utilized to estimate non-additive genetic variation such as dominance and gene-gene interactions, which can account for a high percentage of phenotypic variance. For example, in one GWA of daily weight gain in pigs, additive, dominance, and epistatic variance were found to contribute 35.7%, 5.6%, and 9.5% respectively to total phenotypic variance (Su et al., 2012). Non-additive genetic variance is also expected to be higher in a crossbred population, like the study population used in this dissertation, compared to a pure line due to greater heterozygosity and lower linkage disequilibrium (Su et al., 2012).

Non-additive genetic variance was not addressed in Chapter 6 of this dissertation, partly due to added complexity of working with continuous genotypes. Very few programs designed for association testing with MLMs permit the use of continuous genotypes. The tool used in Chapter 6, GCTA (Yang et al., 2011), required a patch to accommodate continuous genotypes and does not include functions to

estimate and partition dominant and epistatic variances. Additionally, dominance is more difficult to estimate with continuous genotypes because the genotype reflects both uncertainty as well as zygosity.

1.3 Interpretation of Results

Disease causing variants are generally not directly genotyped in GWA studies, which instead use a set of genetic variants, often single nucleotide polymorphisms (SNPs), distributed throughout the genome that serve as markers with known locations. A SNP with an allele state that is associated with the disease being studied may either be causal or highly correlated (in linkage disequilibrium; LD) with the causal allele (Hirschhorn and Daly, 2005). As was demonstrated by Fu et al. (Fu et al., 2015), crossbred broiler populations like the sample population studied throughout this thesis, have much lower LD than their pure line grandparents. This is because the selection that produces a purebred animal or plant acts as a bottleneck in genetic diversity, increasing the frequency of certain alleles at each locus that produce desirable traits and reducing or even eliminating other alleles. As a result, purebred populations have higher homozygosity than crossbred populations as well as higher LD and longer haplotype blocks, or sections of genome where a specific set of alleles is frequently found together.

The use of a 4-way crossbred population in this dissertation was intentional with regard to harnessing low LD for a higher resolution map of quantitative trait loci. In other words, significant SNPs are likely to be physically close to causal mutations. However, because LD is a very noisy statistic with large variation between genomic regions (Paigen and Petkov, 2010), the identification of candidate genes from genetic markers is sometimes an imprecise practice. Grouping SNPs into quantitative trait loci

is challenging for the same reason. It can be difficult to distinguish between multiple variants with smaller independent effects and a single variant of large effect that is in LD with numerous markers.

Complicating matters further, most variants identified in GWA studies explain only a small proportion of heritability. This phenomenon, often called "missing heritability" is true even in well-powered studies with large sample sizes. Rare variants, small effect sizes, non-additive effects, epigenetics, and genetic linkage have all been proposed as contributors to missing heritability, in addition to complications with phenotype measurement (Manolio et al., 2009). Wooden breast is a perfect example of the latter issue, because not only is it difficult to consistently measure disease severity but we also must question (1) if what we call wooden breast is truly a collection of several disorders or (2) if the distinction between wooden breast and white striping is a false dichotomy. With all of this in mind, it's important to realize that the GWA study described in Chapter 6 is just the beginning of our exploration of the genetic basis of wooden breast. The genetic architecture of such quantitative traits can be astoundingly complex, involving variation in thousands of genes interacting with the environment and each other. Every thrilling discovery just raises more questions to explore.

REFERENCES

Bomba, L., Walter, K. & Soranzo, N. The impact of rare and low-frequency genetic variants in common disease. Genome Biol 18, 77 (2017). https://doi.org/10.1186/s13059-017-1212-4

Bumgarner, Roger. "Overview of DNA microarrays: types, applications, and their future." Current protocols in molecular biology vol. Chapter 22 (2013): Unit 22.1. doi:10.1002/0471142727.mb2201s101

Clark, L. V., Lipka, A. E., and Sacks, E. J. (2019). polyRAD: Genotype Calling with Uncertainty from Sequencing Data in Polyploids and Diploids. Genes Genomes Genet. 9, 663–673. doi:10.1534/g3.118.200913.

Dodds, K. G., McEwan, J. C., Brauning, R., Anderson, R. M., Stijn, T. C., Kristjánsson, T., et al. (2015). Construction of relatedness matrices using genotyping-by-sequencing data. BMC Genomics 16, 1–15. doi:10.1186/s12864-015-2252-3.

Elshire RJ, Glaubitz JC, Sun Q, Poland JA, Kawamoto K, Buckler ES, et al. (2011) A Robust, Simple Genotyping-by-Sequencing (GBS) Approach for High Diversity Species. PLoS ONE 6(5): e19379. https://doi.org/10.1371/journal.pone.0019379

Fu, W., Dekkers, J. C. M., Lee, W. R., and Abasht, B. (2015). Linkage disequilibrium in crossbred and pure line chickens. *Genet. Sel. Evol.* 47, 1–12. doi:10.1186/s12711-015-0098-4.

Groenen, M.A., Megens, HJ., Zare, Y. et al. The development and characterization of a 60K SNP chip for chicken. BMC Genomics 12, 274 (2011). https://doi.org/10.1186/1471-2164-12-274

Hirschhorn, J., Daly, M. Genome-wide association studies for common diseases and complex traits. Nat Rev Genet 6, 95–108 (2005). https://doi.org/10.1038/nrg1521

Kang, H., Sul, J., Service, S. et al. Variance component model to account for sample structure in genome-wide association studies. Nat Genet 42, 348–354 (2010). https://doi.org/10.1038/ng.548

Kang, H.M., Zaitlen, N.A., Wade, C.M., Kirby, A., Heckerman, D., Daly, M.J., and Eskin, E. (2008). Efficient Control of Population Structure in Model Organism Association Mapping. Genetics 178,3: 1709–1723. https://doi.org/10.1534/genetics.107.080101

Kranis, A., Gheyas, A.A., Boschiero, C. et al. Development of a high density 600K SNP genotyping array for chicken. BMC Genomics 14, 59 (2013). https://doi.org/10.1186/1471-2164-14-59

Liu, R., Xing, S., Wang, J. et al. A new chicken 55K SNP genotyping array. BMC Genomics 20, 410 (2019). https://doi.org/10.1186/s12864-019-5736-8

Manolio, T., Collins, F., Cox, N. et al. Finding the missing heritability of complex diseases. Nature 461, 747–753 (2009). https://doi.org/10.1038/nature08494

Minias, P., Dunn, P.O., Whittingham, L.A. et al. Evaluation of a Chicken 600K SNP genotyping array in non-model species of grouse. Sci Rep 9, 6407 (2019). https://doi.org/10.1038/s41598-019-42885-5

Paigen, K., & Petkov, P. (2010). Mammalian recombination hot spots: properties, control and evolution. *Nature reviews. Genetics*, *11*(3), 221–233. https://doi.org/10.1038/nrg2712

Ros-Freixedes, R., Whalen, A., Chen, CY. et al. Accuracy of whole-genome sequence imputation using hybrid peeling in large pedigreed livestock populations. Genet Sel Evol 52, 17 (2020). https://doi.org/10.1186/s12711-020-00536-8

Su, G., Christensen, O. F., Ostersen, T., Henryon, M., and Lund, M. S. (2012). Estimating Additive and Non-Additive Genetic Variances and Predicting Genetic Merits Using Genome-Wide Dense Single Nucleotide Polymorphism Markers. *PLoS One* 7, 1–7. doi:10.1371/journal.pone.0045293.

Tam, V., Patel, N., Turcotte, M. et al. Benefits and limitations of genome-wide association studies. Nat Rev Genet 20, 467–484 (2019). https://doi.org/10.1038/s41576-019-0127-1

Yang, Jian et al. “GCTA: a tool for genome-wide complex trait analysis.” American journal of human genetics vol. 88,1 (2011): 76-82. doi:10.1016/j.ajhg.2010.11.011

Zhang, Z., Ersoz, E., Lai, CQ. et al. Mixed linear model approach adapted for genome-wide association studies. Nat Genet 42, 355–360 (2010). https://doi.org/10.1038/ng.546

Zhou, X., & Stephens, M. (2012). Genome-wide efficient mixed-model analysis for association studies. Nature genetics, 44(7), 821.

Chapter 2

GLUCOLIPOTOXICITY: A PROPOSED ETIOLOGY FOR WOODEN BREAST AND RELATED MYOPATHIES IN COMMERCIAL BROILER CHICKENS

(Juniper A. Lake & Behnam Abasht. *Frontiers in Physiology*, 11:169, (2020)).
https://www.frontiersin.org/articles/10.3389/fphys.2020.00169/full

2.1 Abstract

Wooden breast is one of several myopathies of fast-growing commercial broilers that has emerged as a consequence of intensive selection practices in the poultry breeding industry. Despite the substantial economic burden presented to broiler producers worldwide by wooden breast and related muscle disorders such as white striping, the genetic and etiological underpinnings of these diseases are still poorly understood. Here we propose a new hypothesis on the primary causes of wooden breast that implicates dysregulation of lipid and glucose metabolism. Our hypothesis addresses recent findings that have suggested etiologic similarities between wooden breast and type 2 diabetes despite their phenotypic disparities. Unlike in mammals, dysregulation of lipid and glucose metabolism is not accompanied by an increase in plasma glucose levels but generates a unique skeletal muscle phenotype, i.e. wooden breast, in chickens. We hypothesize that these phenotypic disparities result from a major difference in skeletal muscle glucose transport between birds and mammals, and that the wooden breast phenotype most closely resembles complications of diabetes in smooth and cardiac muscle of mammals. Additional basic research on wooden breast and related muscle disorders in commercial broiler

chickens is necessary and can be informative for poultry breeding and production as well as for human health and disease. To inform future studies, this paper reviews the current biological knowledge of wooden breast, outlines the major steps in its proposed pathogenesis, and examines how selection for production traits may have contributed to its prevalence.

2.2 Introduction

The last half century has witnessed remarkable gains in commercial broiler production characterized primarily by rapid growth, high feed efficiency, and high breast muscle yield (Havenstein et al., 2003a, 2003b). Alongside improvements to production traits, intense breeding programs and enhanced management practices may have elicited the emergence of several muscle disorders among fast-growing broiler strains. Myopathies such as wooden breast, white striping, spaghetti meat, and dorsal cranial myopathy significantly impact meat quality, causing substantial economic losses in the poultry industry (Zimermann et al., 2012; Kuttappan et al., 2016; Baldi et al., 2018; Zanetti et al., 2018). Speculation on the causes of these muscle disorders has focused largely on impaired oxygen supply, buildup of metabolic waste, and overstretching or compartmentalization of the muscle due to sustained rapid growth of skeletal muscle and consequent vascular marginalization (Kuttappan et al., 2013; Mudalal et al., 2015; Dalle Zotte et al., 2017; Lilburn et al., 2018). While each of these may well be a contributing factor, a critical analysis of the literature and findings in our laboratory has prompted us to submit a new hypothesis. Here we propose that dysregulation of lipid and glucose metabolism is an important underlying cause of wooden breast and related muscle disorders in commercial broiler chickens (Figure

2.1). Moreover, we suggest that there are substantial similarities in the mechanistic underpinnings of wooden breast in broiler chickens and type 2 diabetes in mammals.

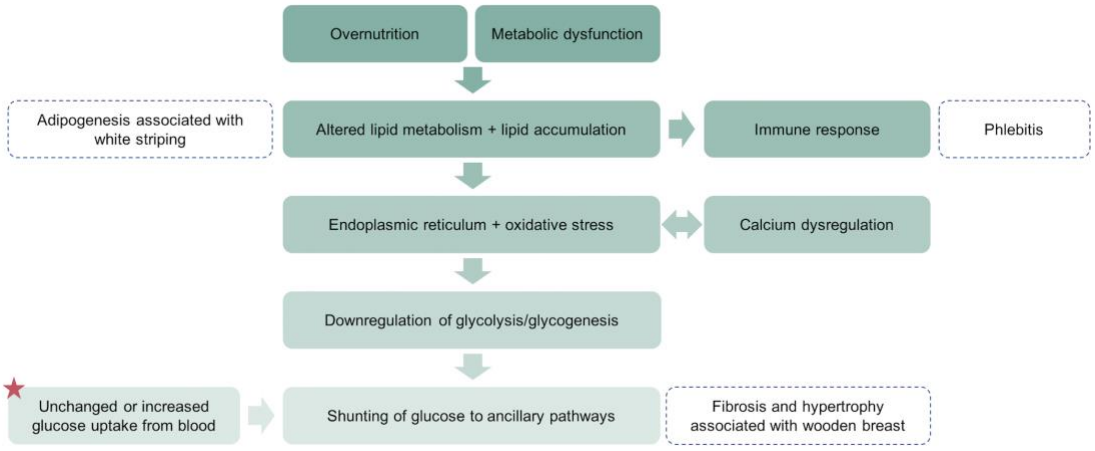

Figure 2.1: A simplified schematic representation of the proposed pathogenesis of wooden breast and white striping in the pectoralis major muscle.

A key difference between wooden breast in broilers and type 2 diabetes in mammals is the dependence on insulin-independent glucose transport in skeletal muscle of chickens. This results in unchanged or increased uptake of glucose from blood (star) even when glycolysis and glycogenesis are substantially downregulated and shunting of that glucose into alternative pathways that contribute to the wooden breast phenotype.

2.3 Lipid Accumulation in Wooden Breast Phenotype

Evidence of lipid accumulation (Papah et al., 2017) and altered lipid metabolism (Papah et al., 2018; Lake et al., 2019) early in the onset of wooden breast suggest that dysregulation of lipid metabolism is a key etiological feature of the myopathy. Lipid accumulation in the pectoralis major of wooden breast affected

chickens is evident at the molecular, microscopic, and macroscopic levels. Affected breast muscle has an overall higher percent composition of fat (Soglia et al., 2016), an altered fatty acid profile (Gratta et al., 2019), and is substantially more likely than unaffected fillets to exhibit signs of white striping, characterized by fatty white striations running parallel to the muscle fiber that are visible to the naked eye (Tasoniero et al., 2016; Dalle Zotte et al., 2017). Microscopic evidence of lipid accumulation and its associated pathological changes includes the presence of lipid droplets, lipogranulomas, and lipid-laden foam cells in the pectoralis major as early as the first week of age (Papah et al., 2017). At the molecular level, metabolomic profiling of 7-week-old birds shows that affected tissues have higher levels of multiple long chain fatty acids, including palmitate, palmitoleate, stearate, and oleate, as well as accumulation of various phospholipid and triglycerides catabolites (Abasht et al., 2016). Lipid accumulation is further supported by the upregulation of lipid metabolism genes in the pectoralis major of 2- and 3-week-old birds that were later diagnosed with wooden breast at 7 weeks of age (Papah et al., 2018; Lake et al., 2019). These genes include *fatty acid translocase* (*CD36*), *fatty acid binding protein 4* (*FABP4*), *lipoprotein lipase* (*LPL*), and *peroxisome proliferator-activated receptor gamma (PPARG)* among others (Lake et al., 2019). Such studies provide overwhelming evidence of altered lipid metabolism in the pectoralis major of wooden breast affected broilers starting in early phases of the disease.

Of the genes mentioned above, *LPL* stands out due to its encoded protein's key role as a metabolic gatekeeper in terms of partitioning circulating lipids among tissues (Wang and Eckel, 2009). The *LPL* gene encodes lipoprotein lipase, an enzyme that attaches to the surface of vascular endothelial cells and serves as the rate-limiting

catalyst for hydrolysis of triglycerides in two types of circulating lipoproteins – portomicrons/chylomicrons and very-low-density lipoproteins (VLDL) – providing non-esterified fatty acids and monoglycerides for use by surrounding tissues (Mead et al., 2002; Wang and Eckel, 2009). Regulation of LPL expression occurs in a tissue-specific manner and alterations to LPL levels in one tissue can affect systemic nutrient partitioning by reducing substrate availability to other tissues (Wang and Eckel, 2009). Increased expression of *LPL* is a consistent and early signal of the overprovision of lipids to the pectoralis major in affected birds. *LPL* is upregulated in 2- and 3-week-old broilers that later develop wooden breast (Papah et al., 2018; Lake et al., 2019), it has been proposed as a contributor to sex-linked differences in wooden breast incidence rate and severity (Brothers et al., 2019), and its increased expression in affected birds has been localized to the site where disease is first microscopically apparent – the endothelium of veins undergoing phlebitis (Papah and Abasht, 2019).

Lipid accumulation in the pectoralis major has been consistently linked to wooden breast, but the mechanism by which it may be involved in the myopathy has not been sufficiently explored. Papah et al. (2017) pointed out the resemblance of the lipid infiltration and phlebitis of wooden breast to atherosclerosis, although symptoms are restricted to the veins of affected broilers. It has also been suggested that increased expression of lipid metabolism genes in the early stages of wooden breast may signify a pathogenetic relationship with metabolic syndrome and type 2 diabetes in humans (Lake et al., 2019). Ectopic fat deposition and the resulting lipotoxicity, specifically in skeletal muscle, are known to be major metabolic risk factors for type 2 diabetes and related conditions (Rasouli et al., 2007), and we believe they play an important etiological role in wooden breast and similar muscle disorders. However, an important

missing link between lipid accumulation and other aspects of the wooden breast phenotype is the fate of glucose in the pectoralis major.

2.4 Lipotoxic Inhibition of Glycolysis and Glycogenesis

The pectoralis major of wooden breast affected birds exhibits signs of severely altered glucose metabolism, specifically inhibition of glycolysis. This is strongly supported by lower levels of glycolytic intermediates, such as glucose-6-phosphate and fructose-6-phosphate, and glycolytic end products, such as pyruvate and lactate, in affected birds (Abasht et al., 2016). Glycogen levels are also significantly lower (Abasht et al., 2016), which discounts the idea that increased synthesis of glycogen (glycogenesis) from glucose-6-phosphate or decreased degradation (such as glycogen storage disease) cause the reduction in glycolytic intermediates and end products. Inhibition of glycolysis is also supported by downregulation of the glycolytic enzyme *6-phosphofructo-2-kinase* (*PFKFB3*) (Mutryn et al., 2015a) as well as the isoform primarily expressed in skeletal muscle, PFKFB1 (unpublished data), in 7-week-old affected birds. In that study, *PFKFB3* and *PFKFB1* were the only detected HIF1-dependent gene that were downregulated rather than upregulated (Mutryn et al., 2015a). The suppression of glycolysis in affected birds is actually at odds with a common hypothesis that hypoxia resulting from breast muscle growth and vascular deficiency is the primary cause of wooden breast and other breast muscle disorders in modern broilers (Boerboom et al., 2018; Sihvo et al., 2018; Livingston et al., 2019a; Petracci et al., 2019). Hypoxia is widely known to stimulate glycolysis in lieu of more oxygen-demanding means of ATP production (Semenza et al., 1994). What must be determined, then, is the trigger for altered glucose metabolism as well as the fate of glucose that doesn't undergo glycolysis in the pectoralis major.

Reduced glucose uptake from plasma is an unlikely cause of reduced glycolysis as there is no difference in plasma glucose levels between affected and unaffected birds (Livingston et al., 2019a, 2019b) and expression of various glucose transporter genes is actually upregulated in the pectoralis major of affected birds (unpublished data). The liver has a major role in maintaining blood glucose levels, compensating for increased plasma glucose by synthesizing more hepatic glycogen (Hers, 1976). However, the livers of wooden breast affected birds also have lower glycogen content than livers of unaffected birds (Kawasaki et al., 2018). Although additional research on glucose uptake in wooden breast is required, this evidence suggests that glucose is taken up by the breast muscle, but not used for energy production or storage as fully as it is in unaffected birds.

We believe that the observed decrease in glycolytic flux is primarily a result of cellular stress responses to lipid accumulation in the pectoralis major. When lipids accumulate in cells and tissues that are not adequately equipped to metabolize or store them, such as liver and muscle, they can activate a broad range of cellular stress and immune responses such as toll-like receptor (TLR) signaling (Lee and Hwang, 2006), increased production of reactive oxygen species (ROS) (Goglia and Skulachev, 2003), endoplasmic reticulum stress, and the unfolded protein response (Volmer and Ron, 2015). These responses create deleterious effects, collectively referred to as lipotoxicity, and can destabilize metabolic functions such as glycolysis. In wooden breast, we believe oxidative stress is the key inhibitor of glycolysis based on downregulation of the glycolytic gene *PFKFB3* in affected broilers (Mutryn et al., 2015a). *PFKFB3* encodes the enzyme that catalyzes the conversion of fructose-6-phosphate to fructose 2,6-bisphosphate, which itself is a potent activator of glycolysis

via allosteric regulation of phosphofructokinase 1. *PFKFB3* is also considered a regulator of oxidative stress because of its ability to sense and respond to redox homeostasis, shunting glucose to the pentose phosphate pathway in response to elevated levels of ROS (Seo and Lee, 2014; Yamamoto et al., 2014).

In mammals, lipotoxic inhibition of glucose oxidation in skeletal muscle and adipose tissue is accompanied by downregulation of insulin-sensitive glucose transporter 4 (GLUT4), resulting in the insulin resistance and high plasma glucose levels that characterize type 2 diabetes (Randle et al., 1965; Groop and Ferrannini, 1993). Reduced GLUT4-mediated glucose transport is especially impactful in skeletal muscle, which is the major site of glucose uptake in the postprandial state (DeFronzo and Tripathy, 2009). This process has been demonstrated in a study of muscle-specific overexpression of LPL in transgenic mice (Kim et al., 2001). In that experiment, overexpression of muscle-specific LPL caused major metabolic changes in skeletal muscle, including a 3-fold increase in triglyceride content, an increased number of lipid droplets around the mitochondrial region, a 52% decrease in insulin-stimulated glucose uptake, a 48% decrease in glycolysis, and an 88% decrease in glycogen synthesis (Kim et al., 2001). The key difference between this mouse model of type 2 diabetes and the wooden breast phenotype is that wooden breast is not associated with a significant change in plasma glucose levels (Livingston et al., 2019a, 2019b). However, this disparity is likely a result of differences between avian and mammalian glucose transport and insulin signaling in skeletal muscle.

2.5 Insulin-Independent Glucose Transport in Chicken Skeletal Muscle

The polarity and size of glucose molecules prevent their transport across lipid membranes by simple diffusion (Navale and Paranjape, 2016). Two families of

glucose transporters, sodium-glucose linked transporters (SGLTs) and facilitated glucose transporters (GLUTs), control the movement of glucose into and out of cells (Navale and Paranjape, 2016) and thus play an important role in glucose homeostasis and regulation of blood glucose levels. In mammals, glucose transport in skeletal muscle relies primarily on the activity of GLUT1 and GLUT4 (Klip et al., 1996). GLUT1 is preferentially restricted to the cell surface and provides insulin-independent basal levels of glucose while GLUT4 is sequestered in intracellular vesicles and rapidly translocated to the cell surface in response to insulin, exercise, or hypoxia (Klip et al., 1996; Shepherd and Kahn, 1999). Impairment of the insulin signaling cascade in skeletal muscle of mammals, which can occur in response to chronic high-fat conditions (Zierath et al., 1997), reduces the insulin-stimulated translocation of GLUT4 to the plasma membrane. Pancreatic β-cells compensate for a reduced insulin response by increasing secretion of insulin, but eventually this becomes insufficient and reduced GLUT4 translocation causes accumulation of glucose in the blood.

Avian glucose transport and insulin signaling are not as well characterized as those of mammals (Braun and Sweazea, 2008), but it is well known that chickens are naturally hyperglycemic and insulin resistant, possessing circulating insulin concentrations approximately equal to those of mammals but extremely high plasma glucose levels (Akiba et al., 1999; Tokushima et al., 2005). Insulin resistance in chickens has been partly attributed to hyperactivity of insulin receptor signaling in skeletal muscle, where phosphatidylinositol 3-kinase (PI3K) activity, a key component of the insulin signaling pathway, was found to be 30 times higher in chickens than in rats (Dupont et al., 2004). In fact, insulin privation via immuno-neutralization was found to have no effect on PI3K activity in chicken skeletal muscle, although it

resulted in altered expression of major metabolic transcription factors in both the liver and skeletal muscle (Godet et al., 2008). Another major contributor is perhaps the intrinsic lack of any GLUT4 homologues in the chicken genome and resulting predominance of insulin-independent glucose transport. An attempt to detect GLUT4 homologues in various tissues of broiler chickens found that GLUT4 cDNA was completely undetectable in any of the 19 chicken tissues that were tested, which included the pectoralis major (Seki et al., 2003). The intrinsic lack of GLUT4 and low expression levels of other common glucose transporters (GLUT1, GLUT2, GLUT3, and GLUT8) in skeletal muscle of broilers (Kono et al., 2005) suggests that glucose transport is regulated differently in chickens than it is in mammals and may primarily be insulin-independent.

The reliance on insulin-independent glucose transporters in chicken skeletal muscle may explain why there are no mammalian skeletal muscle disorders that are equivalent to wooden breast. Rather, the wooden breast phenotype shares striking similarities with various complications of type 2 diabetes in smooth muscle and cardiac muscle, such as atherosclerosis, diabetic cardiomyopathy and myocardial fibrosis, diabetic nephropathy, pulmonary fibrosis, diabetic retinopathy, and non-alcoholic fatty liver disease. These diseases frequently involve lipid accumulation, inflammation, oxidative stress, calcium dysregulation, endoplasmic reticulum stress, hypoxia, hypertrophy, and fibrosis—features that have also been well-documented in wooden breast. The greater role of insulin-independent glucose transport in cardiac and smooth muscle allows glucose uptake even when glycolysis and glycogenesis are impaired. The importance of insulin-insensitive glucose transport in development of diabetic retinopathy (Kumagai, 1999), atherosclerosis (Wall et al., 2018), diabetic

nephropathy (Brosius and Heilig, 2005), pulmonary fibrosis (Cho et al., 2017), diabetic myocardial fibrosis (Asbun and Villarreal, 2006; Gorski et al., 2019) and non-alcoholic fatty liver disease (Nanji et al., 1995) has been demonstrated and is in support of our hypothesis that wooden breast shares substantial etiological factors with type 2 diabetes in mammals.

2.6 Pathological Shunting of Glucose to Ancillary Pathways

The suppression of glycolysis and glycogenesis concurrent with unchanged or increased uptake of glucose from blood results in increased flux of glucose through alternative metabolic pathways (Fantus et al., 2006), including the pentose phosphate, glucuronic acid, hexosamine biosynthesis, and aldose reductase (polyol) pathways. There is evidence that all of these pathways are upregulated in affected birds (Abasht et al., 2016; Papah et al., 2018).

Glucose that is phosphorylated to glucose-6-phosphate can directly enter both the pentose phosphate pathway and the glucuronic acid pathway. In addition to generating carbon skeletons and ribose 5-phosphate, a precursor to nucleotide synthesis, the pentose phosphate pathway is a major source of NADPH, the main reductant that drives free radical detoxification and anabolic growth (Kruger and Von Schaewen, 2003). Accumulation of pentose phosphate pathway intermediates 6-phosphogluconate and sedoheptulose 7-phosphate support the upregulation of this pathway in 7-week-old affected birds (Abasht et al., 2016). Glucose-6-phosphate is also utilized to produce glucuronic acid, a precursor to ascorbic acid and a building block of proteoglycans, glycosaminoglycans, and glycolipids. Elevated levels of ascorbate and UDP-glucuronate in affected birds suggests that this pathway is upregulated as well (Abasht et al., 2016).

Glucose-6-phosphate can also be converted to fructose-6-phosphate and consumed in the hexosamine biosynthesis pathway. The hexosamine biosynthesis pathway is responsible for production of uridine diphosphate N-acetylglucosamine (UDP-GlcNAc), a nucleotide sugar and coenzyme used for protein glycosylation and the synthesis of glycosaminoglycans, proteoglycans, and glycolipids (Fantus et al., 2006). The gene encoding this pathway's rate-limiting enzyme, glutamine-fructose-6-phosphate transaminase 2 (GFPT2), was found to be upregulated in 3-week-old broilers affected by wooden breast (Papah et al., 2018). In fact, three of the four genes involved in the hexosamine biosynthesis pathway – *GFPT2*, *phosphoglucomutase 3* (*PGM3*), and *UDP-N-acteylglucosamine pyrophosphorylase 1* (*UAP1*) – show increased expression in the pectoralis major of high-feed-efficiency broilers, which are more susceptible to wooden breast than those with low feed efficiency (Abasht et al., 2019). In agreement, affected birds have higher levels of hexosamine biosynthesis pathway intermediates isobar UDP-acetylglucosamine and UDP-acetylgalactosamine at 7 weeks of age (Abasht et al., 2016). Increased production of proteoglycans is also supported by Clark and Velleman (Clark and Velleman, 2017), who found greater RNA expression of *decorin* in the pectoralis major of affected birds. The protein encoded by this gene is a small leucine-rich proteoglycan that regulates collagen cross-linking, although it is unclear if increased collagen cross-linking is a universal feature of the wooden breast phenotype (Velleman et al., 2017; Baldi et al., 2019). Proteoglycans and glycosaminoglycans are important components of the extracellular environment and increased production of them is associated with extensive remodeling of the extracellular matrix.

Excess glucose is also consumed in the polyol pathway, a two-step process that converts glucose first to sorbitol and then to fructose (Yan, 2018). Upregulation of the polyol pathway, specifically its first step, in wooden breast and white striping is supported by an accumulation of sorbitol in the pectoralis major (Abasht et al., 2016; Boerboom et al., 2018). One notable effect of polyol pathway stimulation is the induction of collagen synthesis (Bleyer et al., 1994; Ha et al., 1997) due at least in part to transcriptional activation of transforming growth factor-β (TGF- β) (Ishii et al., 1998; Han et al., 1999; Tokudome et al., 2004). All three isoforms of TGF-β are considered important regulators of inflammation, extracellular matrix protein deposition, and fibrosis, and altered activity of TGF-β proteins is known to contribute to various fibroproliferative disorders in humans (Pohlers et al., 2009). Increased expression of *transforming growth factor β 3* (*TGFB3*) in the pectoralis major muscle of affected birds at 7 weeks (Mutryn et al., 2015a) may represent a link between altered glucose metabolism and increased collagen production in wooden breast, the latter of which is widely considered to be an important feature of the myopathy contributing to the characteristic firmness of the pectoralis major (Sihvo et al., 2014; Soglia et al., 2016; Papah et al., 2017).

Finally, glucose can be used in the production of advanced glycation end products (Fantus et al., 2006). Advanced glycation end products are proteins or lipids that become glycated as a result of exposure to sugars and can have numerous pathological effects, such as induction of cytokine production, increased vascular permeability and inflammation, inhibition of vascular dilation, and enhanced oxidative stress (Basta et al., 2004). These effects are consistent with current knowledge of

wooden breast, although altered production of advanced glycation end products has not yet been reported.

Increased flux of glucose through these alternative pathways (Figure 2.2) is a pathological manifestation of altered glucose utilization, likely resulting from reduced glycolysis and glycogenesis alongside unchanged or increased import of glucose from the blood. This process is often referred to as glucose toxicity and is considered a key component of pancreatic β-cell dysfunction, insulin resistance, and chronic complications of diabetes such as diabetic neuropathy, retinopathy, and nephropathy in mammals.

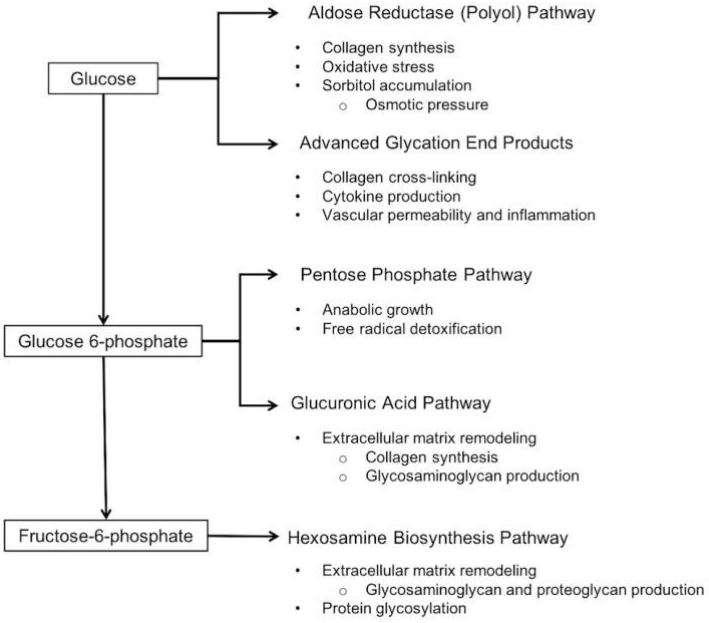

Figure 2.2: Altered carbohydrate metabolism in wooden breast and relevant effects of each pathway.

Wooden breast is associated with a reduced flux of glucose through glycolytic and glycogenic pathways and shunting of glucose into ancillary pathways, including the aldose reductase, pentose phosphate, glucuronic acid, and hexosamine biosynthesis pathways. It has not yet been demonstrated whether or not wooden breast also involves increased synthesis of advanced glycation end products.

2.7 Disruption of Redox Homeostasis and Oxidative Stress

Oxidative stress occurs when the production and accumulation of ROS become unbalanced with an organism's ability to detoxify reactive intermediates and can lead to cell and tissue damage. Broiler chickens show signs of greater oxidative stress in the pectoralis major than layers (Zahoor et al., 2017) and broilers with high feed efficiency have greater oxidative stress response in the breast muscle compared to those with low feed efficiency (Zhou et al., 2015). In wooden breast, affected broilers have metabolite profiles indicative of altered redox homeostasis involving higher free radical exposure than unaffected birds (Abasht et al., 2016). Similarly, various genes involved in oxidative stress response are upregulated in wooden breast birds at both 3 weeks and 7 weeks of age (Abasht et al., 2015; Mutryn et al., 2015a; Papah et al., 2018).

As previously discussed, lipotoxicity is likely a major contributor to oxidative stress in the early stages of wooden breast. Fatty acids are particularly prone to ROS-induced oxidative damage via a process called lipid peroxidation, which proceeds in an aggressively self-propagating chain reaction that can induce damage to proteins and DNA (Goglia and Skulachev, 2003; Schrauwen, 2007). When the supply of fatty acids overwhelms the storage and oxidative capacity of cells, which is more likely in mitochondria-scarce, type IIB pectoralis major muscle fibers, they accumulate in the cell and around the mitochondria where they can have extremely damaging effects

(Schrauwen and Hesselink, 2004; Anderson and Neufer, 2006). Fatty acid transport into the mitochondria is generally regulated by the enzyme carnitine palmitoyltransferase 1 (Schrauwen, 2007). Lower levels of free carnitine in the pectoralis major of affected birds (Abasht et al., 2016) may reflect increased transport of long-chain fatty acids into the mitochondria by carnitine palmitoyltransferase 1. Fatty acids and fatty acid derivatives inside the mitochondrial matrix are extremely vulnerable to ROS-induced lipid peroxidation and can cause substantial mitochondrial damage due to the complex nature of the matrix space (Goglia and Skulachev, 2003). Oxidative damage to the mitochondria due to fatty acid accumulation may be attenuated by mitochondrial energy uncoupling, mediated largely by uncoupling protein 3 (UCP3), an enzyme activated by lipid peroxides (Goglia and Skulachev, 2003; Rousset et al., 2004; Schrauwen and Hesselink, 2004). However, *UCP3* was found to be downregulated in wooden breast affected birds at 3 weeks of age (Papah et al., 2018), suggesting an impaired uncoupling response. High coupling efficiency in an environment with severe lipid accumulation would directly contribute to ROS production and lipid peroxidation and also allow for increased mitochondrial damage by ROS inside the mitochondrial matrix.

After initial derangement of redox homeostasis, multiple factors can contribute to a positive feedback loop of oxidative stress. Most ROS are generated as normal by-products during mitochondrial electron transport, specifically at respiratory complexes I and III of the oxidative phosphorylation pathway (Rousset et al., 2004), and are prevented from reaching damaging levels by various cellular defenses such as superoxide dismutase and glutathione peroxidase (Anderson and Neufer, 2006). Potential genetic variation in antioxidant response may be a key contributor to wooden

breast susceptibility in broilers, as altered redox homeostasis can inhibit the activity of anti-oxidant enzymes and increase ROS production at mitochondrial respiratory complex I (Yabe-Nishimura, 1998; Chung, 2004; Yan, 2018). In diabetes, the polyol pathway is believed to play a critical role in oxidative stress and vascular damage due to its derangement of redox homeostasis (Yabe-Nishimura, 1998; Chung, 2004; Yan, 2018). The first of two reactions in the pathway is conversion of glucose and NADPH to sorbitol and NADP+ by aldose reductase and is suggested to be upregulated in the pectoralis major of affected birds based on the accumulation of sorbitol (Abasht et al., 2016; Boerboom et al., 2018). Mutryn et al. (2015) proposed NADPH-oxidase activity as another contributor to altered NADP+/NADPH homeostasis related to inflammatory and immune responses. The consumption of NADPH by aldose reductase and NADPH-oxidase reduces the activity of other NADPH-dependent enzymes such as glutathione reductase, an important anti-oxidative enzyme, and nitric oxide synthase, which produces nitric oxide from L-arginine (Yabe-Nishimura, 1998). Nitric oxide is a soluble gas produced by endothelial cells that has many functions, including regulation of vascular homeostasis, vasodilation, angiogenesis, endothelial cell growth, and protection of vessels from injury (Tousoulis et al., 2012).

Disruption of NAD+/NADH homeostasis can also increase ROS production, wherein overproduction of the electron donor NADH increases activity of NADH-dependent mitochondrial respiratory complex I (Hirst et al., 2008). The conversion of sorbitol and NAD+ to fructose and NADH by sorbitol dehydrogenase (SORD) in the second reaction of the polyol pathway is one potential contributor to this imbalance; however, this is unlikely in wooden breast as decreased *SORD* expression (unpublished data) and greater accumulation of sorbitol (Abasht et al., 2016) in

affected birds provide testimony for reduced SORD activity. Rather, potentially higher levels of NADH in wooden breast may be partly attributed to lower activity of the glycerol-3-phosphate shuttle (Abasht et al., 2019) or lower activity of lactate dehydrogenase. An imbalance of cytosolic NAD+/NADH would not only increase ROS production but could also limit NAD+ supply to key metabolic enzymes required for sustaining glycolysis and the citric acid cycle. Free NAD+ is a cofactor for glyceraldehyde 3-phosphate dehydrogenase and oxoglutarate dehydrogenase, both of which are downregulated in affected birds according to differential expression analysis (Abasht et al., 2015; Papah et al., 2018). Free NAD+ is also a cofactor for the pyruvate dehydrogenase complex which serves as a link between glycolysis and the citric acid cycle (Yan, 2018).

2.8 Calcium cycling abnormalities

Maintenance of intracellular Ca^{2+} pools is fundamental to generating the Ca^{2+} signals required for numerous cellular processes (Berridge et al., 2003). The pectoralis major of wooden breast affected birds exhibits upregulation of genes encoding both parvalbumin and sarcoplasmic/endoplasmic reticulum calcium ATPase (SERCA) 2 (Mutryn et al., 2015a) as well as increased abundance of SERCA protein (Soglia et al., 2016). Both proteins are involved in sequestering calcium and their upregulation constitutes evidence of a compensatory response to increased intracellular calcium in muscle cells (Mutryn et al., 2015a). Parvalbumin is a Ca^{2+}-binding protein that functions as a calcium buffer and SERCAs are intracellular pumps located in the sarcoplasmic/endoplasmic reticulum (SR) membranes that use ATP to translocate Ca^{2+} from the cytoplasm to the SR lumen (Berridge et al., 2003). Evidence of dysregulated calcium homeostasis and impaired excitation-contraction coupling is also present in 2-

and 3-week-old broilers, prior to manifestation of wooden breast phenotype at market age (Papah et al., 2018; Lake et al., 2019). Increased levels of calcium in the pectoralis major of birds affected by white striping, wooden breast, or both (Sandercock et al., 2009; Tasoniero et al., 2016; Zambonelli et al., 2016) suggests that myocellular uptake of Ca^{2+} from extracellular spaces is affected in addition to dysregulation of intracellular calcium pools.

It is unclear what provides the primary stimulus for calcium dysregulation in wooden breast and, unfortunately, there is no consensus regarding a single cause of altered calcium cycling in diabetes despite extensive research. However, one popular hypothesis contends that chronic exposure to excessive nutrients, specifically glucose and lipids, in tissues unequipped to fully metabolize, store, or dispose of them can initiate SR and mitochondrial stress that result in disruption of calcium homeostasis (Arruda and Hotamisligil, 2015). At least three mechanisms can aid in understanding this process: (1) fatty acids and ROS stimulate release of Ca^{2+} from the SR and inhibit removal of Ca^{2+} from the cytosol, (2) formation of the mitochondrial permeability transition pore and mitochondrial depolarization cause release of Ca^{2+} from the mitochondria, and (3) depolarization of the plasma membrane causes an influx of Ca^{2+} from extracellular spaces. The SR lumen serves as the most important Ca^{2+} store in the cell (Arruda and Hotamisligil, 2015), but an excess of fatty acids, fatty acid derivatives, and ROS can cause release of Ca^{2+} from the SR lumen by activating ryanodine and inositol trisphosphate (IP_3)-sensitive calcium channels (Cheah, 1981; Ursini et al., 2004; Berezhnov et al., 2008; Wei et al., 2009). Certain types of fatty acids can also inhibit SERCA activity, preventing calcium removal from the cytosol (Berezhnov et al., 2008; Fu et al., 2011). Fluxes in intracellular calcium can be

buffered by increased calcium uptake in the mitochondria, where Ca^{2+} can elevate ATP production (Berridge et al., 2003). However, excess mitochondrial Ca^{2+} can sensitize the mitochondrial permeability transition pore, leading to membrane depolarization and the rapid release of Ca^{2+} into the cytosol (Gunter et al., 1994; Berezhnov et al., 2008). High concentrations of long-chain fatty acids could also stimulate formation of the mitochondrial permeability transition pore (Penzo et al., 2002).

Calcium released from internal stores in the SR and mitochondria cannot explain why the pectoralis major of wooden breast birds has an increased percent composition of Ca^{2+}. Dysregulation of cation homeostasis that extends beyond Ca^{2+} in affected birds provides evidence that an influx of Ca^{2+} into the cytoplasm from extracellular spaces involves cell membrane depolarization. Specifically, affected birds show higher sodium and lower magnesium and phosphorus in the pectoralis major as well as higher blood potassium levels (Zambonelli et al., 2016; Livingston et al., 2019b). At resting condition, the concentration of K^+ is higher inside the cell while the concentration of Na^+ and Ca^{2+} is higher outside the cell (Bahar et al., 2016), but the opening of voltage-gated calcium and sodium channels during membrane depolarization results in the rapid influx of Ca^{2+} and Na^+ from extracellular spaces (Bahar et al., 2016). The subsequent efflux of K^+ through voltage-dependent and voltage-independent channels allows repolarization of the membrane (Bahar et al., 2016). Calcium influx in wooden breast might be induced by certain types of fatty acids (Huang et al., 2006), by oxidative damage to the cell membrane (Ursini et al., 2004), or by the gradient-dependent activity of Na^+/Ca^{2+} exchangers that exchange three moles of Na^+ for one mole of Ca^{2+} (Berridge et al., 2003). Opening of voltage

gated calcium channels can exacerbate the release of calcium from endoplasmic reticulum stores in a process called calcium-induced calcium release (Endo, 2009).

One notable effect of altered calcium cycling in skeletal muscle, specifically of increased ATP-dependent SERCA activity, is a substantial increase in oxygen consumption and concurrent elevation of resting metabolic rate (Smith et al., 2013). Disruption of calcium homeostasis is potentially a major contributor to the venous hypercapnia, venous hypoxemia, and muscular hypoxia of the pectoralis major that have been documented in wooden breast affected broilers (Mutryn et al., 2015a; Livingston et al., 2019a, 2019b). Other effects of calcium dysregulation include mitochondrial damage (Orrenius et al., 2015), aberrant excitation/contraction signaling (Berridge et al., 2003), chronic SR stress (Fu et al., 2011), stimulation of skeletal muscle growth (Ermak and Davies, 2001), calcium-dependent proteolysis (Yin et al., 2013), and ultimately cell death (Hajnóczky et al., 2006). As a major site of post-translational protein modification, the SR is crucial to producing functional proteins. Calcium-dependent proteolysis and SR stress could contribute to the lower protein content and lower water holding capacity of wooden breast fillets due to their effects on protein degradation and protein production.

Dysregulation of calcium signaling can also induce expression of genes encoding myoglobin and slow muscle fiber type proteins, a feature of wooden breast discovered through differential expression analysis (Mutryn et al., 2015a) and confirmed with RNA in situ hybridization (RNA ISH) (Papah and Abasht, 2019). Expression of myoglobin and other muscle-specific genes is regulated by a synergistic interaction between transcription factors in the nuclear factor of activated t cells (NFAT) and myocyte enhancer factor-2 (MEF-2) families (Chin et al., 1998).

Transcriptional activation of NFAT and MEF-2 is mediated by calcineurin, a calcium-activated phosphatase, such that calcium fluxes and intracellular concentrations will ultimately determine the fiber type composition within a specific skeletal muscle (Chin et al., 1998). Lipid supplementation and hypoxic conditions have also been demonstrated to stimulate myoglobin expression, possibly through calcium-independent pathways (De Miranda et al., 2012).

2.9 Venous Inflammation and Vascular Permeability

Venous and perivascular inflammation and lipid accumulation are the first microscopic signs of wooden breast, potentially contributing to the edema, petechial hemorrhages, and tissue damage that are macroscopically apparent in late stages of the disease (Papah et al., 2017). It has been noted that these symptoms resemble atherosclerosis in humans (Papah et al., 2017), a condition closely linked to diabetes mellitus that consists of chronic inflammation induced by excessive lipid accumulation (Li et al., 2014). The upregulation of genes associated with vascular disease in 3-week-old broilers that later develop wooden breast (Papah et al., 2018) corroborates this hypothesis, but fails to explain why vascular inflammation is limited to veins. Recent work using RNA ISH to localize expression of a selection of genes in affected pectoralis major muscle provides an important clue. In that study, higher LPL expression was found in the veins of affected breast muscle and not the arteries (Papah and Abasht, 2019), suggesting a causal link between venous and perivascular lipid accumulation and the inflammatory response. This connection between increased LPL activity and inflammation has been thoroughly studied in the context of atherosclerosis.

The participation of LPL in the pathogenesis of atherosclerosis is two-fold: it mediates both the increased hydrolysis of lipoprotein triglycerides as well as the retention of lipoprotein remnants. High LPL activity increases local hydrolysis of triglycerides in portomicrons and VLDL, which produces free fatty acids, portomicron remnants, intermediate-density lipoproteins, and low-density lipoproteins (Alvarenga et al., 2011). Elevated levels of fatty acids and lipoprotein remnants cause damage to vessels as they trigger an inflammatory response, induce endothelial cell apoptosis, and increase endothelial permeability (Toborek et al., 2002; Eiselein et al., 2007; Rocha et al., 2016). A critical element of the inflammatory response caused by fatty acids is the activation of TLRs in the presence of high glucose (Lee and Hwang, 2006; Dasu and Jialal, 2010). TLR activation initiates an inflammatory cascade that includes the release of pro-inflammatory cytokines and cell adhesion molecules as well as T cell activation and the rapid differentiation of monocytes into macrophages (Krutzik et al., 2005). In wooden breast affected birds, *toll-like receptor 2 type 2 precursor* (*TLR2-2*) was one of the top 30 genes identified as a biomarker of wooden breast severity, with significant elevation in moderately-affected birds compared to unaffected or severely-affected birds (Abasht et al., 2015). The author suggested that this expression pattern may be indicative of the progression of the disease involving regulation by some negative feedback mechanism. If disease severity and disease progression are considered more or less equivalent, a similar pattern can be seen with lipid metabolism genes, which are generally upregulated in 2- and 3-week-old birds but relatively unchanged or downregulated in 7-week-old birds (Mutryn et al., 2015a; Papah et al., 2018; Papah and Abasht, 2019). Due to the apparent coupling of lipid

metabolism and venous inflammation, negative feedback regulation of lipid metabolism could be associated with a reduction in the innate immune response.

Endothelial cell damage and apoptosis due to increased lipoprotein metabolism increases the permeability of the endothelium and triggers leukocyte adhesion and transmigration into the vessel wall (Aghajanian et al., 2008). Lipoprotein remnants, which normally enter back into circulation to be cleared by the liver (Alvarenga et al., 2011), can then diffuse into the tunica intima where LPL mediates binding between remnant particles and proteoglycans in the sub-endothelial extracellular matrix (Olin et al., 1999). The subsequent activation of extracellular matrix proteins such as matrix metalloproteinases can elicit remodeling of the extracellular matrix (Amin et al., 2017), a process that is a well-substantiated in the wooden breast pathogenesis (Mutryn et al., 2015a; Papah et al., 2018). LPL-mediated bridging normally occurs between lipoprotein remnants and heparan sulfate proteoglycans on cell surfaces before lipoproteins undergo hydrolysis (Olin et al., 1999). Increased retention of lipoprotein remnants in the extracellular matrix and on cell surfaces increases the likelihood that they will be modified (e.g. oxidized) or taken up by scavenging macrophages to form foam cells, triggering further inflammatory reactions (Botham et al., 2007). The pro-atherosclerotic role of both active and inactive LPL has been demonstrated in mice (Wang et al., 2007), suggesting that both the hydrolysis and bridging functions of LPL are important.

2.10 Broiler Selection and Wooden Breast

Consolidation of poultry breeding and intense selection for production traits have undoubtedly played an oversized role in the rise of muscle disorders such as wooden breast, white striping, and spaghetti meat among commercial broilers. Even

without completely understanding the genetic architectures underlying these traits, it is possible to speculate how selection for specific performance metrics might increase the predisposition of meat-type chickens to these myopathies. Much of this speculation can be framed in the context of supply and demand of nutrients in the pectoralis major muscle. Juvenile growth rate, which has increased substantially since the 1950s independent of improvements to feed formulation (Havenstein et al., 2003b) and which is correlated with wooden breast severity, represents a major component of the supply side of this equation. The rapid growth rate of modern broilers reflects increased delivery of nutrients to the whole body, stemming from some combination of greater appetite, suppressed satiety (Barbato, 1994), as well as improved digestion and absorption in the digestive system (Smith et al., 1990).

Selection for feed efficiency has also raised digestive and absorptive capacity but may not increase the overall supply of nutrients to the body as increased energy absorption from feed is at least partly offset by reduced feed consumption. A larger effect of using feed efficiency as a major selection criterion relates to its correlation with fat distribution and blood lipid levels (Griffin et al., 1989; Zhuo et al., 2015). Unlike selection for juvenile growth rate, which is accompanied by increased fat deposition in adipose tissue depots, selection for increased feed efficiency is accompanied by reduced fat deposition in adipose tissue depots (Abasht et al., 2020). This reflects altered nutrient partitioning in high feed efficiency birds which is likely multifaceted, involving changes to metabolic processes in several organs such as reduced adipogenesis in abdominal fat, reduced lipogenesis in the liver, and increased lipoprotein triglyceride hydrolysis in skeletal muscle. Regardless of the specific biological mechanisms, there is evidence that improvements to such performance traits

are associated with a shifting of fat metabolism away from the liver and normal adipose depots toward skeletal muscle (Griffin et al., 1989; Larkina et al., 2010; Zhuo et al., 2015). In commercial broiler chickens, selection for large breast muscle partitions more nutrients toward the pectoralis major, which may be particularly susceptible to metabolic perturbations due to its primary composition of type IIB glycolytic muscle fibers (Anderson and Neufer, 2006).

Selection for feed efficiency has also raised digestive and absorptive capacity but may not increase the overall supply of nutrients to the body as increased energy absorption from feed is at least partly offset by reduced feed consumption. A larger effect of using feed efficiency as a major selection criterion relates to its correlation with fat distribution and blood lipid levels (Griffin et al., 1989; Zhuo et al., 2015). Unlike selection for juvenile growth rate, which is accompanied by increased fat deposition in adipose tissue depots, selection for increased feed efficiency is accompanied by reduced fat deposition in adipose tissue depots (Abasht et al., 2020). This reflects altered nutrient partitioning in high feed efficiency birds which is likely multifaceted, involving changes to metabolic processes in several organs such as reduced adipogenesis in abdominal fat, reduced lipogenesis in the liver, and increased lipoprotein triglyceride hydrolysis in skeletal muscle. Regardless of the specific biological mechanisms, there is evidence that improvements to such performance traits are associated with a shifting of fat metabolism away from the liver and normal adipose depots toward skeletal muscle (Griffin et al., 1989; Larkina et al., 2010; Zhuo et al., 2015). In commercial broiler chickens, selection for large breast muscle partitions more nutrients toward the pectoralis major, which may be particularly

susceptible to metabolic perturbations due to its primary composition of type IIB glycolytic muscle fibers (Anderson and Neufer, 2006).

2.11 Concluding Remarks

We believe that the wooden breast phenotype in commercial broilers is a manifestation of lipotoxicity and glucotoxicity resulting from the chronic oversupply of both lipids and carbohydrates to the pectoralis major and also the disruption of normal lipid and glucose metabolism. Dependence on insulin-independent glucose transport in the skeletal muscle of chickens causes lipid accumulation in the pectoralis major to be accompanied by unchanged or increased uptake of glucose, causing metabolic and structural alterations that closely resemble complications of diabetes in smooth and cardiac muscle of mammals. In addition to improving our understanding of the etiology and pathogenesis of wooden breast and related myopathies, this hypothesis supports the use of these muscle disorders as models of human metabolic diseases.

2.12 Acknowledgements

The authors wish to thank Dr. Erin Seifert and Dr. Nishanth E. Sunny for their comments and support regarding the manuscript.

REFERENCES

Abasht, B., Fu, W., Mutryn, M. F., Brannick, E. M., and Lee, W. R. (2015). Identification of gene expression biomarkers associated with severity of Wooden Breast disease in broiler chickens. in Proceeding of XXII European symposium on the quality of poultry meat (Nantes, France).

Abasht, B., Mignon-Grasteau, S., Bottje, W., and Lake, J. (2020). "Genetics and genomics of feed utilization efficiency traits in poultry species," in Advances in Poultry Genetics and Genomics, eds. S. E. Aggrey, H. Zhou, M. Tixier-Boichard, and D. D. Rhoads (Burleigh Dodds Science Publishing).

Abasht, B., Mutryn, M. F., Michalek, R. D., and Lee, W. R. (2016). Oxidative stress and metabolic perturbations in wooden breast disorder in chickens. PLoS One 11, 1–16. doi:10.1371/journal.pone.0153750.

Abasht, B., Zhou, N., Lee, W. R., Zhuo, Z., and Peripolli, E. (2019). The metabolic characteristics of susceptibility to wooden breast disease in chickens with high feed efficiency. Poult. Sci., 1–11. doi:10.3382/ps/pez183.

Aghajanian, A., Wittchen, E. S., Allingham, M. J., Garrett, T. A., and Burridge, K. (2008). Endothelial cell junctions and the regulation of vascular permeability and leukocyte transmigration. J. Thromb. Haemost. 6, 1453–1460. doi:10.1111/j.1538-7836.2008.03087.x.

Akiba, Y., Chida, Y., Takahashi, T., Ohtomo, Y., Sato, K., and Takahashi, K. (1999). Persistent hypoglycemia induced by continuous insulin infusion in broiler chickens. Br. Poult. Sci. 40, 701–705. doi:10.1080/00071669987124.

Alvarenga, R. R., Zangeronimo, M. G., Pereira, L. J., Rodrigues, P. B., and Gomide, E. M. (2011). Lipoprotein metabolism in poultry. Worlds. Poult. Sci. J. 67, 431–440. doi:10.1017/s0043933911000481.

Amin, M., Pushpakumar, S., Muradashvili, N., Kundu, S., Tyagi, S. C., and Sen, U. (2017). Regulation and involvement of matrix metalloproteinases in vascular diseases. Front. Biosci. 21, 89–118. doi:10.1002/jmri.25711.PET/MRI.

Anderson, E. J., and Neufer, P. D. (2006). Type II skeletal myofibers possess unique properties that potentiate mitochondrial H2O2 generation. Am. J. Physiol. Physiol. 290, C844–C851. doi:10.1152/ajpcell.00402.2005.

Arruda, A. P., and Hotamisligil, G. S. (2015). Calcium homeostasis and organelle function in the pathogenesis of obesity and diabetes. Cell Metab. 22, 381–397. doi:10.1016/j.cmet.2015.06.010.

Asbun, J., and Villarreal, F. J. (2006). The pathogenesis of myocardial fibrosis in the setting of diabetic cardiomyopathy. J. Am. Coll. Cardiol. 47, 693–700. doi:10.1016/j.jacc.2005.09.050.

Bahar, E., Kim, H., and Yoon, H. (2016). ER stress-mediated signaling: Action potential and Ca2+ as key players. Int. J. Mol. Sci. 17, 1–22. doi:10.3390/ijms17091558.

Baldi, G., Soglia, F., Laghi, L., Tappi, S., Rocculi, P., Tavaniello, S., et al. (2019). Comparison of quality traits among breast meat affected by current muscle abnormalities. Food Res. Int. 115, 369–376. doi:10.1016/j.foodres.2018.11.020.

Baldi, G., Soglia, F., Mazzoni, M., Sirri, F., Canonico, L., Babini, E., et al. (2018). Implications of white striping and spaghetti meat abnormalities on meat quality and histological features in broilers. Animal 12, 164–173. doi:10.1017/S1751731117001069.

Barbato, G. F. (1994). Genetic control of food intake in chickens. J. Nutr. 124, 1340S-1340S. doi:10.1093/jn/124.suppl_8.1340s.

Basta, G., Schmidt, A. M., and De Caterina, R. (2004). Advanced glycation end products and vascular inflammation: Implications for accelerated atherosclerosis in diabetes. Cardiovasc. Res. 63, 582–592. doi:10.1016/j.cardiores.2004.05.001.

Berezhnov, A. V, Fedotova, E. I., Nenov, M. N., Kokoz, Y. M., Zinchenko, V. P., and Dynnik, V. V (2008). Destabilization of the cytosolic calcium level and the death of cardiomyocytes in the presence of derivatives of long-chain fatty acids. Biophysics (Oxf). 53, 564–570. doi:10.1134/s0006350908060183.

Berridge, M. J., Bootman, M. D., and Roderick, H. L. (2003). Calcium signalling: Dynamics, homeostasis and remodelling. Nat. Rev. Mol. Cell Biol. 4, 517–529. doi:10.1038/nrm1155.

Bleyer, A. J., Fumo, P., Snipes, E. R., Goldfarb, S., Simmons, D. A., and Ziyadeh, F. N. (1994). Polyol pathway mediates high glucose-induced collagen synthesis in proximal tubule. Kidney Int. 45, 659–666. doi:10.1038/ki.1994.88.

Boerboom, G., van Kempen, T., Navarro-villa, A., and Perez-Bonilla, A. (2018). Unraveling the cause of white striping in broilers using metabolomics. Poult. Sci. 97, 3977–3986.

Botham, K. M., Moore, E. H., De Pascale, C., and Bejta, F. (2007). The induction of macrophage foam cell formation by chylomicron remnants. Biochem. Soc. Trans. 35, 454–458. doi:10.1042/bst0350454.

Braun, E. J., and Sweazea, K. L. (2008). Glucose regulation in birds. Comp. Biochem. Physiol. - B Biochem. Mol. Biol. 151, 1–9. doi:10.1016/j.cbpb.2008.05.007.

Brosius, F. C., and Heilig, C. W. (2005). Glucose transporters in diabetic nephropathy. Pediatr. Nephrol. 20, 447–451. doi:10.1007/s00467-004-1748-x.

Brothers, B., Zhuo, Z., Papah, M. B., and Abasht, B. (2019). RNA-seq analysis reveals spatial and sex differences in pectoralis major muscle of broiler chickens contributing to difference in susceptibility to wooden breast disease. Front. Physiol. 10. doi:10.3389/fphys.2019.00764.

Cheah, A. M. (1981). Effect of long chain unsaturated fatty acids on the calcium transport of sarcoplasmic reticulum. Biochim. Biophys. Acta 648, 113–119.

Chin, E. R., Olson, E. N., Richardson, J. A., Yang, Q., Humphries, C., Shelton, J. M., et al. (1998). A calcineurin-dependent transcriptional pathway controls skeletal muscle fiber type. Genes Dev. 12, 2499–2509. doi:10.1101/gad.12.16.2499.

Cho, S. J., Moon, J. S., Lee, C. M., Choi, A. M. K., and Stout-Delgado, H. W. (2017). Glucose transporter 1-dependent glycolysis is increased during aging-related lung fibrosis, and phloretin inhibits lung fibrosis. Am. J. Respir. Cell Mol. Biol. 56, 521–531. doi:10.1165/rcmb.2016-0225OC.

Chung, S. S. M. (2004). Contribution of polyol pathway to diabetes-induced oxidative stress. J. Am. Soc. Nephrol. 14, 233S – 236. doi:10.1097/01.asn.0000077408.15865.06.

Clark, D. L., and Velleman, S. G. (2017). Spatial influence on breast muscle morphological structure, myofiber size, and gene expression associated with the wooden breast myopathy in broilers. Poult. Sci. 95, 2930–2945. doi:10.3382/ps/pew243.

Dalle Zotte, A., Tasoniero, G., Puolanne, E., Remignon, H., Cecchinato, M., Catelli, E., et al. (2017). Effect of "Wooden Breast" appearance on poultry meat quality, histological traits, and lesions characterization. Czech J. Anim. Sci. 62, 51–57. doi:10.17221/54/2016-CJAS.

Dasu, M. R., and Jialal, I. (2010). Free fatty acids in the presence of high glucose amplify monocyte inflammation via Toll-like receptors. Am. J. Physiol. Metab. 300, E145–E154. doi:10.1152/ajpendo.00490.2010.

De Miranda, M. A., Schlater, A. E., Green, T. L., and Kanatous, S. B. (2012). In the face of hypoxia: myoglobin increases in response to hypoxic conditions and lipid supplementation in cultured Weddell seal skeletal muscle cells. J. Exp. Biol. 215, 806–813. doi:10.1242/jeb.060681.

DeFronzo, R. A., and Tripathy, D. (2009). Skeletal muscle insulin resistance is the primary defect in type 2 diabetes. Diabetes Care 32 Suppl 2. doi:10.2337/dc09-s302.

Dupont, J., Dagou, C., Derouet, M., Simon, J., and Taouis, M. (2004). Early steps of insulin receptor signaling in chicken and rat: Apparent refractoriness in chicken muscle. Domest. Anim. Endocrinol. 26, 127–142. doi:10.1016/j.domaniend.2003.09.004.

Eiselein, L., Wilson, D. W., Lamé, M. W., and Rutledge, J. C. (2007). Lipolysis products from triglyceride-rich lipoproteins increase endothelial permeability, perturb zonula occludens-1 and F-actin, and induce apoptosis. Am. J. Physiol. Circ. Physiol. 292, H2745–H2753. doi:10.1152/ajpheart.00686.2006.

Endo, M. (2009). Calcium-Induced Calcium Release in Skeletal Muscle. Physiol. Rev. 89, 1153–1176. doi:10.1152/physrev.00040.2008.

Ermak, G., and Davies, K. J. A. (2001). Calcium and oxidative stress: From cell signaling to cell death. Mol. Immunol. 38, 713–721. doi:10.1016/S0161-5890(01)00108-0.

Fantus, I. G., Goldberg, H. J., Whiteside, C. I., and Topic, D. (2007). The hexosamine biosynthesis pathway. Diabet. Kidney, 117–133. doi:10.1007/978-1-59745-153-6_7.

Fu, S., Li, P., Watkins, S. M., Ivanov, A. R., Hofmann, O., Hotamisligil, G. S., et al. (2011). Aberrant lipid metabolism disrupts calcium homeostasis causing liver endoplasmic reticulum stress in obesity. Nature 473, 528–531. doi:10.1038/nature09968.

Godet, E., Porter, T. E., Tesseraud, S., Simon, J., Duclos, M. J., Métayer-Coustard, S., et al. (2008). Insulin immuno-neutralization in chicken: effects on insulin signaling and gene expression in liver and muscle. J. Endocrinol. 197, 531–542. doi:10.1677/joe-08-0055.

Goglia, F., and Skulachev, V. P. (2003). A function for novel uncoupling proteins: antioxidant defense of mitochondrial matrix by translocating fatty acid peroxides from the inner to the outer membrane leaflet. FASEB J. 17, 1585–1591. doi:10.1096/fj.03-0159hyp.

Gorski, D. J., Petz, A., Reichert, C., Twarock, S., Grandoch, M., and Fischer, J. W. (2019). Cardiac fibroblast activation and hyaluronan synthesis in response to hyperglycemia and diet-induced insulin resistance. Sci. Rep. 9, 1–11. doi:10.1038/s41598-018-36140-6.

Gratta, F., Fasolato, L., Birolo, M., Zomeño, C., Novelli, E., Petracci, M., et al. (2019). Effect of breast myopathies on quality and microbial shelf life of broiler meat. Poult. Sci., 1–11. doi:10.3382/ps/pez001.

Griffin, H., Acamovic, F., Guo, K., and Peddie, J. (1989). Plasma lipoprotein metabolism in lean and in fat chickens produced by divergent selection for plasma very low density lipoprotein concentration. J. Lipid Res. 30, 1243–50. Available at: http://www.ncbi.nlm.nih.gov/pubmed/2769076.

Groop, L. C., and Ferrannini, E. (1993). Insulin action and substrate competition. Baillieres. Clin. Endocrinol. Metab. 7, 1007–1032. doi:10.1016/S0950-351X(05)80243-5.

Gunter, T. E., Gunter, K. K., Sheu, S.-S., and Gavin, C. E. (1994). Mitochondrial calcium transport: physiological and pathological relevance. Am. J. Physiol. Physiol. 36, C313–C339.

Ha, S. W., Seo, Y. K., Kim, J. G., Kim, I. S., Sohn, K. Y., Lee, B. H., et al. (1997). Effect of high glucose on synthesis and gene expression of collagen and fibronectin in cultured vascular smooth muscle. Exp. Mol. Med. 29, 59–64. Available at: https://www.nature.com/articles/emm19979.pdf.

Hajnóczky, G., Csordás, G., Das, S., Garcia-Perez, C., Saotome, M., Sinha Roy, S., et al. (2006). Mitochondrial calcium signalling and cell death: Approaches for assessing the role of mitochondrial Ca2+ uptake in apoptosis. Cell Calcium 40, 553–560. doi:10.1016/j.ceca.2006.08.016.

Han, D. C., Isono, M., Hoffman, B. B., and Ziyadeh, F. N. (1999). High glucose stimulates proliferation and collagen type I synthesis in renal cortical fibroblasts: Mediation by autocrine activation of TGF-beta. J. Am. Soc. Nephrol. 10, 1891–1899.

Havenstein, G. B., Ferket, P. R., and Qureshi, M. A. (2003a). Carcass composition and yield of 1957 versus 2001 broilers when fed representative 1957 and 2001 broiler diets. Poult. Sci. 82, 1509–18. doi:10.1093/ps/82.10.1509.

Havenstein, G. B., Ferket, P. R., and Qureshi, M. A. (2003b). Growth, livability, and feed conversion of 1957 versus 2001 broilers when fed representative 1957 an 2001 broiler diets. Poult. Sci. 82, 1500–1508. doi:10.1093/ps/82.10.1509.

Hers, H. G. (1976). The control of glycogen metabolism in the liver. Annu. Rev. Biochem. 45, 167–190. doi:10.1007/978-3-642-66461-8_14.

Hirst, J., King, M. S., and Pryde, K. R. (2008). The production of reactive oxygen species by complex I. Biochem. Soc. Trans. 36, 976–980. doi:10.1042/BST0360976.

Huang, J. M., Xian, H., and Bacaner, M. (2006). Long-chain fatty acids activate calcium channels in ventricular myocytes. Proc. Natl. Acad. Sci. 89, 6452–6456. doi:10.1073/pnas.89.14.6452.

Ishii, H., Tada, H., and Isogai, S. (1998). An aldose reductase inhibitor prevents glucose-induced increase in transforming growth factor-β and protein kinase C activity in cultured human mesangial cells. Diabetologia 41, 362–364. doi:10.1007/s001250050916.

Kawasaki, T., Iwasaki, T., Yamada, M., Yoshida, T., and Watanabe, T. (2018). Rapid growth rate results in remarkably hardened breast in broilers during the middle stage of rearing: A biochemical and histopathological study. PLoS One 13, 1–14. doi:10.1371/journal.pone.0193307.

Kim, J. K., Fillmore, J. J., Chen, Y., Yu, C., Moore, I. K., Pypaert, M., et al. (2001). Tissue-specific overexpression of lipoprotein lipase causes tissue-specific insulin resistance. Proc. Natl. Acad. Sci. 98, 7522–7527. doi:10.1073/pnas.121164498.

Klip, A., Volchuk, A., He, L., and Tsakiridis, T. (1996). The glucose transporters of skeletal muscle. Semin. Cell Dev. Biol. 7, 229–237. doi:10.1006/scdb.1996.0031.

Kono, T., Nishida, M., Nishiki, Y., Seki, Y., Sato, K., and Akiba, Y. (2005). Characterisation of glucose transporter (GLUT) gene expression in broiler chickens. Br. Poult. Sci. 46, 510–515. doi:10.1080/00071660500181289.

Kruger, N. J., and Von Schaewen, A. (2003). The oxidative pentose phosphate pathway: structure and organisation. Curr. Opin. Plant Biol. 6, 236–246. doi:10.1016/S1369-5266(03)00039-6.

Krutzik, S. R., Tan, B., Li, H., Ochoa, M. T., Liu, P. T., Sharfstein, S. E., et al. (2005). TLR activation triggers the rapid differentiation of monocytes into macrophages and dendritic cells. Nat. Med. 11, 653–660. doi:10.1016/j.jaci.2011.08.037.Evidence.

Kumagai, A. K. (1999). Glucose transport in brain and retina: Implications in the management and complications of diabetes. Diabetes. Metab. Res. Rev. 15, 261–273.

Kuttappan, V. A., Hargis, B. M., and Owens, C. M. (2016). White striping and woody breast myopathies in the modern poultry industry: A review. Poult. Sci. 95, 2724–2733. doi:10.3382/ps/pew216.

Kuttappan, V. A., Shivaprasad, H. l., Shaw, D. P., Valentine, B. A., Hargis, B. M., Clark, F. D., et al. (2013). Pathological changes associated with white striping in broiler breast muscles. Poult. Sci. 92, 331–338. doi:10.3382/ps.2012-02646.

Lake, J. A., Papah, M. B., and Abasht, B. (2019). Increased expression of lipid metabolism genes in early stages of wooden breast links myopathy of broilers to metabolic syndrome in humans. Genes (Basel). 10. doi:10.20944/preprints201906.0194.v1.

Larkina, T. A., Sazanova, A. L., Fomichev, K. A., Barkova, O. Y., Malewski, T., Jaszczak, K., et al. (2010). HMG1A and PPARG are differently expressed in the liver of fat and lean broilers. J. Appl. Genet. 52, 225–228. doi:10.1007/s13353-010-0023-z.

Lee, J. Y., and Hwang, D. H. (2006). The modulation of inflammatory gene expression by lipids: mediation through Toll-like receptors. Mol. Cells 21, 174–85. Available at: http://www.ncbi.nlm.nih.gov/pubmed/16682810.

Li, Y., He, P. P., Zhang, D. W., Zheng, X. L., Cayabyab, F. S., Yin, W. D., et al. (2014). Lipoprotein lipase: From gene to atherosclerosis. Atherosclerosis 237, 597–608. doi:10.1016/j.atherosclerosis.2014.10.016.

Lilburn, M. S., Griffin, J. R., and Wick, M. (2018). From muscle to food: oxidative challenges and developmental anomalies in poultry breast muscle. Poult. Sci. doi:10.3382/ps/pey409.

Livingston, M. L., Ferket, P. R., Brake, J., and Livingston, K. A. (2019a). Dietary amino acids under hypoxic conditions exacerbates muscle myopathies including wooden breast and white stripping. Poult. Sci. 98, 1517–1527. doi:10.3382/ps/pey463.

Livingston, M. L., Landon, C. D., Barnes, H. J., Brake, J., and Livingston, K. A. (2019b). Dietary potassium and available phosphorous on broiler growth performance, carcass characteristics, and wooden breast. Poult. Sci. 98, 2813–2822. doi:10.3382/ps/pez015.

Mead, J. R., Irvine, S. A., and Ramji, D. P. (2002). Lipoprotein lipase: Structure, function, regulation, and role in disease. J. Mol. Med. 80, 753–769. doi:10.1007/s00109-002-0384-9.

Mudalal, S., Lorenzi, M., Soglia, F., Cavani, C., and Petracci, M. (2015). Implications of white striping and wooden breast abnormalities on quality traits of raw and marinated chicken meat. Animal 9, 728–734. doi:10.1017/S175173111400295X.

Mutryn, M. F., Brannick, E. M., Fu, W., Lee, W. R., and Abasht, B. (2015). Characterization of a novel chicken muscle disorder through differential gene expression and pathway analysis using RNA-sequencing. BMC Genomics 16, 1–19. doi:10.1186/s12864-015-1623-0.

Nanji, A. A., Fogt, F., and Griniuviene, B. (1995). Alterations in glucose transporter proteins in alcoholic liver disease in the rat. Am J Pathol 146, 329–334.

Navale, A. M., and Paranjape, A. N. (2016). Glucose transporters: physiological and pathological roles. Biophys. Rev. 8, 5–9. doi:10.1007/s12551-015-0186-2.

Olin, K. L., Potter-Perigo, S., Barrett, P. H. R., Wight, T. N., and Chait, A. (1999). Lipoprotein lipase enhances the binding of native and oxidized low density lipoproteins to versican and biglycan synthesized by cultured arterial smooth muscle cells. J. Biol. Chem. 274, 34629–34636. doi:10.1074/jbc.274.49.34629.

Orrenius, S., Gogvadze, V., and Zhivotovsky, B. (2015). Calcium and mitochondria in the regulation of cell death. Biochem. Biophys. Res. Commun. 460, 72–81. doi:10.1016/j.bbrc.2015.01.137.

Papah, M. B., and Abasht, B. (2019). Dysregulation of lipid metabolism and appearance of slow myofiber- specific isoforms accompany the development of Wooden Breast myopathy in modern broiler chickens. Sci. Rep., 1–12. doi:10.1038/s41598-019-53728-8.

Papah, M. B., Brannick, E. M., Schmidt, C. J., and Abasht, B. (2017). Evidence and role of phlebitis and lipid infiltration in the onset and pathogenesis of Wooden Breast Disease in modern broiler chickens. Avian Pathol. 46, 623–643. doi:10.1080/03079457.2017.1339346.

Papah, M. B., Brannick, E. M., Schmidt, C. J., and Abasht, B. (2018). Gene expression profiling of the early pathogenesis of wooden breast disease in commercial broiler chickens using RNA-sequencing. PLoS One 13, e0207346. doi:10.1371/journal.pone.0207346.

Penzo, D., Tagliapietra, C., Colonna, R., Petronilli, V., and Bernardi, P. (2002). Effects of fatty acids on mitochondria: Implications for cell death. Biochim. Biophys. Acta - Bioenerg. 1555, 160–165. doi:10.1016/S0005-2728(02)00272-4.

Petracci, M., Soglia, F., Madruga, M., Carvalho, L., Ida, E., and Estevez, M. (2019). Wooden-breast, white striping, and spaghetti meat: Causes, consequences and consumer perception of emerging broiler meat abnormalities. Compr. Rev. Food Sci. Food Saf. 18, 565–583. doi:10.1111/1541-4337.12431.

Pohlers, D., Brenmoehl, J., Löffler, I., Müller, C. K., Leipner, C., Schultze-Mosgau, S., et al. (2009). TGF-β and fibrosis in different organs - molecular pathway imprints. Biochim. Biophys. Acta - Mol. Basis Dis. 1792, 746–756. doi:10.1016/j.bbadis.2009.06.004.

Randle, P. J., Garland, P. B., Newsholme, E. A., and Hales, C. N. (1965). The glucose fatty acid cycle in obesity and maturity onset diabetes mellitus. Ann. N. Y. Acad. Sci. 131, 324–333. doi:10.1016/0306-9877(81)90134-1.

Rasouli, N., Molavi, B., Elbein, S. C., and Kern, P. A. (2007). Ectopic fat accumulation and metabolic syndrome. Diabetes, Obes. Metab. 9, 1–10. doi:10.1111/j.1463-1326.2006.00590.x.

Rocha, D. M., Caldas, A. P., Oliveira, L. L., Bressan, J., and Hermsdorff, H. H. (2016). Saturated fatty acids trigger TLR4-mediated inflammatory response. Atherosclerosis 244, 211–215. doi:10.1016/j.atherosclerosis.2015.11.015.

Rousset, S., Alves-Guerra, M.-C., Mozo, J., Miroux, B., Cassard-Doulcier, A.-M., Bouillaud, F., et al. (2004). The biology of mitochondrial uncoupling. Diabetes 53, S130–S135. doi:10.2337/diabetes.53.2007.s130.

Sandercock, D. A., Barker, Z. E., Mitchell, M. A., and Hocking, P. M. (2009). Changes in muscle cell cation regulation and meat quality traits are associated with genetic selection for high body weight and meat yield in broiler chickens. Genet. Sel. Evol. 41, 1–8. doi:10.1186/1297-9686-41-8.

Schrauwen, P. (2007). High-fat diet, muscular lipotoxicity and insulin resistance. Proc. Nutr. Soc. 66, 33–41. doi:10.1017/S0029665107005277.

Schrauwen, P., and Hesselink, M. K. C. (2004). Oxidative capacity, lipotoxicity, and mitochondrial damage in type 2 diabetes. Diabetes 53, 1412–1417.

Seki, Y., Sato, K., Kono, T., Abe, H., and Akiba, Y. (2003). Broiler chickens (Ross strain) lack insulin-responsive glucose transporter GLUT4 and have GLUT8 cDNA. Gen. Comp. Endocrinol. 133, 80–87. doi:10.1016/S0016-6480(03)00145-X.

Semenza, G. L., Roth, P. H., Fang, H. M., and Wang, G. L. (1994). Transcriptional regulation of genes encoding glycolytic enzymes by hypoxia-inducible factor 1. J. Biol. Chem. 269, 23757–23763.

Seo, M., and Lee, Y. H. (2014). PFKFB3 regulates oxidative stress homeostasis via its S-glutathionylation in cancer. J. Mol. Biol. 426, 830–842. doi:10.1016/j.jmb.2013.11.021.

Shepherd, P. R., and Kahn, B. B. (1999). Glucose transporters and insulin action: Implications for insulin resistance and diabetes mellitus. N. Engl. J. Med. 341, 248–257.

Sihvo, H. K., Airas, N., Lindén, J., and Puolanne, E. (2018). Pectoral vessel density and early ultrastructural changes in broiler chicken wooden breast myopathy. J. Comp. Pathol. 161, 1–10. doi:10.1016/j.jcpa.2018.04.002.

Sihvo, H. K., Immonen, K., and Puolanne, E. (2014). Myodegeneration with fibrosis and regeneration in the pectoralis major muscle of broilers. Vet. Pathol. 51, 619–623. doi:10.1177/0300985813497488.

Smith, I. C., Bombardier, E., Vigna, C., and Tupling, A. R. (2013). ATP consumption by sarcoplasmic reticulum Ca2+ pumps accounts for 40-50% of resting metabolic rate in mouse fast and slow twitch skeletal muscle. PLoS One 8, 1–11. doi:10.1371/journal.pone.0068924.

Smith, M. W., Mitchell, M. A., and Peacock, M. A. (1990). Effects of genetic selection on growth rate and intestinal structure in the domestic fowl (Gallus domesticus). Comp. Biochem. Physiol. -- Part A Physiol. 97A, 57–63. doi:10.1016/0300-9629(90)90722-5.

Soglia, F., Mudalal, S., Babini, E., Di Nunzio, M., Mazzoni, M., Sirri, F., et al. (2016). Histology, composition, and quality traits of chicken Pectoralis major muscle affected by wooden breast abnormality. Poult. Sci. 95, 651–659. doi:10.3382/ps/pev353.

Tasoniero, G., Cullere, M., Cecchinato, M., Puolanne, E., and Dalle Zotte, A. (2016). Technological quality, mineral profile, and sensory attributes of broiler chicken breasts affected by White Striping and Wooden Breast myopathies. Poult. Sci. 95, 2707–2714. doi:10.3382/ps/pew215.

Toborek, M., Lee, Y. W., Garrido, R., Kaiser, S., and Hennig, B. (2002). Unsaturated fatty acids selectively induce an inflammatory environment in human endothelial cells. Am. J. Clin. Nutr. 75, 119–125. doi:10.1093/ajcn/75.1.119.

Tokudome, T., Horio, T., Yoshihara, F., Suga, S. I., Kawano, Y., Kohno, M., et al. (2004). Direct effects of high glucose and insulin on protein synthesis in cultured cardiac myocytes and DNA and collagen synthesis in cardiac fibroblasts. Metabolism. 53, 710–715. doi:10.1016/j.metabol.2004.01.006.

Tokushima, Y., Takahashi, K., Sato, K., and Akiba, Y. (2005). Glucose uptake in vivo in skeletal muscles of insulin-injected chicks. Comp. Biochem. Physiol. - B Biochem. Mol. Biol. 141, 43–48. doi:10.1016/j.cbpc.2005.01.008.

Tousoulis, D., Kampoli, A.-M., Tentolouris Nikolaos Papageorgiou, C., and Stefanadis, C. (2012). The role of nitric oxide on endothelial function. Curr. Vasc. Pharmacol. 10, 4–18. doi:10.2174/157016112798829760.

Ursini, F., Roveri, A., van Amsterdam, F. T. M., Ratti, E., Maiorino, M., Zamburlini, A., et al. (2004). Effect of hydrogen peroxide on calcium homeostasis in smooth muscle cells. Arch. Biochem. Biophys. 297, 265–270. doi:10.1016/0003-9861(92)90671-i.

Velleman, S. G., Clark, D. L., and Tonniges, J. R. (2017). Fibrillar collagen organization associated with broiler wooden breast fibrotic myopathy. Avian Dis. 61, 481–490. doi:10.1637/11738-080217-Reg.1.

Volmer, R., and Ron, D. (2015). Lipid-dependent regulation of the unfolded protein response. Curr. Opin. Cell Biol. 33, 67–73. doi:10.1016/j.ceb.2014.12.002.

Wall, V. Z., Barnhart, S., Kanter, J. E., Kramer, F., Shimizu-Albergine, M., Adhikari, N., et al. (2018). Smooth muscle glucose metabolism promotes monocyte recruitment and atherosclerosis in a mouse model of metabolic syndrome. JCI Insight 3. doi:10.1172/jci.insight.96544.

Wang, H., and Eckel, R. H. (2009). Lipoprotein lipase: from gene to obesity. Am. J. Physiol. Metab. 297, E271–E288. doi:10.1152/ajpendo.90920.2008.

Wang, J., Xian, X., Huang, W., Chen, L., Wu, L., Zhu, Y., et al. (2007). Expression of LPL in endothelial-intact artery results in lipid deposition and vascular cell adhesion molecule-1 upregulation in both LPL and ApoE-deficient mice. Arterioscler. Thromb. Vasc. Biol. 27, 197–203. doi:10.1161/01.ATV.0000249683.80414.d9.

Wei, Y., Wang, D., Gentile, C. L., and Pagliassotti, M. J. (2009). Reduced endoplasmic reticulum luminal calcium links saturated fatty acid-mediated endoplasmic reticulum stress and cell death in liver cells. Mol. Cell. Biochem. 331, 31–40. doi:10.1007/s11010-009-0142-1.

Yabe-Nishimura, C. (1998). Aldose reductase in glucose toxicity: A potential target for the prevention of diabetic complications. Pharmacol. Rev. 50, 21–33.

Yamamoto, T., Takano, N., Ishiwata, K., Ohmura, M., Nagahata, Y., Matsuura, T., et al. (2014). Reduced methylation of PFKFB3 in cancer cells shunts glucose towards the pentose phosphate pathway. Nat. Commun. 5. doi:10.1038/ncomms4480.

Yan, L. (2018). Redox imbalance stress in diabetes mellitus: Role of the polyol pathway. Anim. Model. Exp. Med. 1, 7–13. doi:10.1002/ame2.12001.

Yin, H., Price, F., and Rudnicki, M. A. (2013). Satellite cells and the muscle stem cell niche. Physiol. Rev. 93, 23–67. doi:10.1152/physrev.00043.2011.

Zahoor, I., De Koning, D. J., and Hocking, P. M. (2017). Transcriptional profile of breast muscle in heat stressed layers is similar to that of broiler chickens at control temperature. Genet. Sel. Evol. 49. doi:10.1186/s12711-017-0346-x.

Zambonelli, P., Zappaterra, M., Soglia, F., Petracci, M., Sirri, F., Cavani, C., et al. (2016). Detection of differentially expressed genes in broiler pectoralis major muscle affected by White Striping - Wooden Breast myopathies. Poult. Sci. 95, 2771–2785. doi:10.3382/ps/pew268.

Zanetti, M. A., Tedesco, D. C., Schneider, T., Teixeira, S. T. F., Daroit, L., Pilotto, F., et al. (2018). Economic losses associated with Wooden Breast and White Striping in broilers. Semin. Ciencias Agrar. 39, 887–892. doi:10.5433/1679-0359.2018v39n2p887.

Zhou, N., Lee, W. R., and Abasht, B. (2015). Messenger RNA sequencing and pathway analysis provide novel insights into the biological basis of chickens' feed efficiency. BMC Genomics 16, 195. doi:10.1186/s12864-015-1364-0.

Zhuo, Z., Lamont, S. J., Lee, W. R., and Abasht, B. (2015). RNA-seq analysis of abdominal fat reveals differences between modern commercial broiler chickens with high and low feed efficiencies. PLoS One 10, e0135810. doi:10.1371/journal.pone.0135810.

Zierath, J. R., Houseknecht, K. L., Gnudi, L., and Kahn, B. B. (1997). High-fat feeding impairs insulin-stimulated GLUT4 recruitment via an early insulin-signaling defect. Diabetes 46, 215–223. doi:10.2337/diab.46.2.215.

Zimermann, F. C., Fallavena, L. C. B., Salle, C. T. P., Moraes, H. L. S., Soncini, R. A., Barreta, M. H., et al. (2012). Downgrading of Heavy Broiler Chicken Carcasses Due to Myodegeneration of the Anterior Latissimus Dorsi: Pathologic and Epidemiologic Studies. Avian Dis. 56, 418–421. doi:10.1637/9860-072111-case.1.

Chapter 3

BLOOD GAS DISTURBANCES AND DISPROPORTIONATE BODY WEIGHT DISTRIBUTION IN BROILERS WITH WOODEN BREAST

(Juniper A. Lake, Erin M. Brannick, Michael B. Papah, Cory Lousenberg, Sandra G. Velleman, & Behnam Abasht. *Frontiers in Physiology*, 11:304, (2020)).
https://www.frontiersin.org/articles/10.3389/fphys.2020.00304/full

3.1 Abstract

Wooden breast syndrome is a widespread and economically important myopathy and vasculopathy of fast growing, commercial broiler chickens, primarily affecting birds with high feed efficiency and large breast muscle yield. To investigate potential systemic physiological differences between birds affected and unaffected by wooden breast, a total of 103 market-age Cobb 500 broilers were sampled for 13 blood parameters and the relative weights of the pectoralis major muscle, pectoralis minor muscle, external oblique muscle, wing, heart, lungs, liver, and spleen. Blood analysis was performed on samples taken from the brachial vein of live birds and revealed significant differences in venous blood gases between affected and unaffected chickens. Chickens with wooden breast exhibited significantly higher potassium (K^+) and lower partial pressure of oxygen (pO_2), oxygen saturation (sO2), and pH. Additionally, affected males had significantly higher partial pressure of carbon dioxide (pCO_2) and total carbon dioxide (TCO_2) than unaffected males. Wooden breast affected broilers also possessed a significantly heavier pectoralis major muscle and whole feathered wing compared to unaffected broilers. Blood gas disturbances characterized by high pCO_2 and low pH are indicative of insufficient respiratory gas

exchange, suggesting that wooden breast affected broilers have an elevated metabolic rate that may also be inadequately compensated due to cardiovascular deficiencies such as poor venous return or respiratory insufficiency. Lung tissues from 12 birds with extreme sO_2 values were subsequently examined to assess whether lung pathology contributed to the observed blood gas disturbance. Comparison of lung morphology between affected and unaffected birds revealed no apparent differences that could contribute to decreased parabronchial gas exchange. However, an interesting finding was the detection of pulmonary phlebitis in one of the wooden breast-affected samples consistent with vascular changes observed in pectoralis major muscle exhibiting the wooden breast phenotype. Our results suggest that the effects of wooden breast are not limited to the pectoralis major muscle and further indicate the importance of research into metabolic changes associated with the myopathy.

3.2 Introduction

Modern commercial broiler chickens have undergone intensive selection for production traits such as high muscle yield, rapid growth, and high feed efficiency to meet consumer demand for low-cost lean chicken meat, specifically chicken breast meat. Such breeding strategies have produced remarkable results, nearly halving the time for birds to reach market weight while simultaneously increasing the breast muscle weight by about two-thirds since the 1950s (Petracci et al., 2015). Unfortunately, modern commercial broilers also experience increased prevalence of breast muscle myopathies, some of which cause substantial economic losses due to negative effects on meat quality (Kuttappan et al., 2016).

One such myopathy, commonly called wooden breast (WB), causes the pectoralis major muscle to become grossly pale, enlarged, and palpably firm, with

visible signs of inflammation such as petechial hemorrhages and tissue edema (Sihvo et al., 2014). These macroscopic manifestations of the disorder are accompanied by considerable degradation of meat quality (Mudalal et al., 2015; Chatterjee et al., 2016) such that moderately or severely affected breast muscle cannot be sold as prime breast muscle fillets and is instead condemned or sold for lower revenue products. In addition, increased locomotor difficulties, decreased wing mobility, and higher rates of dorsal recumbency among affected birds (Papah et al., 2017; Norring et al., 2018; Gall et al., 2019a) suggest that WB may also be detrimental to bird welfare.

Research on WB and related myopathies is focused largely on the pectoralis major muscle, with only minor attention paid to potential systemic disparities accompanying the condition. However, factors that predispose broilers to WB – growth rate, feed efficiency, and breast muscle yield – can broadly be categorized as relating to general metabolism and body form. To date, there has been no comprehensive comparison of muscle and organ weights beyond the pectoralis major muscle weight and abdominal fat percentage between WB affected and unaffected broilers. An analysis of body weight distribution in WB birds may aid in identifying systemic physiological predisposition to or pathophysiologic effects of the myopathy. Intensive selection for commercially valuable traits has been shown to underpin biological imbalances in meat-type chickens, such as insufficient cardiopulmonary capacity to accommodate sustained rapid growth, resulting in pulmonary hypertension syndrome, or ascites (Wideman and French, 2000). It is known that WB-affected broilers possess larger breast muscles relative to body weight (Mutryn et al., 2015b) with higher cross-sectional areas (Dalle Zotte et al., 2017), and lower abdominal fat as

a percentage of body weight (Mutryn et al., 2015b), but other potential differences in body weight distribution have not been examined.

Microscopic characterizations of WB have also largely been limited to the pectoralis major muscle (Sihvo et al., 2014, 2017, 2018; Papah et al., 2017), although evidence of altered blood gas values (Livingston et al., 2019b, 2019a) in affected birds may indicate systemic disturbances or inadequate respiratory gas exchange. Two studies have provided initial insight into differences in blood parameters between WB-affected and unaffected broilers (Livingston et al., 2019a, 2019b). Livingston et al. (2019a) evaluated the venous blood of male broilers at 35 days of age and found that WB severity was significantly associated with reduced partial pressure of oxygen (pO_2) and increased total carbon dioxide (TCO_2), bicarbonate (HCO_3^-), and base excess (BE). The same blood analysis conducted at 42 days of age produced similar results with regard to blood gas changes in WB affected birds, with the additional finding that packed cell volume (PCV, hematocrit; Hct) was significantly associated with WB severity (Livingston et al., 2019a). Livingston et al. (2019b) subsequently reported higher potassium (K^+) levels in affected birds in a study evaluating the venous blood of male broilers at 42 days of age.

Thus, the objective of the current study was to further the systemic characterization of WB myopathy by comparing blood parameters, body weight distribution, and lung histology between affected and unaffected broilers.

3.3 Materials and Methods

3.3.1 Ethics Statement

The University of Delaware Institutional Animal Care and Use Committee approved the animal protocol (48R-2015-0) followed for this scientific study. Euthanasia was performed by means of cervical dislocation, and all efforts were made to maximize bird welfare.

3.3.2 Experimental Animals and Wooden Breast Disease Scoring

This experiment was conducted in chicken houses located at the University of Delaware under environmental conditions simulating a commercial setting. As part of a genome-wide association study, a total of 542 Cobb 500 broilers from the same breeding population were raised in 4 chicken houses and provided free access to feed and water. At 47 days of age, 103 birds were selected for blood analysis based on manual palpation of the breast muscle. These birds were selected to achieve an approximately equal number exhibiting no palpable breast muscle firmness (48 total; 26 male and 22 female) and severe palpable firmness (55 total; 39 male and 16 female). Blood analysis using i-STAT requires sampling of blood from live birds. Therefore, bird selection was performed using breast muscle palpation of live birds while all statistical analyses utilized more accurate scoring of WB based on gross evaluation of the pectoralis major muscle at necropsy, as described below.

This experiment was conducted in chicken houses located at the University of Delaware under environmental conditions simulating a commercial setting. As part of a genome-wide association study, a total of 542 Cobb 500 broilers from the same breeding population were raised in 4 chicken houses and provided free access to feed and water. At 47 days of age, 103 birds were selected for blood analysis based on

manual palpation of the breast muscle. These birds were selected to achieve an approximately equal number exhibiting no palpable breast muscle firmness (48 total; 26 male and 22 female) and severe palpable firmness (55 total; 39 male and 16 female). Blood analysis using i-STAT requires sampling of blood from live birds. Therefore, bird selection was performed using breast muscle palpation of live birds while all statistical analyses utilized more accurate scoring of WB based on gross evaluation of the pectoralis major muscle at necropsy, as described below.

3.3.3 Blood Analysis

At 47 days of age, 1ml of blood was drawn from the brachial wing vein of each bird using a 3 ml syringe with 23-gauge needle that had been prepared by aspirating and expelling a small volume of liquid heparin prior to blood collection. The blood was deposited immediately into a new i-STAT CG8+ cartridge inserted in the i-STAT 1 Analyzer (model 300A, Abbott Point of Care Inc., Princeton, NJ) to perform rapid blood analysis. While designed for clinical use in humans, the i-STAT system's performance in *Gallus gallus* has been demonstrated in previous studies (Steinmetz et al., 2007; Livingston et al., 2019a). CG8+ test cartridges were used to test blood chemistry parameters including sodium (Na^+), K^+, ionized calcium (iCa), and glucose (Glu); hematologic parameters Hct and hemoglobin (Hb); and blood gas parameters including pH, partial pressure of carbon dioxide (pCO_2), TCO_2, HCO_3^-, BE, oxygen saturation (sO_2), and pO_2. After all measurements were completed, data was downloaded from the analyzer and consolidated for statistical analysis. Body weight at 47 days was also measured at this time.

3.3.4 Body Weight Distribution

The same 103 birds used for blood analyses were also used to evaluate body weight distribution. After euthanasia, the left pectoralis major muscle, left pectoralis minor muscle, left external oblique muscle, heart, lungs, liver, spleen, and whole feathered left wing, disarticulated at the shoulder, were dissected from each bird. The weight of each dissected body part was recorded, along with the body weight of the bird before necropsy.

3.3.5 Statistical Analysis

Statistical analyses were performed using JMP software (SAS Institute, Cary, NC, USA). To improve statistical power, birds were grouped according to WB status: unaffected birds included those assigned a WB score of 0-Normal or 1-Very Mild and affected birds included those assigned a score of 2-Mild, 3-Moderate, or 4-Severe. All i-STAT measurements were analyzed using a mixed linear model with WB status, sex, WB-sex interaction, and body weight at 47 days as fixed effects and poultry house as a random effect. Body part weights were analyzed using a mixed linear model with WB status, sex, WB-sex interaction, and body weight at necropsy as fixed effects and poultry house as a random effect. Effects with $P \leq 0.05$ were considered significant for all tests.

3.3.6 Histological Evaluation of Lungs

Of the 103 broilers used in this study, six birds (3 males and 3 females) with the lowest sO_2 values and six birds with the highest sO_2 values (3 males and 3 females) were selected for microscopic examination of lung tissue based on blood gas values measured at 47 days of age. In the low sO_2 group, 5 birds were classified as affected, with WB scores of 3-Moderate or 4-Severe, and 1 bird was classified as

unaffected, with a WB score of 0-Normal. In the high sO_2 group, all 6 birds were classified as unaffected, with a WB score of 0-Normal. From each of the selected birds, lung tissue from the cranial and caudal aspects from either the left or right lung were harvested and fixed by immersion in 10% neutral buffered formalin. Samples were processed routinely for staining with hematoxylin and eosin as described by Papah et al. (Papah et al., 2017) before histologic evaluation with a light microscope and morphometric analysis with the Aperio LV1 digital microscope (Leica Biosystems, IL, USA).

Lung tissue was examined microscopically by a veterinarian (Papah) and a certified veterinary anatomic pathologist (Brannick) for histopathologic lesions or other tissue changes which could affect systemic blood parameters, such as the presence of inflammation, fibrosis, lymphoid follicular hyperplasia (lymphocytic nodules), cartilaginous nodules, edema or hemorrhage in the gas exchange areas, thickening of parabronchial walls, and obstruction of parabronchi. Assessment of all slides was performed in a blinded fashion and later microscopic lesions were assessed for an association with sO_2 status (high or low), sex, or WB status.

3.4 Results and Discussion

3.4.1 Body Weight Distribution

The effects of WB, sex, WB-sex interaction, and body weight on the weights of the dissected left pectoralis major muscle, left pectoralis minor muscle, left external oblique muscle, whole feathered left wing, heart, lungs, liver, and spleen are provided in Table 3.1. Wooden breast had a significant association with the pectoralis major muscle and whole feathered left wing, which were both larger in affected birds

compared to unaffected birds. Previous studies have found similar results with regard to pectoralis major yield (Mutryn et al., 2015b; Livingston et al., 2019b), providing fodder for speculation that high breast muscle yield is responsible for development of the WB and WS phenotypes due to overstretching of the myofibers and a reduction in capillary density (Kuttappan et al., 2013; Dalle Zotte et al., 2017). However, microscopic lesions of WB can be detected as early as 1 week of age in the pectoralis major muscle (Papah et al., 2017). Thus, hypotheses suggesting that WB arises from overstretching and ischemia may be inadequate or incomplete. Without discounting the potential contribution of pectoralis major growth rate to WB development, it is important to consider alternative interpretations of these results. For example, it has been proposed that muscle hypertrophy may be symptomatic of WB rather than causal, similar to the pathological hypertrophy of organs in chronic complications of diabetes mellitus in mammals (Lake et al., 2019; Lake and Abasht, 2020).

Table 3.1: Effects of wooden breast (WB) status (A: affected, U: unaffected), sex (M: male, F: female), the interaction of WB and sex, and body weight on the weight of the left pectoralis major, left pectoralis minor, left whole feathered wing, left external oblique, heart, lungs, liver, and spleen of broiler chickens.

		WB			**Sex**			**WB x Sex**					**Body Weight**
		A	**U**	***P*-value**	**M**	**F**	***P*-value**	**AM**	**AF**	**UM**	**UF**	***P*-value**	***P*-value|**
Broilers (n)		**55**	**48**		**65**	**38**		**39**	**16**	**26**	**22**		
P. major (g)	Mean	425.51	400.59	0.002	402.70	423.41	0.079	417.84	433.19	387.56	413.63	0.505	<0.001
	SE	4.67	4.68		4.54	7.71		6.66	10.42	6.78	9.41		
P. minor (g)	Mean	81.66	83.58	0.305	80.26	84.97	0.074	81.14^{a,b}	82.17^{a,b}	79.38^{a}	87.78^{b}	0.047	<0.001
	SE	1.55	1.61		1.54	2.06		1.89	2.61	1.98	2.41		
Wing (g)	Mean	169.62	160.31	<0.001	169.07	160.87	0.008	174.72	164.53	163.42	157.20	0.350	<0.001
	SE	1.78	1.85		1.77	2.38		2.18	3.01	2.28	2.78		
Ext. obl. (g)	Mean	7.53	7.03	0.213	6.88	7.68	0.153	7.60^{a}	7.46^{a,b}	6.15^{b}	7.90^{a}	0.018	0.006
	SE	0.26	0.28		0.26	0.40		0.35	0.52	0.37	0.48		
Heart (g)	Mean	17.74	17.83	0.867	17.84	17.74	0.893	17.86	17.62	17.81	17.85	0.786	<0.001
	SE	0.32	0.33		0.31	0.50		0.44	0.67	0.46	0.61		
Lungs	Mean	15.51	16.35	0.209	17.23	14.64	0.006	16.58	14.45	17.88	14.83	0.483	0.158

(g)	SE	0.52	0.54		0.52	0.71		0.65	0.91	0.68	0.84		
Liver	Mean	62.43	64.19	0.334	60.09	66.53	0.013	58.17	66.70	62.02	66.35	0.241	<0.001
(g)	SE	1.30	1.36		1.29	1.86		1.68	2.42	1.76	2.22		
Spleen	Mean	4.20	4.46	0.223	4.03	4.62	0.056	3.83	4.57	4.24	4.67	0.460	<0.001
(g)	SE	0.13	0.14		0.14	0.21		0.19	0.27	0.20	0.25		

Analysis was performed using a mixed linear model approach with poultry house included as a random effect. Data are presented as the least square mean and standard error. Means not sharing a common superscript letter within the interaction effect are significantly different ($P < 0.05$, Tukey's HSD test).

The external oblique muscle showed an interesting effect of the WB-sex interaction, with affected males and unaffected females having the highest average weights of those muscles and unaffected males having the lowest weights. Similarly, the weight of the pectoralis minor muscle was highest in unaffected females and lowest in unaffected males. One potential explanation for the observed group means of the external oblique muscle is as an adaptive response to the size of the combined pectoralis major and pectoralis minor muscle. Avian respiration relies on movement of the sternum to allow expansion of the bellows-like air sacs during inhalation (Schmidt-Nielsen, 1971). The external obliques are ventilatory muscles that insert onto the base of the uncinate processes of the ribs, extensions of bone that project caudally from the vertical segment of each rib, and move the sternum dorsally during expiration (Codd, 2005). Because inhalation and exhalation are active processes driven by musculoskeletal movements, additional weight, especially on the sternum increases the metabolic demand of respiration, reduces the overall effectiveness of respiratory movements (Tickle et al., 2014), and may result in strengthening of respiratory muscles. This is in accordance with unaffected males having the smallest pectoralis major muscle, pectoralis minor muscle, and external oblique muscle in the present model.

Compared to females in the present study, males possessed larger wings and lungs, but a smaller liver after accounting for WB and body weight. There was no significant difference in the size of the pectoralis major muscle between males and females in our model. Body weight had a significant effect on the sizes of all body parts except the lungs, with larger birds possessing generally heavier body parts but relatively smaller lungs.

3.4.2 Blood Analysis

The effects of WB, sex, WB-sex interaction, and body weight on 13 blood parameters are shown in Table 3.2. Compared to unaffected birds, WB affected birds exhibited significantly higher venous K^+ and significantly lower pH, sO_2, and pO_2. Affected male birds also possessed significantly higher pCO_2 and TCO_2 values compared to unaffected male birds. Although affected female birds had pCO_2 and TCO_2 values higher than those of unaffected female birds, the effect was not significant potentially due to the smaller number of female birds sampled. These results are largely in accordance with previously published data of blood parameters measured at 42 days of age (Livingston et al., 2019b, 2019a), although no significant effect of WB on Hct or BE was detected in the present study. The present model also detected a significant sex effect for BE and a WB-sex interaction effect for Glu, with males possessing higher BE than females and affected males possessing higher Glu compared to affected females. It is unclear what might be causing these specific sex effects.

Table 3.2: Effects of wooden breast (WB) status (A: affected, U: unaffected), sex (M: male, F: female), the interaction of WB and sex, and body weight on blood sodium (Na^+), potassium (K^+), ionized calcium (iCa), glucose (Glu), hematocrit (Hct), hemoglobin (Hb), pH, partial pressure of carbon dioxide (pCO_2), total carbon dioxide (TCO_2), partial pressure of oxygen (pO_2), oxygen saturation (sO_2), bicarbonate (HCO_3^-), and base excess (BE).

		WB			**Sex**			**WB x Sex**					**Body Weight**
		A	**U**	***P*-value|**	**M**	**F**	***P*-value**	**AM**	**AF**	**UM**	**UF**	***P*-value**	***P*-value|**
Broilers (n)		**55**	**48**		**65**	**38**		**39**	**16**	**26**	**22**		
Na^+	Mean	150.17	149.24	0.123	149.91	149.50	0.611	150.05	150.30	149.78	148.71	0.240	0.320
(mmol/L)	SE	0.42	0.47		0.42	0.60		0.58	0.75	0.56	0.74		
K^+	Mean	5.04	4.86	0.045	4.98	4.91	0.569	5.11	4.97	4.85	4.86	0.372	0.127
(mmol/L)	SE	0.05	0.06		0.05	0.09		0.08	0.11	0.08	0.11		
iCa	Mean	1.41	1.39	0.416	1.40	1.40	0.983	1.41	1.41	1.40	1.39	0.932	0.266
(mmol/L)	SE	0.02	0.02		0.02	0.02		0.02	0.02	0.02	0.02		
Glu	Mean	220.06	222.58	0.366	224.29	218.36	0.119	226.71^{a}	213.42^{b}	221.87^{a,b}	223.30^{a,b}	0.006	0.310
(mmol/L)	SE	1.85	2.08		1.87	2.75		2.61	3.43	2.52	3.39		
Hct	Mean	23.79	22.84	0.151	23.31	23.32	0.994	23.82	23.76	22.80	22.87	0.919	0.216
(%PCV)	SE	0.50	0.55		0.50	0.69		0.67	0.85	0.64	0.83		
Hb	Mean	8.08	7.76	0.161	7.93	7.92	0.989	8.10	8.07	7.75	7.78	0.903	0.211
(g/dL)	SE	0.17	0.19		0.17	0.24		0.23	0.29	0.22	0.29		
pH	Mean	7.360	7.389	0.007	7.382	7.367	0.268	7.364	7.356	7.401	7.377	0.396	0.600
	SE	0.008	0.009		0.008	0.011		0.011	0.014	0.010	0.013		
pCO_2	Mean	47.26	42.16	0.002	44.69	44.73	0.984	48.82^{a}	45.70^{a,b}	40.55^{b}	43.77^{a,b}	0.041	0.825
(mmHg)	SE	0.88	1.02		0.86	1.55		1.42	1.95	1.26	1.96		
TCO_2	Mean	27.81	26.87	0.125	28.01	26.67	0.111	29.06^{a}	26.57^{a,b}	26.96^{b}	26.78^{a,b}	0.045	0.333
(mmol/L)	SE	0.38	0.43		0.38	0.58		0.55	0.74	0.53	0.73		
pO_2	Mean	39.85	44.75	<0.001	42.03	42.57	0.751	39.52	40.18	44.54	44.97	0.923	0.352
(mmHg)	SE	1.16	1.22		1.15	1.48		1.42	1.79	1.38	1.71		
sO_2	Mean	70.57	79.07	<0.001	74.86	74.78	0.974	70.20	70.94	79.52	78.62	0.647	0.452
(%)	SE	1.37	1.49		1.35	1.95		1.83	2.46	1.76	2.34		
HCO_3^-	Mean	26.42	25.55	0.133	26.66	25.31	0.087	27.62	25.22	25.70	25.40	0.052	0.371
(mmol/L)	SE	0.36	0.41		0.36	0.55		0.53	0.70	0.50	0.69		
BE	Mean	1.00	0.46	0.375	1.60	-0.13	0.036	2.32	-0.31	0.88	0.05	0.113	0.443
(mmol/L)	SE	0.42	0.47		1.60	0.61		0.58	0.75	0.56	0.74		

Analysis was performed using a mixed linear model approach with poultry house included as a random effect. Data are presented as the least square mean and standard error. Means not sharing a common superscript letter within the interaction effect are significantly different ($P < 0.05$, Tukey's HSD test).

Elevated pCO_2 in conjunction with a decline in pH in WB affected birds is possibly indicative of an acid-base disorder called respiratory acidosis. While respiratory acidosis is classically defined in terms of arterial blood gas measurements, the high correlation of arterial and venous pCO_2 and pH is well-established in humans,

dogs, and chickens, as is the use of venous measurements for investigation of acid-base disturbances (Forster et al., 1972; Ilkiw et al., 1991; Wideman et al., 2003; Yildizdaş et al., 2004). Respiratory acidosis occurs when the body produces more CO_2 than can be removed by the lungs (D'Addesio, 1992). As carbon dioxide accumulates in the blood, it causes blood pH to decrease, triggering compensatory mechanisms in the kidneys, such as HCO_3^- retention, to mitigate the rising acidity. Elevated HCO_3^- levels are suggestive of renal compensation and possible chronic respiratory acidosis, as the kidneys increase excretion of acid and hydrogen ions and increase reabsorption of HCO_3^- (Carter et al., 1959). Livingston et al. (2019a) previously found increased HCO_3^- levels in WB-affected broilers. In the present study, HCO_3^- values are higher in affected males compared to unaffected males, though the WB-sex interaction effect is not quite significant in our model (*P*-value = 0.052).

Respiratory acidosis is caused either by an increase in CO_2 production (increased metabolism), a relative decrease in respiratory gas exchange (cardiopulmonary insufficiency), or both (Epstein and Singh, 2001). Previous studies comparing feed-restricted vs. non feed-restricted broilers and slow-growing vs. fast-growing broilers (Julian and Mirsalimi, 1992; Olkowski et al., 1999) have demonstrated how an increase in metabolism can cause changes to blood gas values similar to those seen in the present study. Similarly, respiratory acidosis caused by cardiopulmonary insufficiency has been demonstrated by comparing ascitic versus non-ascitic chickens (Malan et al., 2003). In the present study, body weight was investigated for a potential association with blood parameter values but did not show any significant effects (Table 3.2). The weight of the whole feathered left wing was also tested as a main effect for blood gas values as the brachial vein, from which blood

samples were taken, drains the peripheral wing tissue. However, it also showed no significant effects for blood gas values and so was excluded (data not shown). The fact that WB has a significant effect on blood gas values beyond what can be explained by body weight or wing weight suggests that a higher metabolic rate due to faster growth is not the cause of the apparent blood gas disturbance. It is, therefore, important to explore other potential metabolic, respiratory, or cardiovascular differences between WB affected and unaffected birds that might explain the results seen in this study and in previous studies (Livingston et al., 2019b, 2019a).

Metabolically, WB involves substantial alterations in the pectoralis major muscle, including an apparent increase in lipid metabolism and decrease in glycolysis (Mutryn et al., 2015a; Abasht et al., 2016; Papah et al., 2018). Increased reliance on lipids for energy production rather than glucose can raise oxygen consumption due to the lower phosphate/oxygen ratio of fatty acids, but would not be expected to raise CO_2 production (Brand, 2005). Other features of WB, such as hypercontraction of muscle fibers (Velleman et al., 2018) or increased activity of ATP-powered calcium pumps, could raise the body's energy requirements and total metabolic rate without contributing to growth rate. Sarcoplasmic/endoplasmic reticulum Ca^{2+}-ATPase (SERCA) pumps have been found to account for 40-50% of the resting metabolic rate in mouse skeletal muscle, or 12-15% of whole body resting oxygen consumption (Smith et al., 2013). Upregulation of SERCAs in the pectoralis major muscle of affected birds at market age is supported by transcriptional and proteomic evidence (Mutryn et al., 2015a; Soglia et al., 2016), and the disruption of intracellular calcium homeostasis has been identified as a key feature of the early pathogenesis of WB (Papah et al., 2018; Lake et al., 2019). The contribution of sarcoplasmic reticulum

calcium cycling to increased resting energy expenditure in the WB phenotype has been proposed (Lake and Abasht, 2020) but remains unexplored experimentally.

While numerous potential pulmonary causes of insufficient gas exchange exist, none are particularly well-supported by existing knowledge of WB or the results of the present study. Our data indicate WB is not associated with reduced lung size, altered lung morphology (see following section), or reduced respiratory musculature (i.e. the external oblique muscle).

However, the circulatory system is also intimately involved in respiratory exchange and can reduce gas exchange at the blood-gas barrier by decreasing the rate at which blood passes by the gas exchange surface in the lungs (Ludders, 2015). Evaluations of microscopic lesions associated with WB have cataloged extensive damage to the veins in the p. major muscle of affected birds as well as evidence of hemodynamic perturbations resulting from such damage (Papah et al., 2017; Sihvo et al., 2017). In many cases, venous inflammation progresses to circumferential transmural and valvular infiltration of veins by inflammatory cells (Papah et al., 2017). Subsequent congestion, edema, valvular damage, and stenosis (narrowing) or obstruction of the venous lumen (Papah et al., 2017; Sihvo et al., 2017) all indicate significant impairment of venous return and, implicitly, a reduction of cardiac output. Poor venous return in affected birds could lead to increased accumulation of metabolic waste including CO_2, as indicated by blood gas analysis in this study, and negatively affect gas exchange by slowing the flow of blood back to the gas exchange surfaces of the lungs. Impaired venous return from phlebitis may exacerbate what some characterize as existing vascular insufficiency in the pectoralis major of commercial broilers. At the cellular level, large breast muscles are produced by increasing the

number, diameter, and length of muscle fibers (Scheuermann et al., 2004; Roy et al., 2006), causing a reduction of capillary density among other effects (Hoving-Bolink et al., 2000; Joiner et al., 2014).

Apart from blood gases, the only other analyte measurement that was significantly altered in affected birds in the present study was potassium. Hyperkalemia, increased K^+, is a known effect of high blood CO_2 and therefore a common symptom of respiratory acidosis (Scribner et al., 1955; Ladé and Brown, 1963; Kilburn, 1966). Extracellular K^+ concentration is tightly regulated in the body to maintain it within the necessary range for cellular functions such as electrical excitability of cardiac and skeletal muscle (Aronson and Giebisch, 2011). The majority of the body's K^+ is located in the intracellular fluid of skeletal muscle and is shifted between muscle cells and extracellular space by the activity of various ion transport pathways (Youn and McDonough, 2009). A net loss of K+ from cells during respiratory acidosis is mediated primarily by Na^+-H^+ exchange and Na^+/K^+-ATPase activity, although extracellular elevation of bicarbonate enhances Na^+-HCO_3^- cotransport and prevents the severity of hyperkalemia seen in metabolic acidosis where bicarbonate levels are reduced (Aronson and Giebisch, 2011).

3.4.3 Histological Evaluation of the Lungs

Histologic analysis demonstrated that there was no clinically significant lung disease (pneumonia, etc.) observed in tissues from either high sO_2 or low sO_2 birds to explain detectable differences in blood oxygen saturation. A single lung specimen from the low sO_2 group exhibited moderate localized multifocal lymphoplasmacytic phlebitis consistent with vascular changes observed in WB musculature (Figure 3.1a) and was confirmed to have been collected from a low sO_2 WB affected bird following

analysis. All pulmonary tissues examined from both high sO_2 and low sO_2 birds exhibited one or more foci of chondro-osseous metaplasia, characterized by focal to multifocal islands of well-differentiated non-neoplastic cartilage or bone tissue within otherwise healthy pulmonary tissue. Chondro-osseous metaplasia is thought to arise from within pulmonary connective tissue over time in response to low oxygenation in tissues (chronic hypoxia) and has been previously reported in broiler chickens in association with ascites syndrome (Maxwell, 1988). In the present study, there was no gross evidence of fulminant ascites in any of the birds examined. While present in both WB affected and WB unaffected birds, the metaplastic change in pulmonary tissues was more extensive resulting in larger, more numerous metaplastic foci in WB affected birds (Figures 3.1b and c). This finding may indicate that while lung tissues are susceptible to hypoxic injury even in clinically normal broilers, the WB condition may exacerbate tissue changes due to regionalized or systemic hypoxia.

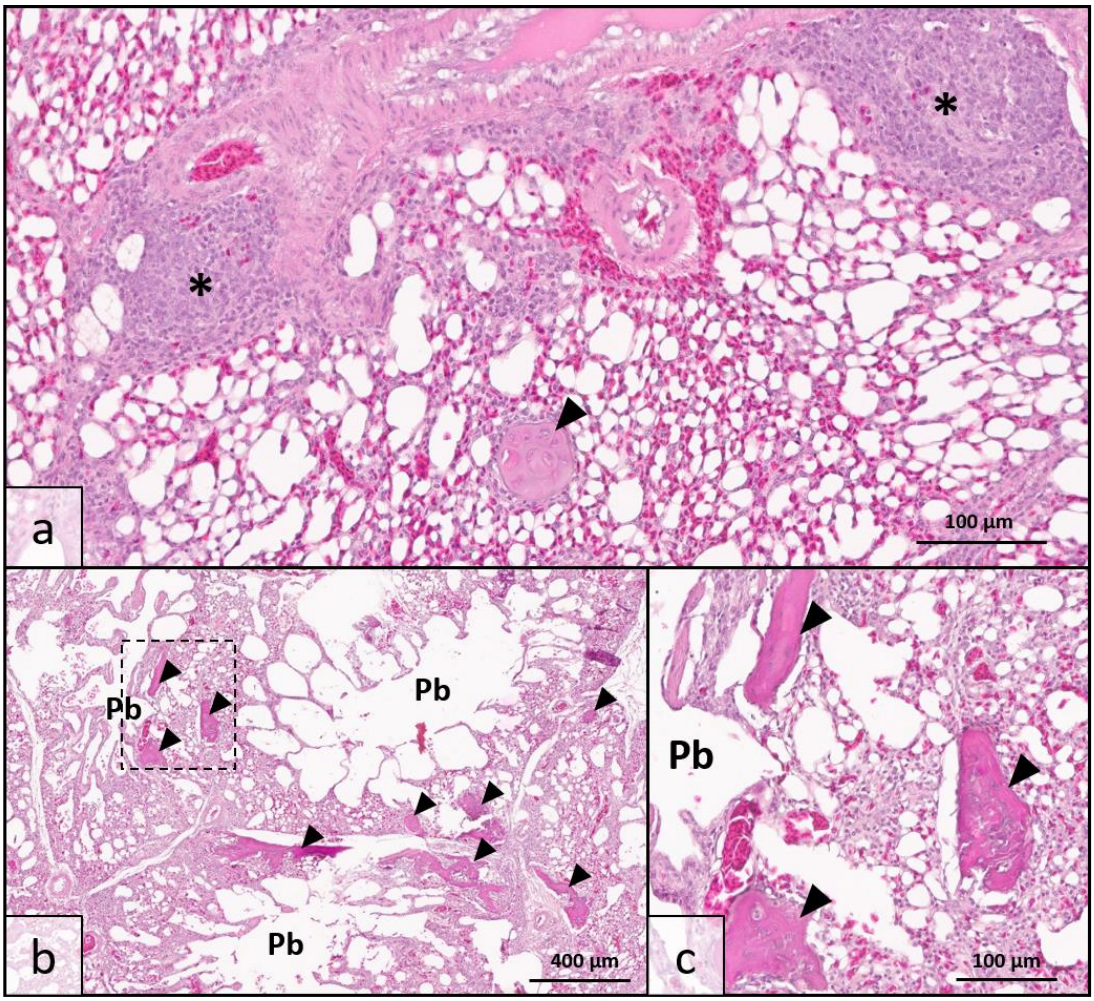

Figure 3.1: Lung histopathology of wooden breast-affected broiler chickens with low venous blood oxygen saturation (sO2).

(a) Obliterative lymphoplasmacytic venous inflammation, interpreted as phlebitis (*), was observed in one bird with sparing of adjacent arterial vessel (top) consistent with the wooden breast phenotype in muscle tissues. Chondro-osseous metaplasia (arrowhead) may be occurring as a sequela of low oxygenation in pulmonary tissues. (b) Multiple parabronchi (Pb) exhibit chondro-osseous metaplasia (arrowheads) in wooden breast-affected birds with low sO2 values. The number and size of metaplastic foci were greater than either wooden breast-affected birds with high sO2 values or unaffected birds. (c) Higher magnification of region demarcated by dotted line in 1b showing metaplastic foci in greater detail. [Hematoxylin & Eosin stain, scale bar indicates 100 µm in (a) and (c) and 400µm in (b)]

Other minor histopathologic findings included bronchus-associated lymphoid tissue (BALT) hyperplasia, occasionally with discrete nodular follicle formation, and extramedullary hematopoiesis (EMH). Generalized and nodular lymphoid hyperplasia likely indicate immune response to inhaled antigens or irritants and are not suspected to be related to WB. The airway associated lymphoid tissues did not appear to impinge upon or obstruct airway lumens. The physiologic process of EMH is common in tissues of young animals, but can sometimes occur to produce additional red blood cells in response to low tissue oxygenation. However, the limited extent and level of EMH in the lung tissues in the present study indicate that EMH is likely an incidental rather than clinically significant finding. Mild, limited EMH is a common finding in avian tissues, including lung, even in clinically normal birds. Artifactual changes from specimen collection and processing, such as acute hemorrhage with no tissue reaction and collapse of air spaces with no indication of true airway obstruction (atelectasis) were observed but disregarded for purposes of analysis.

Other minor histopathologic findings included bronchus-associated lymphoid tissue (BALT) hyperplasia, occasionally with discrete nodular follicle formation, and extramedullary hematopoiesis (EMH). Generalized and nodular lymphoid hyperplasia likely indicate immune response to inhaled antigens or irritants and are not suspected to be related to WB. The airway associated lymphoid tissues did not appear to impinge upon or obstruct airway lumens. The physiologic process of EMH is common in tissues of young animals, but can sometimes occur to produce additional red blood cells in response to low tissue oxygenation. However, the limited extent and level of EMH in the lung tissues in the present study indicate that EMH is likely an incidental rather than clinically significant finding. Mild, limited EMH is a common finding in

avian tissues, including lung, even in clinically normal birds. Artifactual changes from specimen collection and processing, such as acute hemorrhage with no tissue reaction and collapse of air spaces with no indication of true airway obstruction (atelectasis) were observed but disregarded for purposes of analysis.

Previously, our laboratory reported altered gene expression in lung tissue of WB affected broilers (Wong, 2018) which may be connected with the present finding of pulmonary phlebitis. In that study, the top significant canonical pathways identified from the list of differentially expressed genes included atherosclerosis signaling, adipogenesis, and LXR/RXR activation, a pathway involved in the regulation of lipid metabolism and inflammation. Increased expression of genes involved in lipid metabolism and uptake, such as *lipoprotein lipase* (*LPL*), *fatty acid binding protein 4* (*FABP4*), and *adiponectin c1q and collagen domain containing* (*ADIPOQ*), is reminiscent of the transcriptomic changes associated with WB in the pectoralis major muscle (Papah et al., 2018; Lake et al., 2019) and may reflect a similar mechanism. Papah and Abasht (2019) recently found increased *LPL* expression in veins undergoing phlebitis in the pectoralis major muscle of WB affected birds, further substantiating the link between increased lipid metabolism and venous inflammation. In light of this knowledge, it is possible that phlebitis in the lungs is more widespread and not fully represented by the limited number of sections and samples examined in the present study.

3.5 Conclusions

The findings of the present study indicate that WB is associated with blood gas disturbances characterized primarily by increased venous K^+ and pCO_2 and decreased pH, sO_2 and pO_2. The accumulation of carbon dioxide and acidification of venous

blood occurs when the metabolic demands of the tissue exceed the capacity of the respiratory or circulatory system. Factors that may contribute to increased metabolic demand in WB affected birds include hypercontraction of muscle fibers and, importantly, the dysregulation of calcium homeostasis. Cardiovascular and pulmonary deficiencies, specifically venous damage caused by phlebitis and disproportionate growth of the pectoralis major compared to respiratory muscles, potentially also contribute to inadequate respiratory gas exchange in affected birds. Blood gas disturbances, musculature differences, and pulmonary chondro-osseous metaplasia and phlebitis demonstrated herein may further indicate broader systemic implications of the metabolic dysfunction and circulatory insufficiency already described in existing literature regarding WB. Since these results were obtained in 7-week-old birds, findings are more informative of the WB myopathy's effects (sequelae) rather than its etiology and further studies are required to ascertain whether a blood gas disturbance is present during early stages of the disease.

3.6 Acknowledgments

The authors gratefully acknowledge the in-kind support by Cobb-Vantress Inc. in providing chicks and chicken feed. We also greatly appreciate assistance of many graduate and undergraduate students at the University of Delaware Department of Animal and Food Sciences with sample and data collection.

REFERENCES

Abasht, B., Mutryn, M. F., Michalek, R. D., and Lee, W. R. (2016). Oxidative stress and metabolic perturbations in wooden breast disorder in chickens. PLoS One 11, 1–16. doi:10.1371/journal.pone.0153750.

Aronson, P. S., and Giebisch, G. (2011). Effects of pH on potassium: New explanations for old observations. J. Am. Soc. Nephrol. 22, 1981–1989. doi:10.1681/asn.2011040414.

Brand, M. D. (2005). The efficiency and plasticity of mitochondrial energy transduction. Biochem. Soc. Trans. 33, 897. doi:10.1042/bst20050897.

Carter, N., Seldin, D., and Teng, H. (1959). Tissue and renal response to chronic respiratory acidosis. J. Clin. Invest. 38, 949–960. Available at: https://www.jci.org/articles/view/103878/files/pdf.

Chatterjee, D., Zhuang, H., Bowker, B. C., Rincon, A. M., and Sanchez-Brambila, G. (2016). Instrumental texture characteristics of broiler pectoralis major with the wooden breast condition. Poult. Sci. 95, 2449–2454. doi:10.3382/ps/pew204.

Codd, J. R. (2005). Activity of three muscles associated with the uncinate processes of the giant Canada goose Branta canadensis maximus. J. Exp. Biol. 208, 849–857. doi:10.1242/jeb.01489.

D'Addesio, J. (1992). Metabolic and respiratory acidosis. Top. Emerg. Med. 14, 51–55.

Dalle Zotte, A., Tasoniero, G., Puolanne, E., Remignon, H., Cecchinato, M., Catelli, E., et al. (2017). Effect of "Wooden Breast" appearance on poultry meat quality, histological traits, and lesions characterization. Czech J. Anim. Sci. 62, 51–57. doi:10.17221/54/2016-CJAS.

Epstein, S. K., and Singh, N. (2001). Respiratory acidosis. Respir. Care 46, 366–383. Available at: www.draegermedical.com.

Forster, H. V, Dempsey, J. A., Thomson, J., Vidruk, E., and DoPico, G. A. (1972). Estimation of arterial PO2, PCO2, pH, and lactate from arterilazed venous blood. J. Appl. Physiol. 32, 134–137.

Gall, S., Suyemoto, M. M., Sather, H. M. L., Sharpton, A. R., Barnes, H. J., and Borst, L. B. (2019). Wooden breast in commercial broilers associated with mortality, dorsal recumbency, and pulmonary disease. Avian Dis. 63, 514–519. doi:10.1637/11995-111218-case.1.

Hoving-Bolink, A. H., Kranen, R. W., Klont, R. E., Gerritsen, C. L. M., and De Greef, K. H. (2000). Fibre area and capillary supply in broiler breast muscle in relation to productivity and ascites. Meat Sci. 56, 397–402. doi:10.1016/S0309-1740(00)00071-1.

Ilkiw, J. E., Rose, R. J., and Martin, I. C. A. (1991). A comparison of simultaneously collected arterial, mixed venous, jugular venous and cephalic venous blood samples in the assessment of blood-gas and acid-base status in the dog. J. Vet. Intern. Med. 5, 294–298. doi:10.1111/j.1939-1676.1991.tb03136.x.

Joiner, K., Hamlin, G., Lien, R., and Bilgili, S. (2014). Evaluation of capillary and myofiber density in the pectoralis major muscles of rapidly growing, high-yield broiler chickens during increased heat stress. Avian Dis. 58, 377–382.

Julian, A. R. J., and Mirsalimi, S. M. (1992). Blood oxygen concentration of fast-growing and slow-growing broiler chickens , and chickens with ascites from right ventricular failure. Avian Dis. 36, 730–732.

Kilburn, K. H. (1966). Movements of potassium during acute respiratory acidosis and recovery. J. Appl. Physiol. 21, 679–684. doi:10.1152/jappl.1966.21.2.679.

Kuttappan, V. A., Hargis, B. M., and Owens, C. M. (2016). White striping and woody breast myopathies in the modern poultry industry: A review. Poult. Sci. 95, 2724–2733. doi:10.3382/ps/pew216.

Kuttappan, V. A., Shivaprasad, H. l., Shaw, D. P., Valentine, B. A., Hargis, B. M., Clark, F. D., et al. (2013). Pathological changes associated with white striping in broiler breast muscles. Poult. Sci. 92, 331–338. doi:10.3382/ps.2012-02646.

Ladé, R. I., and Brown, E. B. (1963). Movement of potassium between muscle and blood in response to respiratory acidosis. Am. J. Physiol. Content 204, 761–764. doi:10.1152/ajplegacy.1963.204.5.761.

Lake, J. A., and Abasht, B. (2020). Glucolipotoxicity: A proposed etiology for wooden breast and related myopathies in commercial broiler chickens. Front. Physiol. doi:10.3389/fphys.2020.00169.

Lake, J. A., Papah, M. B., and Abasht, B. (2019). Increased expression of lipid metabolism genes in early stages of wooden breast links myopathy of broilers to metabolic syndrome in humans. Genes (Basel). 10. doi:10.20944/preprints201906.0194.v1.

Livingston, M. L., Ferket, P. R., Brake, J., and Livingston, K. A. (2019a). Dietary amino acids under hypoxic conditions exacerbates muscle myopathies including wooden breast and white stripping. Poult. Sci. 98, 1517–1527. doi:10.3382/ps/pey463.

Livingston, M. L., Landon, C. D., Barnes, H. J., Brake, J., and Livingston, K. A. (2019b). Dietary potassium and available phosphorous on broiler growth performance, carcass characteristics, and wooden breast. Poult. Sci. 98, 2813–2822. doi:10.3382/ps/pez015.

Ludders, J. W. (2015). "Respiration in birds," in Duke's Physiology of Domestic Animals, eds. W. O. Reece, H. E. Howard, J. P. Goff, and E. E. Uemura (Ames, IA: Wiley), 245–258.

Malan, D. D., Scheele, C. W., Buyse, J., Kwakernaak, C., Siebrits, F. K., Van Der Klis, J. D., et al. (2003). Metabolic rate and its relationship with ascites in chicken genotypes. Br. Poult. Sci. 44, 309–315. doi:10.1080/000716603100024603.

Maxwell, M. H. (1988). The histology and ultrastructure of ectopic cartilaginous and osseous nodules in the lungs of young broilers with an ascitic syndrome. Avian Pathol. 17, 201–219. doi:10.1080/03079458808436439.

Mudalal, S., Lorenzi, M., Soglia, F., Cavani, C., and Petracci, M. (2015). Implications of white striping and wooden breast abnormalities on quality traits of raw and marinated chicken meat. Animal 9, 728–734. doi:10.1017/S175173111400295X.

Mutryn, M. F., Brannick, E. M., Fu, W., Lee, W. R., and Abasht, B. (2015a). Characterization of a novel chicken muscle disorder through differential gene expression and pathway analysis using RNA-sequencing. BMC Genomics 16, 1–19. doi:10.1186/s12864-015-1623-0.

Mutryn, M. F., Fu, W., and Abasht, B. (2015b). Incidence of Wooden Breast Disease and its correlation with broiler performance and ultimate pH of breast muscle. in Proceedings of XXII European Symposium on Poultry Meat Quality (Nantes, France).

Norring, M., Valros, A., Valaja, J., Sihvo, H., Immonen, K., and Puolanne, E. (2018). Wooden breast myopathy links with poorer gait in broiler chickens. Animal, 1–6. doi:10.1017/S1751731118003270.

Olkowski, A. A., Korver, D., Rathgeber, B., and Classen, H. L. (1999). Cardiac index, oxygen delivery, and tissue oxygen extraction in slow and fast growing chickens, and in chickens with heart failure and ascites: A comparative study. Avian Pathol. 28, 137–146. doi:10.1080/03079459994867.

Papah, M. B., and Abasht, B. (2019). Dysregulation of lipid metabolism and appearance of slow myofiber- specific isoforms accompany the development of Wooden Breast myopathy in modern broiler chickens. Sci. Rep., 1–12. doi:10.1038/s41598-019-53728-8.

Papah, M. B., Brannick, E. M., Schmidt, C. J., and Abasht, B. (2017). Evidence and role of phlebitis and lipid infiltration in the onset and pathogenesis of Wooden Breast Disease in modern broiler chickens. Avian Pathol. 46, 623–643. doi:10.1080/03079457.2017.1339346.

Papah, M. B., Brannick, E. M., Schmidt, C. J., and Abasht, B. (2018). Gene expression profiling of the early pathogenesis of wooden breast disease in commercial broiler chickens using RNA-sequencing. PLoS One 13, e0207346. doi:10.1371/journal.pone.0207346.

Petracci, M., Mudalal, S., Soglia, F., and Cavani, C. (2015). Meat quality in fast-growing broiler chickens. Worlds. Poult. Sci. J. 71, 363–374. doi:10.1017/S0043933915000367.

Roy, B. C., Oshima, I., Miyachi, H., Shiba, N., Nishimura, S., Tabata, S., et al. (2006). Effects of nutritional level on muscle development, histochemical properties of myofibre and collagen architecture in the pectoralis muscle of male broilers. Br. Poult. Sci. 47, 433–442. doi:10.1080/00071660600828334.

Scheuermann, G. N., Bilgili, S. F., Tuzun, S., and Mulvaney, D. R. (2004). Comparison of chicken genotypes: Myofiber number in pectoralis muscle and myostatin ontogeny. Poult. Sci. 83, 1404–1412. doi:10.1093/ps/83.8.1404.

Schmidt-Nielsen, K. (1971). How birds breathe. Sci. Am. 225, 72–79.

Scribner, B. B. H., Fremont-smith, K., and Burnell, J. M. (1955). The effect of acute respiratory acidosis on the internal equilibrium of potassium. J. Clin. Invest. 34, 1276–1285.

Sihvo, H. K., Airas, N., Lindén, J., and Puolanne, E. (2018). Pectoral vessel density and early ultrastructural changes in broiler chicken wooden breast myopathy. J. Comp. Pathol. 161, 1–10. doi:10.1016/j.jcpa.2018.04.002.

Sihvo, H. K., Immonen, K., and Puolanne, E. (2014). Myodegeneration with fibrosis and regeneration in the pectoralis major muscle of broilers. Vet. Pathol. 51, 619–623. doi:10.1177/0300985813497488.

Sihvo, H. K., Lindén, J., Airas, N., Immonen, K., Valaja, J., and Puolanne, E. (2017). Wooden breast myodegeneration of pectoralis major muscle over the growth period in broilers. Vet. Pathol. 54, 119–128. doi:10.1177/0300985816658099.

Smith, I. C., Bombardier, E., Vigna, C., and Tupling, A. R. (2013). ATP consumption by sarcoplasmic reticulum Ca2+ pumps accounts for 40-50% of resting metabolic rate in mouse fast and slow twitch skeletal muscle. PLoS One 8, 1–11. doi:10.1371/journal.pone.0068924.

Soglia, F., Mudalal, S., Babini, E., Di Nunzio, M., Mazzoni, M., Sirri, F., et al. (2016). Histology, composition, and quality traits of chicken Pectoralis major muscle affected by wooden breast abnormality. Poult. Sci. 95, 651–659. doi:10.3382/ps/pev353.

Steinmetz, H. W., Vogt, R., Kästner, S., Riond, B., and Hatt, J.-M. (2007). Evaluation of the i-STAT portable clinical analyzer in chickens (Gallus gallus). J. Vet. Diagnostic Investig. 19, 382–388.

Tickle, P. G., Paxton, H., Rankin, J. W., Hutchinson, J. R., and Codd, J. R. (2014). Anatomical and biomechanical traits of broiler chickens across ontogeny. Part I. Anatomy of the musculoskeletal respiratory apparatus and changes in organ size. PeerJ 2, e432. doi:10.7717/peerj.432.

Velleman, S. G., Clark, D. L., and Tonniges, J. R. (2018). The effect of the Wooden Breast myopathy on sarcomere structure and organization. Avian Dis. 62, 28–35. doi:10.1637/11766-110217-Reg.1.

Wideman, R. F., and French, H. (2000). Ascites resistance of progeny from broiler breeders selected for two generations using chronic unilateral pulmonary artery occlusion. Poult. Sci. 79, 396–401. doi:10.1093/ps/79.3.396.

Wideman, R. F., Hooge, D. M., and Cummings, K. R. (2003). Dietary sodium bicarbonate, cool temperatures, and feed withdrawal: Impact on arterial and venous blood-gas values in broilers. Poult. Sci. 82, 560–570. doi:10.1093/ps/82.4.560.

Wong, E. M. (2018). Differential gene expression in lung tissue of wooden breast syndrome affected and unaffected commercial broiler chickens. [undergraduate thesis]. [Newark (DE)]: University of Delaware.

Yildizdaş, D., Yapicioğlu, H., Yilmaz, H. L., and Sertdemir, Y. (2004). Correlation of simultaneously obtained capillary, venous, and arterial blood gases of patients in a paediatric intensive care unit. Arch. Dis. Child. 89, 176–180. doi:10.1136/adc.2002.016261.

Youn, J. H., and McDonough, A. A. (2009). Recent advances in understanding integrative control of potassium homeostasis. Annu. Rev. Physiol. 71, 381–401. doi:10.1146/annurev.physiol.010908.163241.

Chapter 4

3-METHYLHISTIDINE AS PROMISING PLASMA BIOMARKER OF WOODEN BREAST AND WHITE STRIPING

(Juniper A. Lake, Jack C.M. Dekkers, Yiren Yan, Jing Qiu, Erin M. Brannick, & Behnam Abasht. In Review (2021)).

4.1 Abstract

Current diagnostic methods for wooden breast and white striping, common breast muscle myopathies of modern commercial broiler chickens, rely on subjective examinations of the pectoralis major muscle, time-consuming microscopy, or expensive imaging technologies. Further research on these disorders would benefit from more quantitative and objective measures of disease severity that can be used in live birds. To this end, we utilized untargeted metabolomics alongside two statistical approaches to evaluate plasma metabolites as potential biomarkers of wooden breast and white striping in 250 male commercial broiler chickens. First, mixed linear modeling was employed to identify metabolites with a significant association with these muscle disorders and found 98 metabolites associated with wooden breast and 44 metabolites associated with white striping (q-value < 0.05). Second, a support vector machine was constructed using stepwise feature selection to determine the smallest subset of metabolites with the highest prediction accuracy for wooden breast. The final support vector machine achieved a prediction accuracy of 94% using only 6 metabolites. The metabolite 3-methylhistidine, which is often used as an index of myofibrillar breakdown in skeletal muscle, was the top metabolite for both wooden

breast and white striping in our mixed linear model and was also the metabolite with highest marginal prediction accuracy (82%) for wooden breast in our support vector machine.

4.2 Introduction

Wooden breast and white striping are breast muscle disorders of modern commercial broiler chickens that inflict a substantial economic burden on the poultry industry worldwide due to the high prevalence and detrimental effects of these diseases on meat quality and appearance. Despite distinct appearances, these myopathies are believed to be part of the same disease spectrum or progression (Griffin et al., 2018; Mutryn et al., 2015), frequently manifest together in the same bird, and have high genetic correlation with each other ($r = 0.9$) (Lake et al., 2021). At the microscopic level, both disorders present with similar lesions, including myodegeneration with regeneration, necrosis, lymphocyte and macrophage infiltration, fibrosis, and lipidosis (Kuttappan et al., 2013; Sihvo et al., 2014). However, severe wooden breast is clinically and grossly characterized by palpable firmness of the pectoralis major muscle, particularly at the cranial end, while white striping appears grossly as fatty white striations that run parallel to the muscle fibers.

Although the exact etiologies of these myopathies are still not fully understood, it is clear that both genotype and environmental factors play a role (Bailey et al., 2020; Lake et al., 2021). One major hypothesis proposes shared pathogenesis with metabolic syndrome and type 2 diabetes mellitus in mammals, wherein differences in insulin signaling and glucose transport in the skeletal muscle of chickens produce symptoms most akin to mammalian diabetic complications in the heart, liver, and kidneys (Lake and Abasht, 2020). However, further research into the

biological basis of wooden breast and white striping is hampered by current diagnostic techniques, which rely primarily on manual palpation and visual examination of the breast muscle. Such techniques are either not very accurate in live birds (palpation) or not applicable to live birds (gross examination of muscle at processing or necropsy) and can be biased by the subjectivity and inconsistency of scorers. Diagnosis using histology or muscle metabolomics can be performed on live birds using muscle biopsies (Papah et al., 2017, 2018), but this technique is invasive, substantially affected by sampling site, and not well suited to studies that require repeated measurements over time. A diagnostic model based on blood, plasma, or serum metabolites would allow for objective and repeatable quantification of disease severity in live birds, and would thus vastly improve the quality of diagnostics and research relating to wooden breast and white striping.

Metabolomic approaches have previously been used to identify biomarkers and key metabolic pathways associated with wooden breast and white striping in broiler chickens. For example, Abasht et al. (Abasht et al., 2016) highlighted altered lipid and carbohydrate metabolism in birds affected with wooden breast, as well as changes in histidine and glutathione metabolism that may indicate increased inflammation, oxidative stress, and muscle protein breakdown. Similarly, (Boerboom et al., 2018) found increased levels of long-chain fatty acids and signs of perturbations to the citric acid cycle associated with white striping. However, it has become evident that the effects of such breast muscle myopathies extend beyond the pectoralis major muscle, with systemic changes described in the vasculature, blood, lungs, and other skeletal muscles (Kuttappan et al., 2013; Severyn et al., 2019; Lake et al., 2020; Abasht et al., 2021). As previous metabolomics studies have generally been limited to the pectoralis

major muscle, metabolomics profiling of wooden breast and white striping using blood can provide novel insights about the diseases from a more systemic perspective.

In this study, we applied an untargeted metabolomics approach to identify plasma metabolites associated with wooden breast and white striping in male broiler chickens at market age. The primary objectives of this study were (i) to identify plasma metabolites that can be used to identify and objectively quantify wooden breast and white striping in live birds and (ii) to provide insights into the underlying pathophysiology of these myopathies.

4.3 Materials and Methods

4.3.1 Test Animals, Study Design, and Sampling

All animal procedures were performed in accordance with guidelines set by The University of Delaware Institutional Animal Care and Use Committee (IACUC) and were approved by IACUC under protocol number 48R-2015-0. The sample population consisted of 250 commercial broiler chickens selected from a previously described study population (Lake et al., 2021) according to wooden breast scores and sex determined at necropsy (selection criteria described below). All birds were offspring from the same breeding population of 15 sires and 200 dams, but were raised in two separate hatches (n1 = 109, n2 = 141). Broilers were housed according to optimal industry standards in five poultry houses on the University of Delaware Newark campus farm complex (Newark, DE) and given free access to feed and water until approximately 7 weeks of age, at which time they were euthanized by cervical dislocation. Due to the complexity of sample collection and number of birds, bird necropsy was conducted over 4 days, at 48, 49, 52, and 53 days of age, once the birds

had reached full market weight. Preceding euthanasia, live weight was recorded and whole blood samples were collected from the brachial wing vein of each bird using a 3mL syringe with 23-gauge needle and placed in lithium heparin-coated tubes. Plasma was separated by centrifugation and stored at -80˚C until further analysis. During necropsy, the pectoralis major muscles were evaluated visually and by manual palpation for gross lesions and palpable firmness associated with wooden breast. Each bird was assigned a wooden breast score according to the 5-point scale described by Lake et al. (Lake et al., 2021), with the exception that "1-Very Mild" was renamed "1-Minimal": 0-Normal, 1-Minimal, 2-Mild, 3-Moderate, and 4-Severe. White striping was also assessed at this time and each bird was assigned a white striping score using a 4-point scale described by Lake et al. (Lake et al., 2021): 0-Normal, 1-Mild, 2-Moderate, and 3-Severe.

Plasma samples from 250 birds were selected for metabolomics profiling using the following criteria. First, birds associated with plasma samples with volumes less than 120 µl were not included. Second, birds were filtered to retain only those determined to be males at necropsy and otherwise in good health (e.g. no indication of ascites or leg defects). Third, birds were selected based on wooden breast score to maximize statistical power in detecting differences between the extremes of the wooden breast disease spectrum. Samples from birds receiving extreme scores (0-Normal, 3-Moderate, and 4-Severe) were selected first and then additional samples were randomly selected from the pool of birds with scores of 1-Minimal. No birds with scores of 2-Mild were included in this study. Sex was later confirmed using genetic analysis of sex chromosomes (Lake et al., 2021).

4.3.2 Metabolomic Sample Accessioning and Preparation

Frozen plasma samples were thawed at room temperature and 120 µl aliquots of each sample were placed in individual 2.0 mL polypropylene tubes before being immediately flash frozen in liquid nitrogen. Frozen aliquots were shipped on dry-ice to Metabolon Inc. (Durham, NC) for metabolomics profiling using ultrahigh performance liquid chromatography-tandem mass spectrometry (UPLC-MS/MS).

Following receipt, samples were inventoried and immediately stored at -80˚C until processing. Each sample received was accessioned into the Metabolon Laboratory Information Management System (LIMS) system and was assigned a unique identifier that was used to track all sample handling, tasks, and results. The samples (and all derived aliquots) were tracked by the LIMS system.

Samples were prepared using the automated MicroLab STAR system (Hamilton Company). Several recovery standards were added prior to the first step in the extraction process for quality control purposes. To remove protein, to dissociate small molecules that were bound to protein or trapped in the precipitated protein matrix, and to recover chemically diverse metabolites, proteins were precipitated with methanol under vigorous shaking for 2 min (Glen Mills GenoGrinder 2000), followed by centrifugation. The resulting extract was divided into five fractions for analysis using four different methods, and one sample reserved for backup. Samples were placed briefly on a TurboVap (Zymark) to remove the organic solvent and then stored overnight under nitrogen before preparation for analysis. Several types of controls were analyzed in concert with the experimental samples; a detailed description of the quality control methods can be found in Appendix A.

4.3.3 Ultrahigh Performance Liquid Chromatography-Tandem Mass Spectroscopy (UPLC-MS/MS)

All mass spectroscopy methods utilized a Waters ACQUITY ultra-performance liquid chromatography (UPLC) and a Thermo Scientific Q-Exactive high resolution/accurate mass spectrometer interfaced with a heated electrospray ionization (HESI-II) source and Orbitrap mass analyzer operated at 35,000 mass resolution. The sample extract was dried then reconstituted in solvents compatible to each of the four methods: two separate reverse phase (RP)/UPLC-MS/MS methods with positive ion mode electrospray ionization (ESI), one for analysis by RP/UPLC-MS/MS with negative ion mode ESI, one for analysis by hydrophilic interaction liquid chromatography (HILIC)/UPLC-MS/MS with negative ion mode ESI. The scan range varied slighted between methods but covered 70-1000 m/z.

Samples were balanced across multiple run days to conserve the ratio of wooden breast scores and to help account for inter-day tuning differences in instruments. Additional details on the UPLC-MS/MS methods are available in the Appendix A.

4.3.4 Compound Identification and Quantification

Metabolites were identified and quantified by Metabolon using Metabolon's hardware and software. Compounds were identified by comparison to library entries of purified standards or recurrent unknown entities. Biochemical identification was based on three criteria: retention time within a narrow refractive index window of the proposed identification, accurate mass match to the library +/- 10 ppm, and the MS/MS forward and reverse scores between the sample data and authentic standards. The size of peaks was quantified using area-under-the-curve.

4.3.5 Data Pre-Processing

To account for inter-day tuning differences of instruments, area-under-the curve values for each metabolite were divided by the median value of their associated run-day to equalize the medians across run-day. Metabolites or samples that contained more than 20% missing values were removed and the remaining values were log transformed and standardized to set the mean of each metabolite equal to zero and the standard deviation equal to one. Missing values, which were primarily associated with lower limits of detection, were imputed using the minimum value for that metabolite. All subsequent analyses were performed using these log-transformed, standardized and imputed metabolite values.

4.3.6 Statistical Analysis

Metabolites that passed the filter criteria described above were individually tested for a relationship with wooden breast score using the following linear mixed model implemented with the 'lme4qtl' package version 0.2.2 (Ziyatdinov et al., 2018) in R:

$$\boldsymbol{y} = \boldsymbol{Xb} + \boldsymbol{Zu} + e, \qquad \textit{Equation 1}$$

where $\boldsymbol{y}$ is a vector of standardized metabolite values, $\boldsymbol{b}$ is the vector of fixed effects and the overall mean (a vector of 1's), $\boldsymbol{X}$ an incidence matrix for fixed effects, $\boldsymbol{u}$ is a vector of random polygenic effects, $\boldsymbol{Z}$ is an incidence matrix corresponding to $\boldsymbol{u}$, and e is the residual error. Fixed effects included wooden breast score (or white striping score) and poultry house as discrete class variables and body weight at 7 weeks as a continuous variable. The effects of hatch and age at blood sample collection were both fully nested (collinear) with poultry house and, therefore, not included in the model. Random effects u and e were assumed to follow normal distributions: $\boldsymbol{u} \sim N\left(0, \sigma_g^2 \boldsymbol{G}\right)$

and $e \sim N(0, \sigma_e^2 \boldsymbol{I}_n)$, where σ_g^2 is the genetic variance, σ_e^2 is the variance of the residual errors, $\boldsymbol{G}$ is the genomic relationship matrix acquired from Lake et al. (Lake et al., 2021), and $\boldsymbol{I}_n$ is an identity matrix of dimension n. Since the 'lme4qtl' package does not provide estimates of significance, a type II Wald chi-square test was performed with the R package 'car' version 3.0-10 (Fox and Weisberg, 2019) to test the significance of wooden breast or white striping score for each metabolite. Metabolites were considered to have a significant association with wooden breast or white striping score if the FDR-adjusted p-value was below 0.05 (Benjamini and Hochberg, 1995). Pairwise comparisons of the estimated marginal means for each wooden breast and white striping score were performed for significant metabolites with the R package "emmeans" (Lenth, 2019). Pathway enrichment analysis of significant metabolites associated with wooden breast was conducted with MetaboAnalyst 5.0 (https://www.metaboanalyst.ca) using the *Gallus gallus* KEGG pathway library, with significance assessed using a hypergeometric test.

To assess the usefulness of metabolic traits in genetic studies of wooden breast, heritability was calculated for each metabolite as the ratio of genetic to phenotypic variance, i.e. the sum of genetic and residual variance, and reported only for significant metabolites. Heritability estimation was performed with GCTA version 1.26.0 using the same model described above, except that fixed effects only included poultry house and body weight.

4.3.7 Construction of Support Vector Machine (SVM) Classifier

Support vector machine (SVM) is a supervised machine learning algorithm that is frequently used for classification and prediction. It maps labeled training samples to points in space and selects a decision boundary between categories so as to

maximize the distance between that boundary and the data points in each category (Noble, 2006). Test samples are then mapped into that same space and predicted to belong to a category based on which side of the boundary they fall. To improve this model's classification power, birds with wooden breast scores of 0-Normal and 1-Minimal were consolidated into a single group that will be called "Unaffected" and birds with wooden breast scores of 3-Moderate and 4-Severe were consolidated into a single group that will be called "Affected".

The SVM with the optimal subset of metabolites for classifying birds as wooden breast Affected or Unaffected was constructed using an integrated machine learning feature selection algorithm, implemented in the R package 'caret' version 3.6.3 (Kuhn, 2008). Specifically, stepwise selection was implemented to determine the smallest subset of metabolites with the highest prediction accuracy (proportion of true positives). First, the metabolite with the highest prediction accuracy calculated through leave-one-out cross-validation was added to the SVM. At each subsequent step, a new metabolite was added or an existing metabolite was removed if the prediction accuracy was increased according to leave-one-out cross-validation. The stepwise selection was complete when adding metabolites to the SVM or removing them from the SVM failed to increase prediction accuracy. All metabolites included in the final SVM were considered important for prediction with their relative importance concordant with the order in which they were added to the SVM.

Although radial and linear kernels were both evaluated, the linear kernel produced higher accuracy and is reported here with its only hyperparameter, cost (*C*), which is a misclassification penalty that was tuned to achieve the highest average

prediction accuracy by nested cross-validation. The final SVM had 6 metabolite predictors and a *C* of 0.1.

4.4 Results

4.4.1 Quality Control

A total of 615 metabolites were detected and quantitated, with 581 compounds passing quality control filter criteria. Of the 250 birds from that were sampled for metabolomic profiling, 4 were found to be genetically female despite being recorded as male at necropsy and were excluded from all subsequent analyses. The distributions of wooden breast score and white striping score among the remaining 246 male broilers are described in Table 4.1. One bird with a wooden breast score of 3-Moderate and a white striping score of 2-Moderate did not pass sequencing quality control and was excluded from the linear mixed model analysis, which controlled for relatedness by means of a genomic relatedness matrix constructed from SNP genotype data (Lake et al., 2021).

Table 4.1: Distribution of wooden breast and white striping scores among 7-week-old broiler chickens sampled for metabolomic analysis and confirmed to be genetically male (n=246 total).

	Wooden Breast Score				
	0-Unaffected	1-Minimal	2-Mild	3-Moderate	4-Severe
n	68	23	0	135	20
	White Striping Score				
	0-Unaffected	1-Mild	2-Moderate	3-Severe	
n	59	79	82	25	

4.4.2 Plasma Metabolites Associated with Wooden Breast and White Striping

The association of wooden breast and white striping scores with metabolite levels was first investigated using a mixed linear model, which identified 98 metabolites that were significantly associated with wooden breast score and 44 metabolites that were significantly associated with white striping score. The metabolites that were associated with white striping score were almost entirely a subset of those found to be significant for wooden breast, with only 4 metabolites that were unique to white striping – 1-palmitoyl-2-arachidonoyl-GPE (16:0/20:4), 1-palmitoyl-2-oleoyl-GPE (16:0/18:1), chiro-inositol, and stearoyl sphingomyelin (d18:1/18:0). The majority of significant metabolites were amino acids or lipids, with the greatest effects of wooden breast and white striping relating to histidine metabolism and sphingolipid metabolism (Figure 4.1). The top metabolite for both muscle disorders was 3-methylhistidine, which showed clear differences between birds with no apparent disease and those with even minimal disease.

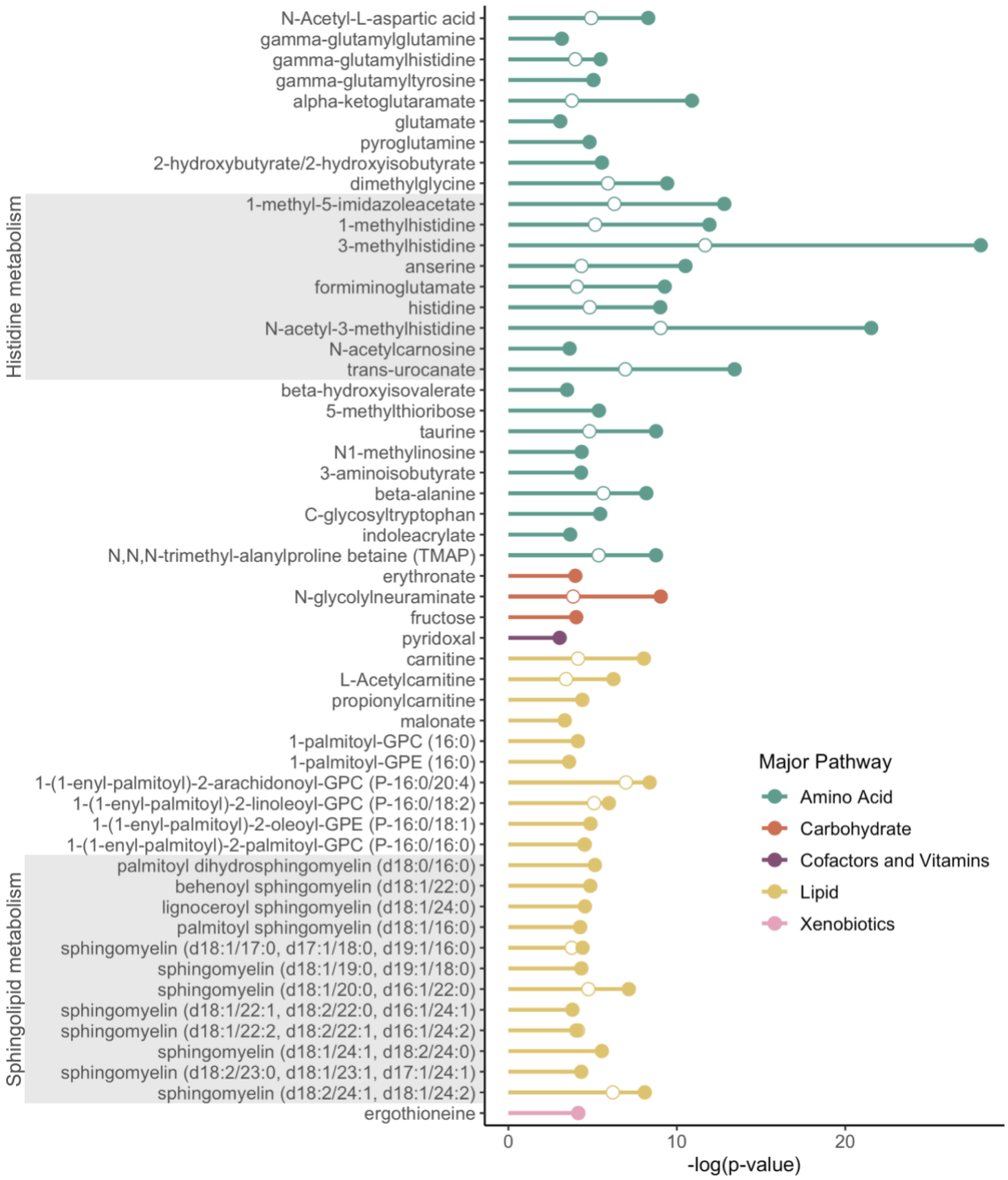

Figure 4.1: Top metabolites (q-value < 0.01) associated with wooden breast (closed circles) and white striping (open circles) in male broiler chickens at market age (7 weeks).

4.4.3 Pathway Enrichment

A total 75 of the 98 metabolites identified as significant for wooden breast were recognized by the MetaboAnalyst database. Pathway enrichment analysis found two significant pathways – histidine metabolism and beta-alanine metabolism. The results of this analysis, including the metabolites associated with each significant pathway, are presented in Table 4.2.

Table 4.2: Results of pathway enrichment analysis for wooden breast metabolites.

Pathway	**FDR**	**Metabolites**
Histidine metabolism	0.000016	3-methylhistidine; anserine; glutamate; histamine; histidine; formiminoglutamate; trans-urocanate
Beta-alanine metabolism	0.073	5,6-dihydrouracil; anserine; beta-alanine, histidine, spermine

4.4.4 Metabolite Heritability

Genetic marker data was used to estimate heritability for metabolites significantly associated with wooden breast score. Metabolite heritability estimates varied widely (Table 4.3), with several metabolites including histamine and pyroglutamine showing no heritability ($h^2 = 0$) and one metabolite, glutarylcarnitine (C5-DC), showing the highest heritability ($h^2 = 1$). Notably, the top metabolite associated with both wooden breast and white striping in this study, 3-methylhistidine, showed high heritability ($h^2 = 0.90 \pm 0.18$).

Table 4.3: Heritability estimates for metabolites significantly associated with wooden breast score in mixed linear model analysis. Heritability was estimated from genetic marker data.

Metabolite Name	Heritability	Standard Error
1-(1-enyl-palmitoyl)-2-arachidonoyl-GPC (P-16:0/20:4)	0.67	0.17
1-(1-enyl-palmitoyl)-2-linoleoyl-GPC (P-16:0/18:2)	0.66	0.16
1-(1-enyl-palmitoyl)-2-oleoyl-GPC (P-16:0/18:1)	0.55	0.16
1-(1-enyl-palmitoyl)-2-oleoyl-GPE (P-16:0/18:1)	0.25	0.14
1-(1-enyl-palmitoyl)-2-palmitoyl-GPC (P-16:0/16:0)	0.38	0.16
1-(1-enyl-stearoyl)-2-arachidonoyl-GPE (P-18:0/20:4)	0.35	0.16
1-(1-enyl-stearoyl)-2-linoleoyl-GPE (P-18:0/18:2)	0.62	0.17
1-(1-enyl-stearoyl)-GPE (P-18:0)	0.36	0.16
1-arachidonoyl-GPC (20:4)	0.33	0.17
1-linoleoyl-GPC (18:2)	0.06	0.10
1-methyl-5-imidazoleacetate	0.50	0.18
1-methylhistidine	0.57	0.20
1-palmitoleoyl-GPC (16:1)	0.17	0.14
1-palmitoyl-GPC (16:0)	0.00	0.13
1-palmitoyl-GPE (16:0)	0.20	0.15
1-stearoyl-GPE (18:0)	0.13	0.13
1,2-dipalmitoyl-GPE (16:0/16:0)	0.20	0.16
2-hydroxybutyrate/2-hydroxyisobutyrate	0.42	0.19
2-hydroxyglutarate	0.09	0.14
2-oxoadipate	0.58	0.18
3-(3-amino-3-carboxypropyl)uridine	0.57	0.17
3-aminoisobutyrate	0.78	0.18
3-methylhistidine	0.90	0.18
4-acetylphenyl sulfate	0.00	0.10
4-ethylphenol glucuronide	0.22	0.15
5-methylthioadenosine (MTA)	0.71	0.18
5-methylthioribose	0.40	0.18
5,6-dihydrouracil	0.05	0.11
aconitate [cis or trans]	0.27	0.16
adenine	0.38	0.17
alpha-ketoglutaramate	0.60	0.18
anserine	0.56	0.18

behenoyl sphingomyelin (d18:1/22:0)	0.53	0.18
beta-alanine	0.43	0.19
beta-hydroxyisovalerate	0.37	0.17
C-glycosyltryptophan	0.89	0.15
carnitine	0.72	0.17
catechol glucuronide	0.11	0.12
cholesterol	0.12	0.16
deoxycarnitine	0.52	0.19
dimethylglycine	0.78	0.17
equol glucuronide	0.02	0.10
ergothioneine	0.36	0.16
erythronate	0.57	0.18
formiminoglutamate	0.58	0.19
fructose	0.49	0.18
gamma-glutamylglutamine	0.23	0.15
gamma-glutamylhistidine	0.61	0.20
gamma-glutamyltyrosine	0.50	0.18
glutamate	0.25	0.16
glutamine	0.14	0.12
glutarylcarnitine (C5-DC)	1.00	0.14
histamine	0.00	0.12
histidine	0.49	0.20
hydroxyasparagine	0.79	0.17
imidazole lactate	0.63	0.18
iminodiacetate (IDA)	0.00	0.10
indoleacrylate	0.10	0.12
indolepropionate	0.00	0.11
indolin-2-one	0.00	0.10
L-Acetylcarnitine	0.54	0.18
lignoceroyl sphingomyelin (d18:1/24:0)	0.41	0.18
linoleoylcarnitine (C18:2)	0.00	0.12
maleate	0.02	0.08
malonate	0.06	0.10
N-acetyl-3-methylhistidine	0.87	0.17
N-Acetyl-L-aspartic acid	0.56	0.19
N-acetylcarnosine	0.47	0.17
N-glycolylneuraminate	0.51	0.19

N,N,N-trimethyl-alanylproline betaine (TMAP)	0.66	0.18
N1-methylinosine	0.23	0.15
N6,N6,N6-trimethyllysine	0.53	0.16
palmitoyl dihydrosphingomyelin (d18:0/16:0)	0.77	0.17
palmitoyl sphingomyelin (d18:1/16:0)	0.55	0.17
propionylcarnitine	0.51	0.17
pyridoxal	0.25	0.16
pyroglutamine	0.00	0.09
spermine	0.01	0.07
sphingomyelin (d17:1/16:0, d18:1/15:0, d16:1/17:0)	0.69	0.17
sphingomyelin (d18:0/18:0, d19:0/17:0)	0.49	0.17
sphingomyelin (d18:1/14:0, d16:1/16:0)	0.51	0.20
sphingomyelin (d18:1/17:0, d17:1/18:0, d19:1/16:0)	0.72	0.16
sphingomyelin (d18:1/19:0, d19:1/18:0)	0.79	0.16
sphingomyelin (d18:1/20:0, d16:1/22:0)	0.75	0.16
sphingomyelin (d18:1/21:0, d17:1/22:0, d16:1/23:0)	0.32	0.16
sphingomyelin (d18:1/22:1, d18:2/22:0, d16:1/24:1)	0.60	0.17
sphingomyelin (d18:1/22:2, d18:2/22:1, d16:1/24:2)	0.58	0.17
sphingomyelin (d18:1/24:1, d18:2/24:0)	0.53	0.17
sphingomyelin (d18:2/23:0, d18:1/23:1, d17:1/24:1)	0.47	0.17
sphingomyelin (d18:2/24:1, d18:1/24:2)	0.69	0.17
stearoylcarnitine (C18)	0.12	0.15
taurine	0.17	0.13
tauroursodeoxycholate	0.53	0.20
threonate	0.11	0.12
trans-urocanate	0.25	0.18
tricosanoyl sphingomyelin (d18:1/23:0)	0.44	0.18
tyrosine	0.28	0.15
xanthosine	0.86	0.16

4.4.5 SVM Classification

The optimized SVM achieved prediction accuracy of 94.3% using the leave-one-out cross-validation method with the following six metabolite predictors: 3-methylhistidine, N-acetyl-L-aspartic acid, glycerate, N,N,N-trimethyl-5-

aminovalerate, alanine, and O-sulfo-L-tyrosine. The marginal prediction accuracy associated with each metabolite in the model is reported in Table 4.4. Only two of these metabolites, 3-methylhistidine and N-acetyl-L-aspartic acid, were identified as significantly associated with wooden breast in the previously described mixed linear model analysis. The relatively low overlap of results between these two analyses is likely due, at least in part, to correlation structure among metabolites, which is considered redundant information with regards to prediction accuracy of a classification model.

Table 4.4: Optimal metabolite set for wooden breast classification using support vector machine with stepwise feature selection and relevant performance measures.

Order	**Metabolite**	**Marginal Accuracy[1,2]**	**Total Accuracy**	**Precision[3]**	**Recall[4]**	**F_1 Score[5]**
1	3-methylhistidine	0.817	0.817	0.844	0.871	0.857
2	N-acetyl-L-aspartic acid	0.073	0.890	0.900	0.929	0.914
3	glycerate	0.017	0.907	0.913	0.942	0.927
4	N,N,N-trimethyl-5-aminovalerate	0.020	0.927	0.925	0.955	0.940
5	alanine	0.012	0.939	0.938	0.968	0.952
6	O-sulfo-L-tyrosine	0.004	0.943	0.938	0.974	0.956

[1]Accuracy = true positives / (true positives + false positives + true negatives + false negatives)
[2]Marginal prediction accuracy is the increase in total prediction accuracy achieved by adding the associated metabolite
[3]Precision = true positives / (true positives + false positives)
[4]Recall = true positives / (true positives + false negatives)
[5]F_1 Score = 2 × (precision × recall)/ (precision + recall)

4.5 Discussion

4.5.1 Histidine Metabolism

Histidine was elevated in association with wooden breast score (Figure 4.2) and white striping score, as well as eight additional metabolites related to histidine metabolism including 1-methylhistidine, 1-methyl-5-imidazoleacetate, 3-methylhistidine, anserine, formiminoglutamate, imidazole lactate, N-acetyl-3-methylhistidine, and trans-urocanate. A histidine derivative called 3-methylhistidine was identified as the most significant metabolite associated with wooden breast and white striping in regression analysis (Figure 4.1; wooden breast q-value = $5.18x10^{-26}$, white striping q-value = $1.21x10^{-09}$) and also the top metabolite for classifying birds as wooden breast affected or unaffected via our linear SVM model (Table 4.4). Using 3-methylhistidine alone in the SVM model achieves an impressively high prediction accuracy of 82% (Table 4.4). 3-methylhistidine is found mainly in the contractile proteins of skeletal muscle, actin and myosin, and is one of the few amino acids that cannot be reutilized for protein synthesis (Ballard and Tomas, 1983). After the intracellular breakdown of actin and myosin, 3-methylhistidine is released into the blood stream and excreted in urine. Its concentration in plasma and urine is used as an index of myofibrillar breakdown in skeletal muscle, though dietary intake of 3-methylhistidine in ingested muscle protein must be restricted in order to obtain accurate measurements (Ballard and Tomas, 1983).

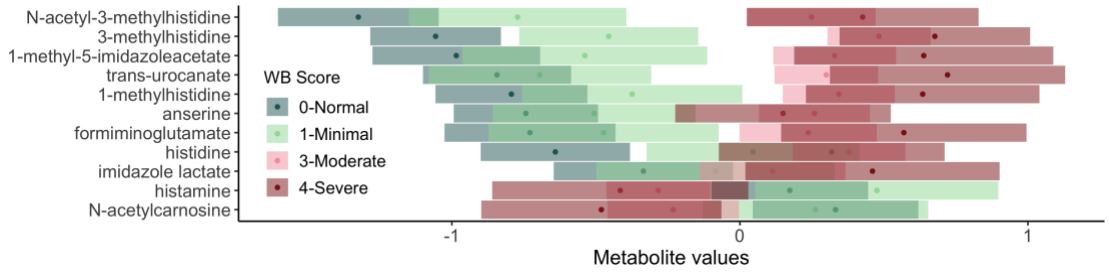

Figure 4.2: Association of wooden breast score with histidine metabolism in plasma of male broiler chickens.

Results of post-hoc analysis of metabolite values by wooden breast score are shown with estimated marginal means (dots) and confidence intervals (bars). Overlapping confidence intervals indicate that there is no significant difference between the two scores. To improve visualization, metabolites are listed in order of the adjusted means for a wooden breast score of 0-Normal.

Previously, Abasht et al. (Abasht et al., 2016) found elevated levels of 3-methylhistidine, histidine, and 1-methylhistidine in wooden breast affected pectoralis major compared to unaffected pectoralis major samples. Vignale et al. (Vignale et al., 2017) also found higher concentrations of 3-methylhistidine, expressed as a higher fractional breakdown rate, in broiler breast muscle samples with severe white striping compared to normal samples. These findings are consistent with histological and compositional observations associated with wooden breast, specifically a decrease in protein content in the pectoralis major and a reduced number of muscle fibers (Soglia et al., 2016). It is important to note that protein breakdown rates and the associated changes to 3-methylhistidine in the breast muscle and excreta of broilers have been associated with differences in body composition and feed efficiency (Tomas et al., 1988; Pym et al., 2004). However, birds that are more susceptible to wooden breast and white striping tend to have high feed efficiency and high breast muscle yield, which are generally associated with reduced protein breakdown, or reduced 3-

methylhistidine, at least in response to greater protein intake (Tomas et al., 1988; Pym et al., 2004).

In humans, increased levels of 1-methylhistidine and 3-methylhistidine in urine are associated with obesity and uncontrolled diabetes mellitus (Marchesini et al., 1982; Tůma et al., 2005). This is consistent with previous findings from our laboratory that support similarities in the pathogenesis of wooden breast and white striping in broilers and metabolic syndrome and type 2 diabetes in mammals (Lake et al., 2019, 2021; Lake and Abasht, 2020), although this comparison does not hold for histidine and histamine. It has been reported that lower plasma concentrations of histidine and higher plasma concentrations of histamine are associated with obesity and type 2 diabetes (Mihalik et al., 2012; Niu et al., 2012), with histidine supplementation contributing to amelioration of metabolic syndrome including improvements to inflammation and oxidative stress (Feng et al., 2013). Histidine supplementation in chickens also produces anti-oxidant benefits (Kopeć et al., 2013), although at high levels it can drastically reduce weight gain in growing birds (Edmonds and Baker, 1987).

4.5.2 Beta-alanine and Taurine Metabolism

One manner by which histidine supplementation improves antioxidant status is by increasing levels of the histidine-derived antioxidants anserine and carnosine in muscle. Anserine and carnosine were previously found to be reduced in wooden breast-affected pectoralis major muscle (Abasht et al., 2016), providing further evidence of altered redox homeostasis associated with the myopathy. In plasma, we found that anserine was increased in birds with greater wooden breast severity (Figure 4.3) although there was no significant association between wooden breast score and

carnosine levels. A likely contributor to low anserine and carnosine in the pectoralis major muscle is insufficient plasma beta-alanine (Figure 4.3), as the rate of carnosine and anserine synthesis in skeletal muscle is limited by circulating availability of the precursor beta-alanine. It is unclear if reduced plasma beta-alanine in wooden breast is caused by its depletion in response to oxidative stress or by some other mechanism.

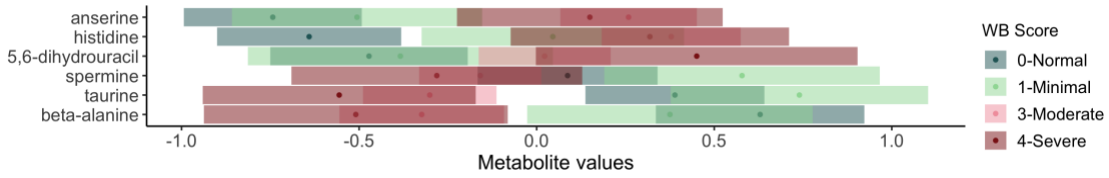

Figure 4.3: Association of wooden breast score with beta-alanine and taurine metabolism in plasma of male broiler chickens.

Results of post-hoc analysis of metabolite values by wooden breast score are shown with estimated marginal means (dots) and confidence intervals (bars). Overlapping confidence intervals indicate that there is no significant difference between the two scores. To improve visualization, metabolites are listed in order of the adjusted means for a wooden breast score of 0-Normal.

In humans, beta-alanine uptake into skeletal muscle cells is thought to be mediated by two transporters, proton-coupled amino acid transporter 1 (PAT1) and taurine transporter (TauT), which also regulate the uptake of another beta amino acid, taurine (Baliou et al., 2020). Taurine exerts a wide range of physiological functions, serving most notably as an antioxidant, calcium modulator, and osmoregulator (Baliou et al., 2020). In the present study, taurine was inversely related to both wooden breast and white striping score (Supplementary Files 3 and 4), potentially due to increased uptake in skeletal as Abasht et al. (Abasht et al., 2016) documented elevated taurine levels in the pectoralis major muscle of wooden breast affected chickens. The

importance of plasma taurine deficiency has mainly been demonstrated by taurine supplementation in animal models and clinical trials where it can prevent or mitigate various aspects of metabolic syndrome, including hyperglycemia, dyslipidemia, hypertension, oxidative stress, and inflammation (Imae et al., 2014). In one study of cardiac disease in Wistar rats, a combined treatment of taurine and beta-alanine had dramatic effects on markers of oxidative stress and inflammation, increasing activity of glutathione peroxidase and superoxide dismutase by more than 175% and reducing serum levels of tumor necrosis factor (TNF)-α and interleukin-6 (IL-6) by nearly 60% (Hou et al., 2020).

4.5.3 Sphingolipid Metabolism

Elevated levels of sphingomyelins among birds with severe wooden breast (Figure 4.4) and white striping may be important with regard to vascular changes and lipid accumulation associated with these myopathies. Inflammation of small- and medium-sized veins accompanied by perivenous lipid infiltration was reported by Papah et al. (Papah et al., 2017) as an early histological lesion associated with wooden breast in birds as young as 1 week post-hatch. These lesions had features in common with atherosclerosis despite being localized to veins alone. Human and rodent studies have found that plasma sphingomyelin levels are highly correlated with and considered a significant risk factor independent of cholesterol for coronary artery disease and subclinical atherosclerosis (Jiang et al., 2000; Nelson et al., 2006). Sphingomyelin is an important component of circulating lipoproteins, and is enriched in atherogenic triglyceride-rich lipoprotein remnants because it is not degraded by plasma enzymes and instead relies on hepatic clearance methods for removal from plasma (Jiang et al., 2000).

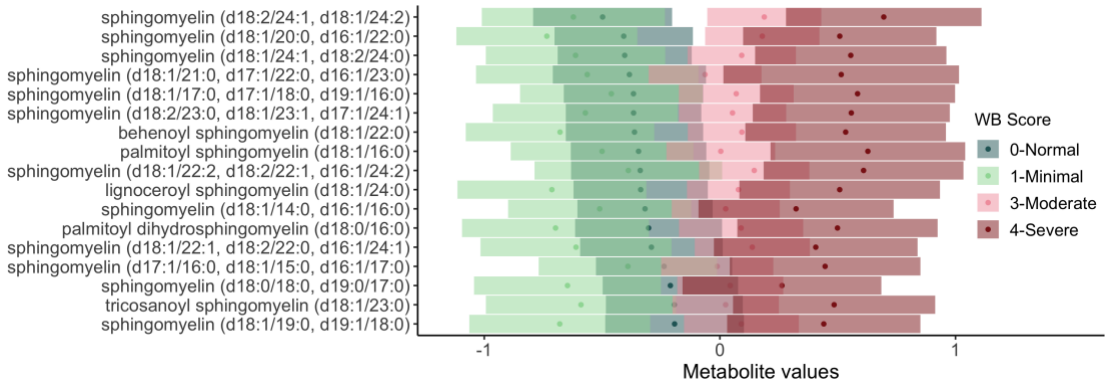

Figure 4.4: Association of wooden breast score with sphingolipid metabolism in plasma of male broiler chickens.

Results of post-hoc analysis of metabolite values by wooden breast score are shown with estimated marginal means (dots) and confidence intervals (bars). Overlapping confidence intervals indicate that there is no significant difference between the two scores. To improve visualization, metabolites are listed in order of the adjusted means for a wooden breast score of 0-Normal.

In wooden breast, there is strong evidence for increased lipoprotein metabolism in the veins of the pectoralis major, where expression of the *lipoprotein lipase* (*LPL*) gene is increased even from an early age (Papah et al., 2018; Lake et al., 2019; Papah and Abasht, 2019). It is possible that greater lipoprotein metabolism in veins of wooden breast affected birds results in higher levels of sphingomyelins in venous plasma, where they may contribute to perivascular lipid leakage, deposition and subsequent inflammation. Sphingomyelins comprise approximately 85% of sphingolipids in humans and serve as structural cell membrane components as well as critical signaling molecules (Kikas et al., 2018). Although sphingolipids have not been well-studied in chickens, they have been proposed to be among the most pathogenic lipids in the development of metabolic disorders related to adiposity in humans, including diabetes and cardiovascular disease (Holland and Summers, 2008).

4.5.4 Purine and Pyrimidine Metabolism

Wooden breast affected birds exhibited altered purine metabolism, with elevated levels of adenine, N1-methylinosine, and xanthosine (Figure 4.5). Metabolites involved in pyrimidine metabolism were also impacted, with wooden breast affected birds showing higher levels of 5,6-dihydrouracil and 3-(3-amino-3-carboxypropyl)uridine, but lower levels of beta-alanine and 3-aminoisobutyrate (Figure 4.5). Abasht et al. (Abasht et al., 2016) previously identified changes to nucleotide metabolism in wooden breast affected pectoralis major muscle involving the accumulation of cytidine, thymidine, adenine, uridine, guanosine, and several nucleotide catabolites. This was believed to result from increased activity of the pentose phosphate pathway or decreased nucleotide utilization (Abasht et al., 2016). While it is unclear if the changes to plasma nucleotide metabolism described here directly reflect alterations occurring in the pectoralis major, one metabolite requires additional scrutiny based on its connection to skeletal muscle.

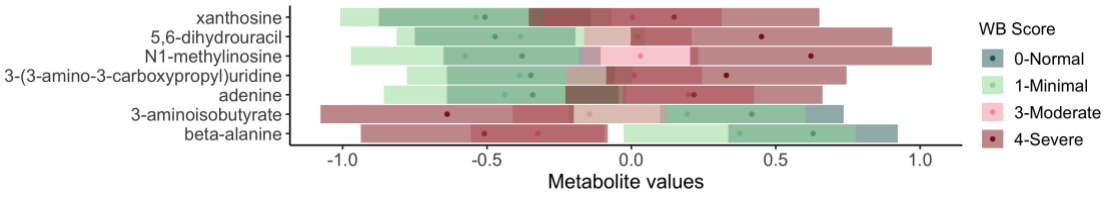

Figure 4.5: Association of wooden breast score with nucleotide metabolism in plasma of male broiler chickens.

Results of post-hoc analysis of metabolite values by wooden breast score are shown with estimated marginal means (dots) and confidence intervals (bars). Overlapping confidence intervals indicate that there is no significant difference between the two scores. To improve visualization, metabolites are listed in order of the adjusted means for a wooden breast score of 0-Normal.

The thymine catabolite 3-aminoisobutyrate, which we found to be reduced in birds severely affected by wooden breast compared to unaffected and minimally affected birds (Figure 4.5), functions as a small molecule myokine that is secreted from skeletal muscle cells both at rest and in response to exercise (Barlow et al., 2020), causing an increase in plasma levels of the metabolite. In mammals and rodents, it is inversely correlated with cardiometabolic risk factors at least partly due to several identified regulatory mechanisms in inflammation and energy metabolism, including expression of brown adipocyte-specific genes, hepatic fatty acid oxidation, insulin release from pancreatic beta cells, and insulin sensitivity of the liver, adipose tissue, and skeletal muscle (Roberts et al., 2014; Shi et al., 2016; Jung et al., 2018). These effects are at least in part mediated by activation of AMP-activated protein kinase (AMPK) and involve major metabolic transcription factors such as peroxisome proliferator-activated receptors α/δ/γ, nuclear factor kappa B (Nf-κB), and sterol regulatory element-binding protein-1c (SREBP-1c) (Tanianskii et al., 2019). A reduction of plasma 3-aminoisobutyrate in wooden breast affected birds may signal dysregulation of lipid and glucose metabolism, which is well-documented in wooden breast (Lake et al., 2019; Papah and Abasht, 2019; Lake and Abasht, 2020).

Plasma adenine, which is moderately increased in birds with a score of 3 or 4 compared to birds with a score of 0 or 1 (Figure 4.5), may also result from altered energy metabolism in wooden breast. In an obese diabetic mouse model, increasing plasma free fatty acids produced a dose-dependent increase in adenine nucleotides and reduction in glucose tolerance (Yang et al., 2019). This effect was limited to the diabetic condition and was not recorded in other obese mouse models. The authors of that study identified two potential sources contributing to the increase in adenine

nucleotides – their release from endothelial cells prior to apoptosis and their release from red blood cells in response to hydrogen peroxide (Yang et al., 2019).

4.5.5 Carnitine and Fatty Acid Metabolism

Carnitine is a branched amino acid that, at least in mammals, can either be absorbed from dietary intake or synthesized in the liver or kidneys from lysine and methionine. It plays critical role in energy metabolism, especially in cardiac and skeletal muscle, via its involvement as a cofactor in the mitochondrial beta-oxidation of long-chain fatty acids along with its most abundant derivative, L-acetylcarnitine. Both carnitine and L-acetylcarnitine are increased in plasma of moderately and severely affected birds compared to unaffected birds (Figure 4.6). In contrast, free carnitine is reduced in the pectoralis major muscle of wooden breast affected birds and multiple long chain fatty acids are increased (Abasht et al., 2016). Together, this may indicate altered uptake of carnitine, which must be transported into skeletal muscle from plasma, either preceding or as a result of other changes in lipid metabolism that have been documented. For example, increased expression of the *lipoprotein lipase* gene in wooden breast- affected pectoralis major suggests an increased uptake of fatty acids from circulating lipoproteins, as *lipoprotein lipase* encodes the rate-limiting enzyme in lipoprotein metabolism (Lake et al., 2019; Papah and Abasht, 2019).

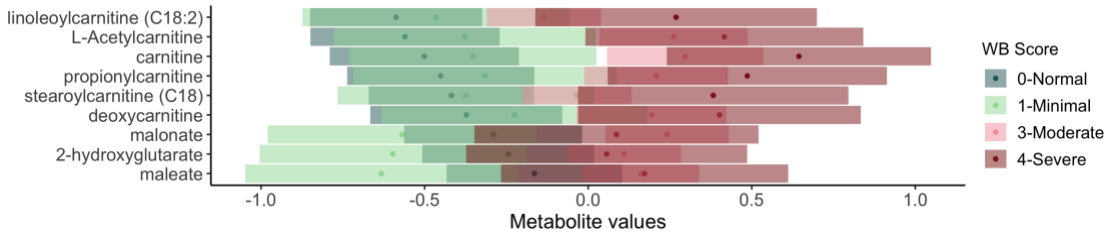

Figure 4.6: Association of wooden breast score with carnitine and fatty acid metabolism in plasma of male broiler chickens.

Results of post-hoc analysis of metabolite values by wooden breast score are shown with estimated marginal means estimated marginal means (dots) and confidence intervals (bars). Overlapping confidence intervals indicate that there is no significant difference between the two scores. To improve visualization, metabolites are listed in order of the adjusted means for a wooden breast score of 0-Normal.

4.5.6 Inositol Metabolism

One of the four metabolites unique to white striping was chiro-inositol, which is reduced in birds with more severe white striping scores (Supplementary File 4). Despite being the only metabolite in this pathway significantly affected by white striping, this compound is worth mentioning because it has been studied mainly as a component of insulin signaling and disposal of intracellular glucose. Chiro-inositol functions as part of a second messenger system for insulin, and even acts as an insulin mimetic, by activating Mg2+-dependent protein phosphatases involved in oxidative and nonoxidative glucose metabolism (Larner et al., 2010). It was also demonstrated in several studies that progression from normal glucose tolerance to type 2 diabetes was associated with growing chiro-inositol deficiency due to the increasing resistance to insulin (Larner et al., 2010). Reduced plasma chiro-inositol in white striping-affected birds suggests that insulin resistance may be a component of the disease,

although substantial differences in insulin signaling between mammals and avians complicate direct comparisons of circulating metabolites.

4.6 Conclusions

Wooden breast and white striping incidence had the most notable association with metabolites involved in histidine metabolism and sphingolipid metabolism, potentially resulting from increased muscle protein breakdown and increased lipoprotein uptake in the pectoralis major of affected birds. This study has also identified plasma metabolites that show potential as biomarkers for wooden breast and white striping in live birds. Specifically, 3-methylhistidine and N-acetyl-L-aspartic acid were both identified as highly significant by mixed linear model analysis for both wooden breast and white striping and were part of the optimal subset of metabolites identified by linear support vector machine. As such, these metabolites are most likely to serve as consistent biomarkers of these myopathies, although their diagnostic performance needs to be confirmed in further studies with larger sample sizes and in comparison to other myopathies of broilers such as deep pectoral myopathy. This research furthers our understanding of the underlying metabolic disturbances present within the wooden breast and white striping conditions and may lead to diagnostic test development toward enhanced field diagnosis and research efficacy for these disorders.

4.7 Acknowledgments

We gratefully acknowledge the in-kind support by Cobb–Vantress Inc. in providing chicks and chicken feed for this experiment. We also greatly appreciate assistance with samples and data collection from many graduate and undergraduate

students at the University of Delaware Department of Animal and Food Sciences. We would like to acknowledge the support from the University of Delaware Center for Bioinformatics and Computational Biology for utilization of their cluster BioMix, which was made possible through support from the Delaware INBRE (NIH GM103446), the state of Delaware and the Delaware Biotechnology Institute (DBI).

REFERENCES

Abasht, B., Mutryn, M. F., Michalek, R. D., and Lee, W. R. (2016). Oxidative stress and metabolic perturbations in wooden breast disorder in chickens. *PLoS One* 11, 1–16. doi:10.1371/journal.pone.0153750.

Abasht, B., Papah, M. B., and Qiu, J. (2021). Evidence of vascular endothelial dysfunction in Wooden Breast disorder in chickens: Insights through gene expression analysis, ultra-structural evaluation and supervised machine learning methods. *PLoS One* 16, e0243983. doi:10.1371/journal.pone.0243983.

Bailey, R. A., Souza, E., and Avendano, S. (2020). Characterising the Influence of Genetics on Breast Muscle Myopathies in Broiler Chickens. *Front. Physiol.* 11, 1–12. doi:10.3389/fphys.2020.01041.

Baliou, S., Kyriakopoulos, A. M., Goulielmaki, M., Panayiotidis, M. I., Spandidos, D. A., and Zoumpourlis, V. (2020). Significance of taurine transporter (TauT) in homeostasis and its layers of regulation (review). *Mol. Med. Rep.* 22, 2163–2173. doi:10.3892/mmr.2020.11321.

Ballard, F. J., and Tomas, F. M. (1983). 3-Methylhistidine as a measure of skeletal muscle protein breakdown in human subjects: The case of its continued use. *Clin. Sci.* 65, 209–215. doi:10.1042/cs0650209.

Barlow, J. P., Karstoft, K., Vigelsø, A., Gram, M., Helge, J. W., Dela, F., et al. (2020). Beta-aminoisobutyric acid is released by contracting human skeletal muscle and lowers insulin release from INS-1 832/3 cells by mediating mitochondrial energy metabolism. *Metab. Open* 7, 100053. doi:10.1016/j.metop.2020.100053.

Benjamini, Y., and Hochberg, Y. (1995). Controlling the False Discovery Rate : A Practical and Powerful Approach to Multiple Testing. *J. R. Stat. Soc. Ser. B* 57, 289–300.

Boerboom, G., van Kempen, T., Navarro-villa, A., and Perez-Bonilla, A. (2018). Unraveling the cause of white striping in broilers using metabolomics. *Poult. Sci.* 97, 3977–3986.

Edmonds, M. S., and Baker, D. H. (1987). Comparative effects of individual amino acid excesses when added to a corn-soybean meal diet: effects on growth and dietary choice in the chick. *J. Anim. Sci.* 65, 699–705. doi:10.2527/jas1987.653699x.

Feng, R. N., Niu, Y. C., Sun, X. W., Li, Q., Zhao, C., Wang, C., et al. (2013). Histidine supplementation improves insulin resistance through suppressed inflammation in obese women with the metabolic syndrome: A randomised controlled trial. *Diabetologia* 56, 985–994. doi:10.1007/s00125-013-2839-7.

Fox, J., and Weisberg, S. (2019). *An R Companion to Applied Regression*. Third Ed. Thousand Oaks, CA: Sage.

Griffin, J. R., Moraes, L., Wick, M., and Lilburn, M. S. (2018). Onset of white striping and progression into wooden breast as defined by myopathic changes underlying Pectoralis major growth. Estimation of growth parameters as predictors for stage of myopathy progression. *Avian Pathol.* 47, 2–13. doi:10.1080/03079457.2017.1356908.

Holland, W. L., and Summers, S. A. (2008). Sphingolipids, insulin resistance, and metabolic disease: New insights from in vivo manipulation of sphingolipid metabolism. *Endocr. Rev.* 29, 381–402. doi:10.1210/er.2007-0025.

Hou, X., Sun, G., Guo, L., Gong, Z., Han, Y., and Bai, X. (2020). Cardioprotective effect of taurine and β-alanine against cardiac disease in myocardial ischemia and reperfusion-induced rats. *Electron. J. Biotechnol.* 45, 46–52. doi:10.1016/j.ejbt.2020.04.003.

Imae, M., Asano, T., and Murakami, S. (2014). Potential role of taurine in the prevention of diabetes and metabolic syndrome. *Amino Acids* 46, 81–88. doi:10.1007/s00726-012-1434-4.

Jiang, X. C., Paultre, F., Pearson, T. A., Reed, R. G., Francis, C. K., Lin, M., et al. (2000). Plasma sphingomyelin level as a risk factor for coronary artery disease. *Arterioscler. Thromb. Vasc. Biol.* 20, 2614–2618. doi:10.1161/01.ATV.20.12.2614.

Jung, T. W., Park, H. S., Choi, G. H., Kim, D., and Lee, T. (2018). β-aminoisobutyric acid attenuates LPS-induced inflammation and insulin resistance in adipocytes through AMPK-mediated pathway. *J. Biomed. Sci.* 25, 1–9. doi:10.1186/s12929-018-0431-7.

Kikas, P., Chalikias, G., and Tziakas, D. (2018). Cardiovascular implications of sphingomyelin presence in biological membranes. *Eur. Cardiol. Rev.* 13, 42–45. doi:10.15420/ecr.2017:20:3.

Kopeć, W., Jamroz, D., Wiliczkiewicz, A., Biazik, E., Pudlo, A., Hikawczuk, T., et al. (2013). Influence of different histidine sources and zinc supplementation of broiler diets on dipeptide content and antioxidant status of blood and meat. *Br. Poult. Sci.* 54, 454–465. doi:10.1080/00071668.2013.793295.

Kuhn, M. (2008). Building Predictive Models in R Using the caret Package. *J. Stat. Software, Artic.* 28, 1–26. doi:10.18637/jss.v028.i05.

Kuttappan, V. A., Shivaprasad, H. l., Shaw, D. P., Valentine, B. A., Hargis, B. M., Clark, F. D., et al. (2013). Pathological changes associated with white striping in broiler breast muscles. *Poult. Sci.* 92, 331–338. doi:10.3382/ps.2012-02646.

Lake, J. A., and Abasht, B. (2020). Glucolipotoxicity: A proposed etiology for wooden breast and related myopathies in commercial broiler chickens. *Front. Physiol.* doi:10.3389/fphys.2020.00169.

Lake, J. A., Brannick, E. M., Papah, M. B., Lousenberg, C., Velleman, S. G., and Abasht, B. (2020). Blood Gas Disturbances and Disproportionate Body Weight Distribution in Broilers With Wooden Breast. *Front. Physiol.* 11, 1–9. doi:10.3389/fphys.2020.00304.

Lake, J. A., Dekkers, J. C. M., and Abasht, B. (2021). Genetic basis and identification of candidate genes for wooden breast and white striping in commercial broiler chickens. *Sci. Rep.* 11. doi:10.1038/s41598-021-86176-4.

Lake, J. A., Papah, M. B., and Abasht, B. (2019). Increased expression of lipid metabolism genes in early stages of wooden breast links myopathy of broilers to metabolic syndrome in humans. *Genes (Basel).* 10, 746. doi:10.20944/preprints201906.0194.v1.

Larner, J., Brautigan, D. L., and Thorner, M. O. (2010). D-chiro-inositol glycans in insulin signaling and insulin resistance. *Mol. Med.* 16, 543–551. doi:10.2119/molmed.2010.00107.

Lenth, R. (2019). Emmeans: estimated marginal means aka Least-Squares Means. R package version 1.5.4-09001. Available at: https://cran.r-project.org/package=emmeans.

Marchesini, G., Forlani, G., Zoli, M., Vannini, P., and Pisi, E. (1982). Muscle protein breakdown in uncontrolled diabetes as assessed by urinary 3-methylhistidine excretion. *Diabetologia* 23, 456–458.

Mihalik, S. J., Michaliszyn, S. F., De Las Heras, J., Bacha, F., Lee, S. J., Chace, D. H., et al. (2012). Metabolomic profiling of fatty acid and amino acid metabolism in youth with obesity and type 2 diabetes: Evidence for enhanced mitochondrial oxidation. *Diabetes Care* 35, 605–611. doi:10.2337/DC11-1577.

Mutryn, M. F., Brannick, E. M., Fu, W., Lee, W.R., and Abasht, B. (2015). Characterization of a novel chicken muscle disorder through differential gene expression and pathway analysis using RNA-sequencing. *BMC Genomics*. 16, 399.

Nelson, J. C., Jiang, X. C., Tabas, I., Tall, A., and Shea, S. (2006). Plasma sphingomyelin and subclinical atherosclerosis: Findings from the multi-ethnic study of atherosclerosis. *Am. J. Epidemiol.* 163, 903–912. doi:10.1093/aje/kwj140.

Niu, Y. C., Feng, R. N., Hou, Y., Li, K., Kang, Z., Wang, J., et al. (2012). Histidine and arginine are associated with inflammation and oxidative stress in obese women. *Br. J. Nutr.* 108, 57–61. doi:10.1017/S0007114511005289.

Noble, W. S. (2006). What is a support vector machine? *Nat. Biotechnol.* 24, 1565–1567. doi:10.1038/nbt1206-1565.

Papah, M. B., and Abasht, B. (2019). Dysregulation of lipid metabolism and appearance of slow myofiber- specific isoforms accompany the development of Wooden Breast myopathy in modern broiler chickens. *Sci. Rep.* 9, 17170. doi:10.1038/s41598-019-53728-8.

Papah, M. B., Brannick, E. M., Schmidt, C. J., and Abasht, B. (2017). Evidence and role of phlebitis and lipid infiltration in the onset and pathogenesis of Wooden Breast Disease in modern broiler chickens. *Avian Pathol.* 46, 623–643. doi:10.1080/03079457.2017.1339346.

Papah, M. B., Brannick, E. M., Schmidt, C. J., and Abasht, B. (2018). Gene expression profiling of the early pathogenesis of wooden breast disease in commercial broiler chickens using RNA-sequencing. *PLoS One* 13, e0207346. doi:10.1371/journal.pone.0207346.

Pym, R. A. E., Leclercq, B., Tomas, F. M., and Tesseraud, S. (2004). Protein utilisation and turnover in lines of chickens selected for different aspects of body composition. *Br. Poult. Sci.* 45, 775–786. doi:10.1080/00071660400012774.

Roberts, L. D., Boström, P., O'Sullivan, J. F., Schinzel, R. T., Lewis, G. D., Dejam, A., et al. (2014). β-Aminoisobutyric acid induces browning of white fat and hepatic β-oxidation and is inversely correlated with cardiometabolic risk factors. *Cell Metab.* 19, 96–108. doi:10.1016/j.cmet.2013.12.003.

Severyn, M. K., Brannick, E. M., Bautista, D. A., and Dekich, M. A. (2019). Wooden Breast Syndrome in Gastrocnemius Muscle of Roaster Chickens Leading to Muscle-Tendon Rupture and Leg Condemnation. *Avian Dis.* 63, 102. doi:10.1637/11957-082418-case.1.

Shi, C. X., Zhao, M. X., Shu, X. D., Xiong, X. Q., Wang, J. J., Gao, X. Y., et al. (2016). B-Aminoisobutyric Acid Attenuates Hepatic Endoplasmic Reticulum Stress and Glucose/Lipid Metabolic Disturbance in Mice With Type 2 Diabetes. *Sci. Rep.* 6, 1–12. doi:10.1038/srep21924.

Sihvo, H. K., Immonen, K., and Puolanne, E. (2014). Myodegeneration with fibrosis and regeneration in the pectoralis major muscle of broilers. *Vet. Pathol.* 51, 619–623. doi:10.1177/0300985813497488.

Soglia, F., Mudalal, S., Babini, E., Di Nunzio, M., Mazzoni, M., Sirri, F., et al. (2016). Histology, composition, and quality traits of chicken Pectoralis major muscle affected by wooden breast abnormality. *Poult. Sci.* 95, 651–659. doi:10.3382/ps/pev353.

Tanianskii, D. A., Jarzebska, N., Birkenfeld, A. L., O'sullivan, J. F., and Rodionov, R. N. (2019). Beta-aminoisobutyric acid as a novel regulator of carbohydrate and lipid metabolism. *Nutrients* 11. doi:10.3390/nu11030524.

Tomas, F. M., Jones, L. M., and Pym, R. A. (1988). Rates of muscle protein breakdown in chickens selected for increased growth rate, food consumption or efficiency of food utilisation as assessed by Nτ-methylhistidine excretion. *Br. Poult. Sci.* 29, 359–370.

Tůma, P., Samcová, E., and Balínová, P. (2005). Determination of 3-methylhistidine and 1-methylhistidine in untreated urine samples by capillary electrophoresis. *J. Chromatogr. B Anal. Technol. Biomed. Life Sci.* 821, 53–59. doi:10.1016/j.jchromb.2005.04.006.

Vignale, K., Caldas, J. V., England, J. A., Boonsinchai, N., Magnuson, A., Pollock, E. D., et al. (2017). Effect of white striping myopathy on breast muscle (Pectoralis major) protein turnover and gene expression in broilers. *Poult. Sci.* 96, 886–893. doi:10.3382/ps/pew315.

Yang, X., Zhao, Y., Sun, Q., Yang, Y., Gao, Y., Ge, W., et al. (2019). An Intermediary Role of Adenine Nucleotides on Free Fatty Acids-Induced Hyperglycemia in Obese Mice. *Front. Endocrinol. (Lausanne).* 10, 1–9. doi:10.3389/fendo.2019.00497.

Ziyatdinov, A., Vázquez-Santiago, M., Brunel, H., Martinez-Perez, A., Aschard, H., and Soria, J. M. (2018). lme4qtl: Linear mixed models with flexible covariance structure for genetic studies of related individuals. *BMC Bioinformatics* 19, 1–5. doi:10.1186/s12859-018-2057-x.

Chapter 5

INCREASED EXPRESSION OF LIPID METABOLISM GENES IN EARLY STAGES OF WOODEN BREAST LINKS MYOPATHY OF BROILERS TO METABOLIC SYNDROME IN HUMANS

(Juniper A. Lake, Michael B. Papah, & Behnam Abasht. *Genes*, 10:746, (2019)).
https://www.mdpi.com/2073-4425/10/10/746

5.1 Abstract

Wooden breast is a muscle disorder affecting modern commercial broiler chickens that causes a palpably firm pectoralis major muscle and severe reduction in meat quality. Most studies have focused on advanced stages of wooden breast apparent at market age, resulting in limited insights into the etiology and early pathogenesis of the myopathy. Therefore, the objective of this study was to identify early molecular signals in the wooden breast transcriptional cascade by performing gene expression analysis on the pectoralis major muscle of two-week-old birds that may later exhibit the wooden breast phenotype by market age at 7 weeks. Biopsy samples of the left pectoralis major muscle were collected from 101 birds at 14 days of age. Birds were subsequently raised to 7 weeks of age to allow sample selection based on the wooden breast phenotype at market age. RNA sequencing was performed on 5 unaffected and 8 affected female chicken samples, selected based on wooden breast scores (0 to 4) assigned at necropsy where affected birds had scores of 2 or 3 (mildly or moderately affected) while unaffected birds had scores of 0 (no apparent gross lesions). Differential expression analysis identified 60 genes found to be significant at an FDR-adjusted p value of 0.05. Of these, 26 were previously demonstrated to exhibit

altered expression or genetic polymorphisms related to glucose tolerance or diabetes mellitus in mammals. Additionally, 9 genes have functions directly related to lipid metabolism and 11 genes are associated with adiposity traits such as intramuscular fat and body mass index. This study suggests that wooden breast disease is first and foremost a metabolic disorder characterized primarily by ectopic lipid accumulation in the pectoralis major.

5.2 Introduction

Wooden breast is one of several muscle abnormalities of modern commercial broiler chickens that causes substantial economic losses in the poultry industry due to its impact on meat quality. Emerging evidence suggests wooden breast may also be detrimental to bird welfare as affected chickens exhibit increased locomotor difficulties, decreased wing mobility, and higher mortality rates (Papah et al., 2017; Norring et al., 2018; Gall et al., 2019b). While the etiology of the myopathy is still poorly understood, many believe it to be a side-effect of improved management practices and selective breeding for performance traits due to increased susceptibility among broilers with high feed efficiency (Mutryn et al., 2015b; Abasht et al., 2019), breast muscle yield (Dalle Zotte et al., 2014; Bailey et al., 2015; Mutryn et al., 2015b), and growth rate (Trocino et al., 2015; Livingston et al., 2019a).

Macroscopic manifestations of the disorder include pale and hardened areas, subcutaneous and fascial edema, petechial hemorrhages, spongy areas with disintegrating myofiber bundles, and white fatty striations characteristic of white striping (Sihvo et al., 2014; Papah et al., 2017). An early study of wooden breast characterized its microscopic presentation as polyphasic myodegeneration and necrosis with regeneration and interstitial connective tissue accumulation (fibrosis),

primarily affecting the cranial end of the pectoralis major muscle (Sihvo et al., 2014). However, it has since been demonstrated that venous inflammation (phlebitis) and perivascular lipid and inflammatory cell infiltration appear in the first week of age and precede other symptoms (Papah et al., 2017). Differential gene expression analysis of the pectoralis major in 7-week-old broilers suggests that hypoxia, oxidative stress, fiber-type switching, and increased intracellular calcium may be important components of the myopathy (Mutryn et al., 2015a). In two- and three-week old birds, differentially expressed genes were mostly associated with increased inflammation, vascular disease, increased oxidative stress, extracellular matrix remodeling, dysregulation of carbohydrates and lipids, and impaired excitation-contraction coupling (Papah et al., 2018). Metabolomic profiling is in agreement with these results and provides evidence of oxidative stress and dysregulated carbohydrate and lipid metabolism in affected birds at 7 weeks of age (Abasht et al., 2016).

The objective of the present study was to better characterize the transcriptional anomalies that exist in the pectoralis major of two-week-old birds that later develop wooden breast by market age at 7 weeks. Only one other gene expression study has investigated early stages of wooden breast (Papah et al., 2018). The current study serves as a continuation of that work, but makes two key changes. First, unlike the previous study that used only male birds, we included only female birds in the RNA-seq analysis. Second, birds in the affected group all possessed mild or moderate wooden breast phenotypes rather than severe symptoms, which allowed us to capture a clearer signal of the earliest transcriptomic perturbations associated with the myopathy.

5.3 Materials and Methods

5.3.1 Experimental Animals and Tissue Collection

The University of Delaware Institutional Animal Care and Use Committee approved the animal conditions and experimental procedures used in this scientific study under protocol number 48R-2015-0. For this experiment, 302 mixed male and female Cobb500 broilers were raised according to industry growing standards in two poultry houses from 1 day to 7 weeks of age. Birds were divided between two poultry houses due to capacity constraints, but both houses were maintained at the same environmental conditions. Chickens were provided with continuous free access to water and feed that met all nutritional recommendations for Cobb500 broilers. At 14 days of age, biopsy samples of the craniolateral area of the left pectoralis major muscle were collected in the same manner described by a previous study (Papah et al., 2018) from 101 birds randomly selected from both houses. After biopsy, all birds were grown out to 7 weeks of age, at which time they were euthanized by cervical dislocation. During necropsy, the pectoralis major muscles were evaluated for gross lesions and palpable firmness associated with wooden breast and each bird was assigned a wooden breast score using a 0-4 scale; 0-Normal indicates the bird had no macroscopic signs of the myopathy, 1-Very Mild indicates 1% or less of the breast muscle was affected, 2-Mild indicates between 1% and 10% of the breast muscle was affected, 3-Moderate indicates between 10% and 50% of the breast muscle was affected, and a score of 4-Severe indicates that more than 50% was affected. This scoring system is slightly different from the one previously used in our laboratory and separates unaffected, mildly and moderately affected chickens with a higher resolution.

5.3.2 Sample Selection and RNA-Sequencing

Selection of samples for use in RNA-seq analysis was based on wooden breast scores assigned at necropsy at 7 weeks of age. A total of 6 unaffected and 8 affected birds were identified; affected birds had scores of 2 or 3 (mildly or moderately affected) while unaffected birds had scores of 0 (no apparent gross lesions). Only samples taken from female birds were used for RNA-seq. Total RNA was extracted from pectoralis major tissue samples using the mirVana miRNA Isolation Kit (Thermo Fisher Scientific) according to the manufacturer's protocol and stored at -80˚C until cDNA library preparation. Each RNA sample was quantified using the NanoDrop 1000 Spectrophotometer (Thermo Fisher Scientific) and quality was assessed with the Fragment Analyzer at the Delaware Biotechnology Institute (DBI). cDNA libraries were constructed using the ScriptSeq Complete Kit (Human/Mouse/Rat) (Illumina) with the optional step of adding a user-defined barcode to the library. The 14 barcoded cDNA libraries were normalized and 10 µl of each sample were pooled in two tubes (7 samples in each pool). Pooled libraries were subsequently submitted to the DBI for paired-end 2x76-nucleotide sequencing on two lanes of a flow cell using the HiSeq 2500 Sequencing System (Illumina).

Raw sequencing reads were demultiplexed and then checked for quality using FastQC v0.11.7 (FastQC). All samples passed the quality check and were submitted to Trimmomatic v0.38 (Bolger et al., 2014) to trim leading and trailing bases with quality below 20, remove reads with an average quality below 15, and remove reads that were shorter than 30 bases in length. Trimmed reads were then mapped to both Gallus_gallus-5.0 (Ensembl release 94) and GRCg6a (Ensembl release 95) chicken reference genomes using HISAT2 v2.1.0 (Kim et al., 2015) with concordant mapping required for both reads in each pair. Cuffdiff v2.2.1 (Trapnell et al., 2013) was used

with the fragment bias correction option to identify differentially expressed genes between affected and unaffected birds. Genes were considered statistically significant if the FDR-adjusted p-value was ≤ 0.05. The use of two reference genome builds, the latter of which was released during the course of this study, provided validation of our results and allowed us to capture differentially expressed genes that may have borderline statistical significance due to assembly errors or bias. One sample (animal ID 424183) in the unaffected group displayed an extreme outlier expression pattern; it was therefore removed and differential expression analysis with Cuffdiff was repeated without this sample (5 unaffected vs. 8 affected). In order to compile the results generated from each reference genome, Ensembl gene IDs from Gallus-gallus-5.0 were mapped to GRCg6a gene IDs using Ensembl's ID History Converter; differentially expressed genes with annotation differences between the two reference genome releases were scrutinized for consistency. Pairwise correlation analysis and visualization of differentially expressed genes was conducted with the "stats" and "corrplot" packages (Wei and Simko, 2017) in R only using expression data generated with the GRCg6a reference genome build.

5.4 Results

An average of 19,616,353 paired-end sequence reads were generated per sample, which was reduced to an average of 19,609,044 paired-end reads after trimming. The average mapping rate per sample was 74.5% with the Gallus_gallus-5.0 reference genome build and 75.1% with GRCg6a. The total number of sequenced reads, trimmed reads, and mapped reads per sample can be found in Table 5.1.

Table 5.1: Sequencing and mapping statistics for RNA-Sequencing of 8 wooden breast affected and 6 unaffected pectoralis major muscle samples.

Sample	Affected/ Unaffected	Total Reads	Reads after trimming	Mapped reads (Gallus_gallus-5.0)	Mapped reads (GRCg6a)
424132	Unaffected	16,115,674	16,109,441	12,373,514	12,451,896
424170	Unaffected	22,690,579	22,681,762	15,695,351	15,802,383
424183	Unaffected	19,863,892	19,856,809	15,109,341	15,140,824
424198	Unaffected	23,296,111	23,287,439	17,729,792	17,861,743
424379	Unaffected	19,665,248	19,658,088	15,101,602	15,217,990
424439	Unaffected	20,665,929	20,658,137	15,761,365	15,906,603
424207	Affected	19,102,198	19,094,968	12,531,596	12,839,571
424222	Affected	18,665,648	18,658,831	13,960,980	14,003,237
424225	Affected	15,090,867	15,085,500	11,827,301	11,878,037
424239	Affected	24,066,744	24,057,973	17,148,124	17,254,850
424246	Affected	16,289,902	16,283,971	11,993,993	12,131,613
424259	Affected	18,199,967	18,193,176	13,255,515	13,308,199
424266	Affected	17,338,445	17,331,673	13,155,931	13,241,165
485907	Affected	23,577,735	23,568,852	18,765,289	18,898,406

Sample 424183 was excluded from differential expression analysis due to an extreme outlier expression pattern.

There were 52 differentially expressed genes identified using the Gallus_gallus-5.0 reference genome build and 29 differentially expressed genes using the GRCg6a genome build. After accounting for changes in annotation of Ensembl Gene IDs between genome releases, a total of 60 genes were found to be differentially expressed between affected and unaffected groups across both analyses, with 18 differentially expressed genes overlapping between both Gallus_gallus-5.0 and GRCg6a. Three Ensembl Gene IDs from the earlier build were deprecated in GRCg6a and were excluded from further analysis. Of the 60 differentially expressed genes used for downstream analysis, 52 were upregulated in affected birds and 8 were downregulated in affected birds (Table 5.2).

Table 5.2: Differentially expressed genes between wooden breast affected pectoralis major muscle samples and unaffected samples at 2 weeks of age.

Gene ID	Gene Symbol	Gene Name	Log2FC Galgal5	Log2FC GRCg6a
Genes upregulated in affected group				
ENSGALG00000046652	-	-	1.55	n.s.
ENSGALG00000052084	-	-	n.s.	2.06
ENSGALG00000006491	ANKRD1	Ankyrin repeat domain 1	1.28	0.99
ENSGALG00000049422*	ATF3	Activating transcription factor 3	1.04	n.s.
ENSGALG00000009846	BBS5	Bardet-Biedl syndrome 5	0.76	n.s.
ENSGALG00000017040	C4A	Complement C4A (Rodgers blood group)	1.24	0.96
ENSGALG00000008439	CD36	CD36 molecule	0.87	n.s.
ENSGALG00000046316	CFAP97D1	CFAP97 domain containing 1	1.14	n.s.
ENSGALG00000027874	CHAC1	ChaC glutathione specific gamma-glutamylcyclotransferase 1	1.99	n.s.
ENSGALG00000037856	CHL1	Cell adhesion molecule L1 like	1.44	n.s.
ENSGALG00000034500	CIDEA	Cell death-inducing DFFA-like effector a	1.51	1.22
ENSGALG00000012790	DSP	Desmoplakin	1.50	n.s.
ENSGALG00000015876	ELOVL4	ELOVL fatty acid elongase 4	2.19	n.s.
ENSGALG00000001204	ENKD1	Enkurin domain containing 1	2.07	n.s.
ENSGALG00000008563	ENTPD6	Ectonucleoside triphosphate diphosphohydrolase 6	0.80	n.s.
ENSGALG00000037050	FABP3	Fatty acid binding protein 3	0.77	0.72
ENSGALG00000030025	FABP4	Fatty acid binding protein 4	1.74	1.52
ENSGALG00000013100	GRB10	Growth factor receptor bound protein 10	0.77	n.s.
ENSGALG00000011404	HOPX	HOP homeobox	1.19	1.04
ENSGALG00000023818	HSPB9	Heat shock protein family B (small) member 9	1.14	1.13
ENSGALG00000032672	KRT5	Keratin 5	n.s.	1.68
ENSGALG00000016174	LMBRD1	LMBR1 domain containing 1	0.87	n.s.
ENSGALG00000008805	LMOD2	Leiomodin 2	1.39	n.s.
ENSGALG00000021286	LOC427654	Parvalbumin beta-like	2.36	2.36
ENSGALG00000023819	LOC772158	Heat shock protein 30C-like	0.74	0.76
ENSGALG00000015425	LPL	Lipoprotein lipase	0.80	n.s.
ENSGALG00000043582	LY6CLEL	Lymphocyte antigen 6 complex, locus E-like	2.25	n.s.
ENSGALG00000036004	MRPL34	Mitochondrial ribosomal protein L34	n.s.	0.82
ENSGALG00000001709	MUSTN1	Musculoskeletal, embryonic nuclear protein 1	n.s.	1.30
ENSGALG00000012783	MYBPC1	Myosin binding protein C, slow type	1.49	1.17
ENSGALG00000003323	NECAB2	N-terminal EF-hand calcium binding protein 2	n.s.	1.10
ENSGALG00000053246*	OCM2	Oncomodulin 2	0.78	n.s.
ENSGALG00000013414	PDLIM3	PDZ and LIM domain 3	0.75	n.s.
ENSGALG00000027207	PERP2	PERP2, TP53 apoptosis effector	1.29	n.s.
ENSGALG00000004974	PPARG	Peroxisome proliferator-activated receptor gamma	0.89	n.s.
ENSGALG00000040434	RAB18L	Ras-related protein Rab-18-B-like	1.23	1.09
ENSGALG00000043694	RAPGEF4	Rap guanine nucleotide exchange factor 4	1.24	n.s.
ENSGALG00000002637	RBP7	Retinol binding protein 7	1.96	1.65
ENSGALG00000025650	RF00009	Ribonuclease P RNA component H1, 2 pseudogene	n.s.	0.75
ENSGALG00000051839	RF00012	-	n.s.	2.02
ENSGALG00000047347*	RF00017	-	1.38	n.s.
ENSGALG00000025557	RF00030	-	n.s.	0.88
ENSGALG00000054841*	RF0017	-	0.83	1.46
ENSGALG00000005140	RRAD	RRAD, Ras related glycolysis inhibitor and calcium channel regulator	1.63	1.20
ENSGALG00000051456	RTN2	Reticulon 2	n.s.	1.00
ENSGALG00000009400	SLC8A3	Solute carrier family 8 member A3	0.70	n.s.
ENSGALG00000042863	SMIM4	Small integral membrane protein 4	n.s.	0.87

ENSGALG00000019157	SMPX	Small muscle protein X-linked	0.94	n.s.
ENSGALG00000009037	SPTLC3	Serine palmitoyltransferase long chain base subunit 3	2.47	n.s.
ENSGALG00000031117	STK17A	Serine/threonine kinase 17a	0.92	n.s.
ENSGALG00000021231	TMEM254	Transmembrane protein 254	1.05	n.s.
ENSGALG00000014261	UCHL1	Ubiquitin C-terminal hydrolase L1	1.07	0.94
Genes downregulated in affected group				
ENSGALG00000025945*	AVD	Avidin	-1.58	-1.69
ENSGALG00000033932	BF1	MHC BF1 class I	-0.84	n.s.
ENSGALG00000006681	BRSK2	BR serine/threonine kinase 2	-2.50	-2.77
ENSGALG00000032220	ELN	Elastin	n.s.	-1.17
ENSGALG00000035309	HBE	Hemoglobin subunit epsilon	-1.59	n.s.
ENSGALG00000002708	LINGO1	Leucine-rich repeat and immunoglobulin-like domain-containing nogo receptor-interacting protein 1	-0.78	-0.77
ENSGALG00000006520	MYH11	Myosin, heavy chain 11, smooth muscle	-0.95	n.s.
ENSGALG00000013045	TUBA8B	Tubulin, alpha 8b	-1.67	n.s.

Log2FC is calculated by log2(FPKMaffected/FPKMunaffected). Unknown gene names are indicated with a dash (-). Non-significant p-values (i.e. FDR-adjusted p-values > 0.05) are indicated as n.s. An asterisk (*) indicates genes with annotation differences between Gallus_gallus-5.0 and GRCg6a reference genome assemblies.

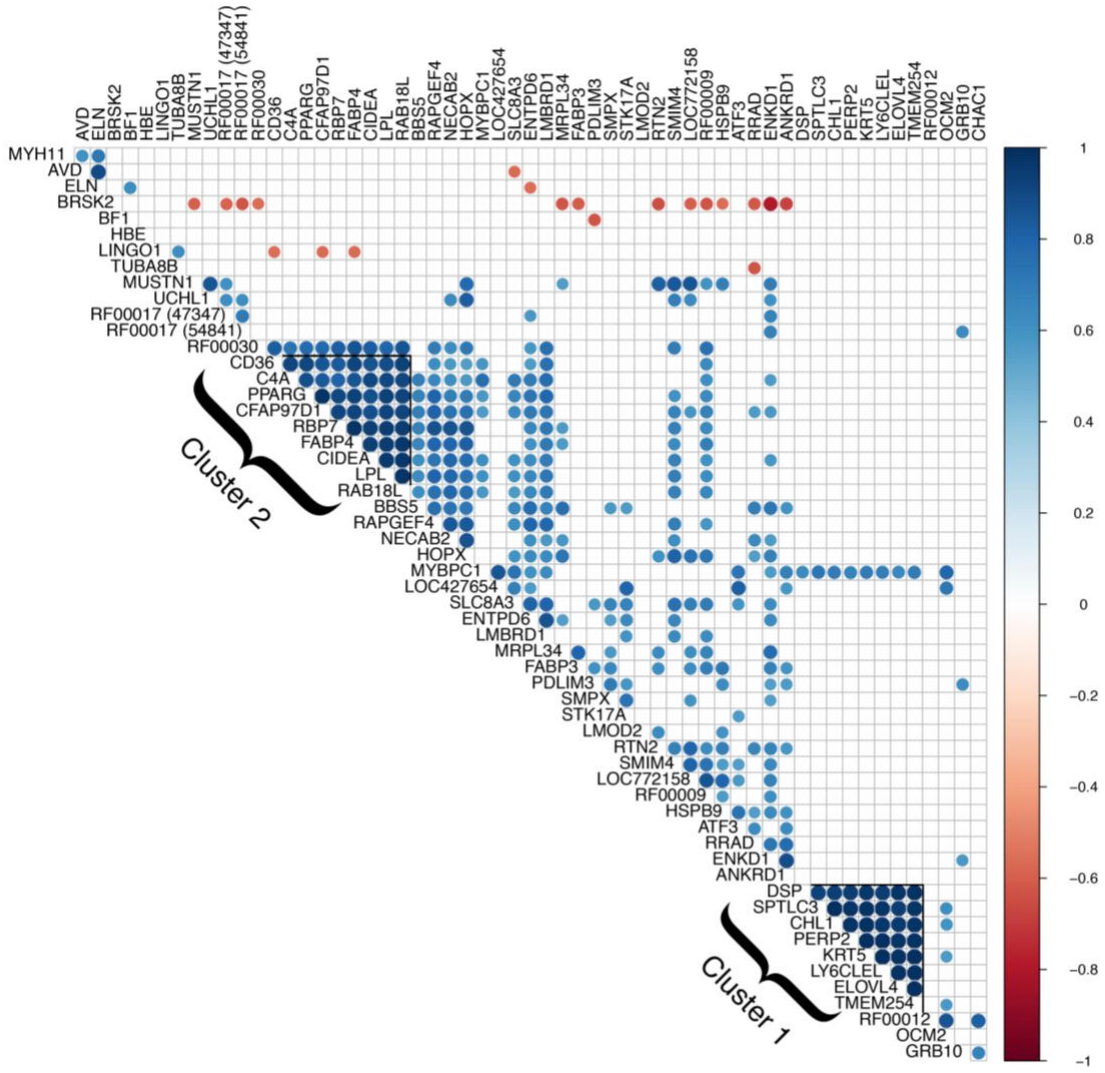

Figure 5.1: Correlation analysis of differentially expressed genes.

Genes with significantly correlated expression (p value ≤ 0.05) are shown in blue (positive correlation) and red (negative correlation). Two major clusters of genes have Pearson's correlation coefficients greater than 0.8 for all gene pairs. Cluster 1 consists of 8 genes, all of which were excluded from further analysis due to presumed skin contamination. Cluster 2 consists of 9 genes related to lipid metabolism or adiposity traits.

Correlation analysis of differentially expressed genes revealed two major clusters with Pearson's correlation coefficients greater than 0.8 for all gene pairs (Figure 5.1). The first is a cluster of 8 genes, all of which were excluded from further analysis due to presumed skin contamination. These include *serine palmitoyltransferase long chain base subunit 3* (*SPTLC3*), *desmoplakin* (*DSP*), *ELOVL fatty acid elongase 4* (*ELOVL4*), *PERP2, TP53 apoptosis effector* (*PERP2*), *keratin 5* (*KRT5*), *cell adhesion molecule L1* like (*CHL1*), *lymphocyte antigen 6 complex, locus E-like* (*LY6CLEL*), and *transmembrane protein 254* (*TMEM254*). Several of these genes are known to be primarily expressed in the skin and a previous biopsy study using the same technique demonstrated that biopsy samples are prone to skin contamination (Papah et al., 2018). Additionally, differential expression of these genes was driven by the same three samples, one unaffected and two affected, and expression in the remaining samples was relatively very low or approximately zero. The second cluster consisted of 9 protein-coding genes with demonstrated or putative involvement in lipid metabolism. Although no other clusters were apparent from correlation analysis, functional groupings of differentially expressed genes included muscle growth and function, calcium signaling, and endoplasmic reticulum (ER) stress response. We also found a substantial number of genes that are differentially expressed, implicated, or otherwise involved in metabolic syndrome in mammals, which is characterized primarily by diabetes, insulin resistance, obesity, elevated blood lipids, and high blood pressure.

5.5 Discussion

Metabolic syndrome refers to a cluster of conditions, including obesity, high blood sugar, high serum triglycerides, low serum HDL cholesterol, and high blood

pressure, that put an individual at greater risk of developing type 2 diabetes and associated complications such as atherosclerosis, cardiomyopathy, non-alcoholic fatty liver disease, and diabetic nephropathy. Our data revealed a surprising number of differentially expressed genes implicated in or associated with metabolic syndrome in humans. Among the 60 differentially expressed genes identified in this study, 20 are previously reported to exhibit altered expression in relation to diabetes or a closely related metabolic condition and 9 genes have been identified as candidate genes in association studies of glucose tolerance or diabetes mellitus (Table 5.3). One of these candidate genes, *Bardet-Biedl syndrome 5* (*BBS5*), is associated with a rare ciliopathy that strongly predisposes individuals to diabetes and other metabolic complications: obesity and diabetes mellitus are actually considered diagnostic features of the disease (Beales et al., 1999; Forsythe and Beales, 2013). Upon further examination, we found that many of the conditions surrounding metabolic syndrome in humans possessed important similarities to the wooden breast phenotype, namely inflammation, ectopic fat deposition, dysregulation of Ca^{2+} homeostasis, ER stress, oxidative stress, altered glucose metabolism, fibrosis, and hypertrophy.

Table 5.3: Differentially expressed genes linked to diabetes and glucose tolerance. Of the 60 differentially expressed genes identified in this study, 26 are either proposed as candidate genes for glucose tolerance or diabetes mellitus or exhibit altered expression in relation to diabetes or a closely related metabolic condition.

Gene Symbol	Gene Name	Connection	Sources
ANKRD1	Ankyrin repeat domain 1	Expression	(Matsuura et al., 2007)
ATF3	Activating transcription factor 3	Expression	(Qi et al., 2009)
BBS5	Bardet-Biedl syndrome 5	Genetic variant	(Beales et al., 1999)
BF1	MHC BF1 class I	Expression	(Faustman et al., 1991)
BRSK2	BR serine/threonine kinase 2	Expression	(Caplen et al., 1990)
C4A	Complement C4A (Rodgers blood group)	Expression	(Lappas, 2011)

C4A	Complement C4A (Rodgers blood group)	Genetic variant	(Caplen et al., 1990)
CD36	CD36 molecule	Expression	(Reynet and Kahn, 1993; Tan et al., 2018)
CIDEA	Cell death-inducing DFFA-like effector a	Expression	(Zhou et al., 2012)
ENTPD6	Ectonucleoside triphosphate diphosphohydrolase 6 (putative)	Genetic variant	(Rich et al., 2009)
FABP3	Fatty acid binding protein 3	Expression	(Husi et al., 2014)
FABP4	Fatty acid binding protein 4	Expression	(Westerbacka et al., 2007; Furuhashi et al., 2014; Husi et al., 2014)
GRB10	Growth factor receptor bound protein 10	Expression	(Lim et al., 2007; Yang et al., 2016)
LINGO1	Leucine-rich repeat and immunoglobulin-like domain-containing nogo receptor-interacting protein 1	Genetic variant	(Morris et al., 2012; Abdullah et al., 2015)
LMBRD1	LMBR1 domain containing 1	Expression	(Tan et al., 2018)
LMOD2	Leiomodin 2	Genetic variant	(Kang et al., 2012)
LPL	Lipoprotein lipase	Expression	(Howard, 1987; Westerbacka et al., 2007)
LPL	Lipoprotein lipase	Genetic variant	(Yang et al., 2003)
MRPL34	Mitochondrial ribosomal protein L34	Expression	(Park et al., 2009; Moreno-Viedma et al., 2016)
MYH11	Myosin, heavy chain 11, smooth muscle	Expression	(Reynet and Kahn, 1993)
PDLIM3	PDZ and LIM domain 3	Genetic variant	(Kang et al., 2012)
PPARG	Peroxisome proliferator-activated receptor gamma	Expression	(Park et al., 1997; Westerbacka et al., 2007)
PPARG	Peroxisome proliferator-activated receptor gamma	Genetic variant	(Stumvoll and Häring, 2002; Scott et al., 2007; Sladek et al., 2007; Zeggini et al., 2008; Sanghera and Blackett, 2012)
RAB18L	Ras-related protein Rab-18-B-like	Expression	(Pulido et al., 2011)
RAPGEF4	Rap guanine nucleotide exchange factor 4	Expression	(Zhang et al., 2009)
RBP7	Retinol binding protein 7	Expression	(Nie et al., 2017)
RRAD	RRAD, Ras related glycolysis inhibitor and calcium channel regulator	Expression	(Reynet and Kahn, 1993)
RTN2	Reticulon 2	Genetic variant	(Caplen et al., 1990)
UCHL1	Ubiquitin C-terminal hydrolase L1	Expression	(Zhang et al., 2016)

5.5.1 Increased Expression of Genes Involved in Lipid Metabolism

The most important connection to metabolic syndrome in our results is the increased expression of genes involved in lipid metabolism in the pectoralis major of affected birds. Many of the differentially expressed genes from our analysis encode proteins with critical or rate-limiting functions in lipid metabolism and homeostasis such as lipoprotein triglyceride hydrolysis, fatty acid transport, and lipid droplet regulation. These genes include *lipoprotein lipase* (*LPL*), *CD36 molecule* (*CD36*),

peroxisome proliferator-activated receptor gamma (*PPARG*), *retinol binding protein 7* (*RBP7*), *fatty acid binding protein 3* (*FABP3*), fatty *acid binding protein 4* (*FABP4*), *cell death-inducing DFFA-like effector a* (*CIDEA*), *ras-related protein Rab-18-B-like* (*RAB18L*), and *LMBR1 domain containing 1* (*LMBRD1*) (Zerega et al., 2001; Mead et al., 2002; Bonen et al., 2004; Zizola et al., 2008; Martin and Parton, 2008; Puri et al., 2008; Wang and Eckel, 2009; Pulido et al., 2011; Rutsch et al., 2011; Furuhashi et al., 2014; Green et al., 2016). Several other genes, some of which are functionally uncharacterized or poorly understood with regard to lipid metabolism, have expression or genetic polymorphisms correlated with adiposity traits such as body mass index, percent intramuscular fat, percent abdominal fat, or blood lipid levels. These include *HOP homeobox* (*HOPX*), *myosin binding protein C, slow type* (*MYBPC1*), *Bardet-Biedl syndrome 5* (*BBS5*), *growth factor receptor bound protein 10* (*GRB10*), *CFAP97 domain containing 1* (*CFAP97D1*), *hemoglobin subunit epsilon* (*HBE*), *ectonucleoside triphosphate diphosphohydrolase 6* (ENTPD6), *complement C4A (Rodgers blood group)* (*C4A*), *mitochondrial ribosomal protein L34* (*MRPL34*), *ATF3*, and *CHAC1* (Heuckeroth et al., 1987; Szatmari et al., 2007; Chen et al., 2011; Zhang et al., 2012; Forsythe and Beales, 2013; Willer et al., 2013; Jang et al., 2013; Liu et al., 2014; Puig-Oliveras et al., 2014; Van Leeuwen et al., 2015; Shi et al., 2015; Surakka et al., 2015; Resnyk et al., 2017; Turcot et al., 2018; Kilpeläinen et al., 2019).

Notably, the present study identified a cluster of 9 genes related to lipid metabolism that may represent a functional group for two main reasons. First, the genes in this cluster exhibit highly correlated expression ($r > 0.8$ for all gene pairs; Figure 5.1). Second, this cluster includes the gene encoding the transcription factor PPARγ and several of its experimentally validated transcriptional targets (*CD36, C4A,*

RBP7, *FABP4*, *CIDEA*, and *LPL*) (Laplante et al., 2003; Szatmari et al., 2007; Lefterova et al., 2008; Puri et al., 2008; Zizola et al., 2008). As a master regulator of adipogenesis, PPARγ plays a crucial role in governing the distribution of lipid deposition in the body and the development of various metabolic conditions (Mitch et al., 1994; Semple et al., 2006; Medina-Gomez et al., 2007; Wang, 2010; Phua et al., 2018). It is also one of the few established genes that has been associated with common forms of type 2 diabetes across multiple genome-wide association studies (Stumvoll and Häring, 2002; Scott et al., 2007; Sladek et al., 2007; Zeggini et al., 2008; Sanghera and Blackett, 2012). In skeletal muscle of broiler chickens and other meat-type animals, increased expression of *PPARG* and PPARγ target genes is frequently associated with higher intramuscular fat content (Wang et al., 2005; Jeong et al., 2012; Liu et al., 2017; Cui et al., 2018).

Increased expression of genes related to lipid metabolism and fat deposition in the pectoralis major is consistent with histological characterization of early stages of wooden breast, in which lipid infiltration and accumulation was established as one of the first signs of disease even before wooden breast is grossly detectable (Papah et al., 2017). The storage of excess lipids in tissues other than adipose tissue, that normally contain only small amounts of fat, is called ectopic lipid deposition and is linked to insulin resistance and metabolic dysfunction in mammals (Tumova et al., 2016). In fact, ectopic lipid deposition and the resulting lipotoxicity are considered to be a major feature of metabolic syndrome with the precise location of ectopic lipid accumulation dictating specific complications such as atherosclerosis, hepatic steatosis, and diabetic nephropathy (Rasouli et al., 2007). This suggests that increased lipid deposition in the pectoralis major may be a major factor contributing to the wooden breast phenotype.

5.5.2 Endoplasmic Reticulum Stress and Dysregulation of Calcium Homeostasis

Results from the current study suggest that ER stress and dysregulation of calcium homeostasis are occurring in the pectoralis major muscle in the early stages of wooden breast. Evidence for ER stress is supported by the upregulation of *activating transcription factor 3* (*ATF3*), *ChaC glutathione specific gamma-glutamylcyclotransferase 1* (*CHAC1*), and *reticulon 2* (*RTN2*) and the downregulation of *BR serine/threonine kinase 2* (*BRSK2*). *ATF3*, *CHAC1*, and *BRSK2* are part of the unfolded protein response (Mungrue et al., 2009; Wang et al., 2012), a highly conserved cellular stress response caused by an accumulation of unfolded or misfolded proteins in the ER (Schröder and Kaufman, 2005). An association between the unfolded protein response, lipid metabolism, dysregulation of calcium homeostasis, and metabolic syndrome has been clearly established, but the direction of causality is controversial (Eizirik et al., 2008; Basseri and Austin, 2012; Cnop et al., 2012; Volmer and Ron, 2015). The role of ATF3 in particular has been studied in the context of type 2 diabetes, non-alcoholic fatty liver disease, diabetic cardiomyopathy, atherosclerosis, and obesity, with some authors suggesting it may have both detrimental and beneficial functions related to insulin resistance, mitochondrial dysfunction, and inflammation in response to high fat diets (Hyun et al., 2006; Qi et al., 2009; Zmuda et al., 2010; Aung et al., 2013; Jang et al., 2013; Kalfon et al., 2017; Kim et al., 2017, 2018). In arterial endothelial cells, ATF3 expression can be induced by exposure to high levels of triglyceride-rich lipoprotein lipolysis products (Aung et al., 2013), substantiating it as a link between high lipid metabolism and cellular stress response.

One of the most compelling links to metabolic syndrome and dysregulation of calcium homeostasis in our data is *ras related glycolysis inhibitor and calcium channel regulator* (*RRAD*), a gene encoding a small GTPase that binds directly to Ca^{2+}

channel beta subunits to regulate intracellular Ca^{2+} signaling in muscle cells (Finlin et al., 2003). RRAD also has regulatory functions via its interaction with calmodulin (Moyers et al., 1997). This gene was originally named *Ras-related associated with diabetes* because it was identified via subtraction cloning as the only gene out of 4000 cDNA clones that was overexpressed in skeletal muscle of type 2 diabetic individuals compared to non-diabetic or type 1 diabetic individuals (Reynet and Kahn, 1993). Overexpression of *RRAD* in cultured myocytes was found to reduce insulin-stimulated glucose uptake by 50-90%, which the authors speculated was due to a decrease in intrinsic activity of glucose transporter 4, the insulin-dependent glucose transporter (Moyers et al., 1996). An in vivo study of transgenic mice overexpressing *RRAD* in skeletal muscle found that high fat feeding produced not only insulin resistance in transgenic mice, but also increased triglyceride metabolism compared to controls (Ilany et al., 2006). This suggests that RRAD may inhibit glycolysis independently from its action on glucose transporters via substrate competition (Randle et al., 1994). Another regulator of intracellular Ca^{2+}, *RAPGEF4*, upregulated in the current study, is the direct target of some anti-diabetic drugs called sulfonylureas (Zhang et al., 2009).

The role of Ca^{2+} in metabolic syndrome and diabetes is complex and not fully understood, but one theory suggests that the disruption of Ca^{2+} homeostasis is a feed-forward pathological cycle resulting from ER dysfunction during chronic exposure to excessive nutrients and energy (Arruda and Hotamisligil, 2015). The majority of intracellular Ca^{2+} pools are contained within the ER, known as the sarcoplasmic reticulum in muscle cells; however, high concentrations of fatty acids can mediate a substantial redistribution of ER luminal Ca^{2+} stores among subcompartments of the

ER and from the ER to the cytosol, leading to ER stress and eventually cell death (Rys-Sikora and Gill, 1998; Wei et al., 2009).

5.5.3 Increased Expression of Genes Related to Hypertrophy and Slow-Twitch Muscle

Several genes involved in myogenic differentiation and muscle hypertrophy are upregulated in affected birds: *musculoskeletal, embryonic nuclear protein 1* (*MUSTN1*), *ankyrin repeat domain 1* (*ANKRD1*), and *HOPX* have roles in myotube formation, myofusion, and regulation of other myoblast differentiation genes (Shin et al., 2002; Yang et al., 2005; Kee et al., 2007; Kojic et al., 2010; Zhang et al., 2012; Ma et al., 2014), although studies of *HOPX* in chickens have found that it's highly expressed in adipose tissue and has functions related to adipocyte differentiation (Zhang et al., 2012; Shi et al., 2015). Other upregulated genes related to development and regeneration of the musculosketal system include *PDZ and LIM domain 3* (*PDLIM3*), *small muscle protein X-linked* (*SMPX*), and *leiomodin 2* (*LMOD2*). Two of these, *SMPX* and *PDLIM3,* encode Z-disc associated proteins with putative mechanosensory or stretch signaling roles in striated muscle (Bagnall et al., 2010; Eftestøl et al., 2014). Expression of *MUSTN1*, *ANKRD1*, *PDLIM3,* and *SMPX* can be induced by eccentric contraction exercises (Chen et al., 2002; Barash et al., 2004; Kostek et al., 2007) or passive stretch (Kemp et al., 2001), suggesting a role in muscle hypertrophy and repair (Eftestøl et al., 2014). Although some of these genes possess roles in muscle fiber regeneration, we do not believe that they are indicative of the regenerative process that characterizes later stages of wooden breast. Regeneration of new muscle fibers occurs in response to degeneration and necrosis and is not apparent microscopically until 3 weeks of age (Papah et al., 2017).

Upregulation of genes related to hypertrophy in affected birds is in line with higher breast muscle yield in affected birds (Dalle Zotte et al., 2014; Bailey et al., 2015; Mutryn et al., 2015b). In fact, speculation on the cause of wooden breast and related muscle disorders has focused largely on impaired oxygen supply and buildup of metabolic waste resulting from sustained rapid growth of the pectoralis major (MacRae et al., 2006; Kuttappan et al., 2013; Mudalal et al., 2015; Lilburn et al., 2018). However, upregulation of genes involved in hypertrophy may also be part of the disease process, causing excessive growth of pectoralis major in affected chickens. Considering the metabolic and physiologic similarities between wooden breast and diabetes, it is possible that mechanisms underlying muscle hypertrophy in wooden breast are similar to those that cause hypertrophy of organs in diabetic complications. For example, diabetic cardiomyopathy, non-alcoholic fatty liver disease, and diabetic nephropathy can cause structural remodeling that includes hypertrophy of the heart, liver, and kidneys respectively (Sharma and McNeill, 2006; Satriano, 2007; Liang et al., 2014) .

Interestingly, our data showed upregulation of several genes, such as *MYBPC1* and *SMPX* (Palmer et al., 2001; Jingting et al., 2017), that are more closely associated with slow-twitch oxidative muscle rather than fast-twitch glycolytic muscle. For example, *LMOD2* has been alternatively called cardiac leiomodin and its levels in cardiac muscle are directly linked to the length of actin-containing thin filaments due to competition for binding with tropomodulin-1 (Tsukada et al., 2010). Overexpression of *LMOD2* in the heart results in elongation of thin filaments and reduced cardiac function as proper thin filament length is necessary to generate contractile force (Tsukada et al., 2010; Pappas et al., 2018). Similarly, *ANKRD1* was

previously named cardiac ankyrin repeat protein (CARP) and has been proposed as a marker of cardiac hypertrophy due to its increased expression in 3 distinct models of cardiac hypertrophy in rats (Aihara et al., 2000). The lipid transporter *FABP3*, which is involved in the uptake, intracellular metabolism and transport of long-chain fatty acids, is most abundantly expressed in slow-twitch skeletal and cardiac muscle of humans (Heuckeroth et al., 1987). Upregulation of these genes is consistent with previous reports of fiber-type switching in 7-week-old birds with wooden breast (Mutryn et al., 2015a) and may suggest that the pectoralis major muscle of affected birds resembles cardiac or slow-twitch muscle at the transcriptional level.

5.5.4 Comparison with Prior Gene Expression Study of Early Stages of Wooden Breast

A considerable number of differentially expressed genes from the current study were previously identified by Papah et al. (Papah et al., 2018), who studied the early pathogenesis of wooden breast in male broilers. Of the 20 genes that were previously identified, the majority were found to be differentially expressed in 3-week-old birds rather than 2-week-old birds (Table 5.4). A key difference between these studies is the use of male birds in the previous study and female birds in the present experiment. Methodological discrepancies, such as broiler line and severity of disease in affected birds, prevent us from drawing conclusions about sex-linked differences in global gene expression that might help explain the higher prevalence and severity of wooden breast among male birds compared to females (Trocino et al., 2015). However, it has been suggested that increased expression of genes related to fat metabolism and deposition in the pectoralis major of male broilers at 3 weeks of age may contribute to their increased susceptibility (Brothers et al., 2019). Incomplete dosage compensation

in male broilers, which are homogametic, may also play an important role (Brothers et al., 2019). The only Z-linked gene found to be differentially expressed in our results is *LPL*, which encodes a rate-limiting catalyst for lipoprotein triglyceride hydrolysis (Mead et al., 2002; Wang and Eckel, 2009). Upregulation of LPL in the pectoralis major of affected birds may increase the rate that lipids are taken up by the muscle, making it a critical gene for ectopic lipid deposition.

Table 5.4: Comparison of differentially expressed genes with previous study of wooden breast in male broilers. A total of 20 genes from the current study were also previously identified at early stages of wooden breast development in 2- and 3-week-old male broilers by Papah et al. (Papah et al., 2018).

Biopsy Age	No. Genes	Gene Symbols
2 weeks	4	*ANKRD1, ATF3, CHAC1, RAPGEF4*
3 weeks	18	*AVD, BBS5, CD36, CHAC1, CIDEA, FABP4, HOPX, LINGO1, LMOD2, LPL, MYBPC1, OCM2, RAPGEF4, RBP7, RRAD, SMPX, STK17A, UCHL1*

Our results highlight the importance of increased lipid metabolism in governing susceptibility to wooden breast and establish high expression of lipid metabolism genes as a much earlier signature of the disease than was previously believed. This is consistent with previous reports of metabolic perturbations in wooden breast (Mutryn et al., 2015a; Abasht et al., 2016; Papah et al., 2018), especially a recent study suggesting that the increased ability to direct alimentary resources, particularly fatty acids, to the pectoralis major muscle may underlie susceptibility to wooden breast (Abasht et al., 2019). While our findings reveal strong parallels between wooden breast in broilers and metabolic syndrome in humans, it is important to recognize that wooden breast is not associated with increased visceral adiposity (Zhuo et al., 2015; Abasht et al., 2019) or elevated blood glucose levels

(Livingston et al., 2019a). Additionally, lipotoxicity in human skeletal muscle causes muscle atrophy (Tamilarasan et al., 2012) while wooden breast affected birds have a significantly larger pectoralis major muscle compared to unaffected birds (Dalle Zotte et al., 2014). It is important to investigate how ectopic lipid accumulation in skeletal muscle can manifest with such disparate phenotypes in humans compared to broilers.

5.6 Conclusions

The findings of this study show that transcriptional changes associated with early stages of wooden breast disease in 2-week-old birds have significant overlap with genes that are dysregulated in metabolic syndrome in humans. Although the underlying causes of metabolic dysfunction possibly leading to pathological progression of wooden breast remain unknown, this study clearly demonstrates that early upregulation of lipid metabolism in the pectoralis major is a key feature of the myopathy. Additionally, the finding that PPARγ and several of its transcriptional target genes are expressed higher in affected chickens provides critical insight into the early pathogenesis of wooden breast. Affected birds also show dysregulation of various genes involved in muscle growth and function as well as calcium signaling and ER stress. Additional research is needed to understand the mechanisms underlying the apparent metabolic dysfunction and to investigate the possible link between wooden breast and metabolic syndrome.

5.7 Acknowledgements

The authors gratefully acknowledge the in-kind support by Cobb-Vantress Inc. in providing chicks and chicken feed for this experiment. We also greatly appreciate assistance with samples and data collection from many graduate and undergraduate

students at the University of Delaware Department of Animal and Food Sciences. We would like to acknowledge the support from the University of Delaware Center for Bioinformatics and Computational Biology for utilization of their cluster BioMix, which was made possible through support from the Delaware INBRE (NIH GM103446), the state of Delaware and the Delaware Biotechnology Institute (DBI). RNA sequencing services at DBI are greatly appreciated.

REFERENCES

Abasht, B., Mutryn, M. F., Michalek, R. D., and Lee, W. R. (2016). Oxidative stress and metabolic perturbations in wooden breast disorder in chickens. *PLoS One* 11, 1–16. doi:10.1371/journal.pone.0153750.

Abasht, B., Zhou, N., Lee, W. R., Zhuo, Z., and Peripolli, E. (2019). The metabolic characteristics of susceptibility to wooden breast disease in chickens with high feed efficiency. *Poult. Sci.* 98, 3246–3256. doi:10.3382/ps/pez183.

Abdullah, N., Abdul Murad, N. A., Attia, J., Oldmeadow, C., Mohd Haniff, E. A., Syafruddin, S. E., et al. (2015). Characterizing the genetic risk for Type 2 diabetes in a Malaysian multi-ethnic cohort. *Diabet. Med.* 32, 1377–1384. doi:10.1111/dme.12735.

Aihara, Y., Kurabayashi, M., Saito, Y., Ohyama, Y., Tanaka, T., Takeda, S., et al. (2000). Cardiac ankyrin repeat protein is a novel marker of cardiac hypertrophy: Role of M-CAT element within the promoter. *Hypertension* 36, 48–53. doi:10.1161/01.hyp.36.1.48.

Arruda, A. P., and Hotamisligil, G. S. (2015). Calcium homeostasis and organelle function in the pathogenesis of obesity and diabetes. *Cell Metab.* 22, 381–397. doi:10.1016/j.cmet.2015.06.010.

Aung, H. H., Lame, M. W., Gohil, K., An, C. Il, Wilson, D. W., and Rutledge, J. C. (2013). Induction of ATF3 gene network by triglyceride-rich lipoprotein lipolysis products increases vascular apoptosis and inflammation. *Arterioscler. Thromb. Vasc. Biol.* 33, 2088–2096. doi:10.1161/ATVBAHA.113.301375.

Bagnall, R. D., Yeates, L., and Semsarian, C. (2010). Analysis of the Z-disc genes PDLIM3 and MYPN in Patients with Hypertrophic Cardiomyopathy. *Int. J. Cardiol.* 145, 601–602. doi:10.1016/j.ijcard.2010.08.004.

Bailey, R. A., Watson, K. A., Bilgili, S. F., and Avendano, S. (2015). The genetic basis of pectoralis major myopathies in modern broiler chicken lines. *Poult. Sci.* 94, 2870–2879. doi:10.3382/ps/pev304.

Barash, I. A., Mathew, L., Ryan, A. F., Chen, J., and Lieber, R. L. (2004). Rapid muscle-specific gene expression changes after a single bout of eccentric contractions in the mouse. *Am. J. Physiol. Physiol.* 286, C355–C364. doi:10.1152/ajpcell.00211.2003.

Basseri, S., and Austin, R. C. (2012). Endoplasmic reticulum stress and lipid metabolism: Mechanisms and therapeutic potential. *Biochem. Res. Int.* 2012. doi:10.1155/2012/841362.

Beales, P. L., Elcioglu, N., Woolf, A. S., Parker, D., and Flinter, F. A. (1999). New criteria for improved diagnosis of Bardet-Biedl syndrome: results of a population survey. *J. Med. Genet.* 36, 437–46. Available at: http://www.ncbi.nlm.nih.gov/pubmed/10874630%0Ahttp://www.pubmedcentral.nih.gov/articlerender.fcgi?artid=PMC1734378.

Bolger, A. M., Lohse, M., and Usadel, B. (2014). Trimmomatic: A flexible trimmer for Illumina sequence data. *Bioinformatics* 30, 2114–2120. doi:10.1093/bioinformatics/btu170.

Bonen, A., Parolin, M. L., Steinberg, G. R., Calles-Escandon, J., Tandon, N. N., Glatz, J. F. C., et al. (2004). Triacylglycerol accumulation in human obesity and type 2 diabetes is associated with increased rates of skeletal muscle fatty acid transport and increased sarcolemmal FAT/CD36. *FASEB J.* 18, 1144–1146. doi:10.1096/fj.03-1065fje.

Brothers, B., Zhuo, Z., Papah, M. B., and Abasht, B. (2019). RNA-seq analysis reveals spatial and sex differences in pectoralis major muscle of broiler chickens contributing to difference in susceptibility to wooden breast disease. *Front. Physiol.* 10. doi:10.3389/fphys.2019.00764.

Caplen, N. J., Patel, A., Millward, A., Campbell, R. D., Ratanachaiyavong, S., Wong, F. S., et al. (1990). Complement C4 and heat shock protein 70 (HSP70) genotypes and type I diabetes mellitus. *Immunogenetics* 32, 427–430.

Chen, Y. W., Nader, G. A., Baar, K. R., Fedele, M. J., Hoffman, E. P., and Esser, K. A. (2002). Response of rat muscle to acute resistance exercise defined by transcriptional and translational profiling. *J. Physiol.* 545, 27–41. doi:10.1113/jphysiol.2002.021220.

Chen, Z., Zhao, T.-J., Li, J., Gao, Y.-S., Meng, F.-G., Yan, Y.-B., et al. (2011). Slow skeletal muscle myosin-binding protein-C (MyBPC1) mediates recruitment of muscle-type creatine kinase (CK) to myosin. *Biochem. J.* 436, 437–445. doi:10.1042/bj20102007.

Cnop, M., Foufelle, F., and Velloso, L. A. (2012). Endoplasmic reticulum stress, obesity and diabetes. *Trends Mol. Med.* 18, 59–68. doi:10.1016/j.molmed.2011.07.010.

Cui, H., Zheng, M., Zhao, G., Liu, R., and Wen, J. (2018). Identification of differentially expressed genes and pathways for intramuscular fat metabolism between breast and thigh tissues of chickens. *BMC Genomics* 19, 1–9. doi:10.1186/s12864-017-4292-3.

Dalle Zotte, A., Cecchinato, M., Quartesan, A., Bradanovic, J., and Puolanne, E. (2014). How does "Wooden Breast" myodegradation affect poultry meat quality? in *60th International Congress of Meat Science and Technology* (Punta Del Este, Uruguay).

Eftestøl, E., Norman Alver, T., Gundersen, K., and Bruusgaard, J. C. (2014). Overexpression of SMPX in adult skeletal muscle does not change skeletal muscle fiber type or size. *PLoS One* 9. doi:10.1371/journal.pone.0099232.

Eizirik, D. L., Cardozo, A. K., and Cnop, M. (2008). The role for endoplasmic reticulum stress in diabetes mellitus. *Endocr. Rev.* 29, 42–61. doi:10.1210/er.2007-0015.

FastQC Available at: https://www.bioinformatics.babraham.ac.uk/projects/fastqc/.

Faustman, D., Li, X., Lin, H. Y., Fu, Y., Eisenbarth, G., Avruch, J., et al. (1991). Linkage of faulty major histocompatibility complex class I to autoimmune diabetes. *Science (80-.).* 254, 1756–1761. doi:10.1126/science.1763324.

Finlin, B. S., Crump, S. M., Satin, J., and Andres, D. A. (2003). Regulation of voltage-gated calcium channel activity by the Rem and Rad GTPases. *Proc. Natl. Acad. Sci. U. S. A.* 100, 14469–74. doi:10.1073/pnas.2437756100.

Forsythe, E., and Beales, P. L. (2013). Bardet-Biedl syndrome. *Eur. J. Hum. Genet.* 21, 8–13. doi:10.1111/j.1442-9071.1984.tb01143.x.

Furuhashi, M., Saitoh, S., Shimamoto, K., and Miura, T. (2014). Fatty acid-binding protein 4 (FABP4): Pathophysiological insights and potent clinical biomarker of metabolic and cardiovascular diseases. *Clin. Med. Insights Cardiol.* 2014, 23–33. doi:10.4137/CMC.S17067.

Gall, S., Suyemoto, M. M., Sather, H. M. L., Sharpton, A. R., Barnes, H. J., and Borst, L. B. (2019). Wooden breast in commercial broilers associated with mortality, dorsal recumbency, and pulmonary disease. *Avian Dis. In-Press*.

Green, C. R., Wallace, M., Divakaruni, A. S., Phillips, S. A., Murphy, A. N., Ciaraldi, T. P., et al. (2016). Branched-chain amino acid catabolism fuels adipocyte differentiation and lipogenesis. *Nat. Chem. Biol.* 12, 15–21. doi:10.1038/nchembio.1961.

Heuckeroth, R. O., Birkenmeier, E. H., Levin, M. S., and Gordon, J. I. (1987). Analysis of the tissue-specific expression, developmental regulation, and linkage relationships of a rodent gene encoding heart fatty acid binding protein. *J. Biol. Chem.* 262, 9709–9717.

Howard, B. V. (1987). Lipoprotein metabolism in diabetes mellitus. *J. Lipid Res.* 28, 613–628. doi:10.1016/s0955-2863(96)00117-9.

Husi, H., Van Agtmael, T., Mullen, W., Bahlmann, F. H., Schanstra, J. P., Vlahou, A., et al. (2014). Proteome-based systems biology analysis of the diabetic mouse aorta reveals major changes in fatty acid biosynthesis as potential hallmark in diabetes mellitus-associated vascular disease. *Circ. Cardiovasc. Genet.* 7, 161–170. doi:10.1161/CIRCGENETICS.113.000196.

Hyun, B. K., Kong, M., Tae, M. K., Young, H. S., Kim, W. H., Joo, H. L., et al. (2006). NFATc4 and ATF3 negatively regulate adiponectin gene expression in 3T3-L1 adipocytes. *Diabetes* 55, 1342–1352. doi:10.2337/db05-1507.

Ilany, J., Bilan, P. J., Kapur, S., Caldwell, J. S., Patti, M.-E., Marette, A., et al. (2006). Overexpression of Rad in muscle worsens diet-induced insulin resistance and glucose intolerance and lowers plasma triglyceride level. *Proc. Natl. Acad. Sci.* 103, 4481–4486. doi:10.1073/pnas.0511246103.

Jang, M. K., Son, Y., and Jung, M. H. (2013). ATF3 plays a role in adipocyte hypoxia-mediated mitochondria dysfunction in obesity. *Biochem. Biophys. Res. Commun.* 431, 421–427. doi:10.1016/j.bbrc.2012.12.154.

Jeong, J., Kwon, E. G., Im, S. K., Seo, K. S., and Baik, M. (2012). Expression of fat deposition and fat removal genes is associated with intramuscular fat content in longissimus dorsi muscle of Korean cattle steers. *J. Anim. Sci.* 90, 2044–2053. doi:10.2527/jas.2011-4753.

Jingting, S., Qin, X., Yanju, S., Ming, Z., Yunjie, T., Gaige, J., et al. (2017). Oxidative and glycolytic skeletal muscles show marked differences in gene expression profile in Chinese Qingyuan partridge chickens. *PLoS One* 12, 1–17. doi:10.1371/journal.pone.0183118.

Kalfon, R., Koren, L., Aviram, S., Schwartz, O., Hai, T., and Aronheim, A. (2017). ATF3 expression in cardiomyocytes preserves homeostasis in the heart and controls peripheral glucose tolerance. *Cardiovasc. Res.* 113, 134–146. doi:10.1093/cvr/cvw228.

Kang, H. P., Yang, X., Chen, R., Zhang, B., Corona, E., Schadt, E. E., et al. (2012). Integration of disease-specific single nucleotide polymorphisms, Expression quantitative trait loci and coexpression networks reveal novel candidate genes for type 2 diabetes. *Diabetologia* 55, 2205–2213. doi:10.1007/s00125-012-2568-3.

Kee, H. J., Kim, J. R., Nam, K. Il, Hye, Y. P., Shin, S., Jeong, C. K., et al. (2007). Enhancer of polycomb1, a novel homeodomain only protein-binding partner, induces skeletal muscle differentiation. *J. Biol. Chem.* 282, 7700–7709. doi:10.1074/jbc.M611198200.

Kemp, T. J., Sadusky, T. J., Simon, M., Brown, R., Eastwood, M., Sassoon, D. A., et al. (2001). Identification of a novel stretch-responsive skeletal muscle gene (Smpx). *Genomics* 72, 260–271. doi:10.1006/geno.2000.6461.

Kilpeläinen, T. O., Bentley, A. R., Noordam, R., Sung, Y. J., Schwander, K., Winkler, T. W., et al. (2019). Multi-ancestry study of blood lipid levels identifies four loci interacting with physical activity. *Nat. Commun.* 10. doi:10.1038/s41467-018-08008-w.

Kim, D., Langmead, B., and Salzberg, S. L. (2015). HISAT: A fast spliced aligner with low memory requirements. *Nat. Methods* 12, 357–360. doi:10.1038/nmeth.3317.

Kim, J. Y., Park, K. J., Hwang, J. Y., Kim, G. H., Lee, D. Y., Lee, Y. J., et al. (2017). Activating transcription factor 3 is a target molecule linking hepatic steatosis to impaired glucose homeostasis. *J. Hepatol.* 67, 349–359. doi:10.1016/j.jhep.2017.03.023.

Kim, S., Song, N. J., Bahn, G., Chang, S. H., Yun, U. J., Ku, J. M., et al. (2018). Atf3 induction is a therapeutic target for obesity and metabolic diseases. *Biochem. Biophys. Res. Commun.* 504, 903–908. doi:10.1016/j.bbrc.2018.09.048.

Kojic, S., Nestorovic, A., Rakicevic, L., Belgrano, A., Stankovic, M., Divac, A., et al. (2010). A novel role for cardiac ankyrin repeat protein Ankrd1/CARP as a co-activator of the p53 tumor suppressor protein. *Arch. Biochem. Biophys.* 502, 60–67. doi:10.1016/j.abb.2010.06.029.

Kostek, M. C., Chen, Y.-W., Cuthbertson, D. J., Shi, R., Fedele, M. J., Esser, K. A., et al. (2007). Gene expression responses over 24 h to lengthening and shortening contractions in human muscle: major changes in CSRP3, MUSTN1, SIX1, and FBXO32. *Physiol. Genomics* 31, 42–52. doi:10.1152/physiolgenomics.00151.2006.

Kuttappan, V. A., Shivaprasad, H. l., Shaw, D. P., Valentine, B. A., Hargis, B. M., Clark, F. D., et al. (2013). Pathological changes associated with white striping in broiler breast muscles. *Poult. Sci.* 92, 331–338. doi:10.3382/ps.2012-02646.

Laplante, M., Sell, H., MacNaul, K. L., Richard, D., Berger, J. P., and Deshaies, Y. (2003). PPAR-gamma activation mediates adipose depot-specific effects on gene expression and lipoprotein lipase activity. *Diabetes* 52, 291–299. Available at: http://diabetes.diabetesjournals.org/content/52/2/291.short.

Lappas, M. (2011). Lower circulating levels of complement split proteins C3a and C4a in maternal plasma of women with gestational diabetes mellitus. *Diabet. Med.* 28, 906–911. doi:10.1111/j.1464-5491.2011.03336.x.

Lefterova, M. I., Zhang, Y., Steger, D. J., Schupp, M., Schug, J., Cristancho, A., et al. (2008). PPARγ and C/EBP factors orchestrate adipocyte biology via adjacent binding on a genome-wide scale. *Genes Dev.* 22, 2941–2952. doi:10.1101/gad.1709008.

Liang, W., Menke, A. L., Driessen, A., Koek, G. H., Lindeman, J. H., Stoop, R., et al. (2014). Establishment of a general NAFLD scoring system for rodent models and comparison to human liver pathology. *PLoS One* 9, 1–17. doi:10.1371/journal.pone.0115922.

Lilburn, M. S., Griffin, J. R., and Wick, M. (2018). From muscle to food: oxidative challenges and developmental anomalies in poultry breast muscle. *Poult. Sci.* doi:10.3382/ps/pey409.

Lim, M. A., Riedel, H., and Liu, F. (2007). Grb10: more than a simple adaptor protein. *Front. Biosci.* 9, 387–403. doi:10.2741/1226.

Liu, L., Cui, H., Fu, R., Zheng, M., Liu, R., Zhao, G., et al. (2017). The regulation of IMF deposition in pectoralis major of fast- and slow- growing chickens at hatching. *J. Anim. Sci. Biotechnol.* 8, 1–8. doi:10.1186/s40104-017-0207-z.

Liu, M., Bai, J., He, S., Villarreal, R., Hu, D., Zhang, C., et al. (2014). Grb10 promotes lipolysis and thermogenesis by phosphorylation-dependent feedback inhibition of mTORC1. *Cell Metab.* 19, 967–980. doi:10.1016/j.cmet.2014.03.018.

Livingston, M. L., Ferket, P. R., Brake, J., and Livingston, K. A. (2019). Dietary amino acids under hypoxic conditions exacerbates muscle myopathies including wooden breast and white stripping. *Poult. Sci.* 98, 1517–1527. doi:10.3382/ps/pey463.

Ma, G., Wang, H., Gu, X., Li, W., Zhang, X., Cui, L., et al. (2014). CARP, a myostatin-downregulated gene in CFM cells, is a novel essential positive regulator of myogenesis. *Int. J. Biol. Sci.* 10, 309–320. doi:10.7150/ijbs.7475.

MacRae, V. E., Mahon, M., Gilpin, S., Sandercock, D. A., and Mitchell, M. A. (2006). Skeletal muscle fibre growth and growth associated myopathy in the domestic chicken (Gallus domesticus). *Br. Poult. Sci.* 47, 264–272. doi:10.1080/00071660600753615.

Martin, S., and Parton, R. G. (2008). "Characterization of Rab18, a lipid droplet-associated Small GTPase," in *Methods in Enzymology*, 109–129. doi:10.1016/S0076-6879(07)38008-7.

Matsuura, K., Uesugi, N., Hijiya, N., Uchida, T., and Moriyama, M. (2007). Upregulated expression of cardiac ankyrin-repeated protein in renal podocytes is associated with proteinuria severity in lupus nephritis. *Hum. Pathol.* 38, 410–419. doi:10.1016/j.humpath.2006.09.006.

Mead, J. R., Irvine, S. A., and Ramji, D. P. (2002). Lipoprotein lipase: Structure, function, regulation, and role in disease. *J. Mol. Med.* 80, 753–769. doi:10.1007/s00109-002-0384-9.

Medina-Gomez, G., Gray, S., and Vidal-Puig, A. (2007). Adipogenesis and lipotoxicity: Role of peroxisome proliferator-activated receptor γ (PPARγ) and PPARγcoactivator-1 (PGC1). *Public Health Nutr.* 10, 1132–1137. doi:10.1017/S1368980007000614.

Mitch, W. E., Medina, R., Grieber, S., May, R. C., England, B. K., Price, S. R., et al. (1994). Metabolic acidosis stimulates muscle protein degradation by activating the adenosine triphosphate-dependent pathway involving ubiquitin and proteasomes. *J. Clin. Invest.* 93, 2127–2133. doi:10.1172/JCI117208.

Moreno-Viedma, V., Amor, M., Sarabi, A., Bilban, M., Staffler, G., Zeyda, M., et al. (2016). Common dysregulated pathways in obese adipose tissue and atherosclerosis. *Cardiovasc. Diabetol.* 15, 1–12. doi:10.1186/s12933-016-0441-2.

Morris, A. D. P., Voight, B. F., Teslovich, T. M., Ferreira, T., Segrè, A. V., Steinthorsdottir, V., et al. (2012). Large-scale association analysis provides insights into the genetic architecture and pathophysiology of type 2 diabetes. *Nat. Genet.* 44, 981–990. doi:10.1038/ng.2383.

Moyers, J. S., Bilan, P. J., Reynet, C., and Ronald Kahn, C. (1996). Overexpression of Rad inhibits glucose uptake in cultured muscle and fat cells. *J. Biol. Chem.* 271, 23111–23116. doi:10.1074/jbc.271.38.23111.

Moyers, J. S., Bilan, P. J., Zhu, J., and Kahn, C. R. (1997). Rad and Rad-related GTPases interact with calmodulin and calmodulin- dependent protein kinase II. *J. Biol. Chem.* 272, 11832–11839. doi:10.1074/jbc.272.18.11832.

Mudalal, S., Lorenzi, M., Soglia, F., Cavani, C., and Petracci, M. (2015). Implications of white striping and wooden breast abnormalities on quality traits of raw and marinated chicken meat. *Animal* 9, 728–734. doi:10.1017/S175173111400295X.

Mungrue, I. N., Pagnon, J., Kohannim, O., Gargalovic, P. S., and Lusis, A. J. (2009). CHAC1/MGC4504 is a novel proapoptotic component of the unfolded protein response, downstream of the ATF4-ATF3-CHOP cascade. *J. Immunol.* 182, 466–476.

Mutryn, M. F., Brannick, E. M., Fu, W., Lee, W. R., and Abasht, B. (2015a). Characterization of a novel chicken muscle disorder through differential gene expression and pathway analysis using RNA-sequencing. *BMC Genomics* 16, 399. doi:10.1186/s12864-015-1623-0.

Mutryn, M. F., Fu, W., and Abasht, B. (2015b). Incidence of Wooden Breast Disease and its correlation with broiler performance and ultimate pH of breast muscle. in *Proceedings of XXII European Symposium on Poultry Meat Quality* (Nantes, France).

Nie, J., DuBois, D. C., Xue, B., Jusko, W. J., and Almon, R. R. (2017). Effects of high-fat feeding on skeletal muscle gene expression in diabetic Goto-Kakizaki rats. *Gene Regul. Syst. Bio.* 11, 1–11. doi:10.1177/1177625017710009.

Norring, M., Valros, A., Valaja, J., Sihvo, H., Immonen, K., and Puolanne, E. (2018). Wooden breast myopathy links with poorer gait in broiler chickens. *Animal*, 1–6. doi:10.1017/S1751731118003270.

Palmer, S., Groves, N., Schindeler, A., Yeoh, T., Biben, C., Wang, C.-C., et al. (2001). The Small Muscle-specific Protein Csl Modifies Cell Shape and Promotes Myocyte Fusion in an... *J. Cell Biol.* 153, 985. Available at: http://search.ebscohost.com/login.aspx?direct=true&db=a9h&AN=5226347&site=ehost-live&scope=site.

Papah, M. B., Brannick, E. M., Schmidt, C. J., and Abasht, B. (2017). Evidence and role of phlebitis and lipid infiltration in the onset and pathogenesis of Wooden Breast Disease in modern broiler chickens. *Avian Pathol.* 46, 623–643. doi:10.1080/03079457.2017.1339346.

Papah, M. B., Brannick, E. M., Schmidt, C. J., and Abasht, B. (2018). Gene expression profiling of the early pathogenesis of wooden breast disease in commercial broiler chickens using RNA-sequencing. *PLoS One* 13, e0207346. doi:10.1371/journal.pone.0207346.

Pappas, C. T., Farman, G. P., Mayfield, R. M., Konhilas, J. P., and Gregorio, C. C. (2018). Cardiac-specific knockout of Lmod2 results in a severe reduction in myofilament force production and rapid cardiac failure. *J. Mol. Cell. Cardiol.* 122, 88–97. doi:10.1016/j.yjmcc.2018.08.009.

Park, K. S., Ciaraldi, T. P., Abrams-carter, L., Mudaliar, S., Nikoulina, S. E., and Henry, R. R. (1997). PPAR-y gene expression is elevated in skeletal muscle of obese and type II diabetic subjects. *Diabetes* 46, 1230–1234.

Park, P. J., Kong, S. W., Tebaldi, T., Lai, W. R., Kasif, S., and Kohane, I. S. (2009). Integration of heterogeneous expression data sets extends the role of the retinol pathway in diabetes and insulin resistance. *Bioinformatics* 25, 3121–3127. doi:10.1093/bioinformatics/btp559.

Phua, W. W. T., Wong, M. X. Y., Liao, Z., and Tan, N. S. (2018). An apparent functional consequence in skeletal muscle physiology via peroxisome proliferator-activated receptors. *Int. J. Mol. Sci.* 19. doi:10.3390/ijms19051425.

Puig-Oliveras, A., Ramayo-Caldas, Y., Corominas, J., Estellé, J., Pérez-Montarelo, D., Hudson, N. J., et al. (2014). Differences in muscle transcriptome among pigs phenotypically extreme for fatty acid composition. *PLoS One* 9. doi:10.1371/journal.pone.0099720.

Pulido, M. R., Diaz-Ruiz, A., Jiménez-Gómez, Y., Garcia-Navarro, S., Gracia-Navarro, F., Tinahones, F., et al. (2011). Rab18 dynamics in adipocytes in relation to lipogenesis, lipolysis and obesity. *PLoS One* 6. doi:10.1371/journal.pone.0022931.

Puri, V., Ranjit, S., Konda, S., Nicoloro, S. M. C., Straubhaar, J., Chawla, A., et al. (2008). Cidea is associated with lipid droplets and insulin sensitivity in humans. *Proc. Natl. Acad. Sci.* 105, 7833–7838. doi:10.1073/pnas.0802063105.

Qi, L., Saberi, M., Zmuda, E., Wang, Y., Altarejos, J., Zhang, X., et al. (2009). Adipocyte CREB promotes insulin resistance in obesity. *Cell Metab.* 9, 277–286. doi:10.1016/j.cmet.2009.01.006.

Randle, P. J., Priestman, D. A., Mistry, S. C., and Halsall, A. (1994). Glucose fatty acid interactions and the regulation of glucose disposal. *J. Cell. Biochem.* 55, 1–11. doi:10.1002/jcb.240550002.

Rasouli, N., Molavi, B., Elbein, S. C., and Kern, P. A. (2007). Ectopic fat accumulation and metabolic syndrome. *Diabetes, Obes. Metab.* 9, 1–10. doi:10.1111/j.1463-1326.2006.00590.x.

Resnyk, C. W., Carré, W., Wang, X., Porter, T. E., Simon, J., Le Bihan-Duval, E., et al. (2017). Transcriptional analysis of abdominal fat in chickens divergently selected on bodyweight at two ages reveals novel mechanisms controlling adiposity: Validating visceral adipose tissue as a dynamic endocrine and metabolic organ. *BMC Genomics* 18, 1–31. doi:10.1186/s12864-017-4035-5.

Reynet, C., and Kahn, C. R. (1993). Rad: A member of the Ras family overexpressed in muscle of type II diabetic humans. *Science (80-.).* 262, 1441. Available at: http://search.proquest.com/docview/213556241/8483B8EB64464EB0PQ/58?accountid=11836z.

Rich, S. S., Goodarzi, M. O., Palmer, N. D., Langefeld, C. D., Ziegler, J., Haffner, S. M., et al. (2009). A genome-wide association scan for acute insulin response to glucose in Hispanic-Americans: The Insulin Resistance Atherosclerosis Family Study (IRAS FS). *Diabetologia* 52, 1326–1333. doi:10.1007/s00125-009-1373-0.

Rutsch, F., Gailus, S., Suormala, T., and Fowler, B. (2011). LMBRD1: The gene for the cblF defect of vitamin B12 metabolism. *J. Inherit. Metab. Dis.* 34, 121–126. doi:10.1007/s10545-010-9083-9.

Rys-Sikora, K. E., and Gill, D. L. (1998). Fatty acid-mediated calcium sequestration within intracellular calcium pools. *J. Biol. Chem.* 273, 32627–32635. doi:10.1074/jbc.273.49.32627.

Sanghera, D. K., and Blackett, P. R. (2012). Type 2 diabetes genetics: Beyond GWAS. *J. Diabetes Metab.* 3, 6948. doi:10.4172/2155-6156.1000198.

Satriano, J. (2007). Kidney growth, hypertrophy and the unifying mechanism of diabetic complications. *Amino Acids* 33, 331–339. doi:10.1007/s00726-007-0529-9.

Schröder, M., and Kaufman, R. J. (2005). ER stress and the unfolded protein response. *Mutat. Res. - Fundam. Mol. Mech. Mutagen.* 569, 29–63. doi:10.1016/j.mrfmmm.2004.06.056.

Scott, L. J., Mohlke, K. L., Bonnycastle, L. L., Willer, C. J., Li, Y., Duren, W. L., et al. (2007). A genome-wide association study of type 2 diabetes in finns detects multiple susceptibility variants. *Science (80-.).* 316, 1341–1345. doi:10.1126/science.1142382.

Semple, R. K., Chatterjee, V. K. K., and Rahilly, S. O. (2006). PPARγ and human metabolic disease. *J. Clin. Invest.* 116, 581–589. doi:10.1172/JCI28003.taglandin.

Sharma, V., and McNeill, J. H. (2006). Diabetic cardiomapathy: Where are we 40 years later? *Can. J. Cardiol.* 22, 305–308. doi:10.1016/S0828-282X(06)70914-X.

Shi, H., He, Q., Cheng, M., Sun, Y., Li, H., and Wang, N. (2015). Effect of HOPX gene overexpression on chicken preadipocyte proliferation. *Sci. Agric. Sin.* 48, 1624–1631. doi:10.3864/j.issn.0578-1752.2015.08.17.

Shin, C. H., Liu, Z. P., Passier, R., Zhang, C. L., Wang, D. Z., Harris, T. M., et al. (2002). Modulation of cardiac growth and development by HOP, an unusual homeodomain protein. *Cell* 110, 725–735. doi:10.1016/S0092-8674(02)00933-9.

Sihvo, H. K., Immonen, K., and Puolanne, E. (2014). Myodegeneration with fibrosis and regeneration in the pectoralis major muscle of broilers. *Vet. Pathol.* 51, 619–623. doi:10.1177/0300985813497488.

Sladek, R., Rocheleau, G., Rung, J., Dina, C., Shen, L., Serre, D., et al. (2007). A genome-wide association study identifies novel risk loci for type 2 diabetes. *Nature* 445, 881–885. doi:10.1038/nature05616.

Stumvoll, M., and Häring, H. (2002). The peroxisome proliferator–activated receptor-gamma2 Pro12Ala polymorphism. *Diabetes* 51, 2341–2347.

Surakka, I., Horikoshi, M., Mägi, R., Sarin, A.-P., Mahajan, A., Lagou, V., et al. (2015). The impact of low-frequency and rare variants on lipid levels. *Nat. Genet.* 47, 589–597. doi:10.1038/ng.3300.

Szatmari, I., Töröcsik, D., Agostini, M., Nagy, T., Gurnell, M., Barta, E., et al. (2007). PPARγ regulates the function of human dendritic cells primarily by altering lipid metabolism. *Blood* 110, 3271–3280. doi:10.1182/blood-2007-06-096222.

Tamilarasan, K. P., Temmel, H., Das, S. K., Al Zoughbi, W., Schauer, S., Vesely, P. W., et al. (2012). Skeletal muscle damage and impaired regeneration due to LPL-mediated lipotoxicity. *Cell Death Dis.* 3, e354-8. doi:10.1038/cddis.2012.91.

Tan, A. L. M., Langley, S. R., Tan, C. F., Chai, J. F., Khoo, C. M., Leow, M. K. S., et al. (2018). Ethnicity-specific skeletal muscle transcriptional signatures and their relevance to insulin resistance in Singapore. *J. Clin. Endocrinol. Metab.* 104, 465–486. doi:10.1210/jc.2018-00309.

Trapnell, C., Hendrickson, D. G., Sauvageau, M., Goff, L., Rinn, J. L., and Pachter, L. (2013). Differential analysis of gene regulation at transcript resolution with RNA-seq. *Nat. Biotechnol.* 31, 46–53. doi:10.1038/nbt.2450.

Trocino, A., Piccirillo, A., Birolo, M., Radaelli, G., Bertotto, D., Filiou, E., et al. (2015). Effect of genotype, gender and feed restriction on growth, meat quality and the occurrence of white striping and wooden breast in broiler chickens. *Poult. Sci.* 94, 2996–3004. doi:10.3382/ps/pev296.

Tsukada, T., Pappas, C. T., Moroz, N., Antin, P. B., Kostyukova, A. S., and Gregorio, C. C. (2010). Leiomodin-2 is an antagonist of tropomodulin-1 at the pointed end of the thin filaments in cardiac muscle. *J. Cell Sci.* 123, 3136–3145. doi:10.1242/jcs.071837.

Tumova, J., Andel, M., and Trnka, J. (2016). Excess of free fatty acids as a cause of metabolic dysfunction in skeletal muscle. *Physiol. Res.* 65, 193–207. Available at: http://www.ncbi.nlm.nih.gov/pubmed/26447514.

Turcot, V., Lu, Y., Highland, H. M., Schurmann, C., Justice, A. E., Fine, R. S., et al. (2018). Protein-altering variants associated with body mass index implicate pathways that control energy intake and expenditure in obesity. *Nat. Genet.* 50, 26–35. doi:10.1038/s41588-017-0011-x.

Van Leeuwen, E. M., Karssen, L. C., Deelen, J., Isaacs, A., Medina-Gomez, C., Mbarek, H., et al. (2015). Genome of the Netherlands population-specific imputations identify an ABCA6 variant associated with cholesterol levels. *Nat. Commun.* 6. doi:10.1038/ncomms7065.

Volmer, R., and Ron, D. (2015). Lipid-dependent regulation of the unfolded protein response. *Curr. Opin. Cell Biol.* 33, 67–73. doi:10.1016/j.ceb.2014.12.002.

Wang, H., and Eckel, R. H. (2009). Lipoprotein lipase: from gene to obesity. *Am. J. Physiol. Metab.* 297, E271–E288. doi:10.1152/ajpendo.90920.2008.

Wang, Y. H., Byrne, K. A., Reverter, A., Harper, G. S., Taniguchi, M., McWilliam, S. M., et al. (2005). Transcriptional profiling of skeletal muscle tissue from two breeds of cattle. *Mamm. Genome* 16, 201–210. doi:10.1007/s00335-004-2419-8.

Wang, Y., Wan, B., Li, D., Zhou, J., Li, R., Bai, M., et al. (2012). BRSK2 is regulated by ER stress in protein level and involved in ER stress-induced apoptosis. *Biochem. Biophys. Res. Commun.* 423, 813–818. doi:10.1016/j.bbrc.2012.06.046.

Wang, Y. X. (2010). PPARs: Diverse regulators in energy metabolism and metabolic diseases. *Cell Res.* 20, 124–137. doi:10.1038/cr.2010.13.

Wei, T., and Simko, V. (2017). R package "corrplot": Visualization of a correlation matrix (Version 0.84). Available at: https://github.com/taiyun/corrplot.

Wei, Y., Wang, D., Gentile, C. L., and Pagliassotti, M. J. (2009). Reduced endoplasmic reticulum luminal calcium links saturated fatty acid-mediated endoplasmic reticulum stress and cell death in liver cells. *Mol. Cell. Biochem.* 331, 31–40. doi:10.1007/s11010-009-0142-1.

Westerbacka, J., Kolak, M., Kiviluoto, T., Arkkila, P., Sire, J., Hamsten, A., et al. (2007). Genes involved in fatty acid partitioning and binding, inflammation are overexpressed in the human fatty liver of insulin-resistant subjects. *Diabetes* 56, 2759–2765. doi:10.2337/db07-0156.ADIPOR.

Willer, C. J., Schmidt, E. M., Sengupta, S., Peloso, G. M., Gustafsson, S., Kanoni, S., et al. (2013). Discovery and refinement of loci associated with lipid levels. *Nat. Genet.* 45, 1274–1285. doi:10.1038/ng.2797.

Yang, S., Deng, H., Zhang, Q., Xie, J., Zeng, H., Jin, X., et al. (2016). Amelioration of diabetic mouse nephropathy by catalpol correlates with down-regulation of Grb10 adn activation of insulin-like growth factor 1/insulin-like growth factor 1 receptor signaling. *PLoS One* 11, e0151857. doi:10.1371/journal.pone.0151857.

Yang, T., Pang, C. P., Tsang, M. W., Lam, C. W., Poon, P. M. K., Chan, L. Y. S., et al. (2003). Pathogenic mutations of the lipoprotein lipase gene in Chinese patients with hypertriglyceridemic type 2 diabetes. *Hum. Mutat.* 21, 453. doi:10.1002/humu.9134.

Yang, W., Zhang, Y., Ma, G., Zhao, X., Chen, Y., and Zhu, D. (2005). Identification of gene expression modifications in myostatin-stimulated myoblasts. *Biochem. Biophys. Res. Commun.* 326, 660–666. doi:10.1016/j.bbrc.2004.11.096.

Zeggini, E., Scott, L. J., Saxena, R., and Voight, B. F. (2008). Meta-analysis of genome-wide association data and large-scale replication identifies additional susceptibility loci for type 2 diabetes. *Nat. Genet.* 40, 638–645. doi:10.1038/ng.120.

Zerega, B., Camardella, L., Cermelli, S., Sala, R., Cancedda, R., and Descalzi Cancedda, F. (2001). Avidin expression during chick chondrocyte and myoblast development in vitro and in vivo: regulation of cell proliferation. *J Cell Sci* 114, 1473–1482. Available at: http://www.ncbi.nlm.nih.gov/entrez/query.fcgi?cmd=Retrieve&db=PubMed&dopt=Citation&list_uids=11282023.

Zhang, C.-L., Katoh, M., Shibasaki, T., Minami, K., Sunaga, Y., Takahashi, H., et al. (2009). The cAMP sensor Epac2 is a direct target of antidiabetic sulfonylurea drugs. *Science* 325, 607–610. doi:10.1126/science.1172256.

Zhang, H., Luo, W., Sun, Y., Qiao, Y., Zhang, L., Zhao, Z., et al. (2016). Wnt/β-catenin signaling mediated-UCH-L1 expression in podocytes of diabetic nephropathy. *Int. J. Mol. Sci.* 17. doi:10.3390/ijms17091404.

Zhang, K., Zhang, Z. W., Wang, W. S., Yan, X. H., Li, H., and Wang, N. (2012). Cloning and expression of chicken HOPX gene. *J. Northeast Agric. Univ.* 43, 46–53.

Zhou, L., Xu, L., Ye, J., Li, D., Wang, W., Li, X., et al. (2012). Cidea promotes hepatic steatosis by sensing dietary fatty acids. *Hepatology* 56, 95–107. doi:10.1002/hep.25611.

Zhuo, Z., Lamont, S. J., Lee, W. R., and Abasht, B. (2015). RNA-seq analysis of abdominal fat reveals differences between modern commercial broiler chickens with high and low feed efficiencies. *PLoS One* 10, e0135810. doi:10.1371/journal.pone.0135810.

Zizola, C. F., Schwartz, G. J., and Vogel, S. (2008). Cellular retinol-binding protein type III is a PPARγ target gene and plays a role in lipid metabolism. *Am. J. Physiol. Metab.* 295, E1358–E1368. doi:10.1152/ajpendo.90464.2008.

Zmuda, E. J., Qi, L., Zhu, M. X., Mirmira, R. G., Montminy, M. R., and Hai, T. (2010). The roles of ATF3 , an adaptive-response gene, in high-fat-diet-induced diabetes and pancreatic β-cell dysfunction. *Mol. Endocrinol.* 24, 1423–1433. doi:10.1210/me.2009-0463.

Chapter 6

GENETIC BASIS AND IDENTIFICATION OF CANDIDATE GENES FOR WOODEN BREAST AND WHITE STRIPING IN COMMERCIAL BROILER CHICKENS

(Juniper A. Lake, Jack C.M. Dekkers, & Behnam Abasht. *Scientific Reports*, 11:6785, (2021)). https://www.nature.com/articles/s41598-021-86176-4

6.1 Abstract

Wooden breast (WB) and white striping (WS) are highly prevalent and economically damaging muscle disorders of modern commercial broiler chickens characterized respectively by palpable firmness and fatty white striations running parallel to the muscle fiber. High feed efficiency and rapid growth, especially of the breast muscle, are believed to contribute to development of such muscle defects; however, their etiology remains poorly understood. To gain insight into the genetic basis of these myopathies, a genome-wide association study was conducted using a commercial crossbred broiler population (n=1193). Heritability was estimated at 0.5 for WB and WS with high genetic correlation between them (0.88). GWAS revealed 28 quantitative trait loci (QTL) on five chromosomes for WB and 6 QTL on one chromosome for WS, with the majority of QTL for both myopathies located in a ~8 Mb region of chromosome 5. This region has highly conserved synteny with a portion of human chromosome 11 containing a cluster of imprinted genes associated with growth and metabolic disorders such as type 2 diabetes and Beckwith-Wiedemann syndrome. Candidate genes include *potassium voltage-gated channel subfamily Q*

member 1 (*KCNQ1*), involved in insulin secretion and cardiac electrical activity, *lymphocyte-specific protein 1* (*LSP1*), involved in inflammation and immune response.

6.2 Introduction

The modern commercial broiler chicken embodies remarkable gains in the economics of meat production realized through intensive breeding programs, optimized nutrition, and enhanced management practices. Compared to the 1950s, modern broilers can be raised to approximately the same market weight in close to half the time using substantially less feed and with substantially higher breast muscle yield (Havenstein et al., 2003b, 2003a; Petracci et al., 2015). However, the financial gains and increased production capacity associated with improvements to production traits are threatened by the concurrent global emergence of numerous muscle disorders that severely affect meat quality and may also impact animal welfare (Sihvo et al., 2014; Papah et al., 2017; Norring et al., 2018). Wooden breast and white striping, often co-occurring and believed to be part of the same disease spectrum (Mutryn et al., 2015a; Griffin et al., 2018), are two such myopathies, which together represent the breast muscle defects with the highest prevalence and greatest economic burden.

First described in the literature in 2014 (Sihvo et al., 2014), wooden breast manifests as palpably firm and discolored pectoralis major with subcutaneous and fascial edema, petechial hemorrhages, and spongy areas with disintegrating myofiber bundles. Birds affected by wooden breast frequently show signs of white striping as well, which is macroscopically characterized by white fatty striations running parallel to the muscle fibers and presents with similar histological lesions as wooden breast, including myodegeneration with regeneration, necrosis, lymphocyte and macrophage infiltration, fibrosis, and lipidosis (Kuttappan et al., 2013; Sihvo et al., 2014). These

muscle disorders present an exceptional challenge to producers, as dietary or management strategies against them often fail to improve meat quality (Livingston et al., 2019b; Zampiga et al., 2019) or lack viability due to impaired live performance (Meloche et al., 2018b) or cost-prohibitive inputs. The tight association between breast muscle disorders and economic traits such as feed efficiency and breast muscle yield suggests that successful mitigation of meat quality defects without simultaneous compromise to desirable traits will require an understanding of the genetic basis of these myopathies and selection against their causal variants.

Several hypotheses exist regarding the underlying causes of wooden breast and white striping. Some implicate the rapid growth of the pectoralis major and relative vascular deficiency for creating a buildup of waste products and hypoxic conditions (Boerboom et al., 2018; Soglia et al., 2019) in the breast muscle, while others suggest shared etiologic underpinnings with type 2 diabetes and other metabolic disorders in mammals (Lake et al., 2019; Lake and Abasht, 2020). However, current knowledge regarding the genetic basis of wooden breast and white striping is extremely limited and somewhat conflicting. Bailey et al. (Bailey et al., 2020) estimated heritability (h^2) of wooden breast and white striping in a pedigree commercial broiler pure line to be low – 0.07 for wooden breast and 0.25 for white striping – but also demonstrated a dramatic 18.4% reduction in wooden breast incidence after only 2 years of genetic selection against breast muscle myopathies. Another study of two broiler lines divergently selected for ultimate pH of the pectoralis major estimated heritability (h^2) of white striping to be 0.65 (Alnahhas et al., 2016). The only genome-wide association study of white striping was performed on a similar population and found no markers

with genome-wide significance (Pampouille et al., 2018), while the genetic architecture of wooden breast currently remains unexplored.

Our poor understanding of these traits at the genetic level is deficient and precludes our ability to adequately mitigate their effects through either broiler breeding or management. Therefore, the aim of this study is to estimate genetic parameters for wooden breast, white striping, and two body weight traits in a hybrid commercial broiler population and to identify quantitative trait loci (QTLs) and candidate genes to elucidate potential molecular mechanisms contributing to myopathy development.

6.3 Results and Discussion

6.3.1 Trait Statistics and Genetic Parameter Estimates

Of the 1,194 progeny that were genotyped for this study, only one bird did not meet the sequence filter criteria and was excluded from all analyses. Sex chromosomes were used to confirm each bird's sex before all analyses, and found that 12 birds were mis-gendered at necropsy. The sex-specific and overall distributions of wooden breast and white striping scores for the remaining 1,193 birds can be found in Table 6.1. The prevalence of wooden breast, i.e. the proportion of birds with a wooden breast score greater than 0, was approximately 79%, although the scoring system implemented in this study was relatively sensitive to mild signs of the myopathy compared to other studies (Meloche et al., 2018b; Livingston et al., 2019b). Meat quality is not substantially affected in birds with scores of 1 or 2, and severe wooden breast (score of 4) was detected only in 2.1% of chickens in our study (Table 6.1). The prevalence of white striping was similarly high, at approximately 80%. Compared

to males, female birds exhibited a lower prevalence of wooden breast (71% vs. 87%; p-value < 0.001) and white striping (73% vs. 87%; p-value < 0.001).

Table 6.1: Distributions of wooden breast and white striping scores among birds included in genetic analyses.

Wooden Breast Score	**Male (n = 557)**	**Female (n = 636)**	**Total (n = 1193)**
0 - Normal	12.6%	28.8%	21.2%
1 - Very Mild	19.0%	23.3%	21.3%
2 - Mild	39.9%	37.7%	38.7%
3 - Moderate	24.8%	9.6%	16.7%
4 - Severe	3.8%	0.6%	2.1%
White Striping Score			
0 - Normal	12.7%	26.9%	20.3%
1 - Mild	50.4%	48.0%	49.1%
2 - Moderate	31.1%	23.7%	27.2%
3 - Severe	5.7%	1.4%	3.4%

Descriptive statistics, heritability estimates, and variance components of the traits are summarized in Table 6.2. In our population, the wooden breast phenotype exhibits substantially higher heritability (h^2 = 0.49) than indicated by previous work, which estimated heritability between 0.1 and 0.24(Bailey et al., 2015). Additionally, we found the heritability of white striping (h^2 = 0.50) to lie between previous estimates ranging from 0.18 (Bailey et al., 2015) to 0.65 (Alnahhas et al., 2016). Variability among these studies is not surprising, as heritability is inherently specific to the population and environment in which it is estimated. For example, the lower estimates for heritability of wooden breast and white striping were for purebred commercial broiler lines that had relatively low incidence rates of myopathy – 0.16% to 0.39% for wooden breast; 14.46% to 49.6% for white striping – compared to other

hybrid commercial broiler populations (Bailey et al., 2015). Moderate heritability for wooden breast and white striping indicates that both genetic and environmental factors exert strong influences on phenotypic differences for these traits, which is consistent with studies that have demonstrated the ability to reduce severity and incidence of breast muscle myopathies through both genetic selection (Bailey et al., 2020) and manipulation of dietary energy (Meloche et al., 2018a, 2018b).

Table 6.2: Trait statistics and estimates (±SE) of heritability and residual variance from univariate analyses of wooden breast, white striping, and body weight at 13 days and at 7 weeks of age.

Trait	**Number of samples**	**Mean**	**SD**	**Heritability**	**Residual variance**
Wooden Breast[2]	1193	1.57	1.06	0.49 ± 0.06	0.51 ± 0.05
White Striping[3]	1193	1.14	0.77	0.50 ± 0.06	0.28 ± 0.03
Body Weight 13d (g)	1193	354	57	0.36 ± 0.06	1,548 ± 124
Body Weight 7wk (g)	1193	3,496	449	0.40 ± 0.06	45,085 ± 3,741

Wooden breast was scored on a 5-point scale from 0-Normal to 4-Severe. White striping was scored on a 4-point scale from 0-Normal to 3-Severe.

Our analysis found genetic correlations (Table 6.3) of wooden breast and white striping with body weight at 13 days (-0.04 and 0.15 respectively) and body weight at 7 weeks (0.16 and 0.09 respectively) to be low, while the estimate of the genetic correlation between the two myopathies was high (0.88). The latter reinforces an existing hypothesis that these two traits are related to each other and may be variations of the same disorder (Mutryn et al., 2015; Griffin et al., 2018). Note that low genetic correlation between the muscle disorders and body weight traits does not signify low genetic correlations of muscle disorders with other performance traits that were not assessed in this study, such as breast muscle yield and feed conversion ratio.

Table 6.3: Estimates (±SE) of phenotypic (above diagonal) and genetic (below diagonal) correlations among wooden breast, white striping, and body weight at 13 days and at 7 weeks of age based on bivariate analyses.

	Wooden Breast	**White Striping**	**Body Weight 13d**	**Body Weight 7wk**
Wooden Breast		0.65 ± 0.02	0.12 ± 0.03	0.25 ± 0.03
White Striping	0.88 ± 0.04		0.17 ± 0.03	0.19 ± 0.03
Body Weight 13d	-0.04 ± 0.12	0.15 ± 0.12		0.49 ± 0.03
Body Weight 7wk	0.16 ± 0.11	0.09 ± 0.11	0.54 ± 0.09	

6.3.2 Sequence and SNP Statistics

Excluding the single sample that did not meet filter criteria, sequencing produced an average of 5.88 million reads per sample, with an average mapping rate of 77.3%. A total of 199,957 SNPs were retained after locus filtering, consisting of 195,617 autosomal SNPs and 4,340 SNPs on the Z chromosome. The average sequence depth for each genotyped SNP was 10.8, with 97.9% of all genotype calls supported by at least 1 read. The average minor allele frequency was 0.24. The filtering criteria implemented in this study were substantially more stringent than in previous studies utilizing low-depth genotyping-by-sequencing methods (Chan et al., 2016) in order to identify QTLs with greater confidence.

6.3.3 Linkage Disequilibrium

Linkage disequilibrium (r^2) in the population decayed at an extremely rapid rate (Table 6.4), dropping below 0.2 at a distance of 2092 base pairs (bp) on macro-chromosomes, at 1410 bp on intermediate chromosomes, and at 1046 bp on micro-chromosomes. This value was substantially higher on the Z chromosome, at about 78 kb, because this chromosome is subjected to lower recombination frequency and a smaller effective population size. Based on $D_{0.2}$ estimates for each chromosome group, SNPs in the current dataset encompassed 27.5% of the genome (autosomes and Z

chromosome), with chromosome-specific capture rates ranging from 84.6% on the Z chromosome to 3.33% on chromosome 31 (Table 6.5).

Table 6.4: Linkage disequilibrium (r2) between markers located on macro-, intermediate, micro-chromosomes and the Z chromosome at distances of 1 kb, 10 kb, 100 kb, 500 kb, 1 Mb, and 5 Mb.

	1 kb	**10 kb**	**100 kb**	**500 kb**	**1Mb**	**5 Mb**	**$D_{0.2}$ (bp)**
Macro-chromosomes	0.23	0.15	0.08	0.05	0.04	0.02	2092
Intermediate chromosomes	0.21	0.14	0.08	0.05	0.04	0.02	1410
Micro-chromosomes	0.2	0.13	0.07	0.04	0.03	0.01	1046
Z chromosome	0.37	0.28	0.19	0.14	0.12	0.09	78370

Linkage disequilibrium values were used to calculate the distance at which LD decayed below the threshold of 0.2 ($D_{0.2}$)

Table 6.5: Approximate genome capture rates by chromosome determined using linkage decay ($D_{0.2}$) estimates for each chromosome group (micro, intermediate, macro, and Z chromosome).

Chromosome	**Not Captured (nucleotides)**	**Chromosome Length (nucleotides)**	**Percent Captured**
1	158939275	197608386	19.57
2	121983977	149682049	18.50
3	87891737	110838418	20.70
4	71014818	91315245	22.23
5	44735818	59809098	25.20
6	28743784	36374701	20.98
7	29083969	36742308	20.84
8	23238131	30219446	23.10
9	17922614	24153086	25.80
10	15288432	21119840	27.61
11	16415568	20200042	18.73
12	15674066	20387278	23.12
13	14429411	19166714	24.72
14	11540722	16219308	28.85

15	9524609	13062184	27.08
16	2615715	2844601	8.05
17	6712316	10762512	37.63
18	7550089	11373140	33.61
19	6728554	10323212	34.82
20	9569075	13897287	31.14
21	4344505	6844979	36.53
22	4340930	5459462	20.49
23	3307158	6149580	46.22
24	3813280	6491222	41.25
25	2515254	3980610	36.81
26	3278913	6055710	45.85
27	5665926	8080432	29.88
28	2660155	5116882	48.01
30	1469321	1818525	19.20
31	5948197	6153034	3.33
32	456255	725831	37.14
33	6124417	7821666	21.70
Z	12691444	82529921	84.62

6.3.4 GWAS Results for Wooden Breast

Single-SNP analysis of the genetic basis of wooden breast identified 51 SNPs that were significantly associated and an additional 71 SNPs that were suggestively associated with wooden breast score (Figure 6.1; Appendix B). These loci are located across 11 chromosomes of the *Gallus gallus* genome, including (GGA) 1, 2, 4, 5, 6, 9, 10, 18, 24, 30, and 32; however, the majority of significant markers (42 SNPs, 82%) and significant/suggestive markers combined (84 SNPs, 69%) were confined to a region on GGA5 from 8.1 Mb to 16.4 Mb. A total of 28 QTLs on chromosomes (GGA) 2, 5, 6, 30, and 32 were identified from significant SNPs that were clustered based on LD (Table 6.6). Bayesian multi-marker regression corroborated results from single-SNP analysis, detecting 9 1-Mb windows, on chromosomes (GGA) 2, 5, 6, 18,

and 30, that each explained more than 1% of genetic variance for the trait (Table 6.7). Together, these 9 windows explained 16.7% of the genetic variance for wooden breast. Three windows on GGA5, from 13.0 Mb to 17.0 Mb, explained a total of 6% of genetic variance, although the single highest-ranking window in this analysis was at the beginning of GGA30, which explained 3.1% of genetic variance. Although no significant QTLs were identified for sex-specific analyses of wooden breast, some markers exceeded the suggestive threshold in female birds and are listed in Appendix B. Genomic windows with suggestive significance in the BayesB analyses are listed in Appendix C for all traits.

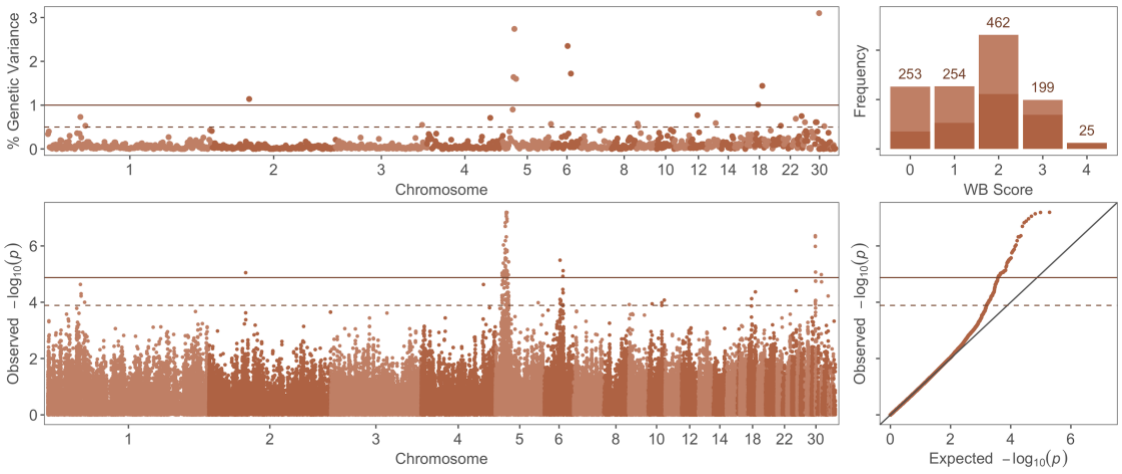

Figure 6.1: Genome-wide association results for wooden breast (WB) score using multi-marker (BayesB) and single-SNP (mixed linear model) analyses.

(Top Left) Percentage of genetic variance explained by 1-Mb regions across the genome for WB score. (Top Right) Distribution of WB scores across progeny used in genome-wide association analyses; dark red = male, light red = female. (Bottom Left) Manhattan plot of single-SNP results showing the −log10(p-value) of SNPs ordered by chromosome and position. (Bottom Right) Quantile-quantile plot of p-values from single-SNP results of WB score. Solid and dashed lines indicate significant and suggestive thresholds, respectively, for each model.

Table 6.6: Wooden Breast quantitative trait loci (QTLs) containing SNPs with FDR adjusted p-values less than 0.05.

QTL				Top SNP in QTL						
Chr	**Start (bp)**	**End (bp)**	**#SNP**	**Pos (bp)**	**Alleles**	**Freq**	**Beta**	**P-value**	**FDR**	**Candidate genes**
2	–	–	1	45199243	T/C	0.473	0.211	8.91e-06	0.043	–
5	8327574	8393723	3	8393723	A/T	0.228	0.289	9.17e-06	0.043	*MICAL2* *DKK3*
5	–	–	1	9797353	A/G	0.240	0.305	4.10e-06	0.031	*NRIP3*
5	9975375	10239083	2	9975375	T/C	0.232	0.325	9.28e-07	0.014	*DENND2B* *RPL27A*
5	–	–	1	10415181	T/A	0.390	0.246	7.83e-06	0.043	–
5	–	–	1	10675242	T/A	0.181	0.291	1.10e-05	0.046	*PSMA1*
5	11903835	11903902	4	11903836	G/A	0.235	-0.197	8.68e-06	0.043	–
5	–	–	1	11913861	A/G	0.163	-0.305	1.15e-05	0.046	–
5	–	–	1	11924135	T/C	0.255	0.300	1.76e-06	0.019	–
5	12196653	12196751	2	12196653	T/C	0.232	-0.352	1.50e-07	0.004	*USH1C*
5	12310175	12310343	7	12310234	T/C	0.244	-0.270	6.52e-07	0.011	–
5	13374229	13429787	2	13429787	T/C	0.240	-0.313	4.75e-07	0.008	*KCNQ1* *SLC22A18* *CDKN1C*
5	13449328	13449379	3	13449367	T/C	0.369	-0.281	6.38e-08	0.004	*KCNQ1*
5	–	–	1	13508017	C/A	0.245	0.301	7.27e-06	0.043	*KCNQ1*
5	–	–	1	13899194	G/C	0.255	-0.284	1.15e-05	0.046	–
5	14280580	14280613	2	14280613	T/C	0.335	0.311	6.47e-08	0.004	*LSP1*
5	14295515	14308280	4	14301905	G/C	0.180	-0.307	1.44e-06	0.018	*TNNI2* *SYT8* *ENSGALG00000006608*
5	14321077	14321102	2	14321077	G/A	0.433	0.280	1.32e-07	0.004	*CTSD* *ENSGALG00000006608*
5	–	–	1	14529930	T/C	0.286	0.065	7.87e-06	0.043	*BRSK1* *ENSGALG00000006608*
5	–	–	1	16063707	T/C	0.174	0.319	1.06e-05	0.046	*ENSGALG00000044313* *PHRF1*
5	16219365	16219383	2	16219365	A/G	0.213	-0.292	3.66e-06	0.029	*HRAS*
6	–	–	1	19640631	T/G	0.389	0.343	3.21e-06	0.027	–
6	–	–	1	23100280	A/G	0.303	0.294	1.20e-05	0.047	*GOT1* *CNNM1*
6	23389752	23391597	3	23389752	A/G	0.119	0.368	7.59e-06	0.043	*LCOR*
30	–	–	1	90012	C/T	0.292	-0.249	4.34e-07	0.008	*DNM2* *QTRT1*
30	96694	97362	2	97362	A/G	0.196	-0.283	4.73e-07	0.008	*DNM2*
30	–	–	1	393145	A/G	0.275	0.240	8.50e-06	0.043	*CNN1* *ZNF653* *ECSIT* *ELOF1* *ACP5*
32	–	–	1	86047	C/G	0.297	-0.261	1.05e-05	0.046	*ACTN4* *ECH1*

Candidate genes include protein-coding genes located within 5000bp upstream or downstream of the QTL start or end site, respectively. Chr: chromosome, bp: base pairs, #SNP: number of significant SNPs in QTL, Pos: position, Alleles: effect/alternative alleles, Freq: effect allele frequency, Beta: effect size estimate.

Table 6.7: Results of Bayesian multi-marker regression for wooden breast and white striping.

Trait	Chromosome	Window (Mb)	# SNPs	Explained genetic variance (%)	P > 0[1]
Wooden Breast	30	0 – 1	327	3.10	0.970
	5	14 – 15	186	2.74	0.808
	6	19 – 20	82	2.35	0.775
	6	23 – 24	990	1.72	0.951
	5	13 – 14	224	1.64	0.622
	5	16 – 17	436	1.60	0.798
	18	9 – 10	1508	1.44	0.987
	2	45 – 46	147	1.14	0.587
	18	4 – 5	791	1.01	0.890
White Striping	5	14 – 15	186	5.38	0.990
	5	58 – 59	604	3.18	0.997
	12	9 – 10	563	1.19	0.990

Windows identified by Bayes B were considered significant if they explained ≥ 1% of genetic variance. Body weight traits did not have any significant 1-Mb windows. P>0 refers to the frequency of sample for which the region had a nonzero effect.

Top candidate genes for wooden breast (Table 6.6) include *cyclin dependent kinase inhibitor 1C* (*CDKN1C*), *cathepsin D* (*CTSD*), *potassium voltage-gated channel subfamily Q member 1* (*KCNQ1*), *lymphocyte-specific protein 1* (*LSP1*), *solute carrier family 22 member 18* (*SLC22A18*) and *USH1 protein network component harmonin* (*USH1C*) on GGA5 and *dynamin 2* (*DNM2*) on GGA30. In humans, variation in all of these genes has been linked to altered insulin expression or secretion (Xu et al., 2011; Mutair et al., 2013; Travers et al., 2013; Fan et al., 2015) despite their having distinct biological functions.

6.3.5 GWAS Results for White Striping

A total of 18 SNPs (10 significant and 8 suggestive) were associated with white striping score (Figure 6.2; Appendix B), all of which are located on GGA5,

except for one marker on GGA11. Similar to the wooden breast association analysis results, most of these loci (9 significant and 6 suggestive, 83% of combined) were on GGA5, between 12.1 Mb and 14.8 Mb (Table 6.8). Bayesian multi-marker regression identified a window in this same region, between 14.0 Mb and 15.0 Mb, as the highest-ranking 1-Mb window, explaining 5.4% of genetic variance (Table 6.7). Two other windows also explain more than 1% of genetic variance, one on the long arm of GGA5 and one on GGA12. Together, the three significant windows for white striping explained 9.8% of the genetic variance for the trait. None of the QTLs identified in this study overlapped with QTLs previously identified for white striping; Pampouille et al. (Pampouille et al., 2018) did not discover QTLs with genome-wide significance, but identified three QTLs with chromosome-wide significance in the 3rd Mb windows of GGA17 and GGA18 and in the 88th Mb window of GGA1. No significant or suggestive SNPs were identified for sex-specific analyses of white striping. Genomic windows with suggestive significance in the BayesB analyses are listed in Appendix C.

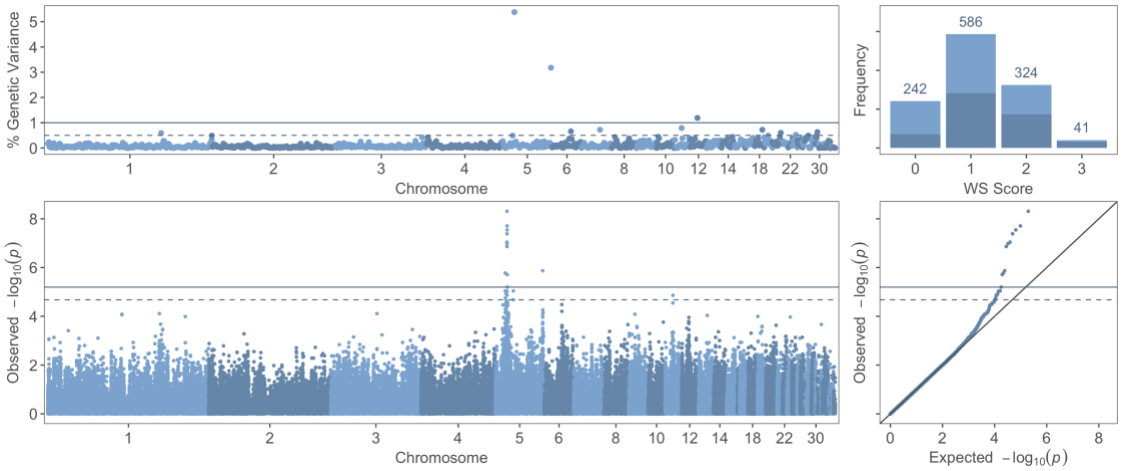

Figure 6.2: Genome-wide association results for white striping (WS) score using multi-marker (BayesB) and single-SNP (mixed linear model) analyses.

(Top Left) Percentage of genetic variance explained by 1-Mb regions across the genome for WS score. (Top Right) Distribution of WS scores across progeny used in genome-wide association analyses; dark blue = male, light blue = female. (Bottom Left) Manhattan plot of single-SNP results showing the −log10(p-value) of SNPs ordered by chromosome and position. (Bottom Right) Quantile-quantile plot of p-values from single-SNP results of WS score. Solid and dashed lines indicate significant and suggestive thresholds, respectively, for each model.

Table 6.8: White Striping quantitative trait loci (QTLs) containing SNPs with FDR adjusted p-values less than 0.05.

QTL				**Top SNP in QTL**						
Chr	**Start (bp)**	**End (bp)**	**#SNP**	**Pos (bp)**	**Alleles**	**Freq**	**Beta**	**P-value**	**FDR**	**Candidate genes**
5	–	–	1	12196653	T/C	0.232	-0.239	1.68e-06	0.036	*USH1C*
5	14280580	14320311	4	14280613	T/C	0.335	0.228	9.07e-08	0.003	*LSP1* *TNNI2* *SYT8* *ENSGALG00000006608* *CTSD*
5	14321077	14321102	2	14321077	G/A	0.433	0.230	4.93e-09	0.001	*ENSGALG00000006608* *CTSD*
5	–	–	1	14477401	T/C	0.238	-0.241	2.86e-08	0.002	*ENSGALG00000006608* *MOB2*
5	–	–	1	14529930	T/C	0.286	0.229	1.95e-06	0.038	*ENSGALG00000006608* *BRSK1*
5	–	–	1	58074636	A/G	0.359	0.166	1.35e-06	0.033	*NIN*

Candidate genes include protein-coding genes located within 5000bp upstream or downstream of the QTL start or end site, respectively. Chr: chromosome, bp: base pairs, #SNP: number of significant SNPs in QTL, Pos: position, Alleles: effect/alternative alleles, Freq: effect allele frequency, Beta: effect size estimate.

Top candidate genes for white striping include *CTSD*, *LSP1*, *troponin I2 fast skeletal type* (*TNNI2*), *synaptotagmin 8* (*SYT8*), and *MOB kinase activator 2* (*MOB2*). As with candidate genes for wooden breast, variation in mammalian homologues of all of these genes is linked to altered insulin expression or secretion in pancreatic beta cells (Xu et al., 2011; Mohlke and Boehnke, 2015). However, they possess additional functions that may be relevant to poultry myopathies, such as calcium-dependent regulation of striated muscle contraction (Kimber et al., 2006) (*TNNI2*), and regulation neutrophil transendothelial migration (*LSP1*) (Liu et al., 2005).

6.3.6 GWAS Results for Body Weight Traits

No QTLs were identified for either body weight trait using single-SNP or multi-marker analyses (Figures 6.3 and 6.4; Appendix C). This may be a result extreme selection for growth rate over many decades, likely resulting in fixed alleles at loci of large effect. By contrast, wooden breast and white striping have a much shorter selection history based on their somewhat recent appearance, and have potentially been subjected to both positive and negative selection if they indeed share a strong genetic basis with performance traits such as feed efficiency and breast muscle yield. This would preserve variation at loci with moderate or large effects, which are easier to detect with lower sample sizes in genome-wide association analyses.

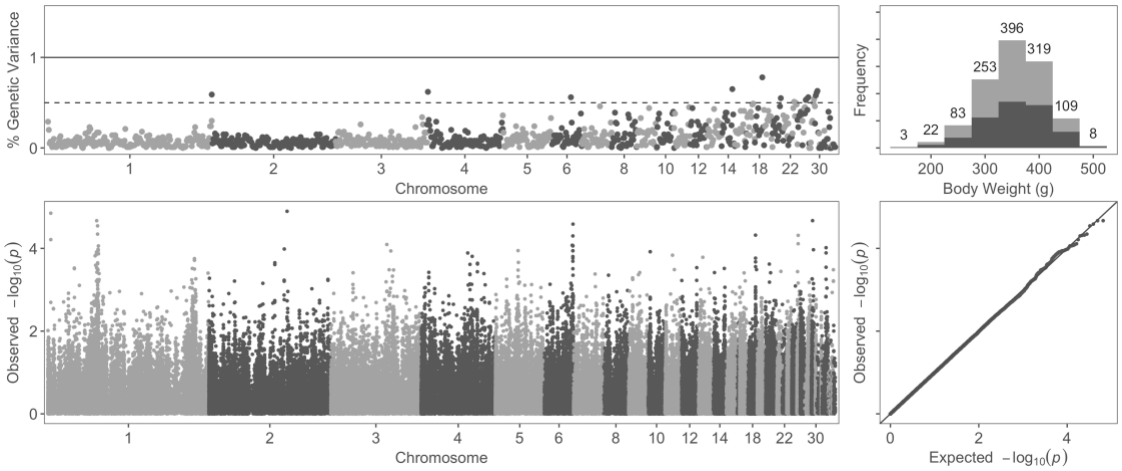

Figure 6.3: Genome-wide association results for body weight at 13 days using multi-marker (BayesB) and single-SNP (mixed linear model) analyses.

(Top Left) Percentage of genetic variance explained by 1-Mb regions across the genome for body weight at 13 days. (Top Right) Distribution of body weight across progeny used in genome-wide association analyses; dark grey = male, light grey = female. (Bottom Left) Manhattan plot of single-SNP results showing the −log10(p-value) of SNPs ordered by chromosome and position. (Bottom Right) Quantile-quantile plot of p-values from single-SNP results. Solid and dashed lines indicate significant and suggestive thresholds, respectively, for each model.

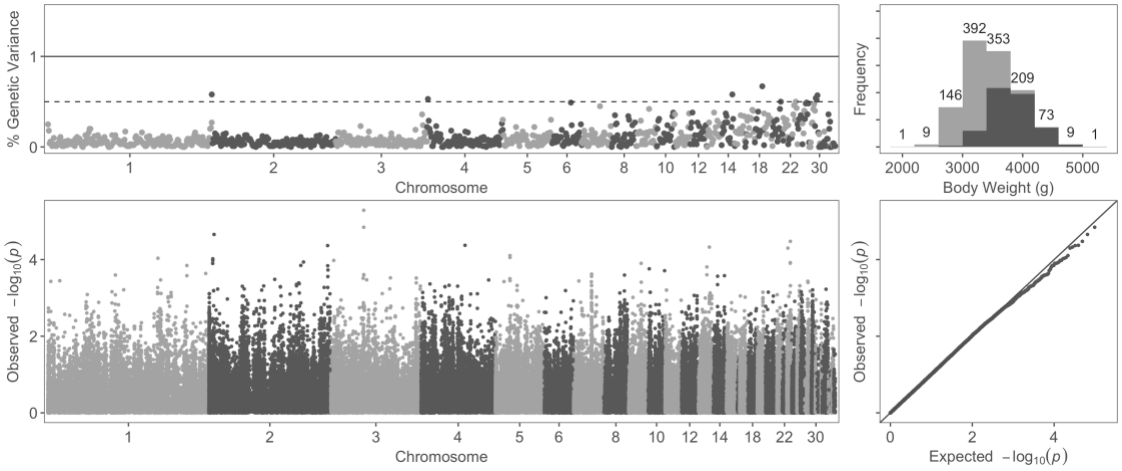

Figure 6.4: Genome-wide association results for body weight at 7 weeks using multi-marker (BayesB) and single-SNP (mixed linear model) analyses.

(Top Left) Percentage of genetic variance explained by 1-Mb regions across the genome for body weight at 7 weeks. (Top Right) Distribution of body weight at 7 weeks across progeny used in genome-wide association analyses; dark grey = male, light grey = female. (Bottom Left) Manhattan plot of single-SNP results showing the −log10(p-value) of SNPs ordered by chromosome and position. (Bottom Right) Quantile-quantile plot of p-values from single-SNP results. Solid and dashed lines indicate significant and suggestive thresholds, respectively, for each model.

QTL detection for both body weight and muscle disorder traits may also have been hindered by the extremely rapid LD decay (Table 6.4) in our 4-way crossbred broiler population relative to the genome coverage achieved by our genotyping methods and filter criteria. Using SNP positions and $D_{0.2}$, we estimated that only 27.52% of autosomes and the Z chromosome were encompassed by SNPs in this study. This is a conservative estimate, as it includes chromosomal regions with extremely low variation, but indicates the strong potential for additional QTLs with large effects that were not captured by this study. Our sample size also prevented detection of small-effect QTLs by limiting statistical power. The rapid LD decay, however, gives us confidence that the QTLs detected in this study are in close proximity to their causal mutations.

6.3.7 Comparative Genomics of GGA5

Chicken chromosome 5 (GGA5) has conserved synteny with portions of human chromosomes 11, 14, and 15 (Pitel et al., 2004). The majority of QTLs identified for both wooden breast and white striping were located in a region that has highly conserved synteny with HSA11 (Figure 6.5). Indeed, there is greater conservation of synteny for genes on HSA11 between chickens and humans than between mice and humans, although numerous intrachromosomal rearrangements are present. The area on HSA11 that is homologous to QTL regions on GGA5 identified

in the present study is associated with numerous metabolic and growth disorders and various forms of diabetes mellitus (Figure 6.5). For example, *KCNQ1* locus in this region is heavily studied in humans as part of an imprinted gene cluster that when dysregulated can cause overgrowth disorders including Beckwith-Wiedemann syndrome (Smith et al., 2007). Even though the size of the region and order of genes is nearly identical between chickens and mammals (Figure 6.5), chickens lack the relevant imprinting control elements present in mammals (Paulsen et al., 2005). This suggests that chickens may serve as an excellent model for studying topics such as evolutionary genomics, imprinting control, and growth disorders.

Figure 6.5: Conserved synteny between chicken chromosome 5 and human chromosome 11.

The wooden breast QTL-rich region of chicken chromosome 5 (GGA5) has highly conserved synteny with human chromosome 11 (HSA11), especially compared to homologous regions in the mouse genome on chromosomes 2 (MMU2) and 7 (MMU7). In humans, this area is associated with a high number of growth and metabolic disorders, which are highlighted here based on existing knowledge of wooden breast and white striping, including a hypothesis suggesting dysregulation of lipid and glucose metabolism as an important underlying factor in development of the myopathies.

The QTL-rich region of GGA5 also contains several areas that show evidence of strong selection sweeps (Figure 6.5) in two commercial purebred male broiler lines selected for breast muscle growth and feed efficiency (Fu et al., 2016). Selective breeding for meat production traits is considered a major culprit for the rapid increase in meat quality issues among broiler chickens, and the genomic co-localization of loci that are beneficial for production traits with loci associated with breast muscle myopathies provides further evidence of this. Targeted sequencing of GGA5 is required to determine if the specific genetic mutations contributing to each trait are simply linked or, in fact, the same. Additionally, targeted sequencing of GGA5 with long-read technologies could reveal copy number variants, which are not captured by SNP data. The *SRY-box transcription factor 6* (*SOX6*) gene is of particular interest because it was identified as a candidate gene for the selection sweep region on GGA5 (Fu et al., 2016) . Although *SOX6* was not identified as a candidate gene for wooden breast based on association analyses described here, a selection sweep in or near this gene would hinder detection of causal variants using many GWAS methods due to filters for minor allele frequency.

6.3.8 Clinical Significance of Candidate Genes

A major functional theme of candidate genes identified in this study is insulin secretion and action, particularly in the QTL-rich region of GGA5 (Figure 6.6), which contains numerous genes previously shown to be associated with metabolic and cardiac disorders in humans (Figure 6.5). For example, *KCNQ1* polymorphisms are associated with altered insulin secretion in pancreatic β cells, short and long QT syndrome in cardiac muscle, and sensorineural deafness in the inner ear (Abbott, 2014). This gene encodes a highly-studied voltage-gated potassium channel, which

interacts with numerous other protein subunits and switches from voltage-dependent to constitutive activity (Abbott, 2014), endowing it with a diverse set of functional roles and associating it with a proportionally diverse number of pathologies. Some pleiotropic *KCNQ1* variants in humans can simultaneously increase insulin secretion in the pancreas, reduce serum potassium upon oral glucose challenge, and cause long QT syndrome, putting individuals at risk of sudden, uncontrollable, arrhythmias which may lead to fainting or sudden death (Torekov et al., 2014). This could represent a potential cause of sudden cardiac death reported in broilers, especially those with wooden breast (Gall et al., 2019a). We re-examined data from a previous study of differential gene expression associated with wooden breast in 2-week-old female broilers (Lake et al., 2019) and found that, although there was no differential expression of *KCNQ1* in the pectoralis major of 2-week-old birds, expression levels of the gene were very low in all birds (data not shown). It is therefore likely that genetic variation in *KCNQ1* would primarily affect organs other than the pectoralis major, potentially including the pancreas.

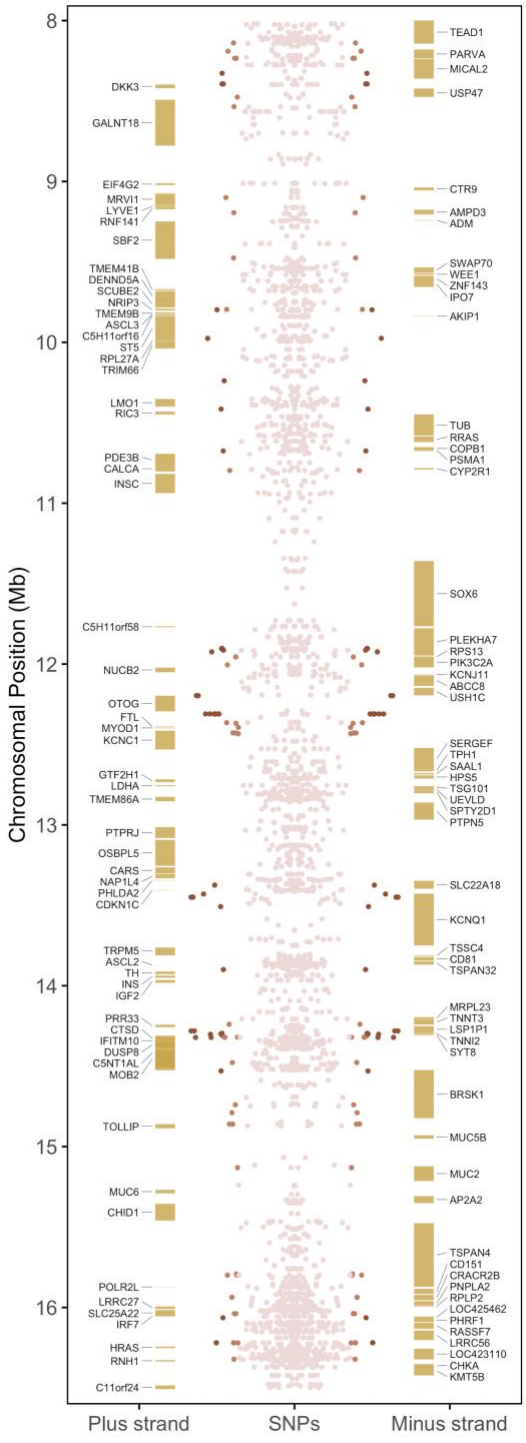

Figure 6.6: Gene landscape of QTL-rich region between 8.0 Mb and 16.5 Mb on chicken chromosome 5.

Mirrored Manhattan plot shows SNPs with significance thresholds indicated by color; dark red = significant, orange = suggestive.

Some candidate genes on GGA5 affect insulin secretion through both gene-gene interactions and protein function, as the insulin gene (*INS*) is located in the middle of this QTL-rich region at approximately 13.94 Mb (Figure 6.6). For instance, *synaptotagmin 8* (*SYT8)* encodes a membrane protein with roles in trafficking and exocytosis, including insulin secretion in pancreatic islet cells (Xu et al., 2011). The *SYT8* gene is located over 300kb away from *INS* in humans, and yet physically interacts with the *INS* locus to elevate *SYT8* expression, especially in the presence of glucose (Xu et al., 2011). This indicates the importance of *SYT8* for both basal and glucose-stimulated insulin secretion in human islets. The same study identified additional interactions of *INS* with *troponin I2, fast skeletal type* (*TNNI2*) and *lymphocyte-specific protein 1 (LSP1*), which are also top candidate genes for wooden breast and white striping.

QTLs outside of GGA5 also have strong ties to insulin as well. The protein encoded by *DNM2* on GGA30 is critical for proper pancreatic function, where it regulates biphasic insulin secretion and glucose homeostasis in mammals. Knockout of *DNM2* in pancreatic β cells in mice causes glucose intolerance via remodeling of the actin cytoskeleton and inefficient endocytosis-exocytosis coupling, indicating a potential pathophysiological link between *DNM2* function and diabetes mellitus (Fan et al., 2015). *DNM2* is best known for its involvement in two distinct congenital neuromuscular diseases of humans, centronuclear myopathy and Charcot-Marie-Tooth neuropathy. Several of the characteristic features of DNM2-associated centronuclear myopathy are reminiscent of the histopathological signs of wooden breast and white striping in broiler breast muscle, including increased variability of myofiber size,

endomysial fibrosis, calcium homeostasis alterations, and abnormal centralization of nuclei in muscle fibers, as also seen in regenerating fibers (Romero, 2010; Fraysse et al., 2016). Although not discussed by Mutryn et al. (Mutryn et al., 2015a), *DNM2* expression was found to be downregulated in wooden breast-affected broilers compared to unaffected broilers at market age (data not shown), which is of particular interest considering findings of a knockout study of this gene in mouse gastrocnemius muscle. Tinelli et al. (Tinelli et al., 2013) found that *DNM2* knockout caused a decrease in the number of muscle fibers, an increase in the proportion of smaller muscle fibers, an increase in lipid droplets, mitochondrial enlargement and disruption of cristae, mitochondrial dysfunction, and altered neuromuscular junctions at various developmental ages (Tinelli et al., 2013). Previously, Papah et al. (Papah et al., 2017) described an increase in acellular lipid droplets and abnormal mitochondrial morphology with degenerated cristae as part of the wooden breast pathogenesis. A decrease in the number of muscle fibers and increase in the proportion of small fibers has also been documented as a characteristic of wooden breast in some broiler lines (Velleman et al., 2018).

A candidate gene on GGA6, *GOT1*, encodes the cytoplasmic version of an enzyme called aspartate transaminase (AST) that catalyzes the interconversion of aspartate and α-ketoglutarate to oxaloacetate and glutamate. Two key roles of AST should be highlighted from this anaplerotic reaction: the replenishment of aspartate, a key intermediate of the citric acid cycle, and the regulation of concentrations of glutamate, which functions as a potentiator of insulin release and precursor of the antioxidant glutathione in human skeletal muscle (Rutten et al., 2005). Thus, variation

in *GOT1* may play an important role in altered energy metabolism and ROS balance in wooden breast.

Genetic variation associated with broiler production traits such as visceral adiposity (Simon and LeClercq, 1982), body weight (Sinsigalli et al., 1987) is already known to affect plasma insulin and glucagon levels, as well as insulin sensitivity and glucose clearance. More generally, commercial broilers have elevated plasma insulin levels compared to layers (Shiraishi et al., 2011) and poorer serum insulin homeostasis compared to Silky chickens (Ji et al., 2020). Insulin is also a key regulator of carbohydrate, lipid, and amino acid metabolism (Tokushima et al., 2005; Godet et al., 2008), which are dysregulated in wooden breast and white striping (Abasht et al., 2016; Papah and Abasht, 2019), although additional research is required to determine whether altered insulin dynamics are a contributing factor to wooden breast and white striping in broilers.

6.4 Conclusions

This study is the first to characterize the genetic basis of wooden breast and white striping in a commercial crossbred broiler population using genetic markers. A major finding of the present work is the identification of a QTL-rich region for both wooden breast and white striping between 8.0 and 16.5 Mb on GGA5, which is homologous to and possesses highly conserved synteny with an imprinted region of human chromosome 11. Further study of this GGA5 region may prove to be critically important for understanding the cause of chicken myopathies as well as the evolution of genomic imprinting and genes involved in growth regulation in humans. Our findings also provide compelling evidence in support of a previous hypothesis describing a shared pathomechanism between breast muscle myopathies in broilers

and type 2 diabetes in mammals (Lake et al., 2019; Lake and Abasht, 2020) and suggest that potential alterations to pancreatic function and insulin action may be involved. There exist substantial differences between mammalian and avian insulin signaling and action – for example, the apparent lack of the insulin responsive glucose transporter *GLUT4* in the chicken genome (Seki et al., 2003) – that warrant additional research, especially with regard to wooden breast and white striping. Investigation into organs involved in regulation of whole-body energy homeostasis, such as the pancreas, liver, and adipose tissue, may also aid in our understanding of these myopathies.

6.5 Methods

6.5.1 Birds

All animal procedures were performed in accordance with guidelines set by The University of Delaware Institutional Animal Care and Use Committee (IACUC) and were approved by IACUC under protocol number 48R-2015-0. The study was carried out in compliance with the ARRIVE guidelines. A total of 1,228 mixed male and female Cobb500 broilers from the same breeding population of 15 sires and 200 dams were raised as two separate hatches ($n_1 = 686$, $n_2 = 542$) with staggered hatch dates. Broilers were housed according to optimal industry standards in five poultry houses and given free access to feed and water until approximately 7 weeks of age (specifically 48, 49, 52, or 53 days), at which time they were euthanized by cervical dislocation. Live weight was recorded for all birds at 13 days of age. Preceding euthanasia (specifically 47, 48, or 52 days of age), live weight was recorded again and whole blood samples were collected from the brachial wing vein of each bird using a

3mL syringe with 23-gauge needle and placed in lithium heparin-coated tubes. Plasma was separated by centrifugation and blood samples were stored at -80˚C until further analysis.

During necropsy, the pectoralis major muscles were evaluated for gross lesions and palpable firmness associated with wooden breast and each bird was assigned a wooden breast score using a 0-4 scale; 0-Normal indicates the bird had no macroscopic signs of the myopathy, 1-Very Mild indicates approximately 1% or less of the breast muscle was affected, 2-Mild indicates approximately between 1% and 10% of the breast muscle was affected, 3-Moderate indicates approximately between 10% and 50% of the breast muscle was affected, and a score of 4-Severe indicates that more than 50% was affected. This scoring system was employed by Lake et al. (Lake et al., 2019) in order to separate unaffected, mildly, and moderately affected chickens with higher resolution and greater sensitivity. White striping was also assessed at this time and each bird was assigned a white striping score using a 0-3 scale; 0-Normal indicates the bird had no macroscopic signs of white striping, 1-Mild indicates approximately 20% or less of the breast muscle was affected, 2-Moderate indicates approximately between 20% and 50% of the breast muscle was affected, and a score of 3-Severe indicates more than 50% of the muscle was affected. The incidence rates of wooden breast and white striping in males and females was compared using Pearson's Chi-squared test implemented in R with Yates' continuity correction.

6.5.2 GBS Library Construction and DNA Sequencing

After the live animal experiment was completed, blood samples from 1,194 birds were selected for DNA extraction and genotyping. These represented all males (n=557) and females (n=636) that did not exhibit any noticeable health conditions or

deformations and had a blood sample of sufficient size with no sign of coagulation. The 15 sires of our chicken population were also included for DNA extraction and genotyping to improve genotype calling of progeny; however, phenotypic data was not recorded for sires. Total DNA was isolated from blood samples using the DNeasy Blood and Tissue Kit (Qiagen) according to the manufacturer's protocol. DNA samples were quantified and quality was assessed using the NanoDrop 1000 Spectrophotometer (Thermo Fisher scientific); all samples had a 260/280 ratio of approximately 1.8 and 260/230 ratio greater than 1.5. Approximately 2.5 µg of DNA per sample was aliquoted into individual wells of a 96-well plate, dried at room temperature, sealed, and shipped to Animal Genomics Research laboratory, AgResearch Invermay, New Zealand for restriction enzyme-based genotyping by sequencing (GBS). The GBS libraries were constructed according to the methods outlined in Elshire et al. (Elshire et al., 2011) with modifications as in Dodds et al. (Dodds et al., 2015) using two restriction enzymes (*MspI* and *ApeKI*). Single-end 1x100 sequencing of 96-plex libraries was performed on an Illumina HiSeq 2500. To control and detect lane bias and batch bias, three samples of control DNA were included in each library and each library was run on at least 4 lanes across at least 2 flowcells. Additionally, one sample (B92023) was included as a positive control in all libraries.

6.5.3 Data Filtering and SNP Calling

AgResearch supplied a single variant call file (VCF) which was constructed by the following methods. Fastq files were demultiplexed using GBSX (Herten et al., 2015) and mapped by sample and lane onto the GRCg6a reference genome (Ensembl release 95) using BWA-MEM (Li, 2013). Samtools v1.9 (Li, 2011) was used to

remove reads with mapping quality below 30, convert the alignment file to BAM format, and merge all alignment files by sample. Variants were detected across all samples on a per chromosome basis using samtools and bcftools v1.9 with parameters set to limit variants to biallelic SNPs (Li, 2011). The results were then combined into a single VCF.

Variants were filtered to only include SNPs with a minimum read depth of 5 for at least 50% of samples, a maximum average read depth of 50, and a minor allele frequency of 5% or greater. Samples were also filtered to only include those with a minimum read depth of 5 for at least 50% of SNPs. Loci on the W chromosome were excluded from all analyses, but were used along with Z chromosome loci to confirm sex of the birds before subsequent analyses. Loci on the Z chromosome were filtered separately using only males to avoid filtering bias from hemizygotic females.

6.5.4 Relatedness and Genetic Parameters

A genomic relationship matrix (***G***) was constructed from the resulting variant data using the R package KGD (Dodds et al., 2015), which implements a method developed to account for GBS with low depth of coverage. Variance components and heritabilities of wooden breast, white striping, body weight at 13 days, and body weight at 7 weeks were estimated using ASReml 4 (Butler et al., 2018) with the following univariate model:

$$\boldsymbol{y} = \boldsymbol{Xb} + \boldsymbol{Zu} + e \qquad \textit{Equation 1}$$

where $\boldsymbol{y}$ is a vector of phenotype values for the relevant trait, $\boldsymbol{b}$ is the vector of fixed effects and the overall mean (a vector of 1's), $\boldsymbol{X}$ an incidence matrix for fixed effects, $\boldsymbol{u}$ is a vector of random polygenic effects, $\boldsymbol{Z}$ is an incidence matrix corresponding to $\boldsymbol{u}$, and e is the residual error. Fixed effects included sex, poultry house, and age at

necropsy for the phenotypes of wooden breast score and white striping score. For analysis of body weight, only sex and poultry house were included as fixed effects; although live weight at 7 weeks was measured on three separate days, this effect was disregarded because it was perfectly correlated with poultry house. Random effects u and e are assumed to follow normal distributions: $\boldsymbol{u} \sim N\left(0, \sigma_g^2 \boldsymbol{G}\right)$ and $e \sim N(0, \sigma_e^2 \boldsymbol{I}_n)$ where σ_g^2 is the genetic variance, σ_e^2 is the variance of the residual errors, $\boldsymbol{G}$ is the genomic relationship matrix as defined above, and $\boldsymbol{I}_n$ is an identity matrix of dimension n. Heritability was calculated as the ratio of genetic to phenotypic variance, i.e. the sum of genetic and residual variance. Pairwise genetic and phenotypic correlations between traits were estimated using bivariate models with the same fixed and random effects as specified for the univariate analyses.

6.5.5 Linkage Disequilibrium Analysis

Pairwise linkage disequilibrium (LD; r^2) of markers within 5 Mb of each other was calculated with Haploview v4.2 using the discrete genotype calls produced during the SNP calling step described above. To characterize LD decay with distance, markers were filtered to only include SNPs with a minimum read depth of 10 in at least 50% of birds. LD on the Z chromosome was determined using genotype calls from only male birds. LD decay curves were generated for macro-chromosomes (GGA1 through GGA5), intermediate chromosomes (GGA6 through GGA10), micro-chromosomes (GGA11 through GGA33), and the Z chromosome by fitting a four-parameter Weibull function (type-1) to r^2 values against physical distance using the R package 'drc' (v3.0–1). The resulting curves were used to estimate r^2 at distances of 1 kb, 10 kb, 100 kb, 500 kb, 1 Mb, and 5 Mb, and to calculate the distance at which LD decayed below the threshold of 0.2 ($D_{0.2}$).

The ability of the present study to capture QTL was evaluated by examining SNP coverage on each chromosome in comparison to corresponding $D_{0.2}$ estimates. Specifically, we calculated the percentage of each chromosome in close enough proximity to a SNP for LD to be considered useful (i.e. $D_{0.2}$), then computed the average percentage weighted by chromosome length. This final value reflects the percentage of the genome (autosomes and Z chromosome) that was captured by SNPs in the present dataset.

6.5.6 Allele Dosage Estimation

Due to the relatively low-depth sequencing methods implemented here, continuous genotype probabilities were used for all association analyses rather than discrete genotype calls. Genotype posterior probabilities were calculated using the Bayesian genotype caller polyRAD v1.1 (Clark et al., 2019), with population structure and LD used as a prior and default parameter values. The minimum correlation coefficient between two alleles (r^2) for LD to be used in genotype estimation was set at 0.2 and the distance within which to search for alleles that may be in LD with the given allele was set to 10,000 base pairs. The maximum mean difference in allele frequencies between iterations to be tolerated before iterations end was set to 0.001. The resulting genotype posterior probabilities were converted to allele dosages (i.e. posterior mean genotypes) for use in association analysis. Genotype calling of markers on the Z chromosome was performed using only male birds.

6.5.7 Genome-Wide Association Analysis

Two separate approaches – Bayesian multi-marker regression and single-SNP analysis – were used to detect quantitative trait loci (QTL) for each trait. Bayesian

models were implemented in GenSel (Fernando and Garrick, 2009) and involved first estimating the proportion of markers with null effect (π) using BayesCπ, followed by computation of the genetic variance explained by each 1 Mb window of SNPs in the genome with BayesB. The BayesCπ algorithm was run for 200,000 MCMC iterations with a burn-in of 150,000 iterations and used a starting value of 0.5 for π. BayesB was run for 60,000 iterations with a burn-in of 20,000 and used the posterior mean of π calculated by BayesCπ for each trait. The following model was used for both Bayesian methods:

$$\boldsymbol{y} = \boldsymbol{Xb} + \sum_{k=1}^{K} \boldsymbol{z}_k a_k + e \qquad \textit{Equation 2}$$

where K is the number of SNPs, z_k is a vector of allele dosages at SNP k, a_k is the additive effect of that SNP, and the remaining variables are as previously described. Loci on the Z chromosome were disregarded for this analysis. Windows explaining greater than 1% of genetic variation were considered significant and those explaining greater than 0.5% were considered suggestive.

Single-SNP analysis was performed with a mixed linear model using GCTA version 1.26.0 (Yang et al., 2011) with software patches provided by van den Berg et al. (Van Den Berg et al., 2019) that adapted the program to accept allele dosages. Eq. 1 was used for all single-SNP analyses with the addition of a SNP effect fitted as a fixed covariate. Single-SNP analysis was performed three separate times for each trait, once using all birds, once with only females, and once with only males. Loci on the Z chromosome were only included when male birds were analyzed separately. For analyses including only male or female progeny, the fixed effect of sex was dropped from the model. Significant and suggestive genome-wide association thresholds were

set at p-values corresponding to FDR-adjusted (Benjamini and Hochberg, 1995) q-values of 0.05 and 0.20, respectively.

Significant intra-chromosomal SNPs that were in high LD ($r^2 > 0.75$) or that were separated by a distance less than or equal to the $D_{0.2}$ value for the relevant chromosome size were assumed to share evidence in association analyses for a given trait and were thus grouped into non-overlapping QTL. Markers considered "suggestive" were not used in the construction of QTL. Candidate genes were identified based on proximity to QTL (within 5000 bp up- or downstream of the start or end position of a QTL, respectively) using Ensembl and NCBI annotation of the *Gallus gallus* genome version GRCg6a (annotation release 99).

6.5.8 Comparative Genomics

An ~8 Mb region of GGA5 was found to be exceedingly rich in QTL for both wooden breast and white striping, and warranted additional attention with regard to existing knowledge of the chromosome's genomic features, which were visualized in a Circos plot (Krzywinski et al., 2009). To this end, sequence alignments between chicken genome assembly GRCg6a and human genome assembly GRCh38 (vertebrate net alignment netHg38) and between human genome assembly GRCh38 and mouse genome assembly GRCm38 (placental net alignment netMm10) were retrieved using the UCSC Table Browser (Karolchik et al., 2004). Associations with human muscular and metabolic disease phenotypes in genomic regions homologous to the QTL-rich section of GGA5 were identified from the OMIM database (Online Mendelian Inheritance in Man, OMIM). Additionally, previously identified selective sweeps on GGA5 in commercial purebred broiler lines that are susceptible to wooden breast (Fu

et al., 2016) were lifted over to the GRCg6a chicken genome assembly using the UCSC liftOver tool (Hinrichs et al., 2006).

6.5.9 Data Availability

The datasets generated during the current study are available in the NCBI Sequence Read Archive (SRA) repository under BioProject PRJNA682423.

6.5.10 Acknowledgements

We would like to thank Muhammed Walugembe, Luke Kramer, and numerous others from the Department of Animal Science at Iowa State University for their excellent technical help. Andrew Hess of AgResearch proved indispensable in providing guidance on analytical methods specific to low-depth GBS and Rudiger Brauning of AgResearch was always immensely helpful and relentlessly cheerful in the face of numerous questions throughout the entirety of this project. We gratefully acknowledge the in-kind support by Cobb–Vantress Inc. in providing chicks and chicken feed for this experiment. We also greatly appreciate assistance with samples and data collection from many graduate and undergraduate students at the University of Delaware Department of Animal and Food Sciences. We would like to acknowledge the support from the University of Delaware Center for Bioinformatics and Computational Biology for utilization of their cluster BioMix, which was made possible through support from the Delaware INBRE (NIH GM103446), the state of Delaware and the Delaware Biotechnology Institute (DBI). RNA-sequencing services at DBI are greatly appreciated.

REFERENCES

Abasht, B., Fu, W., Mutryn, M. F., Brannick, E. M., and Lee, W. R. (2015). Identification of gene expression biomarkers associated with severity of Wooden Breast disease in broiler chickens. in *Proceeding of XXII European symposium on the quality of poultry meat* (Nantes, France).

Abasht, B., Mignon-Grasteau, S., Bottje, W., and Lake, J. (2020). "Genetics and genomics of feed utilization efficiency traits in poultry species," in *Advances in Poultry Genetics and Genomics*, eds. S. E. Aggrey, H. Zhou, M. Tixier-Boichard, and D. D. Rhoads (Burleigh Dodds Science Publishing).

Abasht, B., Mutryn, M. F., Michalek, R. D., and Lee, W. R. (2016). Oxidative stress and metabolic perturbations in wooden breast disorder in chickens. *PLoS One* 11, 1–16. doi:10.1371/journal.pone.0153750.

Abasht, B., Zhou, N., Lee, W. R., Zhuo, Z., and Peripolli, E. (2019). The metabolic characteristics of susceptibility to wooden breast disease in chickens with high feed efficiency. *Poult. Sci.* 98, 3246–3256. doi:10.3382/ps/pez183.

Abbott, G. W. (2014). Biology of the KCNQ1 Potassium Channel. *New J. Sci.* 2014, 1–26. doi:10.1155/2014/237431.

Abdullah, N., Abdul Murad, N. A., Attia, J., Oldmeadow, C., Mohd Haniff, E. A., Syafruddin, S. E., et al. (2015). Characterizing the genetic risk for Type 2 diabetes in a Malaysian multi-ethnic cohort. *Diabet. Med.* 32, 1377–1384. doi:10.1111/dme.12735.

Aghajanian, A., Wittchen, E. S., Allingham, M. J., Garrett, T. A., and Burridge, K. (2008). Endothelial cell junctions and the regulation of vascular permeability and leukocyte transmigration. *J. Thromb. Haemost.* 6, 1453–1460. doi:10.1111/j.1538-7836.2008.03087.x.

Aihara, Y., Kurabayashi, M., Saito, Y., Ohyama, Y., Tanaka, T., Takeda, S., et al. (2000). Cardiac ankyrin repeat protein is a novel marker of cardiac hypertrophy: Role of M-CAT element within the promoter. *Hypertension* 36, 48–53. doi:10.1161/01.hyp.36.1.48.

Akiba, Y., Chida, Y., Takahashi, T., Ohtomo, Y., Sato, K., and Takahashi, K. (1999).

Persistent hypoglycemia induced by continuous insulin infusion in broiler chickens. *Br. Poult. Sci.* 40, 701–705. doi:10.1080/00071669987124.

Alnahhas, N., Berri, C., Chabault, M., Chartrin, P., Boulay, M., Bourin, M. C., et al. (2016). Genetic parameters of white striping in relation to body weight, carcass composition, and meat quality traits in two broiler lines divergently selected for the ultimate pH of the pectoralis major muscle. *BMC Genet.* 17, 1–9. doi:10.1186/s12863-016-0369-2.

Alvarenga, R. R., Zangeronimo, M. G., Pereira, L. J., Rodrigues, P. B., and Gomide, E. M. (2011). Lipoprotein metabolism in poultry. *Worlds. Poult. Sci. J.* 67, 431–440. doi:10.1017/s0043933911000481.

Amin, M., Pushpakumar, S., Muradashvili, N., Kundu, S., Tyagi, S. C., and Sen, U. (2017). Regulation and involvement of matrix metalloproteinases in vascular diseases. *Front. Biosci.* 21, 89–118. doi:10.1002/jmri.25711.PET/MRI.

Anderson, E. J., and Neufer, P. D. (2006). Type II skeletal myofibers possess unique properties that potentiate mitochondrial H2O2 generation. *Am. J. Physiol. Physiol.* 290, C844–C851. doi:10.1152/ajpcell.00402.2005.

Aronson, P. S., and Giebisch, G. (2011). Effects of pH on potassium: New explanations for old observations. *J. Am. Soc. Nephrol.* 22, 1981–1989. doi:10.1681/asn.2011040414.

Arruda, A. P., and Hotamisligil, G. S. (2015). Calcium homeostasis and organelle function in the pathogenesis of obesity and diabetes. *Cell Metab.* 22, 381–397. doi:10.1016/j.cmet.2015.06.010.

Asbun, J., and Villarreal, F. J. (2006). The pathogenesis of myocardial fibrosis in the setting of diabetic cardiomyopathy. *J. Am. Coll. Cardiol.* 47, 693–700. doi:10.1016/j.jacc.2005.09.050.

Aung, H. H., Lame, M. W., Gohil, K., An, C. Il, Wilson, D. W., and Rutledge, J. C. (2013). Induction of ATF3 gene network by triglyceride-rich lipoprotein lipolysis products increases vascular apoptosis and inflammation. *Arterioscler. Thromb. Vasc. Biol.* 33, 2088–2096. doi:10.1161/ATVBAHA.113.301375.

Bagnall, R. D., Yeates, L., and Semsarian, C. (2010). Analysis of the Z-disc genes PDLIM3 and MYPN in Patients with Hypertrophic Cardiomyopathy. *Int. J. Cardiol.* 145, 601–602. doi:10.1016/j.ijcard.2010.08.004.

Bahar, E., Kim, H., and Yoon, H. (2016). ER stress-mediated signaling: Action potential and Ca2+ as key players. *Int. J. Mol. Sci.* 17, 1–22.

doi:10.3390/ijms17091558.

Bailey, R. A., Souza, E., and Avendano, S. (2020). Characterising the Influence of Genetics on Breast Muscle Myopathies in Broiler Chickens. *Front. Physiol.* 11, 1–12. doi:10.3389/fphys.2020.01041.

Bailey, R. A., Watson, K. A., Bilgili, S. F., and Avendano, S. (2015). The genetic basis of pectoralis major myopathies in modern broiler chicken lines. *Poult. Sci.* 94, 2870–2879. doi:10.3382/ps/pev304.

Baldi, G., Soglia, F., Laghi, L., Tappi, S., Rocculi, P., Tavaniello, S., et al. (2019). Comparison of quality traits among breast meat affected by current muscle abnormalities. *Food Res. Int.* 115, 369–376. doi:10.1016/j.foodres.2018.11.020.

Baldi, G., Soglia, F., Mazzoni, M., Sirri, F., Canonico, L., Babini, E., et al. (2018). Implications of white striping and spaghetti meat abnormalities on meat quality and histological features in broilers. *Animal* 12, 164–173. doi:10.1017/S1751731117001069.

Barash, I. A., Mathew, L., Ryan, A. F., Chen, J., and Lieber, R. L. (2004). Rapid muscle-specific gene expression changes after a single bout of eccentric contractions in the mouse. *Am. J. Physiol. Physiol.* 286, C355–C364. doi:10.1152/ajpcell.00211.2003.

Barbato, G. F. (1994). Genetic control of food intake in chickens. *J. Nutr.* 124, 1340S-1340S. doi:10.1093/jn/124.suppl_8.1340s.

Basseri, S., and Austin, R. C. (2012). Endoplasmic reticulum stress and lipid metabolism: Mechanisms and therapeutic potential. *Biochem. Res. Int.* 2012. doi:10.1155/2012/841362.

Basta, G., Schmidt, A. M., and De Caterina, R. (2004). Advanced glycation end products and vascular inflammation: Implications for accelerated atherosclerosis in diabetes. *Cardiovasc. Res.* 63, 582–592. doi:10.1016/j.cardiores.2004.05.001.

Beales, P. L., Elcioglu, N., Woolf, A. S., Parker, D., and Flinter, F. A. (1999). New criteria for improved diagnosis of Bardet-Biedl syndrome: results of a population survey. *J. Med. Genet.* 36, 437–46. Available at: http://www.ncbi.nlm.nih.gov/pubmed/10874630%0Ahttp://www.pubmedcentral.nih.gov/articlerender.fcgi?artid=PMC1734378.

Benjamini, Y., and Hochberg, Y. (1995). Controlling the False Discovery Rate : A Practical and Powerful Approach to Multiple Testing. *J. R. Stat. Soc. Ser. B* 57, 289–300.

Berezhnov, A. V, Fedotova, E. I., Nenov, M. N., Kokoz, Y. M., Zinchenko, V. P., and Dynnik, V. V (2008). Destabilization of the cytosolic calcium level and the death of cardiomyocytes in the presence of derivatives of long-chain fatty acids. *Biophysics (Oxf).* 53, 564–570. doi:10.1134/s0006350908060183.

Berridge, M. J., Bootman, M. D., and Roderick, H. L. (2003). Calcium signalling: Dynamics, homeostasis and remodelling. *Nat. Rev. Mol. Cell Biol.* 4, 517–529. doi:10.1038/nrm1155.

Bleyer, A. J., Fumo, P., Snipes, E. R., Goldfarb, S., Simmons, D. A., and Ziyadeh, F. N. (1994). Polyol pathway mediates high glucose-induced collagen synthesis in proximal tubule. *Kidney Int.* 45, 659–666. doi:10.1038/ki.1994.88.

Boerboom, G., van Kempen, T., Navarro-villa, A., and Perez-Bonilla, A. (2018). Unraveling the cause of white striping in broilers using metabolomics. *Poult. Sci.* 97, 3977–3986.

Bolger, A. M., Lohse, M., and Usadel, B. (2014). Trimmomatic: A flexible trimmer for Illumina sequence data. *Bioinformatics* 30, 2114–2120. doi:10.1093/bioinformatics/btu170.

Bonen, A., Parolin, M. L., Steinberg, G. R., Calles-Escandon, J., Tandon, N. N., Glatz, J. F. C., et al. (2004). Triacylglycerol accumulation in human obesity and type 2 diabetes is associated with increased rates of skeletal muscle fatty acid transport and increased sarcolemmal FAT/CD36. *FASEB J.* 18, 1144–1146. doi:10.1096/fj.03-1065fje.

Botham, K. M., Moore, E. H., De Pascale, C., and Bejta, F. (2007). The induction of macrophage foam cell formation by chylomicron remnants. *Biochem. Soc. Trans.* 35, 454–458. doi:10.1042/bst0350454.

Brand, M. D. (2005). The efficiency and plasticity of mitochondrial energy transduction. *Biochem. Soc. Trans.* 33, 897. doi:10.1042/bst20050897.

Braun, E. J., and Sweazea, K. L. (2008). Glucose regulation in birds. *Comp. Biochem. Physiol. - B Biochem. Mol. Biol.* 151, 1–9. doi:10.1016/j.cbpb.2008.05.007.

Brosius, F. C., and Heilig, C. W. (2005). Glucose transporters in diabetic nephropathy. *Pediatr. Nephrol.* 20, 447–451. doi:10.1007/s00467-004-1748-x.

Brothers, B., Zhuo, Z., Papah, M. B., and Abasht, B. (2019). RNA-seq analysis reveals spatial and sex differences in pectoralis major muscle of broiler chickens contributing to difference in susceptibility to wooden breast disease. *Front. Physiol.* 10. doi:10.3389/fphys.2019.00764.

Butler, D. G., Cullis, B. R., Gilmour, A., Gogel, B. J., and Thompson, R. (2018). ASReml-R Reference Manual Version 4.

Caplen, N. J., Patel, A., Millward, A., Campbell, R. D., Ratanachaiyavong, S., Wong, F. S., et al. (1990). Complement C4 and heat shock protein 70 (HSP70) genotypes and type I diabetes mellitus. *Immunogenetics* 32, 427–430.

Carter, N., Seldin, D., and Teng, H. (1959). Tissue and renal response to chronic respiratory acidosis. *J. Clin. Invest.* 38, 949–960. Available at: https://www.jci.org/articles/view/103878/files/pdf.

Chan, A. W., Hamblin, M. T., and Jannink, J. L. (2016). Evaluating imputation algorithms for low-depth genotyping-by-sequencing (GBS) data. *PLoS One* 11, 1–17. doi:10.1371/journal.pone.0160733.

Chatterjee, D., Zhuang, H., Bowker, B. C., Rincon, A. M., and Sanchez-Brambila, G. (2016). Instrumental texture characteristics of broiler pectoralis major with the wooden breast condition. *Poult. Sci.* 95, 2449–2454. doi:10.3382/ps/pew204.

Cheah, A. M. (1981). Effect of long chain unsaturated fatty acids on the calcium transport of sarcoplasmic reticulum. *Biochim. Biophys. Acta* 648, 113–119.

Chen, Y. W., Nader, G. A., Baar, K. R., Fedele, M. J., Hoffman, E. P., and Esser, K. A. (2002). Response of rat muscle to acute resistance exercise defined by transcriptional and translational profiling. *J. Physiol.* 545, 27–41. doi:10.1113/jphysiol.2002.021220.

Chen, Z., Zhao, T.-J., Li, J., Gao, Y.-S., Meng, F.-G., Yan, Y.-B., et al. (2011). Slow skeletal muscle myosin-binding protein-C (MyBPC1) mediates recruitment of muscle-type creatine kinase (CK) to myosin. *Biochem. J.* 436, 437–445. doi:10.1042/bj20102007.

Chin, E. R., Olson, E. N., Richardson, J. A., Yang, Q., Humphries, C., Shelton, J. M., et al. (1998). A calcineurin-dependent transcriptional pathway controls skeletal muscle fiber type. *Genes Dev.* 12, 2499–2509. doi:10.1101/gad.12.16.2499.

Cho, S. J., Moon, J. S., Lee, C. M., Choi, A. M. K., and Stout-Delgado, H. W. (2017). Glucose transporter 1-dependent glycolysis is increased during aging-related lung fibrosis, and phloretin inhibits lung fibrosis. *Am. J. Respir. Cell Mol. Biol.* 56, 521–531. doi:10.1165/rcmb.2016-0225OC.

Chung, S. S. M. (2004). Contribution of polyol pathway to diabetes-induced oxidative stress. *J. Am. Soc. Nephrol.* 14, 233S – 236. doi:10.1097/01.asn.0000077408.15865.06.

Clark, D. L., and Velleman, S. G. (2017). Spatial influence on breast muscle morphological structure, myofiber size, and gene expression associated with the wooden breast myopathy in broilers. *Poult. Sci.* 95, 2930–2945. doi:10.3382/ps/pew243.

Clark, L. V., Lipka, A. E., and Sacks, E. J. (2019). polyRAD: Genotype Calling with Uncertainty from Sequencing Data in Polyploids and Diploids. *Genes Genomes Genet.* 9, 663–673. doi:10.1534/g3.118.200913.

Cnop, M., Foufelle, F., and Velloso, L. A. (2012). Endoplasmic reticulum stress, obesity and diabetes. *Trends Mol. Med.* 18, 59–68. doi:10.1016/j.molmed.2011.07.010.

Codd, J. R. (2005). Activity of three muscles associated with the uncinate processes of the giant Canada goose Branta canadensis maximus. *J. Exp. Biol.* 208, 849–857. doi:10.1242/jeb.01489.

Cui, H., Zheng, M., Zhao, G., Liu, R., and Wen, J. (2018). Identification of differentially expressed genes and pathways for intramuscular fat metabolism between breast and thigh tissues of chickens. *BMC Genomics* 19, 1–9. doi:10.1186/s12864-017-4292-3.

D'Addesio, J. (1992). Metabolic and respiratory acidosis. *Top. Emerg. Med.* 14, 51–55.

Dalle Zotte, A., Cecchinato, M., Quartesan, A., Bradanovic, J., and Puolanne, E. (2014). How does "Wooden Breast" myodegradation affect poultry meat quality? in *60th International Congress of Meat Science and Technology* (Punta Del Este, Uruguay).

Dalle Zotte, A., Tasoniero, G., Puolanne, E., Remignon, H., Cecchinato, M., Catelli, E., et al. (2017). Effect of "Wooden Breast" appearance on poultry meat quality, histological traits, and lesions characterization. *Czech J. Anim. Sci.* 62, 51–57. doi:10.17221/54/2016-CJAS.

Dasu, M. R., and Jialal, I. (2010). Free fatty acids in the presence of high glucose amplify monocyte inflammation via Toll-like receptors. *Am. J. Physiol. Metab.* 300, E145–E154. doi:10.1152/ajpendo.00490.2010.

De Miranda, M. A., Schlater, A. E., Green, T. L., and Kanatous, S. B. (2012). In the face of hypoxia: myoglobin increases in response to hypoxic conditions and lipid supplementation in cultured Weddell seal skeletal muscle cells. *J. Exp. Biol.* 215, 806–813. doi:10.1242/jeb.060681.

DeFronzo, R. A., and Tripathy, D. (2009). Skeletal muscle insulin resistance is the primary defect in type 2 diabetes. *Diabetes Care* 32 Suppl 2. doi:10.2337/dc09-s302.

Dodds, K. G., McEwan, J. C., Brauning, R., Anderson, R. M., Stijn, T. C., Kristjánsson, T., et al. (2015). Construction of relatedness matrices using genotyping-by-sequencing data. *BMC Genomics* 16, 1–15. doi:10.1186/s12864-015-2252-3.

Dupont, J., Dagou, C., Derouet, M., Simon, J., and Taouis, M. (2004). Early steps of insulin receptor signaling in chicken and rat: Apparent refractoriness in chicken muscle. *Domest. Anim. Endocrinol.* 26, 127–142. doi:10.1016/j.domaniend.2003.09.004.

Eftestøl, E., Norman Alver, T., Gundersen, K., and Bruusgaard, J. C. (2014). Overexpression of SMPX in adult skeletal muscle does not change skeletal muscle fiber type or size. *PLoS One* 9. doi:10.1371/journal.pone.0099232.

Eiselein, L., Wilson, D. W., Lamé, M. W., and Rutledge, J. C. (2007). Lipolysis products from triglyceride-rich lipoproteins increase endothelial permeability, perturb zonula occludens-1 and F-actin, and induce apoptosis. *Am. J. Physiol. Circ. Physiol.* 292, H2745–H2753. doi:10.1152/ajpheart.00686.2006.

Eizirik, D. L., Cardozo, A. K., and Cnop, M. (2008). The role for endoplasmic reticulum stress in diabetes mellitus. *Endocr. Rev.* 29, 42–61. doi:10.1210/er.2007-0015.

Elshire, R. J., Glaubitz, J. C., Sun, Q., Poland, J. A., Kawamoto, K., Buckler, E. S., et al. (2011). A robust, simple genotyping-by-sequencing (GBS) approach for high diversity species. *PLoS One* 6, e19379. doi:10.1371/journal.pone.0019379.

Endo, M. (2009). Calcium-Induced Calcium Release in Skeletal Muscle. *Physiol. Rev.* 89, 1153–1176. doi:10.1152/physrev.00040.2008.

Epstein, S. K., and Singh, N. (2001). Respiratory acidosis. *Respir. Care* 46, 366–383. Available at: www.draegermedical.com.

Ermak, G., and Davies, K. J. A. (2001). Calcium and oxidative stress: From cell signaling to cell death. *Mol. Immunol.* 38, 713–721. doi:10.1016/S0161-5890(01)00108-0.

Fan, F., Ji, C., Wu, Y., Ferguson, S. M., Tamarina, N., Philipson, L. H., et al. (2015). Dynamin 2 regulates biphasic insulin secretion and plasma glucose homeostasis. *J. Clin. Invest.* 125, 4026–4041. doi:10.1172/JCI80652.

Fantus, I. G., Goldberg, H. J., Whiteside, C. I., and Topic, D. (2006). "The Hexosamine Biosynthesis Pathway," in *The Diabetic Kidney. Contemporary Diabetes.*, eds. P. Cortes and C. E. Mogensen (Totowa, NJ: Humana Press), 117–133. doi:10.1007/978-1-59745-153-6_7.

FastQC Available at: https://www.bioinformatics.babraham.ac.uk/projects/fastqc/.

Faustman, D., Li, X., Lin, H. Y., Fu, Y., Eisenbarth, G., Avruch, J., et al. (1991). Linkage of faulty major histocompatibility complex class I to autoimmune diabetes. *Science (80-.).* 254, 1756–1761. doi:10.1126/science.1763324.

Fernando, R. L., and Garrick, D. J. (2009). "GenSel-User manual for a portfolio of genomic selection related analyses," in *Iowa State University*, 0–24.

Finlin, B. S., Crump, S. M., Satin, J., and Andres, D. A. (2003). Regulation of voltage-gated calcium channel activity by the Rem and Rad GTPases. *Proc. Natl. Acad. Sci. U. S. A.* 100, 14469–74. doi:10.1073/pnas.2437756100.

Forster, H. V, Dempsey, J. A., Thomson, J., Vidruk, E., and DoPico, G. A. (1972). Estimation of arterial PO2, PCO2, pH, and lactate from arterilazed venous blood. *J. Appl. Physiol.* 32, 134–137.

Forsythe, E., and Beales, P. L. (2013). Bardet-Biedl syndrome. *Eur. J. Hum. Genet.* 21, 8–13. doi:10.1111/j.1442-9071.1984.tb01143.x.

Fraysse, B., Guicheney, P., and Bitoun, M. (2016). Calcium homeostasis alterations in a mouse model of the dynamin 2-related centronuclear myopathy. *Biol. Open* 5, 1691–1696. doi:10.1242/bio.020263.

Fu, S., Li, P., Watkins, S. M., Ivanov, A. R., Hofmann, O., Hotamisligil, G. S., et al. (2011). Aberrant lipid metabolism disrupts calcium homeostasis causing liver endoplasmic reticulum stress in obesity. *Nature* 473, 528–531. doi:10.1038/nature09968.

Fu, W., Lee, W. R., and Abasht, B. (2016). Detection of genomic signatures of recent selection in commercial broiler chickens. *BMC Genet.* 17, 1–10. doi:10.1186/s12863-016-0430-1.

Furuhashi, M., Saitoh, S., Shimamoto, K., and Miura, T. (2014). Fatty acid-binding protein 4 (FABP4): Pathophysiological insights and potent clinical biomarker of metabolic and cardiovascular diseases. *Clin. Med. Insights Cardiol.* 2014, 23–33. doi:10.4137/CMC.S17067.

Gall, S., Suyemoto, M. M., Sather, H. M. L., Sharpton, A. R., Barnes, H. J., and Borst,

L. B. (2019a). Wooden breast in commercial broilers associated with mortality, dorsal recumbency, and pulmonary disease. *Avian Dis.* 63, 514–519. doi:10.1637/11995-111218-case.1.

Gall, S., Suyemoto, M. M., Sather, H. M. L., Sharpton, A. R., Barnes, H. J., and Borst, L. B. (2019b). Wooden breast in commercial broilers associated with mortality, dorsal recumbency, and pulmonary disease. *Avian Dis. In-Press*.

Godet, E., Porter, T. E., Tesseraud, S., Simon, J., Duclos, M. J., Métayer-Coustard, S., et al. (2008). Insulin immuno-neutralization in chicken: effects on insulin signaling and gene expression in liver and muscle. *J. Endocrinol.* 197, 531–542. doi:10.1677/joe-08-0055.

Goglia, F., and Skulachev, V. P. (2003). A function for novel uncoupling proteins: antioxidant defense of mitochondrial matrix by translocating fatty acid peroxides from the inner to the outer membrane leaflet. *FASEB J.* 17, 1585–1591. doi:10.1096/fj.03-0159hyp.

Gorski, D. J., Petz, A., Reichert, C., Twarock, S., Grandoch, M., and Fischer, J. W. (2019). Cardiac fibroblast activation and hyaluronan synthesis in response to hyperglycemia and diet-induced insulin resistance. *Sci. Rep.* 9, 1–11. doi:10.1038/s41598-018-36140-6.

Gratta, F., Fasolato, L., Birolo, M., Zomeño, C., Novelli, E., Petracci, M., et al. (2019). Effect of breast myopathies on quality and microbial shelf life of broiler meat. *Poult. Sci.*, 1–11. doi:10.3382/ps/pez001.

Green, C. R., Wallace, M., Divakaruni, A. S., Phillips, S. A., Murphy, A. N., Ciaraldi, T. P., et al. (2016). Branched-chain amino acid catabolism fuels adipocyte differentiation and lipogenesis. *Nat. Chem. Biol.* 12, 15–21. doi:10.1038/nchembio.1961.

Griffin, H., Acamovic, F., Guo, K., and Peddie, J. (1989). Plasma lipoprotein metabolism in lean and in fat chickens produced by divergent selection for plasma very low density lipoprotein concentration. *J. Lipid Res.* 30, 1243–50. Available at: http://www.ncbi.nlm.nih.gov/pubmed/2769076.

Griffin, J. R., Moraes, L., Wick, M., and Lilburn, M. S. (2018). Onset of white striping and progression into wooden breast as defined by myopathic changes underlying Pectoralis major growth. Estimation of growth parameters as predictors for stage of myopathy progression. *Avian Pathol.* 47, 2–13. doi:10.1080/03079457.2017.1356908.

Groop, L. C., and Ferrannini, E. (1993). Insulin action and substrate competition.

Baillieres. Clin. Endocrinol. Metab. 7, 1007–1032. doi:10.1016/S0950-351X(05)80243-5.

Gunter, T. E., Gunter, K. K., Sheu, S.-S., and Gavin, C. E. (1994). Mitochondrial calcium transport: physiological and pathological relevance. *Am. J. Physiol. Physiol.* 36, C313–C339.

Ha, S. W., Seo, Y. K., Kim, J. G., Kim, I. S., Sohn, K. Y., Lee, B. H., et al. (1997). Effect of high glucose on synthesis and gene expression of collagen and fibronectin in cultured vascular smooth muscle. *Exp. Mol. Med.* 29, 59–64. Available at: https://www.nature.com/articles/emm19979.pdf.

Hajnóczky, G., Csordás, G., Das, S., Garcia-Perez, C., Saotome, M., Sinha Roy, S., et al. (2006). Mitochondrial calcium signalling and cell death: Approaches for assessing the role of mitochondrial Ca2+ uptake in apoptosis. *Cell Calcium* 40, 553–560. doi:10.1016/j.ceca.2006.08.016.

Han, D. C., Isono, M., Hoffman, B. B., and Ziyadeh, F. N. (1999). High glucose stimulates proliferation and collagen type I synthesis in renal cortical fibroblasts: Mediation by autocrine activation of TGF-beta. *J. Am. Soc. Nephrol.* 10, 1891–1899.

Havenstein, G. B., Ferket, P. R., and Qureshi, M. A. (2003a). Carcass composition and yield of 1957 versus 2001 broilers when fed representative 1957 and 2001 broiler diets. *Poult. Sci.* 82, 1509–18. doi:10.1093/ps/82.10.1509.

Havenstein, G. B., Ferket, P. R., and Qureshi, M. A. (2003b). Growth, livability, and feed conversion of 1957 versus 2001 broilers when fed representative 1957 an 2001 broiler diets. *Poult. Sci.* 82, 1500–1508. doi:10.1093/ps/82.10.1509.

Hers, H. G. (1976). The control of glycogen metabolism in the liver. *Annu. Rev. Biochem.* 45, 167–190. doi:10.1007/978-3-642-66461-8_14.

Herten, K., Hestand, M. S., Vermeesch, J. R., and Van Houdt, J. K. J. (2015). GBSX: A toolkit for experimental design and demultiplexing genotyping by sequencing experiments. *BMC Bioinformatics* 16, 1–6. doi:10.1186/s12859-015-0514-3.

Heuckeroth, R. O., Birkenmeier, E. H., Levin, M. S., and Gordon, J. I. (1987). Analysis of the tissue-specific expression, developmental regulation, and linkage relationships of a rodent gene encoding heart fatty acid binding protein. *J. Biol. Chem.* 262, 9709–9717.

Hinrichs, A., Karolchik, D., Baertsch, R., Barber, G., Bejerano, G., Clawson, H., et al. (2006). The UCSC Genome Browser Database: update 2006. *Nucleic Acids Res*

1, D590-8.

Hirst, J., King, M. S., and Pryde, K. R. (2008). The production of reactive oxygen species by complex I. *Biochem. Soc. Trans.* 36, 976–980. doi:10.1042/BST0360976.

Hoving-Bolink, A. H., Kranen, R. W., Klont, R. E., Gerritsen, C. L. M., and De Greef, K. H. (2000). Fibre area and capillary supply in broiler breast muscle in relation to productivity and ascites. *Meat Sci.* 56, 397–402. doi:10.1016/S0309-1740(00)00071-1.

Howard, B. V. (1987). Lipoprotein metabolism in diabetes mellitus. *J. Lipid Res.* 28, 613–628. doi:10.1016/s0955-2863(96)00117-9.

Huang, J. M., Xian, H., and Bacaner, M. (2006). Long-chain fatty acids activate calcium channels in ventricular myocytes. *Proc. Natl. Acad. Sci.* 89, 6452–6456. doi:10.1073/pnas.89.14.6452.

Husi, H., Van Agtmael, T., Mullen, W., Bahlmann, F. H., Schanstra, J. P., Vlahou, A., et al. (2014). Proteome-based systems biology analysis of the diabetic mouse aorta reveals major changes in fatty acid biosynthesis as potential hallmark in diabetes mellitus-associated vascular disease. *Circ. Cardiovasc. Genet.* 7, 161–170. doi:10.1161/CIRCGENETICS.113.000196.

Hyun, B. K., Kong, M., Tae, M. K., Young, H. S., Kim, W. H., Joo, H. L., et al. (2006). NFATc4 and ATF3 negatively regulate adiponectin gene expression in 3T3-L1 adipocytes. *Diabetes* 55, 1342–1352. doi:10.2337/db05-1507.

Ilany, J., Bilan, P. J., Kapur, S., Caldwell, J. S., Patti, M.-E., Marette, A., et al. (2006). Overexpression of Rad in muscle worsens diet-induced insulin resistance and glucose intolerance and lowers plasma triglyceride level. *Proc. Natl. Acad. Sci.* 103, 4481–4486. doi:10.1073/pnas.0511246103.

Ilkiw, J. E., Rose, R. J., and Martin, I. C. A. (1991). A comparison of simultaneously collected arterial, mixed venous, jugular venous and cephalic venous blood samples in the assessment of blood-gas and acid-base status in the dog. *J. Vet. Intern. Med.* 5, 294–298. doi:10.1111/j.1939-1676.1991.tb03136.x.

Ishii, H., Tada, H., and Isogai, S. (1998). An aldose reductase inhibitor prevents glucose-induced increase in transforming growth factor-β and protein kinase C activity in cultured human mesangial cells. *Diabetologia* 41, 362–364. doi:10.1007/s001250050916.

Jang, M. K., Son, Y., and Jung, M. H. (2013). ATF3 plays a role in adipocyte

hypoxia-mediated mitochondria dysfunction in obesity. *Biochem. Biophys. Res. Commun.* 431, 421–427. doi:10.1016/j.bbrc.2012.12.154.

Jeong, J., Kwon, E. G., Im, S. K., Seo, K. S., and Baik, M. (2012). Expression of fat deposition and fat removal genes is associated with intramuscular fat content in longissimus dorsi muscle of Korean cattle steers. *J. Anim. Sci.* 90, 2044–2053. doi:10.2527/jas.2011-4753.

Ji, J., Tao, Y., Zhang, X., Pan, J., Zhu, X., Wang, H., et al. (2020). Dynamic changes of blood glucose, serum biochemical parameters and gene expression in response to exogenous insulin in Arbor Acres broilers and Silky fowls. *Sci. Rep.* 10, 1–11. doi:10.1038/s41598-020-63549-9.

Jingting, S., Qin, X., Yanju, S., Ming, Z., Yunjie, T., Gaige, J., et al. (2017). Oxidative and glycolytic skeletal muscles show marked differences in gene expression profile in Chinese Qingyuan partridge chickens. *PLoS One* 12, 1–17. doi:10.1371/journal.pone.0183118.

Joiner, K., Hamlin, G., Lien, R., and Bilgili, S. (2014). Evaluation of capillary and myofiber density in the pectoralis major muscles of rapidly growing, high-yield broiler chickens during increased heat stress. *Avian Dis.* 58, 377–382.

Julian, A. R. J., and Mirsalimi, S. M. (1992). Blood oxygen concentration of fast-growing and slow-growing broiler chickens , and chickens with ascites from right ventricular failure. *Avian Dis.* 36, 730–732.

Kalfon, R., Koren, L., Aviram, S., Schwartz, O., Hai, T., and Aronheim, A. (2017). ATF3 expression in cardiomyocytes preserves homeostasis in the heart and controls peripheral glucose tolerance. *Cardiovasc. Res.* 113, 134–146. doi:10.1093/cvr/cvw228.

Kang, H. P., Yang, X., Chen, R., Zhang, B., Corona, E., Schadt, E. E., et al. (2012). Integration of disease-specific single nucleotide polymorphisms, Expression quantitative trait loci and coexpression networks reveal novel candidate genes for type 2 diabetes. *Diabetologia* 55, 2205–2213. doi:10.1007/s00125-012-2568-3.

Karolchik, D., Hinrichs, A., Furey, T., Roskin, K., Sugnet, C., Haussler, D., et al. (2004). The UCSC Table Browser data retrieval tool. *Nucleic Acids Res*, D493-6. doi:10.1093/nar/gkh103.

Kawasaki, T., Iwasaki, T., Yamada, M., Yoshida, T., and Watanabe, T. (2018). Rapid growth rate results in remarkably hardened breast in broilers during the middle stage of rearing: A biochemical and histopathological study. *PLoS One* 13, 1–14. doi:10.1371/journal.pone.0193307.

Kee, H. J., Kim, J. R., Nam, K. Il, Hye, Y. P., Shin, S., Jeong, C. K., et al. (2007). Enhancer of polycomb1, a novel homeodomain only protein-binding partner, induces skeletal muscle differentiation. *J. Biol. Chem.* 282, 7700–7709. doi:10.1074/jbc.M611198200.

Kemp, T. J., Sadusky, T. J., Simon, M., Brown, R., Eastwood, M., Sassoon, D. A., et al. (2001). Identification of a novel stretch-responsive skeletal muscle gene (Smpx). *Genomics* 72, 260–271. doi:10.1006/geno.2000.6461.

Kilburn, K. H. (1966). Movements of potassium during acute respiratory acidosis and recovery. *J. Appl. Physiol.* 21, 679–684. doi:10.1152/jappl.1966.21.2.679.

Kilpeläinen, T. O., Bentley, A. R., Noordam, R., Sung, Y. J., Schwander, K., Winkler, T. W., et al. (2019). Multi-ancestry study of blood lipid levels identifies four loci interacting with physical activity. *Nat. Commun.* 10. doi:10.1038/s41467-018-08008-w.

Kim, D., Langmead, B., and Salzberg, S. L. (2015). HISAT: A fast spliced aligner with low memory requirements. *Nat. Methods* 12, 357–360. doi:10.1038/nmeth.3317.

Kim, J. K., Fillmore, J. J., Chen, Y., Yu, C., Moore, I. K., Pypaert, M., et al. (2001). Tissue-specific overexpression of lipoprotein lipase causes tissue-specific insulin resistance. *Proc. Natl. Acad. Sci.* 98, 7522–7527. doi:10.1073/pnas.121164498.

Kim, J. Y., Park, K. J., Hwang, J. Y., Kim, G. H., Lee, D. Y., Lee, Y. J., et al. (2017). Activating transcription factor 3 is a target molecule linking hepatic steatosis to impaired glucose homeostasis. *J. Hepatol.* 67, 349–359. doi:10.1016/j.jhep.2017.03.023.

Kim, S., Song, N. J., Bahn, G., Chang, S. H., Yun, U. J., Ku, J. M., et al. (2018). Atf3 induction is a therapeutic target for obesity and metabolic diseases. *Biochem. Biophys. Res. Commun.* 504, 903–908. doi:10.1016/j.bbrc.2018.09.048.

Kimber, E., Tajsharghi, H., Kroksmark, A. K., Oldfors, A., and Tulinius, M. (2006). A mutation in the fast skeletal muscle troponin I gene causes myopathy and distal arthrogryposis. *Neurology* 67, 597–601. doi:10.1212/01.wnl.0000230168.05328.f4.

Klip, A., Volchuk, A., He, L., and Tsakiridis, T. (1996). The glucose transporters of skeletal muscle. *Semin. Cell Dev. Biol.* 7, 229–237. doi:10.1006/scdb.1996.0031.

Kojic, S., Nestorovic, A., Rakicevic, L., Belgrano, A., Stankovic, M., Divac, A., et al. (2010). A novel role for cardiac ankyrin repeat protein Ankrd1/CARP as a co-

activator of the p53 tumor suppressor protein. *Arch. Biochem. Biophys.* 502, 60–67. doi:10.1016/j.abb.2010.06.029.

Kono, T., Nishida, M., Nishiki, Y., Seki, Y., Sato, K., and Akiba, Y. (2005). Characterisation of glucose transporter (GLUT) gene expression in broiler chickens. *Br. Poult. Sci.* 46, 510–515. doi:10.1080/00071660500181289.

Kostek, M. C., Chen, Y.-W., Cuthbertson, D. J., Shi, R., Fedele, M. J., Esser, K. A., et al. (2007). Gene expression responses over 24 h to lengthening and shortening contractions in human muscle: major changes in CSRP3, MUSTN1, SIX1, and FBXO32. *Physiol. Genomics* 31, 42–52. doi:10.1152/physiolgenomics.00151.2006.

Kruger, N. J., and Von Schaewen, A. (2003). The oxidative pentose phosphate pathway: structure and organisation. *Curr. Opin. Plant Biol.* 6, 236–246. doi:10.1016/S1369-5266(03)00039-6.

Krutzik, S. R., Tan, B., Li, H., Ochoa, M. T., Liu, P. T., Sharfstein, S. E., et al. (2005). TLR activation triggers the rapid differentiation of monocytes into macrophages and dendritic cells. *Nat. Med.* 11, 653–660. doi:10.1016/j.jaci.2011.08.037.Evidence.

Krzywinski, M. I., Schein, J. E., Birol, I., Connors, J., Gascoyne, R., Horsman, D., et al. (2009). Circos: An information aesthetic for comparative genomics. *Genome Res.* 19, 1639–1645. doi:10.1101/gr.092759.109.

Kumagai, A. K. (1999). Glucose transport in brain and retina: Implications in the management and complications of diabetes. *Diabetes. Metab. Res. Rev.* 15, 261–273. doi:10.1002/(SICI)1520-7560(199907/08)15:4<261::AID-DMRR43>3.0.CO;2-Z.

Kuttappan, V. A., Hargis, B. M., and Owens, C. M. (2016). White striping and woody breast myopathies in the modern poultry industry: A review. *Poult. Sci.* 95, 2724–2733. doi:10.3382/ps/pew216.

Kuttappan, V. A., Shivaprasad, H. l., Shaw, D. P., Valentine, B. A., Hargis, B. M., Clark, F. D., et al. (2013). Pathological changes associated with white striping in broiler breast muscles. *Poult. Sci.* 92, 331–338. doi:10.3382/ps.2012-02646.

Ladé, R. I., and Brown, E. B. (1963). Movement of potassium between muscle and blood in response to respiratory acidosis. *Am. J. Physiol. Content* 204, 761–764. doi:10.1152/ajplegacy.1963.204.5.761.

Lake, J. A., and Abasht, B. (2020). Glucolipotoxicity: A proposed etiology for wooden

breast and related myopathies in commercial broiler chickens. *Front. Physiol.* doi:10.3389/fphys.2020.00169.

Lake, J. A., Papah, M. B., and Abasht, B. (2019). Increased expression of lipid metabolism genes in early stages of wooden breast links myopathy of broilers to metabolic syndrome in humans. *Genes (Basel).* 10, 746. doi:10.20944/preprints201906.0194.v1.

Laplante, M., Sell, H., MacNaul, K. L., Richard, D., Berger, J. P., and Deshaies, Y. (2003). PPAR-gamma activation mediates adipose depot-specific effects on gene expression and lipoprotein lipase activity. *Diabetes* 52, 291–299. Available at: http://diabetes.diabetesjournals.org/content/52/2/291.short.

Lappas, M. (2011). Lower circulating levels of complement split proteins C3a and C4a in maternal plasma of women with gestational diabetes mellitus. *Diabet. Med.* 28, 906–911. doi:10.1111/j.1464-5491.2011.03336.x.

Larkina, T. A., Sazanova, A. L., Fomichev, K. A., Barkova, O. Y., Malewski, T., Jaszczak, K., et al. (2010). HMG1A and PPARG are differently expressed in the liver of fat and lean broilers. *J. Appl. Genet.* 52, 225–228. doi:10.1007/s13353-010-0023-z.

Lee, J. Y., and Hwang, D. H. (2006). The modulation of inflammatory gene expression by lipids: mediation through Toll-like receptors. *Mol. Cells* 21, 174–85. Available at: http://www.ncbi.nlm.nih.gov/pubmed/16682810.

Lefterova, M. I., Zhang, Y., Steger, D. J., Schupp, M., Schug, J., Cristancho, A., et al. (2008). PPARγ and C/EBP factors orchestrate adipocyte biology via adjacent binding on a genome-wide scale. *Genes Dev.* 22, 2941–2952. doi:10.1101/gad.1709008.

Li, H. (2011). A statistical framework for SNP calling, mutation discovery, association mapping and population genetical parameter estimation from sequencing data. *Bioinformatics* 27, 2987–2993. doi:10.1093/bioinformatics/btr509.

Li, H. (2013). Aligning sequence reads, clone sequences and assembly contigs with BWA-MEM. *arXiv Prepr.* Available at: http://arxiv.org/abs/1303.3997.

Li, Y., He, P. P., Zhang, D. W., Zheng, X. L., Cayabyab, F. S., Yin, W. D., et al. (2014). Lipoprotein lipase: From gene to atherosclerosis. *Atherosclerosis* 237, 597–608. doi:10.1016/j.atherosclerosis.2014.10.016.

Liang, W., Menke, A. L., Driessen, A., Koek, G. H., Lindeman, J. H., Stoop, R., et al. (2014). Establishment of a general NAFLD scoring system for rodent models and

comparison to human liver pathology. *PLoS One* 9, 1–17. doi:10.1371/journal.pone.0115922.

Lilburn, M. S., Griffin, J. R., and Wick, M. (2018). From muscle to food: oxidative challenges and developmental anomalies in poultry breast muscle. *Poult. Sci.* doi:10.3382/ps/pey409.

Lim, M. A., Riedel, H., and Liu, F. (2007). Grb10: more than a simple adaptor protein. *Front. Biosci.* 9, 387–403. doi:10.2741/1226.

Liu, L., Cara, D. C., Kaur, J., Raharjo, E., Mullaly, S. C., Jongstra-Bilen, J., et al. (2005). LSP1 is an endothelial gatekeeper of leukocyte transendothelial migration. *J. Exp. Med.* 201, 409–418. doi:10.1084/jem.20040830.

Liu, L., Cui, H., Fu, R., Zheng, M., Liu, R., Zhao, G., et al. (2017). The regulation of IMF deposition in pectoralis major of fast- and slow- growing chickens at hatching. *J. Anim. Sci. Biotechnol.* 8, 1–8. doi:10.1186/s40104-017-0207-z.

Liu, M., Bai, J., He, S., Villarreal, R., Hu, D., Zhang, C., et al. (2014). Grb10 promotes lipolysis and thermogenesis by phosphorylation-dependent feedback inhibition of mTORC1. *Cell Metab.* 19, 967–980. doi:10.1016/j.cmet.2014.03.018.

Livingston, M. L., Ferket, P. R., Brake, J., and Livingston, K. A. (2019a). Dietary amino acids under hypoxic conditions exacerbates muscle myopathies including wooden breast and white stripping. *Poult. Sci.* 98, 1517–1527. doi:10.3382/ps/pey463.

Livingston, M. L., Landon, C. D., Barnes, H. J., Brake, J., and Livingston, K. A. (2019b). Dietary potassium and available phosphorous on broiler growth performance, carcass characteristics, and wooden breast. *Poult. Sci.* 98, 2813–2822. doi:10.3382/ps/pez015.

Ludders, J. W. (2015). "Respiration in birds," in *Duke's Physiology of Domestic Animals*, eds. W. O. Reece, H. E. Howard, J. P. Goff, and E. E. Uemura (Ames, IA: Wiley), 245–258.

Ma, G., Wang, H., Gu, X., Li, W., Zhang, X., Cui, L., et al. (2014). CARP, a myostatin-downregulated gene in CFM cells, is a novel essential positive regulator of myogenesis. *Int. J. Biol. Sci.* 10, 309–320. doi:10.7150/ijbs.7475.

MacRae, V. E., Mahon, M., Gilpin, S., Sandercock, D. A., and Mitchell, M. A. (2006). Skeletal muscle fibre growth and growth associated myopathy in the domestic chicken (Gallus domesticus). *Br. Poult. Sci.* 47, 264–272.

doi:10.1080/00071660600753615.

Malan, D. D., Scheele, C. W., Buyse, J., Kwakernaak, C., Siebrits, F. K., Van Der Klis, J. D., et al. (2003). Metabolic rate and its relationship with ascites in chicken genotypes. *Br. Poult. Sci.* 44, 309–315. doi:10.1080/000716603100024603.

Martin, S., and Parton, R. G. (2008). "Characterization of Rab18, a lipid droplet-associated Small GTPase," in *Methods in Enzymology*, 109–129. doi:10.1016/S0076-6879(07)38008-7.

Matsuura, K., Uesugi, N., Hijiya, N., Uchida, T., and Moriyama, M. (2007). Upregulated expression of cardiac ankyrin-repeated protein in renal podocytes is associated with proteinuria severity in lupus nephritis. *Hum. Pathol.* 38, 410–419. doi:10.1016/j.humpath.2006.09.006.

Maxwell, M. H. (1988). The histology and ultrastructure of ectopic cartilaginous and osseous nodules in the lungs of young broilers with an ascitic syndrome. *Avian Pathol.* 17, 201–219. doi:10.1080/03079458808436439.

Mead, J. R., Irvine, S. A., and Ramji, D. P. (2002). Lipoprotein lipase: Structure, function, regulation, and role in disease. *J. Mol. Med.* 80, 753–769. doi:10.1007/s00109-002-0384-9.

Medina-Gomez, G., Gray, S., and Vidal-Puig, A. (2007). Adipogenesis and lipotoxicity: Role of peroxisome proliferator-activated receptor γ (PPARγ) and PPARγcoactivator-1 (PGC1). *Public Health Nutr.* 10, 1132–1137. doi:10.1017/S1368980007000614.

Meloche, K. J., Fancher, B. I., Emmerson, D. A., Bilgili, S. F., and Dozier, W. A. (2018a). Effects of quantitative nutrient allocation on myopathies of the Pectoralis major muscles in broiler chickens at 32 , 43 , and 50 days of age 1. *Poult. Sci.* 97, 1786–1793. doi:10.3382/ps/pex453.

Meloche, K. J., Fancher, B. I., Emmerson, D. A., Bilgili, S. F., and Dozier, W. A. (2018b). Effects of reduced dietary energy and amino acid density on Pectoralis major myopathies in broiler chickens at 36 and 49 days of age1. *Poult. Sci.* 97, 1794–1807. doi:10.3382/ps/pex454.

Mitch, W. E., Medina, R., Grieber, S., May, R. C., England, B. K., Price, S. R., et al. (1994). Metabolic acidosis stimulates muscle protein degradation by activating the adenosine triphosphate-dependent pathway involving ubiquitin and proteasomes. *J. Clin. Invest.* 93, 2127–2133. doi:10.1172/JCI117208.

Mohlke, K. L., and Boehnke, M. (2015). Recent advances in understanding the genetic architecture of type 2 diabetes. *Hum. Mol. Genet.* 24, R85–R92. doi:10.1093/hmg/ddv264.

Moreno-Viedma, V., Amor, M., Sarabi, A., Bilban, M., Staffler, G., Zeyda, M., et al. (2016). Common dysregulated pathways in obese adipose tissue and atherosclerosis. *Cardiovasc. Diabetol.* 15, 1–12. doi:10.1186/s12933-016-0441-2.

Morris, A. D. P., Voight, B. F., Teslovich, T. M., Ferreira, T., Segrè, A. V., Steinthorsdottir, V., et al. (2012). Large-scale association analysis provides insights into the genetic architecture and pathophysiology of type 2 diabetes. *Nat. Genet.* 44, 981–990. doi:10.1038/ng.2383.

Moyers, J. S., Bilan, P. J., Reynet, C., and Ronald Kahn, C. (1996). Overexpression of Rad inhibits glucose uptake in cultured muscle and fat cells. *J. Biol. Chem.* 271, 23111–23116. doi:10.1074/jbc.271.38.23111.

Moyers, J. S., Bilan, P. J., Zhu, J., and Kahn, C. R. (1997). Rad and Rad-related GTPases interact with calmodulin and calmodulin- dependent protein kinase II. *J. Biol. Chem.* 272, 11832–11839. doi:10.1074/jbc.272.18.11832.

Mudalal, S., Lorenzi, M., Soglia, F., Cavani, C., and Petracci, M. (2015). Implications of white striping and wooden breast abnormalities on quality traits of raw and marinated chicken meat. *Animal* 9, 728–734. doi:10.1017/S175173111400295X.

Mungrue, I. N., Pagnon, J., Kohannim, O., Gargalovic, P. S., and Lusis, A. J. (2009). CHAC1/MGC4504 is a novel proapoptotic component of the unfolded protein response, downstream of the ATF4-ATF3-CHOP cascade. *J. Immunol.* 182, 466–476.

Mutair, A. N. A., Brusgaard, K., Bin-Abbas, B., Hussain, K., Felimban, N., Shaikh, A. Al, et al. (2013). Heterogeneity in phenotype of usher-congenital hyperinsulinism syndrome. *Diabetes Care* 36, 557–561. doi:10.2337/dc12-1174.

Mutryn, M. F., Brannick, E. M., Fu, W., Lee, W. R., and Abasht, B. (2015a). Characterization of a novel chicken muscle disorder through differential gene expression and pathway analysis using RNA-sequencing. *BMC Genomics* 16, 399. doi:10.1186/s12864-015-1623-0.

Mutryn, M. F., Fu, W., and Abasht, B. (2015b). Incidence of Wooden Breast Disease and its correlation with broiler performance and ultimate pH of breast muscle. in *Proceedings of XXII European Symposium on Poultry Meat Quality* (Nantes, France).

Nanji, A. A., Fogt, F., and Griniuviene, B. (1995). Alterations in glucose transporter proteins in alcoholic liver disease in the rat. *Am J Pathol* 146, 329–334. Available at: http://www.ncbi.nlm.nih.gov/entrez/query.fcgi?cmd=Retrieve&db=PubMed&dopt=Citation&list_uids=7856745.

Navale, A. M., and Paranjape, A. N. (2016). Glucose transporters: physiological and pathological roles. *Biophys. Rev.* 8, 5–9. doi:10.1007/s12551-015-0186-2.

Nie, J., DuBois, D. C., Xue, B., Jusko, W. J., and Almon, R. R. (2017). Effects of high-fat feeding on skeletal muscle gene expression in diabetic Goto-Kakizaki rats. *Gene Regul. Syst. Bio.* 11, 1–11. doi:10.1177/1177625017710009.

Norring, M., Valros, A., Valaja, J., Sihvo, H., Immonen, K., and Puolanne, E. (2018). Wooden breast myopathy links with poorer gait in broiler chickens. *Animal*, 1–6. doi:10.1017/S1751731118003270.

Olin, K. L., Potter-Perigo, S., Barrett, P. H. R., Wight, T. N., and Chait, A. (1999). Lipoprotein lipase enhances the binding of native and oxidized low density lipoproteins to versican and biglycan synthesized by cultured arterial smooth muscle cells. *J. Biol. Chem.* 274, 34629–34636. doi:10.1074/jbc.274.49.34629.

Olkowski, A. A., Korver, D., Rathgeber, B., and Classen, H. L. (1999). Cardiac index, oxygen delivery, and tissue oxygen extraction in slow and fast growing chickens, and in chickens with heart failure and ascites: A comparative study. *Avian Pathol.* 28, 137–146. doi:10.1080/03079459994867.

Online Mendelian Inheritance in Man, OMIM *McKusick-Nathans Inst. Genet. Med. Johns Hopkins Univ. (Baltimore, MD)*. Available at: https://omim.org/ [Accessed April 14, 2020].

Orrenius, S., Gogvadze, V., and Zhivotovsky, B. (2015). Calcium and mitochondria in the regulation of cell death. *Biochem. Biophys. Res. Commun.* 460, 72–81. doi:10.1016/j.bbrc.2015.01.137.

Palmer, S., Groves, N., Schindeler, A., Yeoh, T., Biben, C., Wang, C.-C., et al. (2001). The Small Muscle-specific Protein Csl Modifies Cell Shape and Promotes Myocyte Fusion in an... *J. Cell Biol.* 153, 985. Available at: http://search.ebscohost.com/login.aspx?direct=true&db=a9h&AN=5226347&site=ehost-live&scope=site.

Pampouille, E., Berri, C., Boitard, S., Hennequet-Antier, C., Beauclercq, S. A., Godet, E., et al. (2018). Mapping QTL for white striping in relation to breast muscle yield and meat quality traits in broiler chickens. *BMC Genomics* 19, 1–14.

doi:10.1186/s12864-018-4598-9.

Papah, M. B., and Abasht, B. (2019). Dysregulation of lipid metabolism and appearance of slow myofiber- specific isoforms accompany the development of Wooden Breast myopathy in modern broiler chickens. *Sci. Rep.* 9, 17170. doi:10.1038/s41598-019-53728-8.

Papah, M. B., Brannick, E. M., Schmidt, C. J., and Abasht, B. (2017). Evidence and role of phlebitis and lipid infiltration in the onset and pathogenesis of Wooden Breast Disease in modern broiler chickens. *Avian Pathol.* 46, 623–643. doi:10.1080/03079457.2017.1339346.

Papah, M. B., Brannick, E. M., Schmidt, C. J., and Abasht, B. (2018). Gene expression profiling of the early pathogenesis of wooden breast disease in commercial broiler chickens using RNA-sequencing. *PLoS One* 13, e0207346. doi:10.1371/journal.pone.0207346.

Pappas, C. T., Farman, G. P., Mayfield, R. M., Konhilas, J. P., and Gregorio, C. C. (2018). Cardiac-specific knockout of Lmod2 results in a severe reduction in myofilament force production and rapid cardiac failure. *J. Mol. Cell. Cardiol.* 122, 88–97. doi:10.1016/j.yjmcc.2018.08.009.

Park, K. S., Ciaraldi, T. P., Abrams-carter, L., Mudaliar, S., Nikoulina, S. E., and Henry, R. R. (1997). PPAR-y gene expression is elevated in skeletal muscle of obese and type II diabetic subjects. *Diabetes* 46, 1230–1234.

Park, P. J., Kong, S. W., Tebaldi, T., Lai, W. R., Kasif, S., and Kohane, I. S. (2009). Integration of heterogeneous expression data sets extends the role of the retinol pathway in diabetes and insulin resistance. *Bioinformatics* 25, 3121–3127. doi:10.1093/bioinformatics/btp559.

Paulsen, M., Khare, T., Burgard, C., Tierling, S., and Walter, J. (2005). Evolution of the Beckwith-Wiedemann syndrome region in vertebrates. *Genome Res.* 15, 146–153. doi:10.1101/gr.2689805.

Penzo, D., Tagliapietra, C., Colonna, R., Petronilli, V., and Bernardi, P. (2002). Effects of fatty acids on mitochondria: Implications for cell death. *Biochim. Biophys. Acta - Bioenerg.* 1555, 160–165. doi:10.1016/S0005-2728(02)00272-4.

Petracci, M., Mudalal, S., Soglia, F., and Cavani, C. (2015). Meat quality in fast-growing broiler chickens. *Worlds. Poult. Sci. J.* 71, 363–374. doi:10.1017/S0043933915000367.

Petracci, M., Soglia, F., Madruga, M., Carvalho, L., Ida, E., and Estevez, M. (2019).

Wooden-breast, white striping, and spaghetti meat: Causes, consequences and consumer perception of emerging broiler meat abnormalities. *Compr. Rev. Food Sci. Food Saf.* 18, 565–583. doi:10.1111/1541-4337.12431.

Phua, W. W. T., Wong, M. X. Y., Liao, Z., and Tan, N. S. (2018). An apparent functional consequence in skeletal muscle physiology via peroxisome proliferator-activated receptors. *Int. J. Mol. Sci.* 19. doi:10.3390/ijms19051425.

Pitel, F., Abasht, B., Morisson, M., Crooijmans, R. P. M. A., Vignoles, F., Leroux, S., et al. (2004). A high-resolution radiation hybrid map of chicken chromosome 5 and comparison with human chromosomes. *BMC Genomics* 5, 1–9. doi:10.1186/1471-2164-5-66.

Pohlers, D., Brenmoehl, J., Löffler, I., Müller, C. K., Leipner, C., Schultze-Mosgau, S., et al. (2009). TGF-β and fibrosis in different organs - molecular pathway imprints. *Biochim. Biophys. Acta - Mol. Basis Dis.* 1792, 746–756. doi:10.1016/j.bbadis.2009.06.004.

Puig-Oliveras, A., Ramayo-Caldas, Y., Corominas, J., Estellé, J., Pérez-Montarelo, D., Hudson, N. J., et al. (2014). Differences in muscle transcriptome among pigs phenotypically extreme for fatty acid composition. *PLoS One* 9. doi:10.1371/journal.pone.0099720.

Pulido, M. R., Diaz-Ruiz, A., Jiménez-Gómez, Y., Garcia-Navarro, S., Gracia-Navarro, F., Tinahones, F., et al. (2011). Rab18 dynamics in adipocytes in relation to lipogenesis, lipolysis and obesity. *PLoS One* 6. doi:10.1371/journal.pone.0022931.

Puri, V., Ranjit, S., Konda, S., Nicoloro, S. M. C., Straubhaar, J., Chawla, A., et al. (2008). Cidea is associated with lipid droplets and insulin sensitivity in humans. *Proc. Natl. Acad. Sci.* 105, 7833–7838. doi:10.1073/pnas.0802063105.

Qi, L., Saberi, M., Zmuda, E., Wang, Y., Altarejos, J., Zhang, X., et al. (2009). Adipocyte CREB promotes insulin resistance in obesity. *Cell Metab.* 9, 277–286. doi:10.1016/j.cmet.2009.01.006.

Randle, P. J., Garland, P. B., Newsholme, E. A., and Hales, C. N. (1965). The glucose fatty acid cycle in obesity and maturity onset diabetes mellitus. *Ann. N. Y. Acad. Sci.* 131, 324–333. doi:10.1016/0306-9877(81)90134-1.

Randle, P. J., Priestman, D. A., Mistry, S. C., and Halsall, A. (1994). Glucose fatty acid interactions and the regulation of glucose disposal. *J. Cell. Biochem.* 55, 1–11. doi:10.1002/jcb.240550002.

Rasouli, N., Molavi, B., Elbein, S. C., and Kern, P. A. (2007). Ectopic fat accumulation and metabolic syndrome. *Diabetes, Obes. Metab.* 9, 1–10. doi:10.1111/j.1463-1326.2006.00590.x.

Resnyk, C. W., Carré, W., Wang, X., Porter, T. E., Simon, J., Le Bihan-Duval, E., et al. (2017). Transcriptional analysis of abdominal fat in chickens divergently selected on bodyweight at two ages reveals novel mechanisms controlling adiposity: Validating visceral adipose tissue as a dynamic endocrine and metabolic organ. *BMC Genomics* 18, 1–31. doi:10.1186/s12864-017-4035-5.

Reynet, C., and Kahn, C. R. (1993). Rad: A member of the Ras family overexpressed in muscle of type II diabetic humans. *Science (80-.).* 262, 1441. Available at: http://search.proquest.com/docview/213556241/8483B8EB64464EB0PQ/58?accountid=11836z.

Rich, S. S., Goodarzi, M. O., Palmer, N. D., Langefeld, C. D., Ziegler, J., Haffner, S. M., et al. (2009). A genome-wide association scan for acute insulin response to glucose in Hispanic-Americans: The Insulin Resistance Atherosclerosis Family Study (IRAS FS). *Diabetologia* 52, 1326–1333. doi:10.1007/s00125-009-1373-0.

Rocha, D. M., Caldas, A. P., Oliveira, L. L., Bressan, J., and Hermsdorff, H. H. (2016). Saturated fatty acids trigger TLR4-mediated inflammatory response. *Atherosclerosis* 244, 211–215. doi:10.1016/j.atherosclerosis.2015.11.015.

Romero, N. B. (2010). Centronuclear myopathies: A widening concept. *Neuromuscul. Disord.* 20, 223–228. doi:10.1016/j.nmd.2010.01.014.

Rousset, S., Alves-Guerra, M.-C., Mozo, J., Miroux, B., Cassard-Doulcier, A.-M., Bouillaud, F., et al. (2004). The biology of mitochondrial uncoupling. *Diabetes* 53, S130–S135. doi:10.2337/diabetes.53.2007.s130.

Roy, B. C., Oshima, I., Miyachi, H., Shiba, N., Nishimura, S., Tabata, S., et al. (2006). Effects of nutritional level on muscle development, histochemical properties of myofibre and collagen architecture in the pectoralis muscle of male broilers. *Br. Poult. Sci.* 47, 433–442. doi:10.1080/00071660600828334.

Rutsch, F., Gailus, S., Suormala, T., and Fowler, B. (2011). LMBRD1: The gene for the cblF defect of vitamin B12 metabolism. *J. Inherit. Metab. Dis.* 34, 121–126. doi:10.1007/s10545-010-9083-9.

Rutten, E. P. A., Engelen, M. P. K. J., Schols, A. M. W. J., and Deutz, N. E. P. (2005). Skeletal muscle glutamate metabolism in health and disease: State of the art. *Curr. Opin. Clin. Nutr. Metab. Care* 8, 41–51. doi:10.1097/00075197-200501000-00007.

Rys-Sikora, K. E., and Gill, D. L. (1998). Fatty acid-mediated calcium sequestration within intracellular calcium pools. *J. Biol. Chem.* 273, 32627–32635. doi:10.1074/jbc.273.49.32627.

Sandercock, D. A., Barker, Z. E., Mitchell, M. A., and Hocking, P. M. (2009). Changes in muscle cell cation regulation and meat quality traits are associated with genetic selection for high body weight and meat yield in broiler chickens. *Genet. Sel. Evol.* 41, 1–8. doi:10.1186/1297-9686-41-8.

Sanghera, D. K., and Blackett, P. R. (2012). Type 2 diabetes genetics: Beyond GWAS. *J. Diabetes Metab.* 3, 6948. doi:10.4172/2155-6156.1000198.

Satriano, J. (2007). Kidney growth, hypertrophy and the unifying mechanism of diabetic complications. *Amino Acids* 33, 331–339. doi:10.1007/s00726-007-0529-9.

Scheuermann, G. N., Bilgili, S. F., Tuzun, S., and Mulvaney, D. R. (2004). Comparison of chicken genotypes: Myofiber number in pectoralis muscle and myostatin ontogeny. *Poult. Sci.* 83, 1404–1412. doi:10.1093/ps/83.8.1404.

Schmidt-Nielsen, K. (1971). How birds breathe. *Sci. Am.* 225, 72–79.

Schrauwen, P. (2007). High-fat diet, muscular lipotoxicity and insulin resistance. *Proc. Nutr. Soc.* 66, 33–41. doi:10.1017/S0029665107005277.

Schrauwen, P., and Hesselink, M. K. C. (2004). Oxidative capacity, lipotoxicity, and mitochondrial damage in type 2 diabetes. *Diabetes* 53, 1412–1417.

Schröder, M., and Kaufman, R. J. (2005). ER stress and the unfolded protein response. *Mutat. Res. - Fundam. Mol. Mech. Mutagen.* 569, 29–63. doi:10.1016/j.mrfmmm.2004.06.056.

Scott, L. J., Mohlke, K. L., Bonnycastle, L. L., Willer, C. J., Li, Y., Duren, W. L., et al. (2007). A genome-wide association study of type 2 diabetes in finns detects multiple susceptibility variants. *Science (80-.).* 316, 1341–1345. doi:10.1126/science.1142382.

Scribner, B. B. H., Fremont-smith, K., and Burnell, J. M. (1955). The effect of acute respiratory acidosis on the internal equilibrium of potassium. *J. Clin. Invest.* 34, 1276–1285.

Seki, Y., Sato, K., Kono, T., Abe, H., and Akiba, Y. (2003). Broiler chickens (Ross strain) lack insulin-responsive glucose transporter GLUT4 and have GLUT8 cDNA. *Gen. Comp. Endocrinol.* 133, 80–87. doi:10.1016/S0016-6480(03)00145-

X.

Semenza, G. L., Roth, P. H., Fang, H. M., and Wang, G. L. (1994). Transcriptional regulation of genes encoding glycolytic enzymes by hypoxia-inducible factor 1. *J. Biol. Chem.* 269, 23757–23763.

Semple, R. K., Chatterjee, V. K. K., and Rahilly, S. O. (2006). PPARγ and human metabolic disease. *J. Clin. Invest.* 116, 581–589. doi:10.1172/JCI28003.taglandin.

Seo, M., and Lee, Y. H. (2014). PFKFB3 regulates oxidative stress homeostasis via its S-glutathionylation in cancer. *J. Mol. Biol.* 426, 830–842. doi:10.1016/j.jmb.2013.11.021.

Sharma, V., and McNeill, J. H. (2006). Diabetic cardiomapathy: Where are we 40 years later? *Can. J. Cardiol.* 22, 305–308. doi:10.1016/S0828-282X(06)70914-X.

Shepherd, P. R., and Kahn, B. B. (1999). Glucose transporters and insulin action: Implications for insulin resistance and diabetes mellitus. *N. Engl. J. Med.* 341, 248–257.

Shi, H., He, Q., Cheng, M., Sun, Y., Li, H., and Wang, N. (2015). Effect of HOPX gene overexpression on chicken preadipocyte proliferation. *Sci. Agric. Sin.* 48, 1624–1631. doi:10.3864/j.issn.0578-1752.2015.08.17.

Shin, C. H., Liu, Z. P., Passier, R., Zhang, C. L., Wang, D. Z., Harris, T. M., et al. (2002). Modulation of cardiac growth and development by HOP, an unusual homeodomain protein. *Cell* 110, 725–735. doi:10.1016/S0092-8674(02)00933-9.

Shiraishi, J. ichi, Yanagita, K., Fukumori, R., Sugino, T., Fujita, M., Kawakami, S. I., et al. (2011). Comparisons of insulin related parameters in commercial-type chicks: Evidence for insulin resistance in broiler chicks. *Physiol. Behav.* 103, 233–239. doi:10.1016/j.physbeh.2011.02.008.

Sihvo, H. K., Airas, N., Lindén, J., and Puolanne, E. (2018). Pectoral vessel density and early ultrastructural changes in broiler chicken wooden breast myopathy. *J. Comp. Pathol.* 161, 1–10. doi:10.1016/j.jcpa.2018.04.002.

Sihvo, H. K., Immonen, K., and Puolanne, E. (2014). Myodegeneration with fibrosis and regeneration in the pectoralis major muscle of broilers. *Vet. Pathol.* 51, 619–623. doi:10.1177/0300985813497488.

Sihvo, H. K., Lindén, J., Airas, N., Immonen, K., Valaja, J., and Puolanne, E. (2017). Wooden breast myodegeneration of pectoralis major muscle over the growth

period in broilers. *Vet. Pathol.* 54, 119–128. doi:10.1177/0300985816658099.

Simon, J., and LeClercq, B. (1982). Longitudinal study of adiposity in chickens selected for high or low abdominal fat content: Further evidence of a glucose-insulin imbalance in the fat line. *J. Nutr.* 112, 1961–1973. doi:10.1093/jn/112.10.1961.

Sinsigalli, N. A., Mcmurtry, J. P., Cherry, J. A., and Siegel, P. B. (1987). Glucose tolerance, plasma insulin and immunoreactive glucagon in chickens selected for high and low body weight. *J. Nutr.*, 941–947.

Sladek, R., Rocheleau, G., Rung, J., Dina, C., Shen, L., Serre, D., et al. (2007). A genome-wide association study identifies novel risk loci for type 2 diabetes. *Nature* 445, 881–885. doi:10.1038/nature05616.

Smith, A. C., Choufani, S., Ferreira, J. C., and Weksberg, R. (2007). Growth regulation, imprinted genes, and chromosome 11p15.5. *Pediatr. Res.* 61, 43–47. doi:10.1203/pdr.0b013e3180457660.

Smith, I. C., Bombardier, E., Vigna, C., and Tupling, A. R. (2013). ATP consumption by sarcoplasmic reticulum Ca2+ pumps accounts for 40-50% of resting metabolic rate in mouse fast and slow twitch skeletal muscle. *PLoS One* 8, 1–11. doi:10.1371/journal.pone.0068924.

Smith, M. W., Mitchell, M. A., and Peacock, M. A. (1990). Effects of genetic selection on growth rate and intestinal structure in the domestic fowl (Gallus domesticus). *Comp. Biochem. Physiol. -- Part A Physiol.* 97A, 57–63. doi:10.1016/0300-9629(90)90722-5.

Soglia, F., Mazzoni, M., and Petracci, M. (2019). Spotlight on avian pathology: current growth-related breast meat abnormalities in broilers. *Avian Pathol.* 48, 1–3. doi:10.1080/03079457.2018.1508821.

Soglia, F., Mudalal, S., Babini, E., Di Nunzio, M., Mazzoni, M., Sirri, F., et al. (2016). Histology, composition, and quality traits of chicken Pectoralis major muscle affected by wooden breast abnormality. *Poult. Sci.* 95, 651–659. doi:10.3382/ps/pev353.

Steinmetz, H. W., Vogt, R., Kästner, S., Riond, B., and Hatt, J.-M. (2007). Evaluation of the i-STAT portable clinical analyzer in chickens (Gallus gallus). *J. Vet. Diagnostic Investig.* 19, 382–388.

Stumvoll, M., and Häring, H. (2002). The peroxisome proliferator–activated receptor-gamma2 Pro12Ala polymorphism. *Diabetes* 51, 2341–2347.

Surakka, I., Horikoshi, M., Mägi, R., Sarin, A.-P., Mahajan, A., Lagou, V., et al. (2015). The impact of low-frequency and rare variants on lipid levels. *Nat. Genet.* 47, 589–597. doi:10.1038/ng.3300.

Szatmari, I., Töröcsik, D., Agostini, M., Nagy, T., Gurnell, M., Barta, E., et al. (2007). PPARγ regulates the function of human dendritic cells primarily by altering lipid metabolism. *Blood* 110, 3271–3280. doi:10.1182/blood-2007-06-096222.

Tamilarasan, K. P., Temmel, H., Das, S. K., Al Zoughbi, W., Schauer, S., Vesely, P. W., et al. (2012). Skeletal muscle damage and impaired regeneration due to LPL-mediated lipotoxicity. *Cell Death Dis.* 3, e354-8. doi:10.1038/cddis.2012.91.

Tan, A. L. M., Langley, S. R., Tan, C. F., Chai, J. F., Khoo, C. M., Leow, M. K. S., et al. (2018). Ethnicity-specific skeletal muscle transcriptional signatures and their relevance to insulin resistance in Singapore. *J. Clin. Endocrinol. Metab.* 104, 465–486. doi:10.1210/jc.2018-00309.

Tasoniero, G., Cullere, M., Cecchinato, M., Puolanne, E., and Dalle Zotte, A. (2016). Technological quality, mineral profile, and sensory attributes of broiler chicken breasts affected by White Striping and Wooden Breast myopathies. *Poult. Sci.* 95, 2707–2714. doi:10.3382/ps/pew215.

Tickle, P. G., Paxton, H., Rankin, J. W., Hutchinson, J. R., and Codd, J. R. (2014). Anatomical and biomechanical traits of broiler chickens across ontogeny. Part I. Anatomy of the musculoskeletal respiratory apparatus and changes in organ size. *PeerJ* 2, e432. doi:10.7717/peerj.432.

Tinelli, E., Pereira, J. A., and Suter, U. (2013). Muscle-specific function of the centronuclear myopathy and charcot-marie-tooth neuropathy associated dynamin 2 is required for proper lipid metabolism, mitochondria, muscle fibers, neuromuscular junctions and peripheral nerves. *Hum. Mol. Genet.* 22, 4417–4429. doi:10.1093/hmg/ddt292.

Toborek, M., Lee, Y. W., Garrido, R., Kaiser, S., and Hennig, B. (2002). Unsaturated fatty acids selectively induce an inflammatory environment in human endothelial cells. *Am. J. Clin. Nutr.* 75, 119–125. doi:10.1093/ajcn/75.1.119.

Tokudome, T., Horio, T., Yoshihara, F., Suga, S. I., Kawano, Y., Kohno, M., et al. (2004). Direct effects of high glucose and insulin on protein synthesis in cultured cardiac myocytes and DNA and collagen synthesis in cardiac fibroblasts. *Metabolism.* 53, 710–715. doi:10.1016/j.metabol.2004.01.006.

Tokushima, Y., Takahashi, K., Sato, K., and Akiba, Y. (2005). Glucose uptake in vivo in skeletal muscles of insulin-injected chicks. *Comp. Biochem. Physiol. - B*

Biochem. Mol. Biol. 141, 43–48. doi:10.1016/j.cbpc.2005.01.008.

Torekov, S. S., Iepsen, E., Christiansen, M., Linneberg, A., Pedersen, O., Holst, J. J., et al. (2014). KCNQ1 long QT syndrome patients have hyperinsulinemia and symptomatic hypoglycemia. *Diabetes* 63, 1315–1325. doi:10.2337/db13-1454.

Tousoulis, D., Kampoli, A.-M., Tentolouris Nikolaos Papageorgiou, C., and Stefanadis, C. (2012). The role of nitric oxide on endothelial function. *Curr. Vasc. Pharmacol.* 10, 4–18. doi:10.2174/157016112798829760.

Trapnell, C., Hendrickson, D. G., Sauvageau, M., Goff, L., Rinn, J. L., and Pachter, L. (2013). Differential analysis of gene regulation at transcript resolution with RNA-seq. *Nat. Biotechnol.* 31, 46–53. doi:10.1038/nbt.2450.

Travers, M. E., Mackay, D. J. G., Nitert, M. D., Morris, A. P., Lindgren, C. M., Berry, A., et al. (2013). Insights into the molecular mechanism for type 2 diabetes susceptibility at the KCNQ1 locus from temporal changes in imprinting status in human islets. *Diabetes* 62, 987–992. doi:10.2337/db12-0819.

Trocino, A., Piccirillo, A., Birolo, M., Radaelli, G., Bertotto, D., Filiou, E., et al. (2015). Effect of genotype, gender and feed restriction on growth, meat quality and the occurrence of white striping and wooden breast in broiler chickens. *Poult. Sci.* 94, 2996–3004. doi:10.3382/ps/pev296.

Tsukada, T., Pappas, C. T., Moroz, N., Antin, P. B., Kostyukova, A. S., and Gregorio, C. C. (2010). Leiomodin-2 is an antagonist of tropomodulin-1 at the pointed end of the thin filaments in cardiac muscle. *J. Cell Sci.* 123, 3136–3145. doi:10.1242/jcs.071837.

Tumova, J., Andel, M., and Trnka, J. (2016). Excess of free fatty acids as a cause of metabolic dysfunction in skeletal muscle. *Physiol. Res.* 65, 193–207. Available at: http://www.ncbi.nlm.nih.gov/pubmed/26447514.

Turcot, V., Lu, Y., Highland, H. M., Schurmann, C., Justice, A. E., Fine, R. S., et al. (2018). Protein-altering variants associated with body mass index implicate pathways that control energy intake and expenditure in obesity. *Nat. Genet.* 50, 26–35. doi:10.1038/s41588-017-0011-x.

Ursini, F., Roveri, A., van Amsterdam, F. T. M., Ratti, E., Maiorino, M., Zamburlini, A., et al. (2004). Effect of hydrogen peroxide on calcium homeostasis in smooth muscle cells. *Arch. Biochem. Biophys.* 297, 265–270. doi:10.1016/0003-9861(92)90671-i.

Van Den Berg, S., Vandenplas, J., Van Eeuwijk, F. A., Bouwman, A. C., Lopes, M.

S., and Veerkamp, R. F. (2019). Imputation to whole-genome sequence using multiple pig populations and its use in genome-wide association studies. *Genet. Sel. Evol.* 51, 1–13. doi:10.1186/s12711-019-0445-y.

Van Leeuwen, E. M., Karssen, L. C., Deelen, J., Isaacs, A., Medina-Gomez, C., Mbarek, H., et al. (2015). Genome of the Netherlands population-specific imputations identify an ABCA6 variant associated with cholesterol levels. *Nat. Commun.* 6. doi:10.1038/ncomms7065.

Velleman, S. G., Clark, D. L., and Tonniges, J. R. (2017). Fibrillar collagen organization associated with broiler wooden breast fibrotic myopathy. *Avian Dis.* 61, 481–490. doi:10.1637/11738-080217-Reg.1.

Velleman, S. G., Clark, D. L., and Tonniges, J. R. (2018). The effect of the Wooden Breast myopathy on sarcomere structure and organization. *Avian Dis.* 62, 28–35. doi:10.1637/11766-110217-Reg.1.

Volmer, R., and Ron, D. (2015). Lipid-dependent regulation of the unfolded protein response. *Curr. Opin. Cell Biol.* 33, 67–73. doi:10.1016/j.ceb.2014.12.002.

Wall, V. Z., Barnhart, S., Kanter, J. E., Kramer, F., Shimizu-Albergine, M., Adhikari, N., et al. (2018). Smooth muscle glucose metabolism promotes monocyte recruitment and atherosclerosis in a mouse model of metabolic syndrome. *JCI Insight* 3. doi:10.1172/jci.insight.96544.

Wang, H., and Eckel, R. H. (2009). Lipoprotein lipase: from gene to obesity. *Am. J. Physiol. Metab.* 297, E271–E288. doi:10.1152/ajpendo.90920.2008.

Wang, J., Xian, X., Huang, W., Chen, L., Wu, L., Zhu, Y., et al. (2007). Expression of LPL in endothelial-intact artery results in lipid deposition and vascular cell adhesion molecule-1 upregulation in both LPL and ApoE-deficient mice. *Arterioscler. Thromb. Vasc. Biol.* 27, 197–203. doi:10.1161/01.ATV.0000249683.80414.d9.

Wang, Y. H., Byrne, K. A., Reverter, A., Harper, G. S., Taniguchi, M., McWilliam, S. M., et al. (2005). Transcriptional profiling of skeletal muscle tissue from two breeds of cattle. *Mamm. Genome* 16, 201–210. doi:10.1007/s00335-004-2419-8.

Wang, Y., Wan, B., Li, D., Zhou, J., Li, R., Bai, M., et al. (2012). BRSK2 is regulated by ER stress in protein level and involved in ER stress-induced apoptosis. *Biochem. Biophys. Res. Commun.* 423, 813–818. doi:10.1016/j.bbrc.2012.06.046.

Wang, Y. X. (2010). PPARs: Diverse regulators in energy metabolism and metabolic diseases. *Cell Res.* 20, 124–137. doi:10.1038/cr.2010.13.

Wei, T., and Simko, V. (2017). R package “corrplot”: Visualization of a correlation matrix (Version 0.84). Available at: https://github.com/taiyun/corrplot.

Wei, Y., Wang, D., Gentile, C. L., and Pagliassotti, M. J. (2009). Reduced endoplasmic reticulum luminal calcium links saturated fatty acid-mediated endoplasmic reticulum stress and cell death in liver cells. *Mol. Cell. Biochem.* 331, 31–40. doi:10.1007/s11010-009-0142-1.

Westerbacka, J., Kolak, M., Kiviluoto, T., Arkkila, P., Sire, J., Hamsten, A., et al. (2007). Genes involved in fatty acid partitioning and binding, inflammation are overexpressed in the human fatty liver of insulin-resistant subjects. *Diabetes* 56, 2759–2765. doi:10.2337/db07-0156.ADIPOR.

Wideman, R. F., and French, H. (2000). Ascites resistance of progeny from broiler breeders selected for two generations using chronic unilateral pulmonary artery occlusion. *Poult. Sci.* 79, 396–401. doi:10.1093/ps/79.3.396.

Wideman, R. F., Hooge, D. M., and Cummings, K. R. (2003). Dietary sodium bicarbonate, cool temperatures, and feed withdrawal: Impact on arterial and venous blood-gas values in broilers. *Poult. Sci.* 82, 560–570. doi:10.1093/ps/82.4.560.

Willer, C. J., Schmidt, E. M., Sengupta, S., Peloso, G. M., Gustafsson, S., Kanoni, S., et al. (2013). Discovery and refinement of loci associated with lipid levels. *Nat. Genet.* 45, 1274–1285. doi:10.1038/ng.2797.

Wong, E. M. (2018). Differential gene expression in lung tissue of wooden breast syndrome affected and unaffected commercial broiler chickens.

Xu, Z., Wei, G., Chepelev, I., Zhao, K., and Felsenfeld, G. (2011). Mapping of INS promoter interactions reveals its role in long-range regulation of SYT8 transcription. *Nat. Struct. Mol. Biol.* 18, 372–378. doi:10.1038/nsmb.1993.

Yabe-Nishimura, C. (1998). Aldose reductase in glucose toxicity: A potential target for the prevention of diabetic complications. *Pharmacol. Rev.* 50, 21–33.

Yamamoto, T., Takano, N., Ishiwata, K., Ohmura, M., Nagahata, Y., Matsuura, T., et al. (2014). Reduced methylation of PFKFB3 in cancer cells shunts glucose towards the pentose phosphate pathway. *Nat. Commun.* 5. doi:10.1038/ncomms4480.

Yan, L. (2018). Redox imbalance stress in diabetes mellitus: Role of the polyol pathway. *Anim. Model. Exp. Med.* 1, 7–13. doi:10.1002/ame2.12001.

Yang, J., Lee, S. H., Goddard, M. E., and Visscher, P. M. (2011). GCTA: A tool for genome-wide complex trait analysis. *Am. J. Hum. Genet.* 88, 76–82. doi:10.1016/j.ajhg.2010.11.011.

Yang, S., Deng, H., Zhang, Q., Xie, J., Zeng, H., Jin, X., et al. (2016). Amelioration of diabetic mouse nephropathy by catalpol correlates with down-regulation of Grb10 adn activation of insulin-like growth factor 1/insulin-like growth factor 1 receptor signaling. *PLoS One* 11, e0151857. doi:10.1371/journal.pone.0151857.

Yang, T., Pang, C. P., Tsang, M. W., Lam, C. W., Poon, P. M. K., Chan, L. Y. S., et al. (2003). Pathogenic mutations of the lipoprotein lipase gene in Chinese patients with hypertriglyceridemic type 2 diabetes. *Hum. Mutat.* 21, 453. doi:10.1002/humu.9134.

Yang, W., Zhang, Y., Ma, G., Zhao, X., Chen, Y., and Zhu, D. (2005). Identification of gene expression modifications in myostatin-stimulated myoblasts. *Biochem. Biophys. Res. Commun.* 326, 660–666. doi:10.1016/j.bbrc.2004.11.096.

Yildizdaş, D., Yapicioğlu, H., Yilmaz, H. L., and Sertdemir, Y. (2004). Correlation of simultaneously obtained capillary, venous, and arterial blood gases of patients in a paediatric intensive care unit. *Arch. Dis. Child.* 89, 176–180. doi:10.1136/adc.2002.016261.

Yin, H., Price, F., and Rudnicki, M. A. (2013). Satellite cells and the muscle stem cell niche. *Physiol. Rev.* 93, 23–67. doi:10.1152/physrev.00043.2011.

Youn, J. H., and McDonough, A. A. (2009). Recent advances in understanding integrative control of potassium homeostasis. *Annu. Rev. Physiol.* 71, 381–401. doi:10.1146/annurev.physiol.010908.163241.

Zahoor, I., De Koning, D. J., and Hocking, P. M. (2017). Transcriptional profile of breast muscle in heat stressed layers is similar to that of broiler chickens at control temperature. *Genet. Sel. Evol.* 49. doi:10.1186/s12711-017-0346-x.

Zambonelli, P., Zappaterra, M., Soglia, F., Petracci, M., Sirri, F., Cavani, C., et al. (2016). Detection of differentially expressed genes in broiler pectoralis major muscle affected by White Striping - Wooden Breast myopathies. *Poult. Sci.* 95, 2771–2785. doi:10.3382/ps/pew268.

Zampiga, M., Soglia, F., Petracci, M., Meluzzi, A., and Sirri, F. (2019). Effect of different arginine-to-lysine ratios in broiler chicken diets on the occurrence of breast myopathies and meat quality attributes. *Poult. Sci.* 98, 2691–2697.

Zanetti, M. A., Tedesco, D. C., Schneider, T., Teixeira, S. T. F., Daroit, L., Pilotto, F.,

et al. (2018). Economic losses associated with Wooden Breast and White Striping in broilers. *Semin. Ciencias Agrar.* 39, 887–892. doi:10.5433/1679-0359.2018v39n2p887.

Zeggini, E., Scott, L. J., Saxena, R., and Voight, B. F. (2008). Meta-analysis of genome-wide association data and large-scale replication identifies additional susceptibility loci for type 2 diabetes. *Nat. Genet.* 40, 638–645. doi:10.1038/ng.120.

Zerega, B., Camardella, L., Cermelli, S., Sala, R., Cancedda, R., and Descalzi Cancedda, F. (2001). Avidin expression during chick chondrocyte and myoblast development in vitro and in vivo: regulation of cell proliferation. *J Cell Sci* 114, 1473–1482. Available at: http://www.ncbi.nlm.nih.gov/entrez/query.fcgi?cmd=Retrieve&db=PubMed&dopt=Citation&list_uids=11282023.

Zhang, C.-L., Katoh, M., Shibasaki, T., Minami, K., Sunaga, Y., Takahashi, H., et al. (2009). The cAMP sensor Epac2 is a direct target of antidiabetic sulfonylurea drugs. *Science* 325, 607–610. doi:10.1126/science.1172256.

Zhang, H., Luo, W., Sun, Y., Qiao, Y., Zhang, L., Zhao, Z., et al. (2016). Wnt/β-catenin signaling mediated-UCH-L1 expression in podocytes of diabetic nephropathy. *Int. J. Mol. Sci.* 17. doi:10.3390/ijms17091404.

Zhang, K., Zhang, Z. W., Wang, W. S., Yan, X. H., Li, H., and Wang, N. (2012). Cloning and expression of chicken HOPX gene. *J. Northeast Agric. Univ.* 43, 46–53.

Zhou, L., Xu, L., Ye, J., Li, D., Wang, W., Li, X., et al. (2012). Cidea promotes hepatic steatosis by sensing dietary fatty acids. *Hepatology* 56, 95–107. doi:10.1002/hep.25611.

Zhou, N., Lee, W. R., and Abasht, B. (2015). Messenger RNA sequencing and pathway analysis provide novel insights into the biological basis of chickens' feed efficiency. *BMC Genomics* 16, 195. doi:10.1186/s12864-015-1364-0.

Zhuo, Z., Lamont, S. J., Lee, W. R., and Abasht, B. (2015). RNA-seq analysis of abdominal fat reveals differences between modern commercial broiler chickens with high and low feed efficiencies. *PLoS One* 10, e0135810. doi:10.1371/journal.pone.0135810.

Zierath, J. R., Houseknecht, K. L., Gnudi, L., and Kahn, B. B. (1997). High-fat feeding impairs insulin-stimulated GLUT4 recruitment via an early insulin-signaling defect. *Diabetes* 46, 215–223. doi:10.2337/diab.46.2.215.

Zimermann, F. C., Fallavena, L. C. B., Salle, C. T. P., Moraes, H. L. S., Soncini, R. A., Barreta, M. H., et al. (2012). Downgrading of Heavy Broiler Chicken Carcasses Due to Myodegeneration of the Anterior Latissimus Dorsi: Pathologic and Epidemiologic Studies. *Avian Dis.* 56, 418–421. doi:10.1637/9860-072111-case.1.

Zizola, C. F., Schwartz, G. J., and Vogel, S. (2008). Cellular retinol-binding protein type III is a PPARγ target gene and plays a role in lipid metabolism. *Am. J. Physiol. Metab.* 295, E1358–E1368. doi:10.1152/ajpendo.90464.2008.

Zmuda, E. J., Qi, L., Zhu, M. X., Mirmira, R. G., Montminy, M. R., and Hai, T. (2010). The roles of ATF3 , an adaptive-response gene, in high-fat-diet-induced diabetes and pancreatic β-cell dysfunction. *Mol. Endocrinol.* 24, 1423–1433. doi:10.1210/me.2009-0463.

Chapter 7

GENERAL DISCUSSION AND CONCLUSIONS

Many of the results presented in this dissertation support the hypothesis that wooden breast and white striping may be related to type 2 diabetes and metabolic disorder in humans and mammals. This hypothesis raises numerous research questions that can be directly tested in future studies; for instance, measuring changes in insulin and glucagon levels that may be associated with these myopathies and evaluating transcriptomic and metabolomic changes in the pancreas and liver. Much of the research on these diseases focuses on local changes in the pectoralis major muscle associated with myopathy development, resulting in blind spots in our perspective of disease pathogenesis.

Based on the metabolomics work presented in this dissertation, future research may also benefit from the use of plasma biomarkers, such as 3-methylhistidine, as non-invasive, objective, and quantitative measures of disease severity. Although major advances have been made in high-throughput ‘omics technologies, phenotyping remains a major challenge in scientific studies. Disease scoring for wooden breast and white striping is the perfect example of a challenging phenotype where there is room for improvement.

Perhaps the most important findings in this dissertation are from the genome-wide association study, which can be viewed as a preliminary study with substantial room for growth. Linkage disequilibrium analysis revealed that only about 27% of the genome was captured by genetic markers, largely due to the low LD of the crossbred

broiler population that was used. Future studies would benefit from finer mapping, which could be accomplished simply by reducing the number of samples that are pooled in each DNA library or by acquiring whole-genome sequences of their pure line ancestors to facilitate imputation of additional loci. Increasing the average sequencing depth would not only help with fine-scale mapping, but would also permit higher-confidence genotype calling that would be useful in analyzing additional variance components such as dominance and epistatic variance.

Targeted long-read sequencing of known quantitative trait loci, such as those found on chromosome 5 and 30, will be necessary to pinpoint causal variants, if possible, and predict their specific biological effects. In-vitro knock-out experiments of certain promising candidate genes such as *KCNQ1* and *DNM2* may also be valuable in demonstrating the effects of their dysfunction in skeletal muscle cell culture. While understanding the biological mechanisms contributing to these myopathies is of great interest, the use of genetic markers to inform breeding programs has much greater practical application. Marker assisted selection could allow substantial mitigation of broiler breast myopathies due to greater precision of selection criteria.

Appendix A

ADDITIONAL DETAILS ON SAMPLE PREPARATION AND METABOLOMIC PROFILING PERFORMED BY METABOLON

A.1 Quality Control

Several types of controls were analyzed in concert with the experimental samples: a pooled matrix sample generated by taking a small volume of each experimental sample (or alternatively, use of a pool of well-characterized human plasma) served as a technical replicate throughout the data set; extracted water samples served as process blanks; and a cocktail of QC standards that were carefully chosen not to interfere with the measurement of endogenous compounds were spiked into every analyzed sample, allowed instrument performance monitoring and aided chromatographic alignment. Tables A.1 and A.2 describe these QC samples and standards. Instrument variability was determined by calculating the median relative standard deviation (RSD) for the standards that were added to each sample prior to injection into the mass spectrometers. Overall process variability was determined by calculating the median RSD for all endogenous metabolites (i.e., non-instrument standards) present in 100% of the pooled matrix samples. Experimental samples were randomized across the platform run with QC samples spaced evenly among the injections, as outlined in Figure A.1.

Table A.1: Description of Metabolon quality control samples.

Type	Description	Purpose
MTRX	Large pool of human plasma maintained by Metabolon that has been characterized extensively.	Assure that all aspects of the Metabolon process are operating within specifications.
CMTRX	Pool created by taking a small aliquot from every customer sample.	Assess the effect of a non-plasma matrix on the Metabolon process and distinguish biological variability from process variability.
PRCS	Aliquot of ultra-pure water	Process Blank used to assess the contribution to compound signals from the process.
SOLV	Aliquot of solvents used in extraction.	Solvent Blank used to segregate contamination sources in the extraction.

Table A.2: Metabolon quality control standards.

Type	Description	Purpose
RS	Recovery Standard	Assess variability and verify performance of extraction and instrumentation.
IS	Internal Standard	Assess variability and performance of instrument.

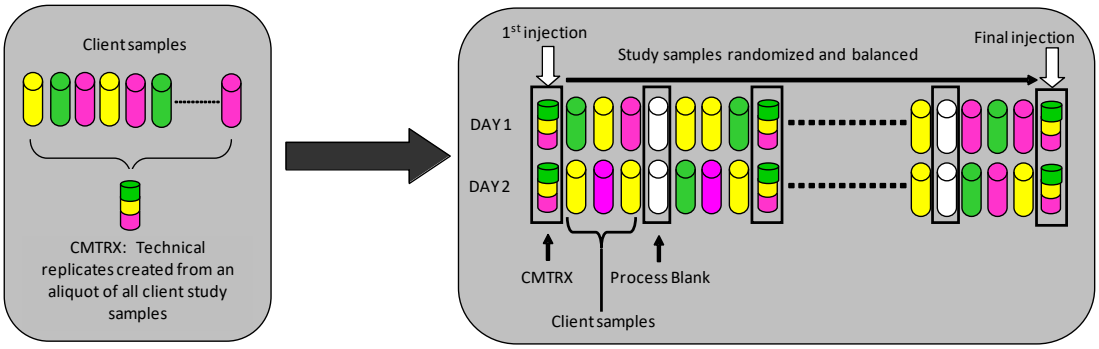

Figure A.1: Preparation of client-specific technical replicates for metabolomics analysis.

A small aliquot of each client sample (colored cylinders) is pooled to create a CMTRX technical replicate sample (multi-colored cylinder), which is then injected periodically

throughout the platform run. Variability among consistently detected biochemicals can be used to calculate an estimate of overall process and platform variability.

A.2 Ultrahigh Performance Liquid Chromatography-Tandem Mass Spectroscopy (UPLC-MS/MS)

Each reconstitution solvent contained a series of standards at fixed concentrations to ensure injection and chromatographic consistency. One aliquot was analyzed using acidic positive ion conditions, chromatographically optimized for more hydrophilic compounds. In this method, the extract was gradient eluted from a C18 column (Waters UPLC BEH C18-2.1x100 mm, 1.7 µm) using water and methanol, containing 0.05% perfluoropentanoic acid (PFPA) and 0.1% formic acid (FA). Another aliquot was also analyzed using acidic positive ion conditions, however it was chromatographically optimized for more hydrophobic compounds. In this method, the extract was gradient eluted from the same afore mentioned C18 column using methanol, acetonitrile, water, 0.05% PFPA and 0.01% FA and was operated at an overall higher organic content. Another aliquot was analyzed using basic negative ion optimized conditions using a separate dedicated C18 column. The basic extracts were gradient eluted from the column using methanol and water, however with 6.5mM Ammonium Bicarbonate at pH 8. The fourth aliquot was analyzed via negative ionization following elution from a HILIC column (Waters UPLC BEH Amide 2.1x150 mm, 1.7 µm) using a gradient consisting of water and acetonitrile with 10mM Ammonium Formate, pH 10.8. The MS analysis alternated between MS and data-dependent MS^n scans using dynamic exclusion.

Appendix B

SIGNIFICANT AND SUGGESTIVE MARKERS FROM SINGLE-SNP GENOME-WIDE ASSOCIATION ANALYSES

Table B.1: Significant (q-value < 0.05) and suggestive (0.05 ≤ q-value < 0.20) SNP markers for wooden breast using all progeny, both male and female.

Chr	Position (bp)	A1	A2	A1 Freq.	beta	se	FDR	Nearest gene within 5000bp	Consequence	dbSNP ID
1	39837932	A	G	0.16	-0.29	0.07	0.07	RPS16	downstream	rs318074938
1	40656409	T	C	0.15	-0.27	0.07	0.13	–	intergenic	rs316589473
1	40656451	C	G	0.15	-0.27	0.07	0.14	–	intergenic	–
1	45019726	G	A	0.27	-0.24	0.06	0.18	–	intergenic	rs15251160
2	45199243	T	C	0.47	0.21	0.05	0.04	–	intergenic	rs14175506
4	76698492	C	T	0.32	0.25	0.06	0.07	CC2D2A	intron	rs315539724
5	8139028	A	G	0.27	0.26	0.07	0.14	–	intergenic	rs317152756
5	8190401	T	A	0.32	0.25	0.06	0.07	PARVA	intron	rs316881438
5	8234205	A	C	0.27	0.23	0.06	0.17	ENSGALG00000054963	intron	rs737477701
5	8234281	A	C	0.27	0.24	0.06	0.15	ENSGALG00000054963	intron	rs317840977
5	8327574	G	A	0.24	0.28	0.06	0.04	MICAL2	intron	rs313323205
5	8393628	C	A	0.23	0.28	0.06	0.05	DKK3	upstream	rs794267517
5	8393723	A	T	0.23	0.29	0.07	0.04	DKK3	upstream	rs794348453
5	8475530	A	C	0.35	0.22	0.06	0.18	USP47	upstream	rs313108206
5	8534954	C	T	0.33	0.23	0.06	0.14	GALNT18	upstream	rs740386531
5	9099844	T	C	0.25	0.28	0.07	0.06	–	intergenic	rs736088841
5	9194281	T	C	0.34	0.23	0.06	0.14	AMPD3, RNF141	intron	rs312667549
5	9475448	A	T	0.26	-0.23	0.06	0.14	SBF2	intron	rs732697357
5	9795454	G	A	0.24	0.28	0.07	0.06	NRIP3	intron	rs313488769
5	9797353	A	G	0.24	0.31	0.07	0.03	NRIP3	intron	rs731178344
5	9975375	T	C	0.23	0.32	0.07	0.01	DENND2B	intron	–
5	10239083	T	C	0.21	0.29	0.07	0.05	–	intergenic	–
5	10415181	T	A	0.39	0.25	0.05	0.04	–	intergenic	rs13706093

5	10675242	T	A	0.18	0.29	0.07	0.05	PSMA1	intron	rs315271009
5	10796757	A	G	0.17	0.28	0.07	0.09	CALCA	intron	–
5	11903835	T	C	0.23	-0.20	0.04	0.04	–	intergenic	rs16465660
5	11903836	G	A	0.23	-0.20	0.04	0.04	–	intergenic	rs16465661
5	11903844	C	T	0.23	-0.20	0.04	0.04	–	intergenic	rs16465662
5	11903902	G	A	0.24	-0.20	0.04	0.04	–	intergenic	rs737998140
5	11913861	A	G	0.16	-0.30	0.07	0.05	ENSGALG00000051449	upstream	rs736880111
5	11924135	T	C	0.26	0.30	0.06	0.02	ENSGALG00000051449	intron	rs314967616
5	11955725	T	C	0.33	0.24	0.06	0.17	RPS13	intron	rs316761972
5	12005079	C	T	0.12	-0.31	0.07	0.07	PIK3C2A	intron	rs1058194263
5	12196653	T	C	0.23	-0.35	0.07	0.00	USH1C	upstream	rs732419382
5	12196751	A	G	0.22	-0.34	0.07	0.00	USH1C	upstream	rs313557028
5	12310175	A	G	0.18	-0.31	0.06	0.02	ENSGALG00000050417	intron	rs736732768
5	12310186	A	G	0.18	-0.30	0.06	0.03	ENSGALG00000050417	intron	rs734005321
5	12310234	T	C	0.24	-0.27	0.05	0.01	ENSGALG00000050417	intron	rs317457748
5	12310309	C	A	0.24	-0.25	0.05	0.03	ENSGALG00000050417	intron	rs738193605
5	12310310	T	C	0.24	-0.25	0.05	0.03	ENSGALG00000050417	intron	rs731027506
5	12310322	C	T	0.25	-0.24	0.05	0.04	ENSGALG00000050417	intron	rs1057899587
5	12310343	C	T	0.25	-0.24	0.05	0.04	ENSGALG00000050417	intron	rs1058116708
5	12364690	G	A	0.25	-0.26	0.06	0.06	ENSGALG00000047047	intron	rs316099496
5	12368625	T	C	0.17	-0.26	0.07	0.17	ENSGALG00000047047	intron	rs737347790
5	12393944	A	G	0.50	0.21	0.05	0.20	MYOD1	upstream	rs14515728
5	12428250	G	A	0.26	-0.23	0.06	0.13	KCNC1	intron	rs15663849
5	12428251	C	T	0.16	-0.26	0.07	0.16	KCNC1	intron	rs738826119
5	12433114	T	A	0.15	-0.26	0.07	0.20	KCNC1	intron	rs315627994
5	13374229	G	A	0.25	-0.28	0.06	0.03	SLC22A18	intron	rs737986697
5	13429787	T	C	0.24	-0.31	0.06	0.01	KCNQ1	missense	rs314148590
5	13449328	A	C	0.37	-0.28	0.05	0.00	KCNQ1	intron	rs317846952
5	13449367	T	C	0.37	-0.28	0.05	0.00	KCNQ1	intron	rs312714261
5	13449379	G	A	0.37	-0.28	0.05	0.00	KCNQ1	intron	rs312662826
5	13508017	C	A	0.25	0.30	0.07	0.04	KCNQ1	intron	rs737511869
5	13899194	G	C	0.25	-0.28	0.06	0.05	ENSGALG00000054949	upstream	rs736998338
5	14239370	A	G	0.31	-0.25	0.06	0.09	TNNT3	upstream	rs315939359
5	14280580	A	C	0.30	0.33	0.06	0.00	LSP1	intron	rs1057848124
5	14280613	T	C	0.34	0.31	0.06	0.00	LSP1	intron	rs316544133
5	14295515	G	C	0.11	-0.34	0.08	0.04	TNNI2	upstream	rs739911666

5	14298811	C	T	0.11	-0.35	0.08	0.04	TNNI2	upstream	rs741315284
5	14301905	G	C	0.18	-0.31	0.06	0.02	SYT8	downstream	rs315541073
5	14308280	T	C	0.11	-0.34	0.08	0.04	SYT8	intron	rs739144609
5	14319885	A	G	0.41	0.24	0.06	0.05	ENSGALG00000006608 (cytosolic 5'-nucleotidase 1A-like)	intron	rs315734391
5	14320013	A	G	0.13	-0.30	0.08	0.19	ENSGALG00000006608 (cytosolic 5'-nucleotidase 1A-like)	intron	rs734156129
5	14320311	A	G	0.31	0.27	0.06	0.05	ENSGALG00000006608 (cytosolic 5'-nucleotidase 1A-like)	intron	rs313176621
5	14321077	G	A	0.43	0.28	0.05	0.00	CTSD	intron	rs734894055
5	14321102	G	T	0.46	0.26	0.05	0.02	CTSD, ENSGALG00000006608 (cytosolic 5'-nucleotidase 1A-like)	intron	rs736987423
5	14477401	T	C	0.24	-0.24	0.06	0.12	MOB2, ENSGALG00000006608 (cytosolic 5'-nucleotidase 1A-like)	intron	rs314346393
5	14529930	T	C	0.29	0.29	0.07	0.04	BRSK1	intron	rs317011817
5	14740059	T	C	0.47	0.23	0.06	0.16	BRSK1	intron	rs732958141
5	14789244	A	C	0.28	0.25	0.06	0.12	BRSK1	intron	rs740340467
5	14859530	A	C	0.22	0.28	0.07	0.09	TOLLIP	upstream	rs731299034
5	14860213	T	C	0.25	0.26	0.06	0.13	TOLLIP	intron	rs741587750
5	15130898	A	T	0.22	0.26	0.07	0.19	–	upstream	rs737205331
5	15791803	G	A	0.44	0.17	0.04	0.17	TSPAN4	intron	rs732618786
5	15798092	G	T	0.28	-0.19	0.05	0.18	TSPAN4	intron	rs739312534
5	15798095	G	C	0.28	-0.19	0.05	0.18	TSPAN4	intron	rs316904875
5	15798156	G	A	0.28	-0.19	0.05	0.19	TSPAN4	intron	rs315274042
5	15798957	T	C	0.31	-0.23	0.05	0.07	TSPAN4	intron	rs318045000
5	15936430	C	T	0.23	-0.23	0.06	0.12	CRACR2B	synonymous	rs317727101
5	16038215	C	T	0.37	0.23	0.06	0.15	SLC25A22	intron	rs80773900
5	16038238	T	C	0.20	0.25	0.06	0.17	SLC25A22	intron	rs316273614
5	16063707	T	C	0.17	0.32	0.07	0.05	ENSGALG00000044313 (malignant fibrous histiocytoma-amplified sequence 1 homolog)	intron	–
5	16219329	T	C	0.18	-0.26	0.06	0.14	HRAS	intron	rs1058469740
5	16219353	C	T	0.18	-0.26	0.06	0.14	HRAS	intron	rs739279765
5	16219365	A	G	0.21	-0.29	0.06	0.03	HRAS	intron	rs736506336
5	16219383	T	C	0.21	-0.29	0.06	0.03	HRAS	intron	rs1060172062
5	16219605	G	A	0.22	-0.26	0.06	0.14	HRAS	intron	–
5	16219948	A	G	0.35	0.24	0.06	0.19	HRAS	intron	rs739071280

5	16321466	C	G	0.37	0.22	0.05	0.14	ENSGALG00000039221 (USP6 N-terminal like)	intron	rs731596612
5	52613622	A	G	0.22	-0.23	0.06	0.18	ENSGALG00000053496	intron	rs736589267
6	19633163	T	C	0.45	0.24	0.06	0.16	–	intergenic	rs312821901
6	19640631	T	G	0.39	0.34	0.07	0.03	–	intergenic	rs317231865
6	19757662	T	C	0.41	0.27	0.07	0.19	–	intergenic	rs732413595
6	20457816	A	G	0.24	-0.24	0.06	0.17	RPP30	intron	rs741367161
6	20457984	T	C	0.24	-0.25	0.06	0.17	RPP30	intron	rs317940783
6	23051337	A	G	0.26	0.28	0.07	0.10	ABCC2	5' UTR	rs316559857
6	23081542	T	A	0.25	0.27	0.07	0.20	ENSGALG00000046861	intron	–
6	23100280	A	G	0.30	0.29	0.07	0.05	GOT1	synonymous	rs735653913
6	23389752	A	G	0.12	0.37	0.08	0.04	LCOR	intron	rs314449385
6	23391580	G	T	0.11	0.33	0.08	0.12	LCOR	intron	rs16553285
6	23391597	T	C	0.11	0.33	0.08	0.12	LCOR	intron	rs315103144
9	1346895	T	G	0.06	0.37	0.10	0.20	ATG16L1	intron	rs1059774978
10	5287329	C	T	0.19	-0.36	0.09	0.19	RORA	intron	rs312843434
10	17159976	G	A	0.21	0.23	0.06	0.18	IGF1R	intron	rs794596837
10	20295224	A	G	0.06	0.39	0.10	0.17	FRMD5	upstream	rs314009265
18	4494393	G	A	0.08	0.33	0.08	0.16	FOXJ1	upstream	rs14110243
18	9125404	A	G	0.49	0.25	0.06	0.12	GPR142	upstream	rs313258278
24	5503009	C	G	0.45	0.21	0.05	0.11	ENSGALG00000054900	upstream	rs733169339
30	79633	G	A	0.19	-0.23	0.06	0.18	ENSGALG00000050235 (queuine tRNA-ribosyltransferase catalytic subunit 1)	intron	–
30	90012	C	T	0.29	-0.25	0.05	0.01	DNM2	intron	–
30	96694	T	C	0.19	-0.28	0.06	0.01	DNM2	intron	–
30	97362	A	G	0.20	-0.28	0.06	0.01	DNM2	intron	–
30	198870	A	G	0.11	-0.26	0.07	0.19	ENSGALG00000050608 (ribonucleoprotein PTB-binding 1-like)	exon	–
30	385373	A	G	0.38	0.18	0.05	0.17	ENSGALG00000047517 (zinc finger protein 653)	3' UTR	–
30	385374	A	G	0.38	0.18	0.05	0.17	ENSGALG00000047517 (zinc finger protein 653)	3' UTR	–
30	393145	A	G	0.27	0.24	0.05	0.04	CNN1	intron	–
30	395750	T	C	0.28	0.21	0.05	0.17	ELOF1	downstream	–
30	409427	A	G	0.06	-0.40	0.09	0.06	NFIX	intron	–
30	480215	C	T	0.08	0.35	0.08	0.06	PGLS	downstream	–
32	86047	C	G	0.30	-0.26	0.06	0.05	ACTN4	exon	–
32	387490	G	A	0.17	-0.27	0.06	0.06	SMARCA4	upstream	–

AADN 05001253.1	268	C	G	0.48	0.18	0.05	0.14	–	intergenic	–

Chr: chromosome, A1: effect allele, A2: alternate allele

Table B.2: Significant (q-value < 0.05) and suggestive (0.05 ≤ q-value < 0.20) SNP markers for wooden breast using only female progeny.

Chr	**Position (bp)**	**A1**	**A2**	**A1 Freq.**	**beta**	**se**	**FDR**	**Nearest gene within 5000bp**	**Consequence**	**dbSNP ID**
1	38013957	T	C	0.49	-0.24	0.06	0.16	PHLDA1	downstream	rs313675359
1	136464100	A	G	0.35	-0.29	0.07	0.11	FHL2	intron	rs317244712
2	45199243	T	C	0.45	0.26	0.06	0.16	–	intergenic	rs14175506
5	8045595	T	C	0.36	-0.29	0.06	0.10	TEAD1	intron	rs737849103
5	8234281	A	C	0.27	0.30	0.08	0.20	ENSGALG00000054963	intron	rs317840977
5	8275509	G	A	0.31	0.31	0.07	0.11	MICAL2	intron	rs733028144
5	8276158	T	C	0.27	0.35	0.08	0.11	MICAL2	intron	rs734168940
5	8327574	G	A	0.24	0.35	0.08	0.10	MICAL2	intron	rs313323205
5	8393628	C	A	0.23	0.35	0.08	0.11	DKK3	upstream	rs794267517
5	8393723	A	T	0.23	0.37	0.08	0.10	DKK3	upstream	rs794348453
5	8475530	A	C	0.35	0.29	0.07	0.15	USP47	upstream	rs313108206
5	8534954	C	T	0.33	0.33	0.07	0.10	GALNT18	upstream	rs740386531
5	8604008	C	T	0.46	0.23	0.06	0.13	GALNT18	intron	rs316321212
5	9010796	A	T	0.27	-0.37	0.08	0.10	EIF4G2	upstream	rs738468379
5	9194281	T	C	0.33	0.30	0.08	0.19	AMPD3, RNF141	intron	rs312667549
5	9797353	A	G	0.24	0.35	0.08	0.15	NRIP3	intron	rs731178344
5	9975375	T	C	0.23	0.37	0.08	0.10	DENND2B	intron	–
5	10089685	G	C	0.26	0.32	0.08	0.12	ENSGALG00000047228	downstream	rs16463571
5	10089707	T	C	0.26	0.32	0.08	0.13	ENSGALG00000047228	downstream	rs13705936
5	10102413	C	T	0.34	0.32	0.07	0.10	–	intergenic	rs737972763
5	10239083	T	C	0.21	0.37	0.09	0.10	–	intergenic	–
5	10617493	T	C	0.16	0.41	0.09	0.10	RRAS	intron	rs741545263
5	11903835	T	C	0.25	-0.25	0.06	0.10	–	intergenic	rs16465660
5	11903836	G	A	0.25	-0.25	0.06	0.10	–	intergenic	rs16465661
5	11903844	C	T	0.25	-0.25	0.06	0.10	–	intergenic	rs16465662
5	11903902	G	A	0.25	-0.25	0.06	0.10	–	intergenic	rs737998140
5	12196653	T	C	0.23	-0.47	0.09	0.01	USH1C	upstream	rs732419382

5	12196751	A	G	0.22	-0.41	0.08	0.04	USH1C	upstream	rs313557028
5	12310175	A	G	0.19	-0.34	0.08	0.11	ENSGALG00000050417	intron	rs736732768
5	12310186	A	G	0.18	-0.35	0.08	0.10	ENSGALG00000050417	intron	rs734005321
5	12310234	T	C	0.25	-0.27	0.07	0.14	ENSGALG00000050417	intron	rs317457748
5	12310309	C	A	0.25	-0.26	0.07	0.19	ENSGALG00000050417	intron	rs738193605
5	12310310	T	C	0.25	-0.26	0.07	0.19	ENSGALG00000050417	intron	rs731027506
5	12428250	G	A	0.26	-0.32	0.07	0.10	KCNC1	non coding transcript exon variant	rs15663849
5	12754295	A	T	0.19	-0.36	0.09	0.14	LDHA	intron	rs733539786
5	12801766	C	G	0.46	0.27	0.06	0.12	SPTY2D1	intron	rs15664878
5	13305983	T	C	0.17	-0.36	0.08	0.11	NAP1L4	intron	rs731375845
5	13336422	T	C	0.43	0.36	0.08	0.10	NAP1L4	downstream	rs318048978
5	13374229	G	A	0.26	-0.30	0.08	0.19	SLC22A18	intron	rs737986697
5	13429787	T	C	0.25	-0.36	0.08	0.08	KCNQ1	missense	rs314148590
5	13449328	A	C	0.38	-0.34	0.07	0.01	KCNQ1	intron	rs317846952
5	13449367	T	C	0.38	-0.35	0.07	0.01	KCNQ1	intron	rs312714261
5	13449379	G	A	0.38	-0.35	0.07	0.01	KCNQ1	intron	rs312662826
5	13465671	C	T	0.18	-0.36	0.08	0.11	KCNQ1	intron	–
5	13508017	C	A	0.24	0.43	0.09	0.03	KCNQ1	intron	rs737511869
5	13710050	T	C	0.31	0.32	0.08	0.20	KCNQ1	intron	–
5	13899194	G	C	0.26	-0.33	0.08	0.18	ENSGALG00000054949	upstream	rs736998338
5	14280580	A	C	0.30	0.37	0.08	0.05	LSP1	intron	rs1057848124
5	14280613	T	C	0.34	0.34	0.07	0.06	LSP1	intron	rs316544133
5	14295515	G	C	0.11	-0.41	0.10	0.16	TNNI2	upstream	rs739911666
5	14301905	G	C	0.18	-0.36	0.08	0.10	SYT8	downstream	rs315541073
5	14308280	T	C	0.11	-0.42	0.10	0.16	SYT8	intron	rs739144609
5	14320311	A	G	0.30	0.32	0.08	0.15	ENSGALG00000006608 (cytosolic 5'-nucleotidase 1A-like)	intron	rs313176621
5	14529930	T	C	0.28	0.38	0.08	0.10	BRSK1	intron	rs317011817
5	14789244	A	C	0.30	0.35	0.08	0.10	BRSK1	intron	rs740340467
5	14859530	A	C	0.22	0.36	0.09	0.15	TOLLIP	upstream	rs731299034
5	14860213	T	C	0.25	0.35	0.08	0.10	TOLLIP	intron	rs741587750
5	14871372	T	G	0.26	0.30	0.07	0.18	TOLLIP	intron	rs316792341
5	15130898	A	T	0.22	0.35	0.09	0.15	–	upstream	rs737205331
5	15791803	G	A	0.39	0.24	0.06	0.15	TSPAN4	intron	rs732618786
5	15936430	C	T	0.23	-0.33	0.07	0.10	CRACR2B	synonymous	rs317727101

5	15960632	A	C	0.18	-0.37	0.09	0.16	CRACR2B; PNPLA2	upstream; downstream	rs317322542
5	16038215	C	T	0.39	0.35	0.07	0.05	SLC25A22	intron	rs80773900
5	16038238	T	C	0.22	0.32	0.08	0.15	SLC25A22	intron	rs316273614
5	55130617	C	T	0.25	-0.34	0.08	0.16	ENSGALG00000049009	intron	–
6	16259130	T	C	0.22	0.34	0.08	0.12	VCL	intron	rs15785172
6	16259131	G	A	0.22	0.34	0.08	0.12	VCL	intron	rs15785175
6	23051337	A	G	0.25	0.39	0.09	0.10	ABCC2	5' UTR	rs316559857
6	23100280	A	G	0.30	0.37	0.09	0.10	GOT1	synonymous	rs735653913
30	90012	C	T	0.29	-0.27	0.07	0.19	DNM2	intron	–
30	393145	A	G	0.27	0.30	0.07	0.15	CNN1	intron	–

Chrom: chromosome, A1: effect allele, A2: alternate allele

Table B.3: Significant (q-value < 0.05) and suggestive (0.05 ≤ q-value < 0.20) SNP markers for white striping, using both male and female progeny

Chr	**Position (bp)**	**A1**	**A2**	**A1 Freq.**	**beta**	**se**	**FDR**	**Nearest gene within 5000bp**	**Consequence**	**dbSNP ID**
5	12196653	T	C	0.23	-0.24	0.05	0.04	USH1C	upstream	rs732419382
5	12310175	A	G	0.18	-0.20	0.05	0.19	ENSGALG00000050417	intron	rs736732768
5	12310234	T	C	0.24	-0.18	0.04	0.13	ENSGALG00000050417	intron	rs317457748
5	13090486	G	T	0.41	0.20	0.05	0.16	OSBPL5	upstream	rs317668507
5	14280580	A	C	0.30	0.24	0.05	0.00	LSP1	intron	rs1057848124
5	14280613	T	C	0.34	0.23	0.04	0.00	LSP1	intron	rs316544133
5	14308280	T	C	0.11	-0.26	0.06	0.13	SYT8	intron	rs739144609
5	14319885	A	G	0.41	0.23	0.04	0.00	ENSGALG00000006608	intron	rs315734391
5	14320311	A	G	0.31	0.24	0.05	0.00	ENSGALG00000006608	intron	rs313176621
5	14321077	G	A	0.43	0.23	0.04	0.00	CTSD	intron	rs734894055
5	14321102	G	T	0.46	0.22	0.04	0.00	CTSD, ENSGALG00000006608	intron	rs736987423
5	14418699	G	A	0.24	-0.16	0.04	0.16	MOB2, ENSGALG00000006608	intron	rs313920846
5	14477401	T	C	0.24	-0.24	0.04	0.00	MOB2, ENSGALG00000006608	intron	rs314346393
5	14529930	T	C	0.29	0.23	0.05	0.04	BRSK1	intron	rs317011817
5	14789244	A	C	0.28	0.21	0.05	0.11	BRSK1	intron	rs740340467
5	22076599	G	A	0.10	-0.30	0.07	0.13	–	intergenic	rs739005238
5	58074636	A	G	0.36	0.17	0.03	0.03	NIN	synonymous	rs736108284
11	9772478	A	C	0.20	-0.20	0.05	0.16	DPY19L3	upstream	rs735361284

Chr: chromosome, A1: effect allele, A2: alternate allele

Appendix C

SIGNIFICANT AND SUGGESTIVE WINDOWS FROM MULTI-MARKER GENOME-WIDE ASSOCIATION ANALYSES

Table C.1: Results of Bayesian multi-marker regression for wooden breast, white striping, body weight at 13 days, and body weight at 7 weeks.

Trait	**Chr**	**Window (Mb)**	**# SNPs**	**Explain Genetic Variance (%)**	**P>0**	**Pi (Prior)**
Wooden Breast	30	0 – 1	327	3.1	0.97	0.998
Wooden Breast	5	14 – 15	186	2.74	0.808	0.998
Wooden Breast	6	19 – 20	82	2.35	0.775	0.998
Wooden Breast	6	23 – 24	990	1.72	0.951	0.998
Wooden Breast	5	13 – 14	224	1.64	0.622	0.998
Wooden Breast	5	16 – 17	436	1.6	0.798	0.998
Wooden Breast	18	9 – 10	1508	1.44	0.987	0.998
Wooden Breast	2	45 – 46	147	1.14	0.587	0.998
Wooden Breast	18	4 – 5	791	1.01	0.89	0.998
Wooden Breast	5	12 – 13	197	0.9	0.587	0.998
Wooden Breast	12	9 – 10	563	0.77	0.837	0.998
Wooden Breast	24	5 – 6	653	0.75	0.83	0.998
Wooden Breast	1	39 – 40	105	0.73	0.443	0.998
Wooden Breast	4	76 – 77	134	0.71	0.542	0.998
Wooden Breast	23	4 – 5	979	0.69	0.893	0.998
Wooden Breast	28	1 – 2	1023	0.61	0.876	0.998
Wooden Breast	25	3 – 4	787	0.61	0.844	0.998
Wooden Breast	28	2 – 3	1039	0.61	0.861	0.998
Wooden Breast	13	11 – 12	440	0.59	0.758	0.998
Wooden Breast	9	1 – 2	288	0.58	0.638	0.998
Wooden Breast	5	58 – 59	604	0.57	0.791	0.998
Wooden Breast	3	104 – 105	592	0.55	0.767	0.998
Wooden Breast	20	10 – 11	1039	0.53	0.89	0.998

Wooden Breast	1	45 – 46	246	0.53	0.548	0.998
Wooden Breast	32	0 – 1	361	0.52	0.619	0.998
Wooden Breast	9	2 – 3	316	0.52	0.621	0.998
White Striping	5	14 – 15	186	5.38	0.99	0.994
White Striping	5	58 – 59	604	3.18	0.997	0.994
White Striping	12	9 – 10	563	1.19	0.99	0.994
White Striping	11	9 – 10	151	0.79	0.807	0.994
White Striping	18	9 – 10	1508	0.72	1	0.994
White Striping	7	22 – 23	890	0.72	0.995	0.994
White Striping	6	23 – 24	990	0.66	0.997	0.994
White Striping	28	3 – 4	1226	0.63	1	0.994
White Striping	20	10 – 11	1039	0.6	1	0.994
White Striping	1	136 – 137	137	0.59	0.737	0.994
White Striping	23	4 – 5	979	0.52	1	0.994
Body Weight 13d	18	9 – 10	1508	0.78	1	0.690
Body Weight 13d	14	13 – 14	1122	0.65	1	0.690
Body Weight 13d	28	3 – 4	1226	0.63	1	0.690
Body Weight 13d	4	1 – 2	1092	0.62	1	0.690
Body Weight 13d	28	2 – 3	1039	0.61	1	0.690
Body Weight 13d	6	23 – 24	990	0.56	1	0.690
Body Weight 13d	26	4 – 5	1034	0.56	1	0.690
Body Weight 13d	20	10 – 11	1039	0.55	1	0.690
Body Weight 13d	27	6 – 7	899	0.54	1	0.690
Body Weight 13d	26	2 – 3	958	0.54	1	0.690
Body Weight 13d	26	1 – 2	1023	0.53	1	0.690
Body Weight 13d	23	2 – 3	997	0.51	1	0.690
Body Weight 13d	23	4 – 5	979	0.5	1	0.690
Body Weight 13d	27	5 – 6	839	0.5	1	0.690
Body Weight 7w	18	9 – 10	1508	0.67	1	0.581
Body Weight 7w	14	13 – 14	1122	0.58	1	0.581
Body Weight 7w	2	0 – 1	1077	0.58	1	0.581
Body Weight 7w	28	3 – 4	1226	0.57	1	0.581
Body Weight 7w	28	1 – 2	1023	0.54	1	0.581
Body Weight 7w	4	1 – 2	1092	0.53	1	0.581
Body Weight 7w	28	2 – 3	1039	0.52	1	0.581
Body Weight 7w	20	10 – 11	1039	0.5	1	0.581

Body Weight 7w	23	4 – 5	979	0.5	1	0.581

Windows identified by Bayes B were considered significant if they explained ≥ 1% of genetic variance and suggestive if they explained ≥ 0.5% of genetic variance. Chr: chromosome.

Appendix D

PERMISSIONS

Chapters that were previously published in peer-reviewed journals are open-access articles distributed under the terms of the Creative Commons Attribution License (CC BY). No special permission is required to reuse all or part of those articles, including figures and tables. For articles published under an open access Creative Common CC BY license, any part of the article may be reused without permission provided that the original article is clearly cited. The use, distribution or reproduction in other forums is permitted, provided the original author(s) and the copyright owner(s) are credited and that the original publication in this journal is cited, in accordance with accepted academic practice. No use, distribution or reproduction is permitted which does not comply with these terms.